University of Southampton

Structure/Function Analysis of Amino Acid Permeases in Higher Plants.

by
Ian David Beech

A thesis submitted at the University of Southampton in partial fulfilment of the requirements for the degree of

Doctor of Philosophy

in the department of Biological Science, Cell Science division.

September 2001

UNIVERSITY OF SOUTHAMPTON

ABSTRACT

FACULTY OF SCIENCE
SCHOOL OF BIOLOGICAL SCIENCES – DIVISION OF CELL SCIENCES

Doctor of Philosophy

STRUCTURE/FUNCTION ANALYSIS OF AMINO ACID PERMEASES IN HIGHER PLANTS

By Ian David Beech

Nitrogen is essential in all living organisms for growth and development. Nitrogen is redistributed in the plant mainly in the form of amino acids. An essential part of this redistribution is the ability to transport amino acids across plasma membranes. The proteins responsible for this transport are of significant physiological importance in plants. The aim of the work described in this thesis has been to further characterise the amino acid permeases, RcAAP1 and RcAAP3, from Ricinus communis and to correlate the structural properties of these transporters with their functional characteristics.

RcAAP3 was expressed in Xenopus laevis oocytes. Radiolabelled uptake analysis and electrophysiological methods were used to determine the kinetic parameters of this permease. A transport model was presented in which the permease operates as an amino acid:proton symport for neural amino acids, with a transport ratio of two protons to two amino acid molecules. Binding of amino acid and proton is random and positively co-operative.

Random mutagenesis combined with a suitable selection procedure is a useful technique for isolating mutants with desired functional properties. Three random mutagenesis protocols were investigated in this project with the aim of isolating mutated amino acid permeases. DNA-shuffling (a technique that involves the random fragmentation of a pool of related sequences and then recombination using self-primered PCR) and error-prone PCR (a method in which Mn^{2+} is added to the PCR or the dNTP ratio is altered) failed to produce DNA in sufficient yield or of sufficient quality for ligation and subsequent transformation into yeast. Chemical mutagenesis, a procedure involving EMS mutagenesis of yeast expressing wild type transporters, was the most successful in terms of isolating potential mutants. Chemical mutagenesis was used to produce a library of mutated permeases for screening with specifically designed selection conditions. The first selection condition involved the inclusion of the toxic amino acid canavanine in the selective medium. The aim was to isolate yeast expressing mutated transporters with altered amino acid recognition sites that would allow growth on this medium that was normally toxic. Several isolates were obtained from this selection although these were not pursued further. The second selection was on a high pH medium. The aim was to isolate mutated transporters with an altered affinity for protons. The sequences of transporters in yeast isolates obtained from the high pH selection were compared to wild-type transporters to determine the functional significance and position of mutated residues. Seven potential RcAAP1 mutants were sequenced and three were found to contain mutations. In two of these mutated sequences, Gln68 had been replaced by histidine, although the DNA mutation was different in each. In the third isolate, a DNA mutation was identified, but this had no effect on the amino acid sequence. The structure/function relationships are discussed.

Contents

Acknowledgements

I would like to thank my two supervisors, Dr. Lorraine Williams and Dr. Tony Miller, who have both given me a phenomenal amount of time and support throughout this work.

I am grateful to the following for supplying yeast and vectors: Dr. Daniel Bush for supplying the JT-16 yeast mutant (Tanaka and Fink 1985); Dr. Julie Bick for supplying the GAP yeast mutant (Grenson *et al* 1970); Prof. Norbert Sauer for the Nev-N shuttle vector and sequence (Sauer and Stolz 1994); Dr. Freddie Theodoulou for supplying the *Xenopus* expression vector pXE2; Dr. Alison Marvier for supplying all yeast wild-type transformants.

I would also like to acknowledge the following: Mrs. Carol Roberts for her technical assistance; Dr. Mark Dixon for advice with sequencing; Dr. Richard Foreman, Dr. Di Oakley and the staff of the Southampton Animal House for help with *Xenopus* and oocytes while in Southampton. A special thanks to Dr. Jing-Jiang Zhou for help with *Xenopus*, oocytes and electrophysiological analysis while in Rothamsted.

Thanks to my friends and colleagues in the laboratories at Southampton – Alison, Jon, Martin, Kate, Anne, Sue, Esther, Becky, Vas, Stickle, Aram, Mel, Russ, Paul, Gerard, Jane, Ann; and Rothamsted – Nick, Jacqui, Darren, Sarah, Sue. Thanks to my brother Jim B and also to Lingard, Alex, Fay, Sam, Lee, Ste, Sarah, Karen, Catherine and all my other friends who helped me through.

Thanks to James, Peter and Hilary for help with accommodation in Harpenden.

A very big thanks to Lucy for constant help and support in every way imaginable.

Of course an extra big thanks to my Mum Pat and my Dad Dave for mental and financial support from start to finish.

Abbreviations

A	-	Adenine
AAP	-	Amino acid permease
APC	-	Amino acid-polyamine-choline facilitator
AtAAP	-	*Arabidopsis thaliana* amino acid permease
ATF	-	Amino acid transport family
ATP	-	Adenosine 5'-triphosphate
bp	-	Base pairs
C	-	Cytosine
cDNA	-	Complimentary deoxyribonucleic acid
$CaCl_2$	-	Calcium chloride
CAT	-	Cationic amino acid transporter
CCCP	-	Carbonyl cyanide-m-chlorophenyl hydrazone
CIAP	-	Calf intestinal alkaline phosphatase
CTP	-	Cytodine 5'-triphosphate
DEPC	-	Diethyl pyrocarbonate
DNA	-	Deoxyribonucleic acid
DNase	-	Deoxyribonuclease
DNTP	-	Deoxynucleotidetriphosphate
DPM	-	Disintegrations per minute
E.coli	-	*Escherichia coli*
EDTA	-	Ethylenediaminetetraacetic acid
EMBL	-	European Molecular Biology Laboratory
EMS	-	Ethyl Methyl Sulfonate (Methanesulfonic acid ester)
ER	-	Endoplasmic reticulum
EST	-	Expressed sequence tag
G	-	Guanine
GAP	-	General amino acid permease
GFP	-	Green fluorescent protein
GOGAT	-	Glutamine synthetase-glutamate synthase
GS	-	Glutamine synthetase
GTP	-	Guanosine 5'-triphosphate
Hepes	-	(N-92-hydrpxyethyl) piprazene-N'-(2-ethanesulphonic acid)
IAA	-	Isoamyl alcohol
IPTG	-	Isopropyl-β-D-thiogalactoside
JT-16	-	(yeast mutant - Mat-a, *hip1-614, his4-401, can1, ino1, ura3-52*) (Tanaka and Fink 1985)

Kb	-	Kilobase pairs
KDa	-	Kilo-Daltons
LB	-	Luria-Bertani broth
MBS	-	Modified Barths` saline
MES	-	2-(N-morpholino) ethansulfonic acid
MIPS	-	Munich Information center for Protein Sequences
MOPS	-	3-(N-morpholino) propanesulphonic acid
mRNA	-	Messenger ribonucleic acid
mV	-	Millivolts
NEM	-	N-ethylmaleimide
OD	-	Optical density
PAGE	-	Polyacrylamide gel electrophoresis
pCMBS	-	p-chloromercurobenzosulfonate
PCR	-	Polymerase chain reaction
PEG	-	Polyethylene glycol
PMF	-	Proton motive force
RcAAP	-	*Ricinus communis* amino acid permease
RNA	-	Ribonucleic acid
RNase	-	Ribonuclease
Rpm	-	Revolutions per minute
RT-PCR	-	Reverse Transcriptase-Polymerase Chain Reaction
SC	-	Synthetic complete media
SDS	-	Sodium dodecyl sulphate
S.E.	-	Standard error
SE-CC	-	Sieve element companion cell complex
SOS	-	Standard oocyte saline
T	-	Thymine
TAE	-	Tris/acetic acid/EDTA
TE	-	Tris/EDTA
TEG	-	Tris/EDTA/glucose
TMHMM	-	Transmembrane hidden Markov model
UTP	-	Uradine 5'-triphosphate
UV	-	Ultraviolet
WT	-	Wild type
Xgal	-	5-Bromo-4-chloro-3-indolyl-β-D-galactoside
YPD	-	Yeast extract/peptone/dextrose

Chapter 1 Introduction

1.1 *Nitrogen assimilation.*

Nitrogen is essential for growth and development in all living organisms, where it constitutes the fourth most abundant element. The largest requirement for this element is in the synthesis of amino acids, which function as the building blocks of proteins as well as precursors to many other compounds. Nitrogen is also an essential constituent of nucleic acids, cofactors and other common metabolites; it is a major component of chlorophyll, and forms part of several plant hormones.

In higher plants, elemental nitrogen cannot be assimilated directly and so several diverse strategies have been employed to acquire nitrogen. Plant roots can take up a variety of nitrogenous compounds from the soil including nitrate, ammonium and amino acids. The ratio of nitrogen sources used depends on the particular plant species and its environmental conditions (Schobert and Komor 1987). For incorporation into organic material, nitrogen must be in the form of ammonium. Nitrate assimilation involves the reduction to ammonium in a two-step process followed by conversion to the amino acid glutamine (for a review see Crawford *et al* 2000b). These reactions are shown in figure 1.1. Nitrate is reduced to nitrite via nitrate reductase in the cytosol. Nitrite enters the plastid and is reduced to ammonium by nitrite reductase and this is subsequently converted to glutamine via an ATP-dependent reaction using glutamate as a substrate. This is catalysed by glutamine synthetase (GS). GS functions in a cycle with glutamate synthetase (GOGAT: glutamine-2-oxoglutarate aminotransferase), which catalyses the reductive transfer of the amide group from glutamine to α-ketoglutarate, forming two molecules of glutamate (figure 1.2). Depending on the plant species or growth conditions, nitrate taken up by the roots may be reduced and assimilated in the root or transported as nitrate to the shoot for reduction and assimilation there. Alternatively nitrate may also be stored in vacuoles in cells of the root or shoot. In *Ricinus* (the plant species used in this project), assimilation is reported to occur in both shoot and root (Kirkby and Armstrong 1980, Van Beusichem *et al* 1985).

Nodulated plants can obtain ammonia efficiently from N_2 by participating in a symbiosis with nitrogen-fixing bacteria. Ammonia, released by the nitrogen-fixing bacteria, is first assimilated in the plant into amino acids by glutamine synthetase and other enzymes, sometimes employing nodule-specific isozymes (Crawford *et al* 2000a). Ammonia is also produced from glycine decarboxylation during photorespiration in the mesophyll of the source

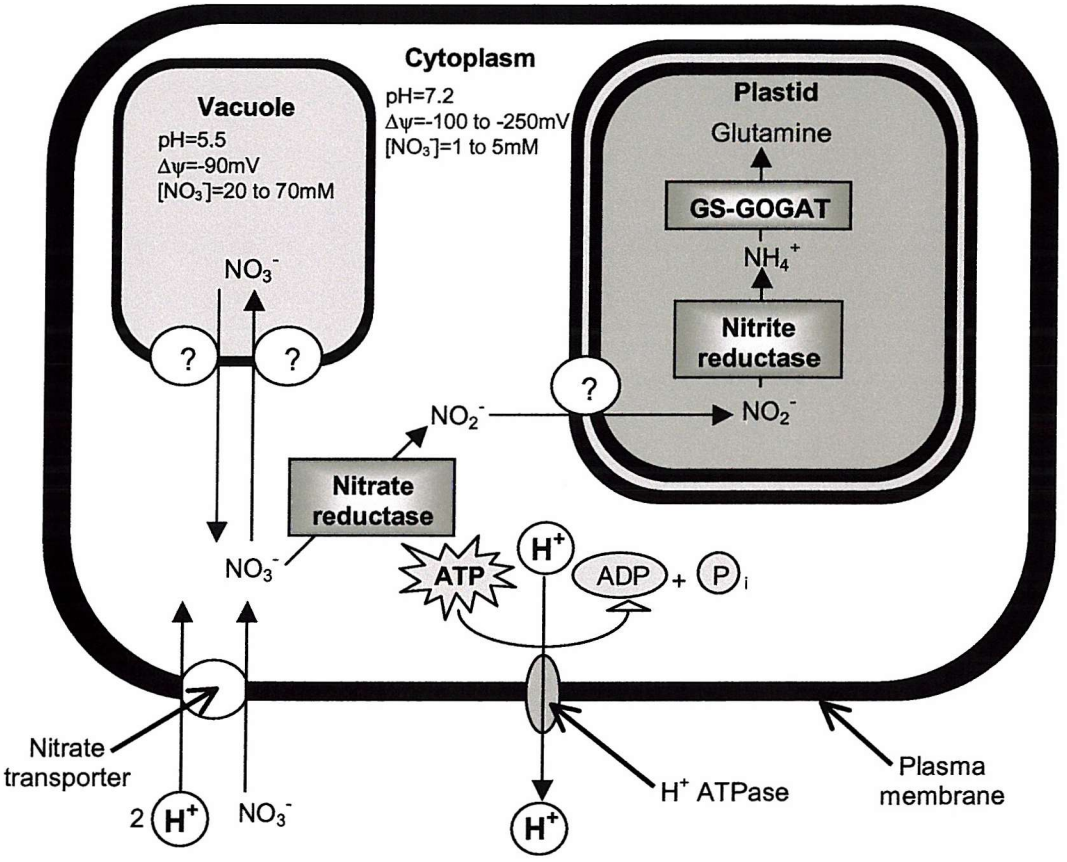

Figure 1.1 – Nitrate assimilation by higher plants. A proton motive force is maintained by the plant cell to transport many solutes across the Plasma membrane (PM), including nitrate (NO_3^-). Inside the cell, nitrate is reduced to ammonia (NH_4^+) by the action of nitrate reductase in the cytoplasm and nitrite reductase in the plastid. Ammonia is then assimilated into glutamate via the glutamine synthetase-glutamate synthase pathway (GS-GOGAT). This pathway is further described in figure 1.2. (Adapted from Crawford *et al* 2000b).

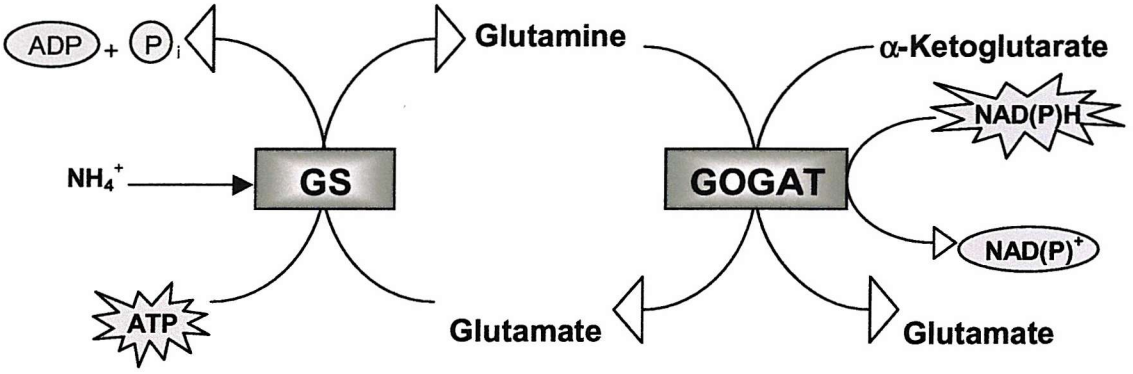

Figure 1.2 – The glutamine synthetase-glutamate synthase pathway (GS-GOGAT). Ammonium and glutamate are combined via glutamine synthetase (GS) to form glutamine. This in turn is used in conjunction with α-ketoglutarate to form two glutamate molecules via the action of glutamate synthase. The net product of this two step procedure is a single glutamate molecule. (Adapted from Coruzzi and Last 2000).

leaves (Crawford *et al* 2000b). This must be re-assimilated into amino acids to prevent nitrogen loss and also to avoid toxicity (McGrath and Coruzzi 1991).

1.2 Nitrogen distribution

Organic and inorganic nitrogenous solutes are transported via the vascular system of the xylem and phloem from their tissue of uptake or production to areas of the plant that require a supply of nitrogenous compounds, such as developing leaves or fruits. Ammonium assimilation usually occurs in the roots whereas nitrate assimilation can occur both in roots and leaves. Transport of nitrate or amino acids from the roots to the leaves occurs in the xylem, whereas redistribution from the leaves to other organs is via the phloem, predominantly in the form of amino acids (Williams and Miller 2001). Xylem and phloem exudates vary considerably in their composition and concentration (tables 1.1 and 1.2) and differences occur not only among plant species but also within the same plant depending on changing physiological conditions and time of day (Fischer 2000). The amino acids glutamine and asparagine are the primary organic nitrogenous compounds transported within the plant (Urquhart and Joy 1981). Glutamine is the preferred compound in light-grown plants, while asparagine is preferred in dark-grown plants (Grant and Bevan 1994). These amino acids are also the primary products of nitrate assimilation reactions (McGrath and Coruzzi 1991), and have high nitrogen to carbon ratios making them suitable as nitrogen transport compounds. Other amino acids such as arginine have a lower nitrogen to carbon ratio, and are often metabolised in the root cells (parenchyma) rather than transported in the xylem (Schobert and Komor 1990). A scheme showing the intercellular transport routes for the main nitrogenous solutes is shown in figure 1.3. In nodules, ammonium from nitrogen fixation is ultimately incorporated into amide amino acids (gluatamine or asparagine) or ureides for export to the leaves (see figure 1.4).

Most relevant to this study is the transport of amino acids and the following sections concentrate on the long distance transport of amino acids in the vascular system.

1.3 Long distance transport of amino acids

Amino acids are the building blocks of proteins and are also precursors for other nitrogen-containing molecules in the cell (e.g. nucleic acids, photosynthetic pigments and growth regulators). They are important in a number of metabolic pathways and they are vital for

Table 1.1 - Amino acid composition in root tissue and xylem sap of 7-day old *Ricinus communis* seedlings (taken from Schobert and Komor 1990).

Amino acid	Amino acid composition	
	Xylem sap (mM)	Root tissue (μmol g^{-1} Fresh Weight)
Neutral amino acids	22.5	14.2
Glutamine	12.0	5.5
Valine	2.2	3.0
Alanine	2.2	0.3
γ-aminobutyric acid	2.0	0.1
Isoleucine	1.3	2.1
Others	2.8	3.2
Basic amino acids	1.0	4.4
Arginine	0.4	2.5
Others	0.6	1.9
Acidic amino acids	1.9	1.2
Glutamate	1.6	0.6
Aspartate	0.3	0.6

Table 1.2 - Concentration of amino acids (in mM - calculated on water content) in those parts of the *Ricinus* seedling important for transport (taken from Schobert and Komor 1989).

Amino Acid	Endosperm	Apopiast between endosperm and cotyledons	Cotyledons	Sieve-tube exudate	Hypocotyl	Root
Neutrai amino acids	**15.6**	**14.1**	**29.4**	**119.3**	**83.2**	**14.2**
Glutamine	1.3	2.7	16.5	49.9	46.9	5.5
Valine	2.0	1.6	6.7	16.1	9.0	3.0
Isoleucine	1.4	1.3	3.7	10.6	6.3	2.1
Serine	1.9	0.8	4.5	8.8	3.4	0.4
Threonine	1.3	1.3	3.6	8.2	2.5	0.9
Leucine	1.6	0.7	2.2	6.1	1.4	0.6
Amino butyric acid	0.2	2.2	4.6	5.8	5.6	0.1
Phenylalanine	1.2	0.7	2.5	5.5	1.6	0.4
Asparagine	0.4	0.3	2.0	4.9	2.4	0.6
Alanine	2.8	2.1	1.9	1.1	2.7	0.3
Glycine	1.0	0.4	0.8	0.7	0.7	0.2
Tyrosine	0.2	0	0.4	0.7	0.2	0.1
Cysteine	0.1	0	0	0.5	0	0
Methionine	0.2	0	0	0.4	0.5	0
Acidic amino acids	**3.6**	**1.0**	**14.1**	**5.9**	**19.6**	**1.2**
Glutamic acid	2.9	0.5	11.5	5.0	16.3	0.6
Aspartic acid	0.7	0.5	2.6	0.9	3.3	0.6
Basic amino acids	**4.2**	**3.4**	**27.6**	**32.4**	**20.6**	**4.4**
Lysine	0.5	1.7	2.6	13.6	2.4	1.2
Arginine	2.5	1.0	20.0	11.1	14.7	2.5
Histidine	1.0	0.5	3.6	5.7	3.0	0.7
1-Methyl-histidine	0.1	0	1.1	1.4	0.3	0
Ornithine	0.1	0.2	0.3	0.6	0.3	0

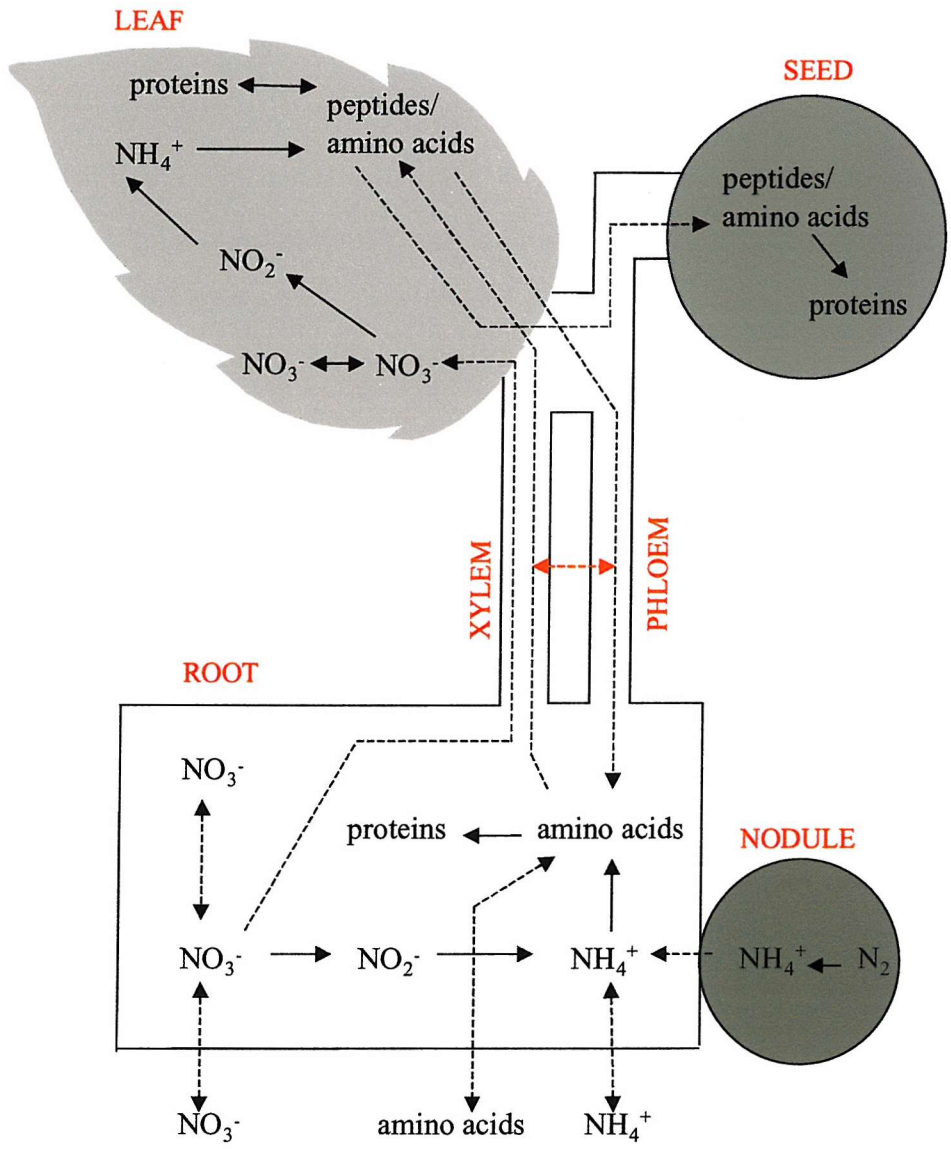

Figure 1.3 – Intercellular routes for the main nitrogenous solutes in a generalised plant. In this diagrammatic representation of a general plant, full lines represent chemical conversions and dashed lines represent transport steps (from Williams and Miller 2001).

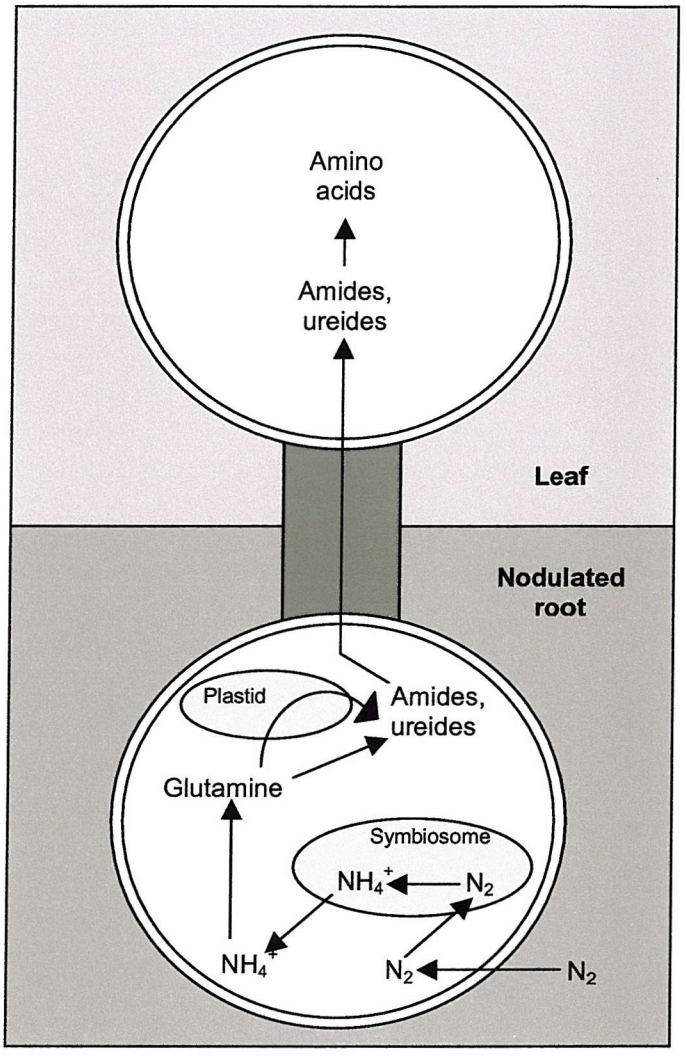

Figure 1.4 – Overview of nitrogen uptake by nodulated plants, with nitrogen-fixing symbionts. Nodulated plants are able to take up fixed nitrogen (N_2) from the soil and through the action of symbiotic bacteria generate ammonia (NH_4^+). This can then be transformed into amino acids for redistribution (adapted from Crawford *et al* 2000b).

the transport and storage of nitrogen. Long distance transport of amino acids occurs in the vascular system and this is essential for supplying tissues that do not participate in nitrogen assimilation. In roots, the release of ions and organic solutes into the xylem (xylem loading) is not well understood although the PM H^+-ATPase in the xylem parenchyma cells is thought to play a key role in pumping protons into the xylem (Mizuno *et al* 1985, DeBoer 1989). The proton and/or electrical gradient could then be used to energise the transport of other ions and solutes (see Marschner 1995 for discussion). Xylem loading as an energised process has been questioned with suggestions that the release of solutes may be thermodynamically passive (Wegner and Raschke 1994). However, there is general agreement that xylem loading is separately regulated from solute uptake in cortical cells offering control over selectivity and rate of transport to the shoot (Marschner 1995).

There is a difference in the relative concentrations of different amino acids that accumulate within the root cells and the xylem (table 1.1; Schobert and Komor 1990). For example in *Ricinus*, there is a six-fold higher concentration of arginine in root cells than in the xylem, and a two-fold higher concentration of glutamic acid in the xylem than in the root cells. In both root cells and xylem, the neutral amino acids are accumulated to much higher concentrations than either the basic or acidic amino acids, and glutamine occurs at the highest concentration in both tissues. The higher concentration in the xylem suggests a selective loading mechanism (Schobert and Komor 1990). It was postulated that specific transporters which differ in their amino acid affinities and transport rates exist within different root tissues. Possible functions of these transporters could be to retrieve amino acids that leak out from the phloem into the apoplastic space or to load specific amino acids into the xylem (Schobert and Komor 1987). This is discussed in more detail in sections 1.5.

Most of the solutes and water in the xylem are transported to the leaves, apart from some reabsorption along the pathway in the stem. A model has been presented for scavenging solutes from the xylem sap (xylem unloading) in leaf cells (Marschner 1995) based on work carried out on the uptake of amino acids in legumes (Canny 1988). In this model, the cells of the bundle sheath are sites of intensive PM proton pumping causing acidification of the apoplast; this proton gradient provides the driving force for cotransport of amino acids and ureides. Further evidence in support of this model is the presence of amino acid cotransporter activity in leaf tissue, although their precise cellular location has not yet been determined (Li and Bush 1991).

The pressure-flow hypothesis of Münch (1930) is commonly accepted for describing the mechanism of long-distance solute movement through the phloem. In this model, the movement of solutes through the sieve tubes occurs by mass flow; it is passive, non-selective

and driven entirely by pressure gradients that are maintained by active loading of photosynthate in source tissues (actively photosynthesising leaves) and unloading of materials in sink tissues (immature leaves, growing root tips, developing flowers, fruit and seed). The mechanisms of phloem loading and unloading have received much attention mainly with regard to the movement of sugars. Two main pathways are available for solutes to be loaded into the phloem, symplastic and apoplastic (for a review see Van Bel 1993). Symplastic loading involves transport from cell to cell via interconnecting cytoplasmic tubes called plasmodesmata. Apoplastic loading involves active uptake across the PM of the companion cell and/or sieve elements from the apoplast via transmembrane carriers. The mechanism of loading appears to differ among plant species (Van Bel 1993).

The amino acid composition in the phloem sap can vary along the length of the phloem, but generally the major components are the amides glutamine and asparagine and also the acidic amino acids, glutamate and aspartate (table 1.2). Amino acid uptake in the phloem of *Ricinus* cotyledons has been investigated by comparing the levels of amino acids present in the cotyledons and the sieve tube sap (table 1.2, Schobert and Komor 1989). Higher relative concentrations of certain amino acids e.g. glutamine were reported in the sap, suggesting a selective transport mechanism.

When nitrogen assimilation occurs in the root, amino acids are transported to the mature leaves in the xylem in the transpiration stream. A high proportion of the amino acids arriving in the mature leaves is cycled from the xylem into the phloem for redistribution to N sinks. When assimilation occurs predominantly in the shoot, it is essential that phloem loading of amino acids take place in order to cover the demand of the roots for these compounds (Marschner *et al* 1997). In the root, excess amino acids can move from the phloem to the xylem for recycling (Larsson *et al* 1991, Cooper and Clarkson 1989). In many cases large amounts of reduced N are cycled from the shoot in excess of root demand (Marschner *et al* 1997). It is thought that the vascular cycling of nutrients allows continued root growth when the external nutrient supply is low. This is important for root extension through nutrient deficient soil layers (Marschner *et al* 1997). Because of their side to side arrangement there is ample opportunities for solute exchange between the xylem and the phloem, especially in the highly branched vascular system of source and sink regions (Fisher 2000). Evidence for feedback control of nitrate uptake by various phloem-translocated amino acids has been presented (Muller and Touraine 1992). This has lead to the suggestion that cycling of amino acids between shoots and roots provides information about whole-plant N status, which allows roots to regulate N uptake accordingly (Cooper and Clarkson 1989, Muller and Touraine 1992). However, there is also evidence arguing against the role of phloem amino acids as the primary signals in shoot-

to-root control of nitrate uptake systems (Tillard *et al* 1998). Evidence that amino acids may play a part in regulating the uptake of ammonium in roots comes from studies of the high affinity ammonium transporter AtAMT1.1. A negative correlation between influx and glutamine accumulation in roots suggests that this amino acid might be the feedback signal for repression of influx and *AtAMT1.1* expression (Rawat *et al* 1999, Von Wiren *et al* 2000, Williams and Miller 2001).

The process of solute unloading from phloem to sink tissue is less well defined than loading, possibly due to the diversity in unloading methods between species and also the organ under consideration. Most work again has concentrated on sugars. Evidence is accumulating suggesting that the most common unloading pathway in rapidly growing sink tissues is symplastic as the efflux rates typically exceed membrane transport rates by an order of magnitude (Fisher and Cash-Clark 2000). Symplastic unloading occurs in the vegetative apex, elongating axis of dicot stem, mature axis of primary dicots, mature axis of primary monocot stem and mature primary root. Efficient and rapid unloading can be achieved if the post-phloem symplast does not place major constraints on the exit of solutes from the SE-CC complex (Oparka and Santa Cruz 2000). The similarity in the pattern of unloading in sink leaves for a diverse range of phloem transported compounds has been cited as evidence that SE-CC complexes in the sink tissue do not discriminate between different solutes and macromolecules arriving in the phloem (Oparka and Santa-Cruz 2000). Thus the information obtained for sucrose unloading could be equally applicable to the unloading of amino acids and macromolecules. Evidence of symplastic phloem unloading has recently come from the barley leaf (Haupt *et al* 2001). Carboxyfluorescein transport and systemic movement of barley stripe mosaic virus expressing GFP showed patterns of unloading that could only be explained by a symplastic method. This evidence alongside electron microscope images of plasmodesmata density collectively indicated a symplastic phloem unloading mechanism.

In most cases, selectivity is not observed and this is characteristic of bulk flow through plasmodesmata (Fisher and Cash-Clark 2000). However, there are examples where very low plasmodesmatal frequencies have been reported between the SE/CC and surrounding cells (e.g. growing corn leaves (*Zea mays*) and sugar beet (*Beta vulgaris*) storage roots (Evert and Russin 1993, Fieuw and Willenbrink 1990) and in such cases an apoplastic pathway may operate. Developing seeds are also another specialised sink where apoplastic unloading must be in place; the symplasm is always discontinuous between embryonic and maternal tissues (Patrick and Offler 1996).

Schobert and Komor (1987) investigated phloem unloading of amino acids in the root of *Ricinus* seedlings. Radiolabelled glutamine, applied to the cotyledons, was transported to the

roots via the phloem. If glutamine was then applied externally to the root, the radiolabelled glutamine appeared in the medium. It was suggested that amino acids are lost from the phloem to the apoplast, as externally applied glutamine could compete with the radiolabelled glutamine for uptake from the apoplast (Schobert and Komor 1987). However, glutamine may not have effluxed from the SE/CC but from other cells following symplastic unloading. Apoplastic unloading has been shown in potato stolons undergoing extension growth using carboxyfluorescein and ^{14}C-assimilates (Viola *et al* 2001). This mechanism however, does not persist through the life of the plant. Symplastic unloading is adopted after tuberization. This shift from apoplastic to symplastic unloading involves a change in the expression patterns of amino acid permeases on a temporal basis. Temporal expression of amino acid transporters has also been shown in *Arabidopsis (*Fischer *et al* 1998), with certain permeases being expressed in mature tissues and others in developing tissues. For example, the amino acid permease, *AtProT1,* is expressed in both developing and mature leaves while *AtProT2* is only expressed in mature leaves (Rentsch *et al* 1996, Fischer *et al* 1998). This could suggest that particular stages in development may depend on apoplastic unloading.

1.4 Membrane transport of amino acids

An apoplastic step in the loading and unloading process means that amino acids would have to cross the PM. The highly hydrophobic nature of the PM makes it an effective barrier to amino acids and other solutes. Membrane spanning proteins exist to selectively facilitate the movement of certain solutes across the membrane. In passive transport, a molecule will move through the membrane down its electrochemical potential gradient, via the transport protein. In active transport, energy is required in order to move the molecule across the PM against its electrochemical potential gradient, via the transport protein. Active transport can be distinguished as primary or secondary active transport. In primary active transport, translocation is directly linked to a chemical reaction, such as ATP hydrolysis in the H^+/ATPase system. In secondary active transport, the translocation of a molecule against its electrochemical potential gradient is linked to the transport of another solute down its electrochemical potential gradient. An antiporter facilitates the movement of two solutes to opposite sides of a membrane, while a symporter facilitates the movement of two solutes to the same side of a membrane. In plants, the proton gradient created across the PM by the H^+/ATPase is, in most cases, the energy source for secondary active transporters (Morsomme and Boutry 2000). For the movement of amino acids against their electrochemical gradient

(Schobert and Komor 1989), a secondary active symport system using a proton gradient is the most commonly proposed mechanism in plants (Bush 1993, Young *et al* 1999, Ortiz-Lopez *et al* 2000) (figure. 1.5).

1.5 Amino acid transporters in plants

Early physiological studies carried out on whole tissues, suspension cells, and protoplasts indicated that several transporters, exhibiting a wide specificity (reviewed in Reinhold and Kaplan 1984) mediate amino acid transport across the PM. Later work with purified membrane vesicles investigated the mechanism of transport (Li and Bush 1990, 1991, 1992 Weston *et al* 1994, 1995). This important foundation work will be discussed in detail here only in relation to *Ricinus communis* (see below). This report will then concentrate on more recent advances in the identification, cloning and molecular characterisation of members of amino acid transporter families (see sections 1.5.2).

1.5.1 Amino acid transport in *Ricinus communis*

The *Ricinus* seedling has been used in a number of studies investigating proton-amino acid cotransport (Kriedeman and Beevers 1967, Robinson and Beevers 1981a,b). The growing *Ricinus* seedling receives nutrients such as sucrose and amino acids from the endosperm, which acts as a storage facility until the seedling germinates. Amino acids are stored in the form of storage protein, which represents a major source of nitrogen for the seedling (Stewart and Beevers 1967). The level of nitrogen contained within the endosperm decreases after the beginning of germination, as it is converted into amino nitrogen by hydrolysis. The level of amino nitrogen rises initially within the endosperm, but then rapidly decreases as the amino acids are absorbed by the cotyledons (Stewart and Beevers 1967). The cotyledons retain the ability to absorb sucrose and amino acids after the endosperm has been removed (Kriedemann and Beevers 1967, Robinson and Beevers 1981a). Therefore the cotyledons are an ideal system in which to study nutrient transport. The accumulation of sucrose and amino acids into the intact cotyledon is thought to occur via active transport processes (Komor 1977, Robinson and Beevers 1981a,b). An alkalinisation response occurrs on the addition of various amino acids to *Ricinus* cotyledons (Robinson and Beevers 1981a). This response is saturable, and inhibited by the protein modifier N-ethylmaleimide (NEM). These results are consistent with the

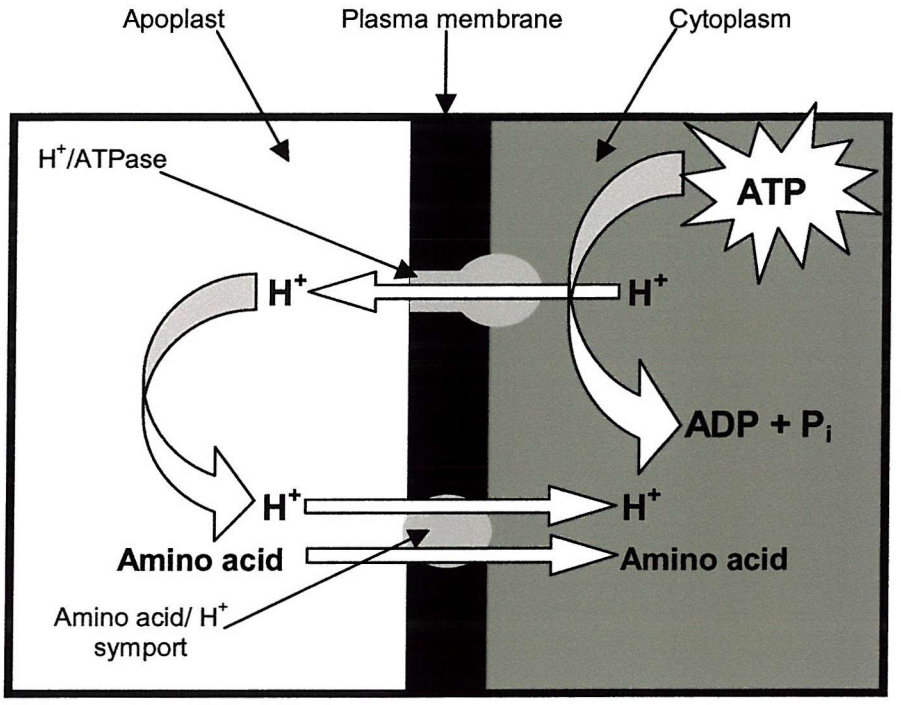

Figure 1.5 - Diagrammatic representation of secondary active amino acid transport. The proton motive force is supplied by a H^+-ATPase through the hydrolysis of ATP. The PMF is then used to transport solutes, such as amino acids against their electrochemical potential gradient.

operation of a proton-coupled carrier mediated transport process. In general, apoplastic alkalinisation is stronger with neutral amino acids than with basic or acidic amino acids, and transport is specific for the L-isomers of all the amino acids tested (Robinson and Beevers 1981b). Inhibition of glutamine transport by other amino acids is greatest for the neutral amino acids compared to basic and acidic amino acids. It is unclear from these results whether one carrier protein transports all the different amino acids and has a different affinity for neutral, acidic and basic amino acids, or whether several carrier proteins are present which transport different groups of amino acids.

Experiments with membrane vesicles overcame several of the problems associated with experiments on whole tissues, cells and protoplasts. For instance, the problem of intracellular metabolism of amino acids is removed as the vesicles do not contain any cytoplasm, and any metabolic enzymes present are those associated with the membrane itself. Artificial electrical and chemical gradients can be created across the membrane to investigate the effect of each gradient on solute transport (Ramos and Kaback 1977a and b, Williams *et al* 1992). The technique of aqueous two-phase partitioning, which separates microsomal membranes based on their charge and hydrophobicity (Lundborg 1983), produces highly purified PM preparations which can be used to study membrane transport processes (Williams *et al* 1990a). The membrane vesicle system also has several disadvantages. It is very difficult to achieve a completely pure membrane vesicle population. The purification procedure may damage the membrane, and affect the permeability and orientation of the membrane vesicles. Finally, the transport protein may be inactivated during the isolation and purification of the membrane, or other important regulatory molecules may be lost. Therefore, the demonstration of specific transport activity in membrane vesicles is a strong indication of its presence in the intact cell, but these results should always be related to transport studies in intact systems (Sze 1985).

Studies of amino acid transport in PM vesicles isolated from *Ricinus*, initially focused on the cotyledons (Williams *et al* 1990a,b), since amino acid transport had already been partially characterised in this tissue (Robinson and Beevers 1981a,b). Studies using the isolated PM vesicle system found that glutamine transport was dependent on both an electrical and chemical proton gradient, which was created artificially across the vesicular membrane (Williams *et al* 1990b). The process was inhibited by the protonophore CCCP suggesting a proton-coupled symport. Further studies with isolated cotyledon vesicles observed saturation kinetics for proton-glutamine cotransport, consistent with carrier-mediated transport, with a K_m of 0.35mM (Williams *et al* 1992). A range of protein modifiers such as pCMBS, phenylglyoxal and NEM, had only slight inhibitory effects on glutamine transport. Glutamine transport was inhibited by a range of amino acids but studies with vesicles cannot decide whether glutamine

transport is the result of one or several carriers which differ in their amino acid specificity; molecular studies carried out subsequently suggested that the latter may be the case (see section 1.5.2).

An electrogenic uptake mechanism was proposed for glutamine transport in *Ricinus* cotyledons. However, the cellular localisation of this amino acid transport system is not known. It could be involved in phloem loading since amino acids are transferred to the phloem in this tissue. Another possibility is localisation in the epidermal cells for the initial uptake of amino acids following release from the endosperm. Experiments localising the expression of a sucrose carrier in *Ricinus* have shown high levels of expression in the lower epidermal cells (these lie adjacent to the endosperm in the germinating seedling) and also in the phloem tissue (Bick *et al* 1998). A similar localisation may occur for *Ricinus* amino acid permeases in the cotyledons, although this remains to be investigated.

Detailed studies of amino acid transport were also carried out in PM vesicles derived from *Ricinus* roots (Weston *et al* 1994, Weston *et al* 1995). Schobert and Komor (1990) had already demonstrated the presence of two distinct active transport systems in *Ricinus* roots, one for neutral amino acids and one for acidic amino acids. However, their work did not show whether these transporters were proton/amino acid symporters. Using similar methods to those described for cotyledon vesicles, (Weston *et al* 1994) but with a wider variety of radiolabelled amino acids, the uptake of acidic, neutral and basic amino acids could be compared (Weston *et al* 1994, Weston *et al* 1995). Competition studies provided evidence for at least two different neutral amino acid transporters (system I and II). Both transport all the neutral amino acids, but system I has a lower affinity for asparagine and system II has a lower affinity for isoleucine and valine (Weston *et al* 1995). Some amino acids, such as alanine, exhibited simple competitive inhibition of transport of both glutamine and isoleucine, with a similar K_i value for each. This suggests that alanine is transported by both transporters with an equivalent binding affinity. These carriers are analogous to those observed in sugar beet leaves, except that neutral system II described for sugar beet had a lower affinity for proline and threonine as well as for isoleucine and valine (Li and Bush 1990). In the *Ricinus* system, however, threonine exhibited a similar level of inhibition of glutamine and isoleucine, and proline was found to be a competitive inhibitor of both carriers (Weston *et al* 1995).

Evidence was provided in the root vesicle system that the basic amino acids may be transported via an additional separate carrier (Weston *et al* 1995). However, it was noted that the neutral amino acids generally inhibited the uptake of the basic amino acids (generally greater than 50%), with the exception of asparagine and proline. Since the data obtained for competition studies of glutamine and lysine did not fit to the equation for competitive or non-

competitive inhibition it is possible that the neutral amino acids may bind to the basic amino acid carriers but not be transported. This would prevent the transport of the basic amino acids and lead to the large percentage inhibitions observed (Weston *et al* 1995). Basic amino acids inhibited the transport of glutamine and isoleucine to lesser extents (less than 50% in each case), therefore it is possible that they are transported via the neutral carriers, but with a lower affinity than the neutral amino acids. Again it is also possible that the basic amino acids could bind to the neutral transporters without being transported, and thereby hinder the transport of the neutral amino acids. These observations could be confirmed if individual amino acid permeases could be isolated and characterised separately.

The transport mechanism of the basic amino acids, arginine and lysine, appears to be different from that of the neutral amino acids, as the electrical gradient is the only driving force for transport of arginine and lysine (Weston *et al* 1995). This suggests that the basic amino acids are transported via a voltage-driven uniporter. This contrasts with the situation in sugar beet leaf vesicles where the transport of basic amino acids appears to be proton-coupled (Li and Bush 1990). The transport mechanism of basic amino acids is controversial, with various studies reporting proton-cotransport mechanisms (Johannes and Felle 1985, Li and Bush 1990), whilst other studies suggested a uniport mechanism (Kinraide and Etherton 1980, Wyse and Komor 1984).

1.5.2 Molecular characterisation of amino acid transporters

To date, the majority of work on amino acid transporters at the molecular level has been carried out using *Arabidopsis thaliana* (for a review see Fischer *et al* 1998, Williams and Miller 2001). Amino acid transporters have been cloned and characterised from other species e.g. *Lycopersicon esculentum* (tomato), *Nicotiana sylvestris* (tobacco), *Vicia faba* (broad bean), *Nepenthes alata* (pitcher plant) and *Pisum sativum* (pea). These have been recently reviewed in Williams and Miller (2001) and will not be discussed in detail here. This report will focus on the *Arabidopsis* amino acid permeases, as this probably gives a good indication of the types of amino acid permeases found in other plants. In addition, the properties of the *Ricinus* amino acid permeases discovered to date will be discussed.

1.5.2.1 *Arabidopsis thaliana* amino acid transporters.

All plant amino acid transporters identified to date are part of either the AAAP superfamily (Amino Acid/ Auxin Permease family) (table 1.3) or the APC (amino acid, polyamine and

choline) superfamily (Fischer *et al* 1998, Ortiz-Lopez 2000, Williams and Miller 2001) (table 1.4). The plant transporters in the AAAP family form a sub-group known as the ATF (amino acid transporter family; Fischer *et al* 1998, Ortiz-Lopez 2000, Williams and Miller 2001). The AAAP family includes over two dozen proteins from plants, animals, yeast and fungi (http://www-biology.ucsd.edu/~msaier/transport). Individual permeases of the AAAP family transport auxin (indole-3-acetic acid), a single amino acid or multiple amino acids. Some of these permeases exhibit very broad specificity, transporting all twenty naturally occurring amino acids (http://www-biology.ucsd.edu/~msaier/transport). The APC superfamily includes members that function as solute:cation symporters and solute:solute antiporters and they occur in bacteria, archaea, yeast, fungi, unicellular eukaryotic protists, slime moulds, plants and animals (http://www-biology.ucsd.edu/~msaier/transport). Two sub-families of the APC superfamily have been identified in plants to date: the CATs (cationic amino acid transporters) and the GABA (4-aminobutyrate) permease-related family (Fischer *et al* 1998). The two members of the CAT family cloned to date are *AtCAT1* (previously *AtAAT1* - Frommer *et al* 1995) and *AtCAT2* (Fisher *et al* 1998, Rentsch *et al* 1998). These are in the same family as the mammalian CATs such as the murine leukaemia virus receptor, a system y^+ high-affinity basic amino acid transporter (Palacin *et al* 1998). AtCAT1 is a high affinity transporter of basic amino acids and is expressed in mature leaf veins, root, flower and stem (Fischer *et al* 1998). AtCAT2 is a putative amino acid transporter (Fisher *et al* 1998) but no information is yet available on its pattern of expression. There are six other related sequences in the *Arabidopsis* genome that have been designated AtCAT3-8 (At3g10600, At5g04770, At1g17120, At3g03720, At5g36940 and At1g05940 in the MIPS database; 'http://www.mips.biochem.mpg.de/'). The GABA - like permeases, which show some homology to amino acid transporters from yeast (Fischer *et al* 1998, Williams and Miller 2001) have yet to be characterised in any detail. There is only one member of this family identified in the *Arabidopsis* genome so far (Breitkreuz *et al* 1999).

The plant ATF is far better characterised than the APC superfamily. The ATF has been sub-divided into five gene families: AAPs (amino acid permease), ProTs (proline transporter), LHTs (lysine histidine transporter), AUXs (auxin transporter) and ANTs (Aromatic and neutral transporter) (Fischer *et al* 1998, Ortiz-Lopez 2000, Chen *et al* 2001, Williams and Miller 2001) (table 1.3).

Table 1.3 - The transport characteristics and spatial expression patterns of the currently identified members of the ATF superfamily from *Arabidopsis thaliana*.

Family	Gene	Transport	Expression	Reference number*	Reference
AAP	AtAAP1/ NAT2	Neutral and acidic amino acids	Flower and silique.	At1g58360	Frommer *et al* 1993, Hsu *et al* 1993
	AtAAP2	Neutral and acidic amino acids	Stem, silique, flower, root, source leaf.	AT5g09220	Kwart *et al* 1993
	AtAAP3	General amino acid permease	Root.	At1g77380	Frommer *et al* 1995
	AtAAP4	Neutral and acidic amino acids	Stem, source leaf, flower.	At5g63850	Frommer *et al* 1995
	AtAAP5	General amino acid permease	Source leaf, stem, flower, silique, root.	At1g44100	Frommer *et al* 1995
	AtAAP6	Neutral and acidic amino acids	Sink leaf, roots.	At5g49630	Rentsch *et al* 1996
	AtAAP7	Predicted amino acid transport		At5g23810	
	AtAAP8	Predicted amino acid transport		At1g10010	
	AtAAP9	Predicted amino acid transport		At5g41800	
	AtAAP10	Predicted amino acid transport		At1g08230	
ProT	AtProT1	Proline	Roots, stems, flowers.	At2g39890	Rentsch *et al* 1996
	AtProT2	Proline	Throughout, increased under water/salt stress.	At3g55740	Rentsch *et al* 1996
	AtProT3	Predicted amino acid transport		At2g36590	
LHT	AtLHT1	Lysine and histidine	Young leaves, flower, silique, pollen, seedling roots.	At5g40780	Chen and Bush 1997
	AtLHT2	Putative amino acid transport		At1g24400	
	AtLHT3	Putative amino acid transport		At1g61270	
	AtLHT4	Predicted amino acid transport		At1g25530	
	AtLHT5	Predicted amino acid transport		At3g01760	
	AtLHT6	Predicted amino acid transport		At1g47670	
	AtLHT7	Predicted amino acid transport		At4g35180	
	AtLHT8	Predicted amino acid transport		At1g67640	
	AtLHT9	Predicted amino acid transport		At1g71680	
	AtLHT10	Predicted amino acid transport		At1g48640	
AUX	AtAUX1	Putative auxin transporter	Root.	At2g38120	Marchant *et al* 1999
	AtAUXR2	Predicted auxin transport		At2g21050	
	AtAUXR3	Predicted auxin transport		At1g77690	
	AtLAX1	Predicted auxin transport		At5g01240	
ANT	AtANT1	Aromatic and neutral amino acids, histidine and arginine		U39783 (EMBL accession number)	Chen *et al* 2001
	AtANT2	Predicted amino acid transport		At5g65990	
	AtANT3	Predicted amino acid transport		AL035539 (EMBL accession number)	

*- In the MIPS database ('http://www.mips.biochem.mpg.de/').

Table 1.4 - The transport characteristics and spatial expression patterns of the currently identified members of the APC superfamlly from *Arabidopsis thaliana*.

Family	Gene	Transport	Expression	Reference number*	Reference
CAT	AtCAT1	Basic amino acids	Mature leaf veins, roots, flower, stem.	At4g21120	Fischer *et al* 1998
	AtCAT2	Putative amino acid transporter		At2g34960	Fischer *et al* 1998
	AtCAT3	Predicted amino acid transport		At3g10600	
	AtCAT4	Predicted amino acid transport		At5g04770	
	AtCAT5	Predicted amino acid transport		At1g17120	
	AtCAT6	Predicted amino acid transport		At3g03720	
	AtCAT7	Predicted amino acid transport		At5g36940	
	AtCAT8	Predicted amino acid transport		At1g05940	
GABA	AtGABA	4-aminobutyrate (GABA)		AF019637 (EMBL accession number)	Breitkreuz *et al* 1999

* - In the MIPS database ('http://www.mips.biochem.mpg.de/').

1.5.2.1.1 AtAAPs

AtAAP1/AtNAT2 was the first amino acid transporter to be cloned from higher plants (Frommer *et al* 1993, Hsu *et al* 1993). Subsequently five other genes have been identified: *AtAAP2 – 6* (for a review see Williams and Miller 2001) and four other related sequences (AtAAP7-10) have been identified in the *Arabidopsis* genome (At5g23810, At1g10010, At5g41800 and At1g08230 in the MIPS database; http://www.mips.biochem.mpg.de/). The AAP family has many common features but all members differ slightly in substrate specificity and patterns of expression (Fischer *et al* 1998, Chen *et al* 2001, Williams and Miller 2001). All have a similar size (51-56kDa) and from hydrophobicity plots are thought to have 9-12 putative membrane spanning regions (Frommer *et al* 1993, Kwart *et al* 1993, Frommer *et al* 1995, Rentsch and Frommer 1996, Rentsch *et al* 1998). Experimental evidence using epitope tagging has indicated that the C- and N-terminal regions are on opposite sides of the membrane for AtAAP1, suggesting an odd number of putative membrane spanning regions. Partial proteolysis was used to show that AtAAP1 has six regions accessible to lysis (external extra-membranous regions). These two experimental findings suggest 11 membrane-spanning domains (Chang and Bush 1997).

All the AtAAP transporters characterised to date (AtAAP1-6) were isolated through complementation of yeast transport mutants (Frommer *et al* 1993, Hsu *et al* 1993, Kwart *et al* 1993, Fischer *et al* 1995, Rentsch *et al* 1996). This technique has become a very powerful tool in plant membrane biology for identifying plant transporter genes (Frommer and Ninnemann 1995). For the isolation of amino acid permeases, a yeast mutant with a particular amino acid uptake deficiency is used which is unable to grow with this particular amino acid as a nitrogen source when supplied at low levels. This yeast is transformed with a cDNA library (inserted into an *E.coli* / yeast shuttle vector) from the plant under investigation. The transformed yeast are then grown on the selective media and those complemented with a plant amino acid transporter that can take up the particular amino acid will grow. *AtAAP1* and *AtAAP2* were found to complement the *Saccharomyces cerevisiae* GAP (General Amino acid Permease) (a, *gap, ura3-52*) mutant (Grenson *et al* 1970, Frommer *et al* 1993, Kwart *et al* 1993). The GAP mutant is defective in citrulline uptake and so cannot grow on media supplemented with citrulline as a nitrogen source. GAP expressing either *AtAAP1* or *2* were able to take up citrulline from the medium and so utilise this amino acid as a nitrogen source. This allowed only GAP expressing these genes to grow on this media. AtAAP3-5 were isolated using the JT-16 (*Mat-a, hip1-614, his4-401, can1, ino1, ura3-52*) mutant *Saccharomyces cerevisiae*, which is deficient in histidine uptake (Tanaka and Fink 1985, Frommer *et al* 1995). The JT-16 mutant is able to grow on media supplemented with a high concentration of histidine (3.86 mM) as a

source of nitrogen. However, when the histidine concentration is reduced (0.13 mM) the yeast mutant is no longer able to grow. Only when expressing AtAAP3, 4 or 5 is the yeast able to take up enough histidine to allow it to grow at low histidine concentrations. AtAAP6 was isolated by complementation of the SHR3 yeast mutant, which lacks the ability to correctly target its own amino acid transporters to the PM (Rentsch *et al* 1996). This yeast was transformed with an *Arabidopsis* library and placed on a selective medium. This method isolated an oligopeptide transporter (NTR family), the two cloned *AtProT* genes and five *AtAAP* genes, one of which was *AtAAP6*. Expression of *AtAAP6* restored yeast growth.

The substrate specificity of the AtAAPs was determined through competition of the uptake of radiolabelled amino acids by other amino acids. If an amino acid is recognised by the permease it inhibits the uptake of the radiolabelled amino acid (Frommer *et al* 1993, Kwart *et al* 1993, Fischer *et al* 1995). However this method does not clearly distinguish between competition for uptake and that for binding. A more detailed study of the substrate specificity of AtAAP1 and AtAAP5 has been achieved by expression in *Xenopus laevis* oocytes (Boorer *et al* 1996, 1997). These experiments have revealed further information about the nature of substrate binding and transport mechanisms. Both appeared to function as proton-coupled amino acid symporters. A model for AtAAP1 transport has been proposed with a stoichiometry of 2 protons : 2 amino acid molecules. Binding of amino acid and proton was random and positively co-operative (Boorer *et al* 1996, 1997) (see chapter 5).

Structure / function relationships have been investigated for AtAAP1 using site-directed mutagenesis. Preliminary evidence discussed in reviews indicates that his47 (Ortiz-Lopez *et al* 2000) and his337 (Bush *et al* 1996) are critical for function. Also implicated were asp252 and ala254 (Ortiz-Lopez *et al* 2000) which when substituted, differentially altered apparent K_ms for alanine and histidine. This is discussed further in section 1.6.

1.5.2.1.2 AtProTs

AtProt1 and 2 were isolated by complementation of the SHR3 yeast mutant (PM targeting deficient strain) (Rentsch *et al* 1996). A transporter designated AtProt3 has been identified in the *Arabidopsis* genome (At2g36590 in the MIPS database; http://www.mips.biochem.mpg.de/), but this has not yet been characterised (table 1.3). *AtProT1* and *2* encode proteins of 48kDa with 10 putative membrane-spanning domains that are distantly related to the AtAAPs (Rentsch *et al* 1996). AtProT1 and 2 are nearly identical in respect to transport characteristics, showing high specificity for proline transport. Unlike the AAPs no stereospecificity is displayed (Rentsch *et al* 1996). The expression pattern of the *AtProT1* and *2* is quite different in tissue specificity

(table 1.3). *AtProT1* expression is down regulated following fertilisation and its major tissue of expression is the floral stalk phloem that enters the carpels, suggesting a role in supplying the ovules with proline (Rentsch *et al* 1996). *AtProT2* expression is strongly induced in leaves under water or salt stress, implying a role in nitrogen redistribution during this stress. AtAAP4 and 6 were found to be repressed under similar conditions of water stress, corroborating the findings that under abiotic stress proline export is increased and other amino acid export is reduced (Delauney and Verma 1993, Rentsch *et al* 1996).

1.5.2.1.3 AtLHTs

AtLHT1 was first identified by a computer database search of the *Arabidopsis thaliana* expressed sequence tag (EST) cDNA collection, for any sequence demonstrating similarity to the AAP1 sequence (Chen and Bush 1997). The transporter was then expressed in the histidine-transport deficient JT-16 yeast mutant and rescued growth on low histidine-containing media. AtLHT1 is a 50.5kDa membrane protein with 9-10 putative membrane spanning domains (Chen and Bush 1997). Uptake of various radiolabelled amino acids has revealed AtLHT1 to be specific for lysine and histidine transport. The expression of AtLHT1 on the surface of seedling roots suggests a role in uptake of histidine and lysine directly from the soil (Chen and Bush 1997). There are nine related sequences in the *Arabidopsis* genome that have been designated AtLHT2-9 (At1g24400, At1g61270, At1g25530, At3g01760, At1g47670, At4g35180, At1g67640, At1g71680, At1g48640 in the MIPS database; http://www.mips.biochem.mpg.de/) based purely on their sequence similarity to AtLHT1. These transporters have yet to be studied in any detail.

1.5.2.1.4 AtAUXs

AtAUX1 was first identified in an agravitropic *Arabidopsis* mutant that displayed an altered growth response to IAA and 2,4-dichlorophenoxyacetic acid (Maher and Martindale 1980). *Arabidopsis* plants were mutagenised using EMS and then selected on medium containing 2,4-dichlorophenoxyacetic acid. WT plants displayed very little root growth on this medium, whereas the *aux1* mutant had a well developed root system. The same phenotypes were observed on medium containing IAA (Maher and Martindale 1980). Using an *Agrobacterium*-mediated transfer DNA-tagging procedure with the *aux1* mutant plant, the *AUX1* gene was isolated and characterised (Bennett *et al* 1996). *AtAUX1* encodes a highly hydrophobic 485 amino acid membrane protein with a predicted mass of 54.1kDa. AtAUX1 is

predicted to have between 10 and 12 membrane-spanning domains and its primary sequence is distantly related to the AAP transporter family (Bennett *et al* 1996, Fisher *et al* 1998, Marchant *et al* 1999). Also the similarity of auxin to the amino acid tryptophan (a major substrate of the AAPs) suggests that AtAUX1 may be related to the AAP family (Bennett *et al* 1996, Fisher *et al* 1998, Marchant *et al* 1999). From the *Arabidopsis* genome sequencing project it has been shown that *AtAUX1* is closely related to At*LAX1* (Like *AUX*) and *AtAUXR2* and *3* (*AUX* Related) (also known as *LAX2* and *3*) (At5g01240, At2g21050 and At1g77690 respectively in the MIPS database; http://www.mips.biochem.mpg.de/). None of these transporters have been isolated or characterised to date, so it is not known if they will have similar transport characteristics to one another. Further evidence that AtAUX1 codes for an auxin transporter is the reduced response of the *aux1* mutant to IAA and 2,4-dichlorophenoxyacetic acid, but its continued WT response to 1-naphthalene-acetic acid, a membrane permeable auxin (Marchant *et al* 1999).

In the plant, *AtAUX1* is expressed predominantly in the primary root apex and root epidermal cells (Bennett *et al* 1996) and has been shown to play a role in gravitropism. The *aux1* mutant plant has an agravitropic root phenotype. A closer look at the root apical expression of AtAUX1 has revealed that it is expressed in tissue associated with transduction and response rather than in tissue associated with the initial perception of the gravitropic stimulus (Marchant *et al* 1999). It is thought to be unlikely that AtAUX1 plays a role in amino acid uptake into the roots as the *aux1* mutant plant shows identical uptake rates for the indole amino acid, tryptophan, as the WT plants (Marchant *et al* 1999).

1.5.2.1.5 AtANTs

AtANT1 was identified by screening a library of *Arabidopsis* EST cDNAs for sequences similar to identified amino acid permeases (Chen *et al* 2001). Initially the partial sequence of an EST suggested consistency with known amino acid transporters, but this EST failed to complement JT-16 on its standard selection medium supplemented with 0.13mM histidine and 6mM arginine. It was hypothesised that this protein may transport arginine preferentially to histidine, or to toxic levels to the yeast. The selectable medium was therefore altered to only contain 0.6mM arginine. Consequently the EST cDNA was able to complement the growth of JT-16. This arginine uptake analysis was verified in uptake analysis experiments (Chen *et al* 2001). AtANT1 transports aromatic and neutral amino acids and also the basic amino acids histidine and arginine. This is the first reported example of a plant transporter with significant aromatic amino acid transport rates. AtANT1 is also believed to facilitate the uptake of 2,4-

dichlorophenoxyacetic acid and indol-3-acetic acid (Chen *et al* 2001). Further evidence will be required however, to show whether the ANT family has a physiologically significant role in auxin transport. AtANT1 is a 50kDa protein with 11 predicted trans-membrane domains. Four other AtANT genes have been identified through Southern analysis and a search of the *Arabidopsis* sequence database (Chen *et al* 2001). To date the sequences for AtANT2 and 3 have been designated in the *Arabidopsis* genome sequence as AtANT2 BAC locus - K2A18_5 and AtANT3 accession number - AL035539. These permeases have yet to be investigated further.

1.5.2.1.6 Other sequences in the *Arabidopsis* genome

The sequencing of the *Arabidopsis* genome has revealed many putative amino acid transporters related at the sequence level to existing cloned transporters. Many of these have been mentioned in previous sections (1.5.2.1.1), alongside the transporters they are similar too. Only functional analysis will eventually reveal if these transporters do in fact belong in the groups to which they have been allocted.

A sequence exists in the *Arabidopsis* genome (At2g01170 in the MIPS database; http://www.mips.biochem.mpg.de/) which is suggested to be a member of the HAAAP family (http://www-biology.ucsd.edu/~msaier/transport). The HAAAP family includes three well characterised aromatic amino acid: H^+ symport permeases as well as two hydroxy amino acid permeases, a serene permease and a threonine permease all from *E.coli.* These proteins exhibit topological features common to the AAAP family and some sequence similarity with a number of the members indicating that they may be distantly related. Further characterisation of this *Arabidopsis* gene is required in order to determine its transport properties and whether it is expressed in the plant.

1.5.2.2 *Ricinus communis* amino acid transporters

Following the broad characterisation of amino acid transport in *Ricinus* PM vesicles (Weston *et al* 1995), work was carried out to clone the transporter cDNAs in order to investigate the biochemical and molecular properties of the individual amino acid permeases in more detail. From the conserved regions of the published sequences of the *Arabidopsis AAPs* then available *(AtAAP1* and *AtAAP2)* degenerate primers were designed for use in RT-PCR. Two partial-length cDNA clones were obtained. *Ricinus communis* amino acid permease 1 and 2 (*RcAAP1* and *RcAAP2*), which both show high homology to *AtAAP1* and *AtAAP2* of *Arabidopsis* (Bick *et al* 1998). Northern analysis indicated that both *RcAAP1* and *RcAAP2* were

expressed most highly in cotyledons and roots, with relatively minimal levels in hypocotyl, endosperm and leaves (Williams *et al* 1996). Subsequently, a full-length cDNA of *RcAAP1* was isolated using yeast complementation (Marvier *et al* 1998). This involved complementation of the *Saccharomyces cerevisiae* mutant lacking the general amino acid permease (GAP mutant). The GAP mutant is defective in citrulline uptake and therefore cannot grow with this amino acid as a nitrogen source. Expression of a *Ricinus* cDNA library in this mutant resulted in the isolation of a cDNA that could restore growth on citrulline media. This was sequenced and was found to be a full-length *RcAAP1* (Marvier *et al* 1998). RcAAP1 has an open reading frame of 486 amino acids and shares 62% homology with the partial length *RcAAP2* clone (Williams *et al* 1996). In a further study, another amino acid permease, *RcAAP3* was isolated from *Ricinus communis* seedlings (Neelam *et al* 1999). Using sequence derived from the partial-length *RcAAP1* clone, a full-length cDNA was isolated (Neelam *et al* 1999) using a PCR-based screening method (Israel 1993). RcAAP1 and RcAAP3 show high homology to each other (86%) (Neelam *et al* 1999) and also to other members of the AAP family (Table 1.5). Radiolabelled amino acid uptake experiments have been conducted for both RcAAP1 and RcAAP3 following expression in yeast. Although RcAAP1 could restore growth of the GAP mutant when grown on citrulline, no appreciable uptake of radiolabelled citrulline could be detected. Therefore the *Saccharomyces cerevisiae* mutant, JT-16, which is deficient in the high-affinity histidine uptake system was used. *RcAAP1* was able to restore growth of this yeast mutant at low histidine concentrations. Radiolabelled histidine uptake experiments showed that RcAAP1 could take up histidine in a linear manner for up to one hour. Saturatable kinetics were observed indicating carrier-mediated transport. Uptake was inhibited by the protonophore CCCP and was maximum at acidic pH suggesting, although not proving, that RcAAP1 functions as a proton/amino acid symport. The transport characteristics were also studied for RcAAP3 following expression in the GAP mutant, using radiolabelled citrulline. This permease also showed saturation kinetics with evidence suggesting a proton/amino acid symport system. However, RcAAP1 and RcAAP3 appeared to differ markedly in their amino acid specificity. RcAAP3 transported a wide range of amino acids (neutral, acidic and basic) whereas RcAAP1 seemed to show a preference for basic amino acids, which is similar to AtAAP3 and AtAAP1 (Fischer *et al* 1995). The competition analysis is shown in figure 1.6.

The physiological roles of RcAAP1 and 3 in *Ricinus* have still not been ascertained. Studies have shown that cotyledons have a carrier responsible for uptake of amino acids from the endosperm (Williams *et al* 1996) and that *RcAAP1* and *3* are both expressed in cotyledons (Bick *et al* 1998, Neelam *et al* 1999). These permeases could serve the uptake function as

Table 1.5 - The % identities for the AAPs from *Ricinus communis* and *Arabidopsis thaliana*. Compiled using the ALIGN program from Genestream network server, IGH, Montpellier, France (http://vega.igh.cnrs.fr/bin/align-guess.cgi).

	RcAAP1	*RcAAP2	RcAAP3	AtAAP1	AtAAP2	AtAAP3	AtAAP4	AtAAP5	AtAAP6	AtAAP7	AtAAP8	AtAAP9	AtAAP10
RcAAP1	100	37	82	58	74	80	72	69	59	48	57	23	26
*RcAAP2		100	36	44	36	38	38	35	48	30	42	19	18
RcAAP3			100	55	70	75	71	66	56	47	55	23	26
AtAAP1				100	55	56	55	53	71	46	75	23	26
AtAAP2					100	71	84	64	55	45	53	22	27
AtAAP3						100	72	71	58	48	57	23	25
AtAAP4							100	65	56	46	54	24	27
AtAAP5								100	55	45	54	24	25
AtAAP6									100	46	66	24	25
AtAAP7										100	50	24	25
AtAAP8											100	24	27
AtAAP9												100	44
AtAAP10													100

*RcAAP2 is only a partial-length sequence.

proposed by Schobert and Komor (1989,1990) at the PM of parenchyma and phloem cells. The expression of *RcAAP1* and *3* in roots may suggest a role in amino acid uptake from the soil (Weston *et al* 1994, Marvier *et al* 1998), in retrieval to the phloem or in recycling of amino acid between xylem and phloem (Weston *et al* 1994, Weston *et al* 1995). However, *RcAAP1* is mainly expressed in the cells adjacent to the xylem pole (Bick *et al* 1998). It is possible that RcAAP1 may be present here to actively accumulate amino acids in these cells for subsequent movement to the xylem (Bick *et al* 1998). However, xylem loading may not be a likely role for RcAAP1 as the xylem sap is not highly concentrated in basic amino acids (Schobert and Komor 1990). It may instead be possible that RcAAP1 is loading these cells with amino acids in order to supply the high amino acid requirement necessary for lateral root development (Bick *et al* 1998).

An important consideration in the nitrogen nutrition of the plant, which is perhaps worthy of investigation, is the level of efflux of amino acids from the roots to the soil. Plant roots were initially considered as amino acid exuding systems (Frenzel 1960), and this has raised the question as to whether plants mainly donate amino acids to or absorb them from the soil (Schobert *et al* 1988). It was demonstrated that intact *Ricinus* roots can compete effectively for amino acids with soil-borne micro-organisms (Schobert *et al* 1988), and evidence exists for the presence of a number of high affinity transporters at the PM of *Ricinus* root cells (Weston *et al* 1995). It will be important to determine however, whether any transporters exist which operate in the efflux of amino acids into the soil.

Members of the RcAAP family show many similarities to particular members of the AtAAP family e.g. high homology at the DNA level, similarities in substrate specificity and expression patterns and also similar kinetics. The phylogenetic relationship between a range of amino acid permeases based on amino acid sequence is shown in figures 1.7 and 1.8. Figure 1.7 shows all the known amino acid transport to date from *Ricinus communis* (castor bean), *Arabidopsis thaliana* (thale cress), *Vicia faba* (broad bean), *Pisum sativum* (pea), *Solanum tuberosum* (potato), *Nepentes alata* (pitcher plant), *Nicotiana sylvestris* (tobacco), *Lycopersicon esculentum* (tomato) and *Oryza sativa* (rice). In this figure it should be noted that AtAAP7-10, AtProT3, AtLHT2-10 and AtAUXR2-3 have not been cloned but have been given their designation following the *Arabidopsis* genome sequencing project, purely due to sequence similarities. The grouping of the AAAP superfamily into discreet sub-families can be seen in figures 1.7 and 1.8 (the later figure just shows the *Ricinus* and *Arabidopsis* members). Three sequences appear not to fit into their designated family domains on the tree in figure 1.7. AtAAP9 and 10 appear to be more closely related to the ProTs than the other AAPs (this is also seen in figure 1.8). NsAAP1 appears to be more closely related to AtLHT transporters. AtAAP9

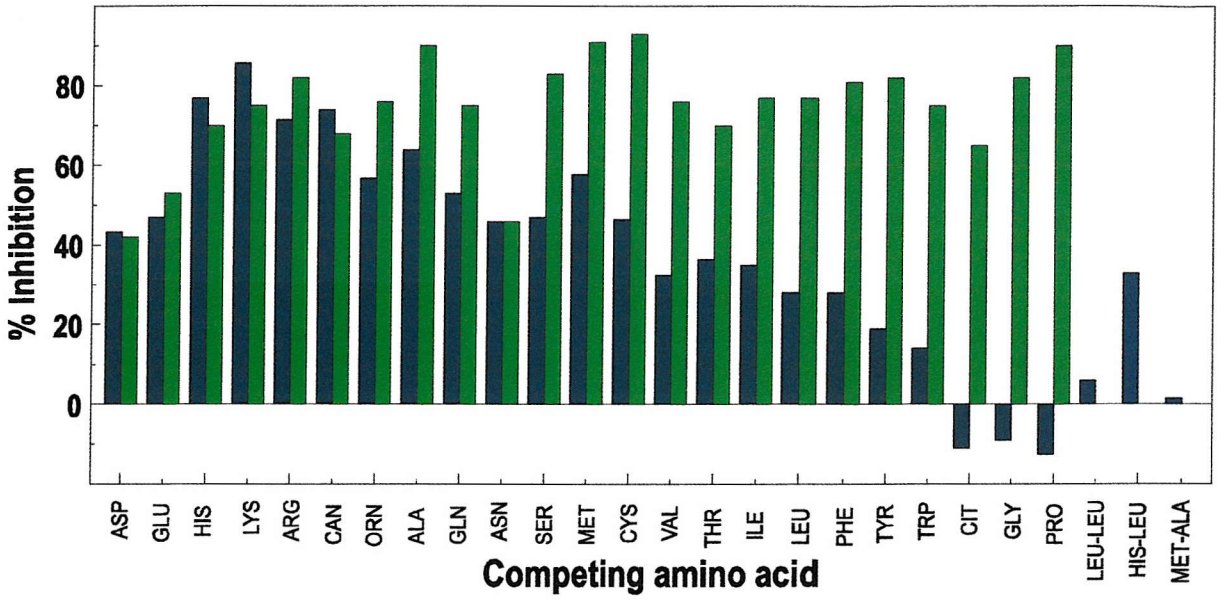

Figure 1.6 – Competition analysis of RcAAP1 (blue) and RcAAP3 (green) expressed in yeast. Radiolabelled uptake of histidine (RcAAP1) or citrulline (RcAAP3) was measured in the presence of a range of non-labelled amino acids. Results show the % inhibition of the radiolabelled amino acid uptake. These results for RcAAP1 are the mean of 3 replicates. These results for RcAAP3 are the mean of 2 replicates (Adapted from Marvier *et al* 1998 and Neelam *et al* 1999).

and 10, and many of the AtLHT transporters have not been characterised beyond sequence similarity. It will be interesting to see how these transporters operate when properly characterised. Looking at the members of the AAP family in more detail, it can be seen from figures 1.7 and 1.8 that the AAPs do not form a single cluster but rather show evidence of three sub-clusters. For example in figure 1.9, AtAAP1, 2, 3 and 4 and RcAAP1 and 3 form one sub-cluster, RcAAP2 and AtAAP1, 6 and 8 a second and AtAAP7 a third. This may suggest that several independent genes existed early in higher plant development, which subsequently evolved into the genes contained in these sub-clusters. If there is any functional significance to the sub-clusters, it will not become apparent until further members have been characterised.

1.5.3 Membrane localisation of amino acid permeases

We know very little about the membrane localisation of any of the cloned transporters to date. One particularly interesting area yet to be investigated is targeting to the vacuolar. Studies indicate that the concentration of vacuole amino acids is lower than that in the cytosol (Riens *et al* 1991, Winter *et al* 1992). This suggests that entry into the vacuole may occur passively while retrieval from the vacuole would require active transport, possibly via a H^+/amino acid symport (Glass and Siddiqi 1995). Martinoia *et al* (1991) proposed that at least three amino acid transport systems mediate transfer across the vacuolar membrane. Two systems (a basic amino acid porter and a broad specificity importer) which appear to be regulated but not energised by ATP and a third system transporting aromatic amino acids that is dependent on the PMF generated by the tonoplast PPase and ATPase.

It is assumed that because cloned transporters can complement nutrient-uptake deficient yeast mutants, they are targeted to the PM. However, immunogold labelling and localisation of GFP fusions are required to prove their sub-cellular location.

Evidence for transport of the sucrose transporter SUT1 mRNA and possibly the protein through the plasmodesmata connecting companion cells and sieve elements of the phloem has been provided (Kuhn *et al* 1997). It will be interesting to determine whether such a phenomenon is observed for amino acid transporters, as amino acids, like sucrose, are major components of the phloem sap.

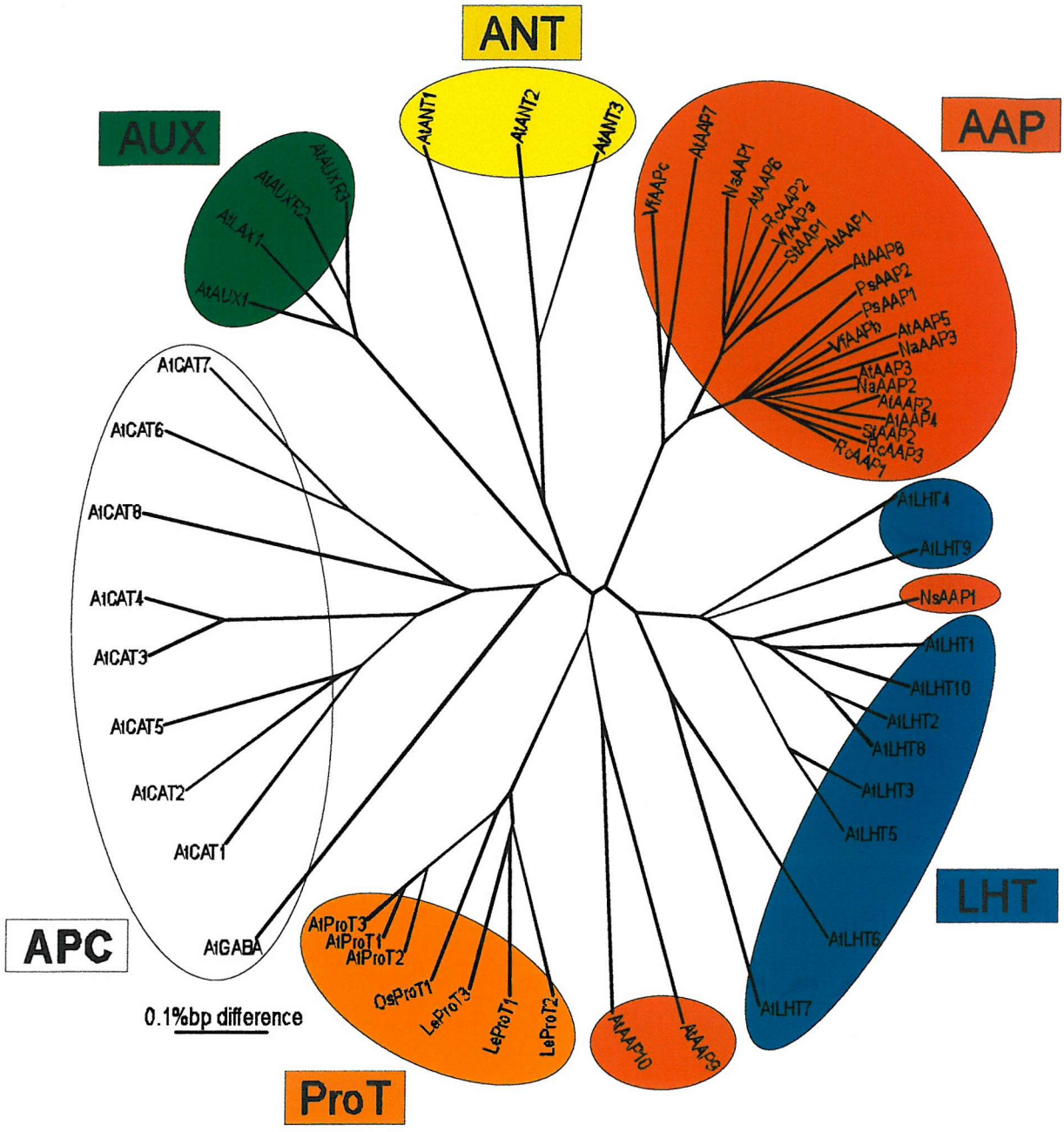

Figure 1.7 - Phylogenetic analysis of all the known plant amino acid transporters to date. AtAAP7-9, AtLHT2-10, AtAUXR2-3 and AtProT3 are products of the *Arabidopsis* genome sequencing project and have been named from sequence similarity alone The colour code shows the APC family in white and the members of the AAAP family in colour. Phylogenetic tree constructed using TreeView (http://taxonomy.zoology.gla.ac.uk/rod/treeview.html) (Page 1996).

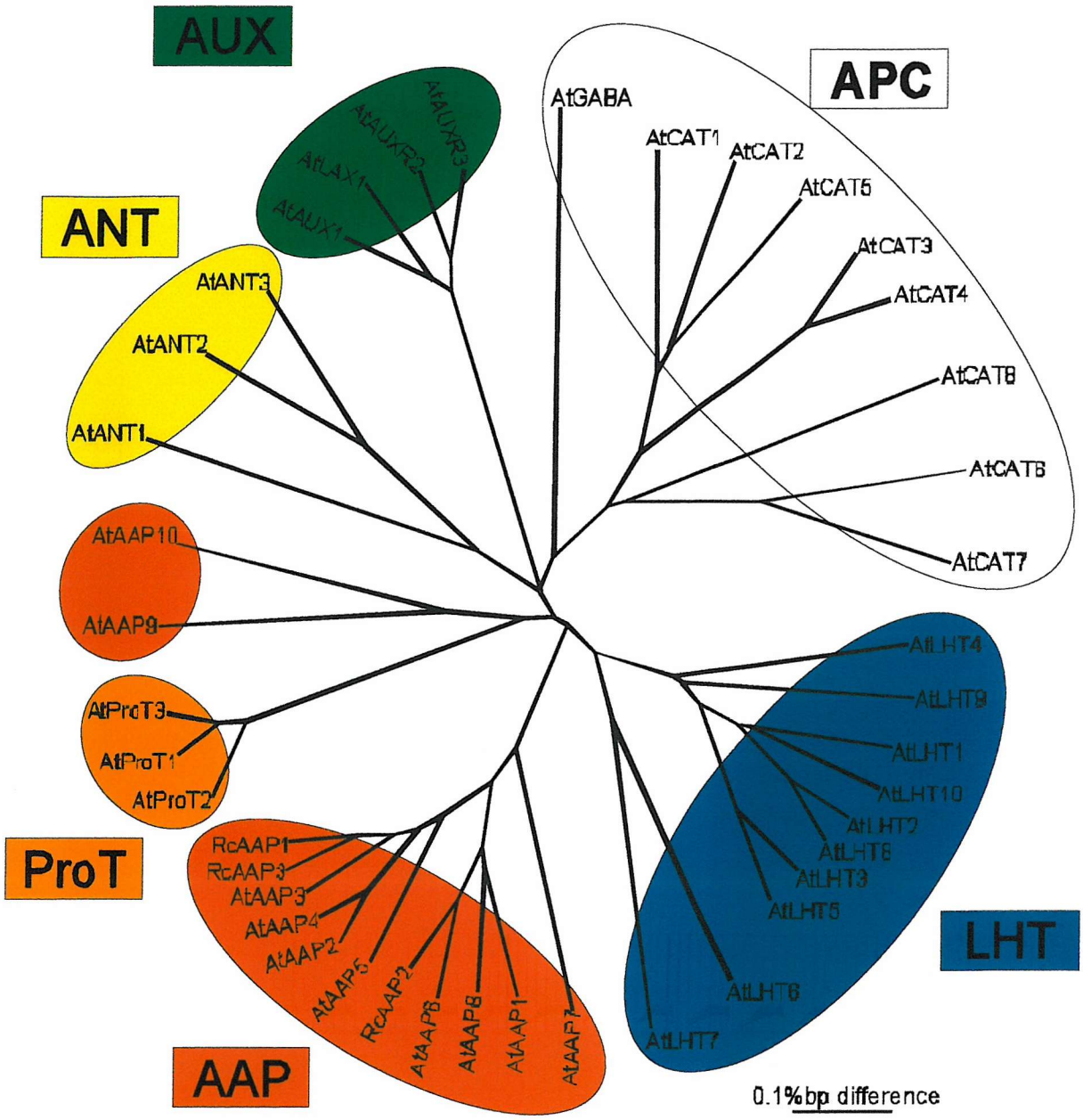

Figure 1.8 – Unrooted phylogenetic analysis showing all the known amino acid transporters to date from *Arabidopsis thaliana* and *Ricinus communis*. AtAAP7-9, AtLHT2-10, AtAUXR2-3 and AtProT3 are products of the *Arabidopsis* genome sequencing project and have been named from sequence similarity alone. The colour code shows the APC family in white and the members of the AAAP family in colour. Phylogenetic tree constructed using TreeView (http://taxonomy.zoology.gla.ac.uk/rod/treeview.html) (Page 1996).

1.5.4 Studies of in vivo function of amino acid permeases using mutants

To provide more information about the role of amino acid transporters, mutant plants have been studied. Mutants have been isolated mainly following exposure to toxic concentrations of certain amino acids or to toxic analogues. Two aminoethylcysteine-resistant mutants were isolated in barley, which were impaired in basic amino acid uptake but not in neutral and acidic amino acid transport (Bright *et al* 1983). The effect was observed in roots and not leaves and only the high affinity system was affected suggesting that the mutation is in a root-specific amino acid permease.

Val^r-2 mutants of *Nicotiana tabacum* (tobacco) were selected from UV-irradiated haploid tobacco mesophyll protoplasts following exposed to toxic valine concentrations (Bourgin 1978). Evidence was presented suggesting that at least three physically distinct transport systems for valine were present in leaves of WT plants and that the mutant was defective in the high affinity system (Pilon and Borstlap 1987, Borstlap and Schuurmans 1988). Several other neutral and acidic amino acids were taken up more slowly by the mutant, whereas uptake rates of basic amino acids were only slightly lower than in WT tobacco (Borstlap *et al* 1985). Valine-resistant mutants were also obtained from *Nicotiana plumbaginifolia* (tex-mex tobacco) by a similar selection procedure (Marion-Poll *et al* 1987). They were resistant to high concentrations of valine and threonine but only slightly affected in lysine uptake (Marion-Poll *et al* 1987). These results suggest that neutral and acidic amino acids share the same transporter in leaves whereas basic amino acids (lysine and histidine) are taken up by another system (Borstlap *et al* 1985).

More recently, several amino acid transport mutants have been isolated from ethyl methanesulfonate mutagenised *Arabidopsis*. The *raz1* mutant was selected on the basis of its resistance to the toxic proline analogue, azetidine-2-carboxylic acid (2AZ) (Verbruggen *et al* 1996). The mutant showed a reduced uptake in 2AZ. Proline uptake in the roots of WT seedlings could be dissected into high and low-affinity components with the *raz1* mutation only affecting the high affinity system (Verbruggen *et al* 1996). High-affinity uptake was considerably inhibited but not eliminated and it was suggested that the residual uptake in the mutant represents the activity of another transporter (Verbruggen *et al* 1996). It would be useful to determine which other amino acids are affected in their uptake by this mutation in order to help clarify which amino acid permease is involved. One of the ProTs has been implicated but several properties of these transporters do not fit the proposed model. The Michaelis-Menten constant is much higher for proline uptake by the ProTs (360μM) than the system impaired in the mutant (60μM) and also 2AZ does not appear to compete with proline transport by ProT1

and 2. Under normal growth and several stress conditions *raz1* was indistinguishable from the WT (Verbruggen *et al* 1996).

raec1 and *rlt11 Arabidopsis* mutants were selected as resistant to concentrations of S-2-aminoethyl-L-cysteine (AEC) and L-lysine plus L-threonine respectively, that inhibit the growth of the WT (Heremans and Jacobs 1994, Heremans *et al* 1997). Both mutants have the same phenotype and mapped to chromosome 1 but it is not yet known whether they are allelic. The resistance was attributed to a reduced influx of basic amino acids (Heremans and Jacobs 1994). Two saturable components of lysine uptake were observed in roots of WT plants, one of low affinity (K_m 159μM) and the other of high affinity (K_m 2.2μM). Only the low affinity component was impaired in the mutants and competition studies suggested that this system probably represents the activity of a transporter for basic amino acids, although an extensive analysis was not carried out for other amino acids (Heremans *et al* 1997). Since AtLHT1 does not transport arginine, is an unlikely candidate for the low affinity system.

The high-affinity system showed biphasic inhibition by valine, indicating that two different transporters may be responsible for this component, both having similar affinities for lysine but differing in their affinity for valine (Heremans *et al* 1997). The authors speculated as to whether the transport activities revealed in the kinetic analysis could be attributed to any of the amino acid permeases identified to date. Although the possibility was raised that AtAAP3 and AtAAP5 may correspond to the high affinity systems, the discrepancies in their K_m values and those determined for *Arabidopsis* roots make this unlikely. AtCAT1, a basic amino acid transporter that also has affinity for a spectrum of other amino acids (including valine), may also be a possible candidate for one of the high affinity systems, although again the K_ms do not equate precisely.

1.5.5 *Signalling and sensing*

Very little is known about the regulation of plant amino acid transporters in response to changes in amino acid concentrations. Glutamine levels have been shown to have an effect on the expression of the *Arabidopsis* ammonium transporter AtAMT1 (Coruzzi and Bush 2001). In the roots of *Arabidopsis*, at high concentrations of glutamine, AtAMT1 is down-regulated (Rawat *et al* 1999). The high glutamine concentration is presumably indicating high nitrogen levels to the plant. Glutamate receptor genes have also been reported in *Arabidopsis* (Lam *et al* 1998). Although these findings certainly suggest possibilities for sensing of amino acids and subsequent signalling, a pathway linking nutrient signal to a morphological response has yet to be uncovered. There is recent evidence that such systems exist in *Saccharomyces cerevisiae*.

Studies have shown that the yeast permease-like sensor Ssy1 controls the expression of a range of other amino acid and peptide transporter genes in response to various amino acids (Didion *et al* 1998, Iraqui *et al* 1999). A transcriptional response was induced from the addition of amino acids extracellularly rather than intracellularly (Iraqui *et al* 1999). It was therefore proposed that Ssy1 detects external amino acids and activates a transduction pathway leading to transcriptional activation of several permease genes. Ssy1 displays structural features reminiscent of those displayed by the Snf3 and Rgt2 glucose sensors from *Saccharomyces cerevisiae*. All three have extended cytoplasmic C-terminal domains, which in Snf3 and Rgt2 are essential in glucose sensing (Ozcan *et al* 1996, 1998). It has been proposed that the large N-terminal domain of Ssy1 might play an important role in generating the amino acid signal (Iraqui *et al* 1999). It remains to be determined whether a similar sensing system operates in plants.

1.6 Mutagenesis and structure/function analysis

Structure/function studies of amino acid permeases are necessary in order to understand the areas of functional significance in these physiologically important proteins. The process of using random mutagenesis to produce a library of mutants, followed by a carefully designed screening process, can be used to identify residues that have a functional role. This technique is useful as it does not require any prior detailed knowledge of functionally significant residues and so avoids bias. A recent major advance in random mutagenesis has been the use of DNA shuffling, which is also known as "sexual" or recombinant PCR (Smith 1994, Stemmer 1994). This powerful technique generates diversity by recombination and provides a form of directed evolution (Crameri *et al* 1998). In this process, random fragmentation of a pool of related genes is carried out followed by re-assembly of the fragments in a self-priming PCR (Stemmer 1994, Crameri *et al* 1998) This process was used successfully to increase the level of fluorescence of green fluorescent protein (GFP) (Crameri *et al* 1996). Three rounds of DNA shuffling were used to randomly mutate the GFP cDNA. The shuffled library was then expressed in *E.coli*. As a selection process, the brightest colonies were picked off. The final improvement was a 45-fold greater signal compared to the original WT gene product. DNA shuffling has also been used to improve an arsenate resistance operon (Crameri *et al* 1997). Multiple rounds of DNA shuffling followed by selection in *E.coli* over a range of arsenate concentrations yielded a 40-fold increase in resistance. In the case of amino acid permeases this technique could be employed using a range of permeases or using a pool of mutated

variations of a single gene. The technique itself incorporates mutation into individual start products and so would work from a single gene through multiple rounds. Alternatively, more classical forms of mutation could be employed to produce a pool of mutants. These methods (described below) can also be used as modes of mutant production in their own right.

Error-prone PCR is a PCR-based procedure for producing random mutations. In this method either Mn^{2+} is included in the reaction or the ratio of one dNTP is altered, both of which have the effect of increasing the rate at which errors occur. The non-proof reading enzyme, *Taq* polymerase, is used and so these errors are left uncorrected. The dihydrofolate reductase gene from *E.coli* was successfully mutated using a combination of base bias and the inclusion of Mn^{2+} (Vartanian *et al* 1996). It was found that a dNTP bias could successfully introduce mis-matches during PCR and not drastically reduce yield. It was also found that a mixture of dNTP bias and the presence of Mn^{2+} caused such a high level of mutation that products were often no longer viable. Mutagenesis with the inclusion of Mn^{2+} alone has been shown to increase the rate of base pair mis-insertion and deplete the proof-reading ability of polymerase enzymes (Goodman *et al* 1993). This method successfully produces point mutations in DNA strands but the concentration of Mn^{2+} is a crucial factor; too low and mutagenesis is not significant, too high and the yield is reduced below useful levels (Fromant *et al* 1995).

A third method of random mutagenesis, one of chemical mutagenesis, has been used successfully by Curran *et al* (2000) to investigate structure/function relationships of a plant Ca^{2+}-ATPase. In this method a mutant yeast, complemented by the expression of a heterologous protein (in this example, a plant Ca^{2+}-pump), is exposed to the chemical mutagen, Ethyl Methyl Sulfonate (EMS). Following mutagenesis, the yeast are washed clean of the mutagen and plated to selective media, which would not normally support growth of the yeast expressing the WT protein. Thus only yeast that are complemented by mutated proteins that are still able to operate to a sufficient level are selected The main advantage of this method is the removal of any transformation steps in the isolation of yeast which express the mutated transporters. The transporter is already expressed in the yeast during mutation and so selection and basic characterisation can take place directly following mutation. However, the drawback of this method is that the yeast genome is present during mutagenesis, whereas in the two previously described methods the plasmid DNA is isolated during mutagenesis. This means there is always a possibility that any alteration in the growth capabilities of the yeast on selective media may be due to a mutation of its genome. It is therefore necessary to either cure the mutated yeast of its plasmid DNA, and show it reverts to normal behaviour or, alternatively, to isolate the mutated insert DNA and re-transform WT yeast, demonstrating that this then confers the particular phenotype.

There have been few published reports investigating structure/function relationships of plant amino acid permeases and those to date have concentrated on AtAAP1. In an attempt to identify regions of the *AtAAP* genes essential to the transport mechanism, specific point mutations have been made to AtAAP1 (unpublished results discussed in Bush *et al* 1996, Ortiz-Lopez *et al* 2000). The effects of these mutations on the transport properties were investigated by expression and characterisation in amino acid transport deficient yeast. The substitutions made at His337 were all found to obliterate transport to below the level of complementation for the yeast mutant on selective media. His47 was also substituted and this also had major effects on the transport capability of the permease (unpublished results discussed in Bush *et al* 1996, Ortiz-lopez *et al* 2000). These particular residues were chosen for point mutation as previously, amino acid permeases from *Beta vulgaris* had been inhibited by the histidine modifier, diethylpyrocarbonate (Li and Bush 1990), and these two histidine residues are conserved throughout the AAP family (Bush *et al* 1996). This shows that both His337 and His47 are essential for the operation of AAPs. Further mutation of AtAAP1 has been carried out using a random mutagenesis protocol but only preliminary unpublished observations have been discussed (Bush *et al* 1996, Ortiz-Lopez *et al* 2000). Substitutions of both Ala254 and Asp252 altered apparent K_ms for alanine and histidine but it was not reported whether the K_ms observed were increased or decreased compared to those of the WT. However it was suggested that these residues may be involved in defining the substrate-binding site (Ortiz-Lopez *et al* 2000).

1.7 Biotechnological implications

Manipulation of physiologically important proteins such as amino acid transporters has implications for improving resource allocation and plant growth. More efficient xylem loading and unloading, phloem loading and unloading and amino acid uptake from the soil are all improvements that could possibly be achieved through altering expression levels of amino acid transporters or indeed expressing mutated transporters with beneficial properties. For example, the nutritional quality of seeds could be improved by expressing a permease with altered substrate specificity or affinity. Knowledge of structure/function relationships will be essential in engineering transporters with desired characteristics.

1.8 Project aims

This study investigates structure/function relationships of amino acid permeases present in the PMs of higher plants, using *Ricinus communis* as a model. The permeases under investigation were RcAAP1 and RcAAP3 (Marvier *et al* 1998, Neelam *et al* 1999). The main aims of this study were firstly to introduce random mutations into the *Ricinus communis* amino acid transporter cDNAs, *RcAAP1* and *3* to create a library of mutated transporters. Secondly, to develop a selection procedure in yeast to isolate mutated transporters with altered transport characteristics that would confer on the yeast mutants the ability to grow under selective conditions. Thirdly, to sequence the mutated transporters and compare this with the sequence of the WT transporters to ascertain which residues may be important in the transport mechanism.

The yeast mutants used for this investigation were JT-16 and GAP, which are defective in histidine and citrulline transport respectively. At the start of this project, *RcAAP1* was available in both mutants whereas *RcAAP3* had only been expressed in GAP. Therefore an initial aim was to determine whether *RcAAP3* would complement JT-16. The next step was to study the behaviour of the yeast mutants expressing the WT transporters under a range of conditions. This was necessary in order to develop a selection procedure that could be used to isolate mutated transporters with altered transport characteristics. The aim was to find selective conditions under which the WT transporters could no longer operate efficiently, thus no longer restoring the growth of the yeast mutants. These conditions would then be used to select for mutations in the transporter that would alter the transport characteristics of the permeases and allow them to operate more efficiently than WT and hence restore yeast growth.

A further aim was to provide a more detailed characterisation of the transport properties of RcAAP1 and RcAAP3. The strategy was to express these amino acid permeases in oocytes and use electrophysiological techniques to determine their kinetic parameters under a range of conditions. The aim was to investigate whether these permeases are amino acid symports as suggested from previous studies in yeast and to determine the stoichiometry of the translocation process. It was also important to develop this system and provide preliminary data with WT transporters so that work in the future could be carried out with promising mutated transporters arising from the random mutagenesis and yeast selection experiments.

Chapter 2 Materials and Methods

2.1 Maintenance of yeast

Two yeast mutant strains were used to express plant amino acid transporters. JT-16 of the genotype a, *hip-64, his4-40, can1, Inol, ura3-52* and GAP (general amino acid permease) ura3 mutant of the genotype a, *gap, ura3-52*. For routine growth of all yeast strains YPD media containing 1%(w/v) yeast extract, 2%(w/v) peptone and 2%(w/v) dextrose was used, solid YPD media also containing 18 mg/ml DIFCO (Detroit, Michigan 48232 USA) agar. For selective growth conditions a defined synthetic media was produced using DIFCO nitrogen base without amino acids, 0.02 g/ml dextrose and 0.5%(w/v) ammonium sulphate, supplemented as required with the appropriate carbon, nitrogen and nucleoside base sources to sustain growth. For JT-16, media was supplemented with 5.74 mM arginine, 3.86 mM histidine, 0.002%(w/v) inosine and 0.02 mg/ml uracil (high histidine + uracil media). For JT-16 containing the Nev-N shuttle vector (figure 2.1) (Sauer and Stolz 1994) the same medium was used but no uracil was required (high histidine media) as the vector contains the URA3 gene. For JT-16 transformed with either *RcAAP1* or *RcAAP3* cloned into the NotI site of the Nev-N shuttle vector, media were supplemented with 5.74 mM arginine and 0.13 mM histidine (Low histidine media). Less histidine was required in the media as the expressed plant transporter complements the uptake deficiency of the yeast. For GAP with the Nev-N vector incorporated, media was not supplemented (simple dextrose media). For GAP with *RcAAP1* or *RcAAP3* cloned into the Nev-N Not I site, media were supplemented with 0.2 mg/ml citrulline (+citrulline media) and the ammonium sulphate was left out.

2.2 Transformation of *S.ceravisiae* with plasmid DNA

Yeast mutants were transformed using a method described in Dohmen *et al* (1991). A 2.5 ml overnight culture of the yeast in YPD medium was used to inoculate 50 ml of YPD media. The yeast were grown at 30 °C with vigorous shaking to an OD_{600nm} of between 0.6 and 1.0 (approximately 7 hours). The cells were pelleted by centrifugation at 1142 x *g* in a Sorvall RC 5B refrigerated centrifuge for 5 minutes at 4 °C and resuspended in 20 ml of ice cold

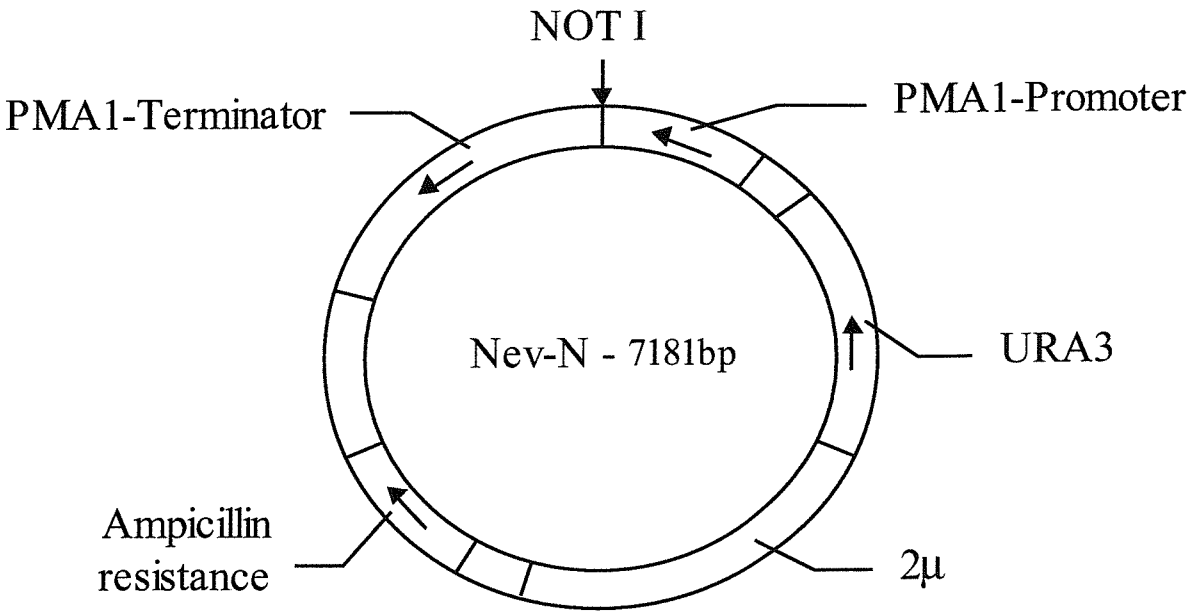

Figure 2.1 - Nev-N shuttle vector (Sauer and Stolz 1994).

competent cell storage buffer, containing 10 mM bicine (pH 8.35), 1 M sorbitol and 3%(v/v) ethylene glycol. The cells were pelleted again by centrifugation at 1142 x *g* in a Sorvall RC 5B refrigerated centrifuge at 4 °C for 5 minutes, resuspended in 2 ml of cold competent cell storage buffer and stored in 200 µl aliquots at -70 °C until required. For each transformation a 200 µl aliquot was defrosted in a 37 °C water bath. Once defrosted, 1 µg of plasmid DNA and 5 µl of herring sperm DNA (100 µg/ml) were added. The mixture was then incubated at 37 °C for 5 minutes with vigorous agitation every 30 seconds. 1 ml of transformation buffer, containing 200 mM bicine (pH 8.35) and 4%(w/v) PEG 1000 was added, mixed by inversion and left at 35 °C for 1 hour. The cells were pelleted by centrifugation at 1142 x *g* in a Sorvall RC 5B refrigerated centrifuge at 4 °C for 5 minutes and resuspended in 800 µl of cell resuspension buffer, containing 10 mM bicine (pH 8.35) and 150 mM sodium chloride. The cells were once again pelleted by centrifugation at 1142 x *g* in a Sorvall RC 5B refrigerated centrifuge at 4 °C for 5 minutes and then resuspended in 300 µl of cell resuspension buffer and plated on the appropriate selective media.

2.3 Isolation of plasmid DNA from yeast

This DNA isolation was carried out as described in Ward (1990). The yeast cells from 1 ml of overnight culture of YPD medium were pelleted by centrifugation at 13000 x *g* in a Sorvall RMC 14 chilled microfuge for 5 minutes. The pellet was resuspended in 200 µl of 'breaking' buffer containing 100 mM NaOH, 1 mM EDTA, 0.1%(w/v) SDS and 10 mM Tris/HCl (pH 8.0). The yeast cells were lysed by the addition of an equal volume of sterile glass beads (acid washed 0.45 mm diameter) and vigorous mixing for 5 minutes. Following two phenol:chloroform:IAA (25:24:1) extractions, the aqueous phase containing the plasmid DNA was transferred to a fresh tube. The plasmid DNA was isolated by ethanol precipitation (2 volumes of ethanol and 0.1 volume 3 M sodium acetate) overnight at -20 °C. The DNA was pelleted by centrifugation at 13000 x *g* in a Sorvall RMC 14 chilled microfuge at 4 °C for 20 minutes. The pellet was then resuspended in 50 µl TE buffer (10 mM Tris and 1mM EDTA, pH 8) and stored at -20 °C until required.

With certain yeast an alternative method was employed which gave lower levels of contamination from genomic DNA. The yeast were grown and harvested as described above. They were then resuspended in 300 µl new lysis buffer (1%(w/v) SDS, 2%(w/v) Triton X100, 100 mM NaCl, 10 mM Tris HCl (pH 8.0), 1 mM EDTA), an equal volume of sterile glass beads (acid washed, 0.45 mm diameter) and 300 µl of phenol:chloroform:IAA (25:24:1). 1 µl RNaseA

(2 mg/ml) was also added to the reaction The cells were then lysed by rigorous vortexing for 1 minute. The resulting solution was centrifuged at 13000 x *g* in an MC 12V microfuge for 5 minutes. Following centrifugation the aqueous top phase was carefully removed and placed in a fresh tube. The DNA in this solution was then concentrated by ethanol precipitation. 2 volumes ethanol and 0.1 volume 3 M sodium acetate were added to the tube and this was precipitated at -20 °C for 1 hour. The DNA was pelleted by centrifugation at 13000 x *g* in a Sorvall MC 12V microfuge, 4 °C for 20 minutes. The pellet was then resuspended in 50 µl TE buffer (10 mM Tris and 1 mM EDTA, pH 8.0) or H_2O and stored at -20 °C until required.

2.4 Ligation of DNA into plasmid vector

Plasmid DNA was linearised at the site of ligation with an appropriate restriction enzyme. The DNA to be ligated was prepared by the same restriction digest. A 50 µl reaction mix in TE was prepared containing 10 units restriction enzyme, 10 µg DNA and 5 µl 10 x specific enzyme buffer. The reaction was incubated at 37 °C for 2 hours. To prevent the plasmid DNA from re-circularising the 'sticky ends' were treated with calf intestinal alkaline phosphatase. A 100 µl reaction mix in sterile water was prepared containing 10 µl of the resultant restriction digest reaction, 10 µl 10x calf intestinal alkaline phosphatase buffer and 2 µl calf intestinal alkaline phosphatase (1 unit/µl). This was incubated for 1 hour at 37°C, with an additional 1 µl calf intestinal alkaline phosphatase being added after 30 minutes. The addition of 2 µl 0.5 M EDTA and incubation at 65 °C for 30 minutes arrested the reaction by inactivation of the calf intestinal alkaline phosphatase. The reaction was then extracted using 150 µl phenol:chloroform:IAA (25:24:1) and precipitated with 2 volumes ethanol, 0.1 volume 3 M sodium acetate (pH 5.2) at –20 °C for 1 hour. After centrifugation at 13000 x *g* in a Sorvall MC 12V microfuge for 20 minutes, pelleted DNA was resuspended in 10 µl TE. The concentration of linearised plasmid DNA was measured using a spectrophotometer (see section 2.9) and diluted to approximately 100 ng/µl. For ligations a ratio of 3:1 insert to vector is used. Using 100 ng of vector DNA (1 µl) the amount of insert DNA required was calculated using the following formula. A 10 µl reaction mix was

$$\frac{\text{ng of vector} \times \text{Kb size of insert}}{\text{Kb size of vector}} \times \text{insert : vector ratio} = \text{ng of insert}$$

prepared containing the previously calculated insert, 100 ng vector, 1 µl T4 DNA ligase (1 unit/µl) and 1 µl 10x ligase buffer in sterile water. The reaction was incubated either at room temperature for 2 hours or at 4 °C for between 16 and 18 hours. The product was then ready to be incorporated into competent *E.coli* (see section 2.5) or yeast (see section 2.2).

2.5 Transformation of *E.coli* with plasmid DNA (containing ampicillin resistance gene)

2.5.1 Heat shock

100 ml of LB was inoculated with 1 ml of overnight *E.coli* culture. This was incubated on a shaker at 37°C until an $O.D_{550nm}$ of between 0.4 and 0.5 was reached (approximately 2.5 to 3 hours). The 100 ml was split evenly between two 50 ml falcon tubes (Greiner Labortechnik Ltd. Gloucestershire, UK) and placed on ice for 5 minutes. The tubes were then centrifuged at 1142 x *g* in a Sorvall RC 5B refrigerated centrifuge at 4 °C for 5 minutes. The supernatant was removed and the cells resuspended in 20 ml of ice-cold 100 mM $CaCl_2$. With storage on ice the cells were used within a few hours. For longer storage, 1.6 ml of 60%(v/v) glycerol was added to 5 ml aliquots of culture to give a final concentration of 15% glycerol. These aliquots could then be stored at –70 °C until required.

2.5 µl of recovered plasmid was added to 200 µl of heat shock competent cells and left on ice for 10 minutes. The mixture was heat shocked at 42 °C for 90 seconds in a water bath, then immediately placed on ice for 5 minutes. 200 µl of LB at 42 °C was then added and 50 µl, 100 µl and 200 µl samples plated to LB agar (1.5%(w/v) agar) media containing an appropriate antibiotic (e.g ampicillin (40 µg/ml)). The plates were then incubated at 37 °C overnight. Any colonies formed on the plate represented a successful transformation and between 4 and 6 were picked off and grown up overnight in liquid LB containing ampicillin (40 µg/ml).

If the plasmid used in the transformation of *E.coli* also contained the Lac-Z gene flanking the cloning site, Xgal (40 ng/ml) and IPTG (119 ng/ml) were included in the LB agar media. After overnight growth, colonies with a blue colouration represented transformation of the bacteria with a plasmid containing no ligated fragment. White colonies represented transformation by successful ligations. The disruption of the Lac-Z gene by the insertion of the ligated fragment prevents the production of β-galactosidase. This enzyme cuts X-gal to produce an indole called 5-bromo-4-chloro-indole which is blue in colour. The inclusion of IPTG induces the expression of the Lac-Z gene.

2.5.2 Electroporation

100 ml of LB was inoculated with 1 ml of overnight *E.coli* culture. This was grown at 37 °C with shaking to an $O.D_{600nm}$ of 0.5 to 1.0 (approximately 2.5 to 3 hours). The culture was chilled on ice for 20 minutes then centrifuged at 1142 x *g* in a Sorvall RC 5B refrigerated centrifuge at 4 °C for 10 minutes. The supernatant (LB) was removed with a pipette and the cells were resuspended in 100 ml of ice-cold sterile water. An important part in the preparation of cells for electroporation is to ensure a minimal level of salt in the solutions. For this reason the water used in this method was purified through a milli-pore filter (Maxima analytical, USF ECCA, Bucks, UK) and then autoclaved. Following resuspension, the cells were centrifuged again as describe and resuspended in 50 ml of ice-cold sterile water. The cells were then centrifuged at 1142 x *g* in a Sorvall RC 5B refrigerated centrifuge at 4 °C for 10 minutes and resuspended in 2 ml ice-cold sterile 10%(v/v) glycerol. At this stage the cell concentration was approximately 1-3 $x10^{10}$ cells/ml. The cells were split into 40 µl aliquots and either stored on ice for up to 2 hours if they were to be used immediately, or stored at –70 °C for up to 6 months until required. After storage at -70°C, the cells were defrosted at room temperature and then stored on ice before use.

1-2 µl of plasmid DNA was added to 40 µl of electroporation competent cells and left on ice for 1 minute. A gene pulser (Bio-Rad laboratories Ltd., Herts. UK) was set to 25 µF and 2.5 kV. The pulse controller was set to 200 Ω to give a pulse of 4-5 msec. The cells and DNA mixture was transferred to the bottom of an ice-cold electroporation cuvette (ECU-102, Equibio, UK). The cuvette was placed into the safety chamber and slid into position so the cuvette was between the electrical contacts. A single pulse was used with the settings described. This produced a field strength of 12.5 kV/cm^2. The cuvette was immediately removed from the chamber and 1 ml of SOC (2%(w/v) bacto-tryptone, 0.5%(w/v) bacto-yeast extract, 10 mM NaCl, 2.5 mM KCl, 10 mM $MgCl_2$, 10 mM $MgSO_4$, 20mM glucose) added. The rapid addition of SOC maximises the recovery of transformants. The cells resuspended in SOC were transferred to a 1.5 ml eppendorf tube and incubated at 37 °C for 1 hour to recover. The cells were then spread onto LB agar plates as described in section 2.5.1. Selection with a suitable antibiotic and the Lac-Z system were again possible.

2.6 Small scale isolation of plasmid DNA from *E.coli*

Plasmid DNA was isolated using the Hybaid Recovery Plasmid Mini Prep kit (Hybaid Ltd, Ashford, UK), following the manufacturers instructions. 1.5 ml of cultured cells were centrifuged at 13000 x *g* in a Sorvall MC 12V microfuge for 1 minute. The resulting pellet of cells was resuspended in 210 µl of cell suspension solution (50 mM Tris/HCl (pH 8.0), 10 mM EDTA, 100mg/ml RNaseA). 210 µl of cell lysis solution (200 mM NaOH, 1%(w/v) SDS) was then added to the eppendorf. The contents were mixed by gentle inversion and left at room temperature for 5 minutes. 280 µl of neutralisation solution (containing acetate and guanidine hydrochloride) was then added and the eppendorf immediately inverted to form a white precipitate. The contents were centrifuged for 10 minutes at 13000 x *g* in a Sorvall MC 12V microfuge. The resulting supernatant was transferred to a spin cup in a receiver tube. After centrifugation at 13000 x *g* in a Sorvall MC 12V microfuge for 1 minute the through-flow was discarded. 700 µl of wash solution (containing ethanol, NaCl, EDTA and Tris/HCl) was added to the spin cup and centrifuged through to the receiver tube at 13000 x *g* in a Sorvall MC 12V microfuge for 1 minute. The remaining contents of the spin cup was recovered in a new receiver tube by adding 75 µl of TE (10 mM Tris and 1 mM EDTA, pH 8) to the spin cup and centrifuging at 13000 x *g* in a Sorvall MC 12V microfuge for 2 minutes. The recovered DNA was cleaned by adding 1 volume phenol:chloroform:IAA (25:24:1), mixing thoroughly then centrifuging at 13000 x *g* in a Sorvall MC 12V microfuge for 5 minutes. The top phase was carefully removed and 2 volumes ethanol, 0.1 volume 3 M sodium acetate added and precipitated for at least 1 hour at -20 °C. The DNA was pelleted by centrifuging at 13000 x *g* in a Sorvall MC 12V microfuge, 4 °C for 20 minutes. This was then resuspended in 10 µl TE (or more if required).

Alternatively a 1.5 ml overnight culture was centrifuged at 13000 x *g* in a Sorvall MC 12V microfuge for 1 minute. The pelleted cells were resuspended in 100 µl TEG (25 mM Tris, 50 mM EDTA, 1%(w/v) glucose (pH 8)) and left at room temperature for 5 minutes. 176 µl or sterile H_2O, 20 µl of 10%(w/v) SDS and 4 µl of 10 M NaOH were then added to give a final mixture of 200 mM NaOH and 1%(w/v) SDS. 1µl RNaseA (2 mg/ml) was also added at this stage to remove any RNA contamination. The contents were mixed by inversion and left on ice for 5 minutes. 150 µL of 3 M potassium acetate (pH 5.5) were added and again the contents mixed by inversion. This was left on ice for 10 minutes before centrifuging at 13000 x *g* in a Sorvall MC 12V microfuge for 10 minutes. The supernatant was transferred to a new container, avoiding transfer of any white precipitate. 900 µl of 100%(w/v) ethanol was added and the

mixture left to precipitate at -20 °C for at least 15 minutes. The contents were centrifuged at 13000 x *g* in a Sorvall MC 12V microfuge, 4 °C for 20 minutes; the pellet was washed in 500 µl of 70%(v/v) ethanol and pelleted again by brief centrifugation. The pellet was then resuspended in 50 µl TE and stored at -20 °C.

2.7 Medium scale isolation of plasmid DNA from *E.coli*

25 ml of overnight culture was centrifuged at 2782 x *g* in a Sorvall MC 12V microfuge for 5 minutes. The pelleted cells were resuspended in 2 ml of TEG (25 mM Tris, 50 mM EDTA, 1%(w/v) glucose (pH 8)) and left at room temperature for 5 minutes. 3280 µl of sterile H_2O, 600 µl of 10%(w/v) SDS and 120 µl of 10 M NaOH were then added to give a final mixture of 200 mM NaOH and 1%(w/v) SDS. The contents were mixed by inversion and left on ice for 5 minutes. 3 ml of 3 M potassium acetate (pH 5.5) were added and again the contents mixed by inversion. This was left on ice for 10 minutes before centrifuging at 2782 x *g* in a Sorvall MC 12V microfuge for 1 hour. The supernatant was transferred to a new container, avoiding transfer of any white precipitate. 10 ml of 100%(v/v) ethanol were added and the mixture left to precipitate at -20 °C for at least 15 minutes. The contents were centrifuged at 2782 x *g* in a Sorvall MC 12V microfuge for 1 hour and then the pellet was washed in 5 ml of 70%(v/v) ethanol and pelleted again by brief centrifugation. The pellet was resuspended in 200 µl of TE. 2 µL of RNaseA (2 mg/ml) was added and incubated at 37 °C for 30 minutes. This removed any RNA contamination. The remaining DNA was stored in TE at -20 °C until required. The DNA was cleaned further with 1 volume phenol:chloroform:IAA (25:24:1) and precipitated with 2 volumes ethanol, 0.1 volume 3 M sodium acetate at -20 °C. This was stored in TE at -20 °C

2.8 Spectrophotometric determination of nucleic acid concentration

An aliquot of a nucleic acid sample was diluted in 250 µl of TE. The absorbance of the sample held in a quartz cuvette with a 0.5 cm path length was measured at 260 nm and 280 nm. The absorbance of 1 mg/ml of double stranded DNA at 260 nm is known to be 20. The concentration of the sample was therefore: -

$$\frac{(OD_{260nm}) \times (\text{dilution factor})}{20} \times 2 = \text{concentration in } \mu g/\mu l$$

Similarly the absorbance of 1 mg/ml at 260 nm of single stranded DNA and RNA is known to be 25. The concentration was therefore: -

$$\frac{(OD_{260nm}) \times (\text{dilution factor})}{25} \times 2 = \text{concentration in } \mu g/\mu l$$

The purity of nucleic acid samples was calculated using the ratio of the absorbance measurements at 260 nm and 280 nm. Where OD_{260}/OD_{280} = 1.8 - 2.0 the sample was considered pure. A lower ratio may have indicated protein, phenol or ethanol contamination whereas a higher ratio possibly indicates polysaccharide contamination or sample degradation, especially for RNA.

2.9 Analysis of DNA on an agarose gel

DNA was separated on an agarose gel as described in Sambrook et al (1989). For DNA samples over approximately 500 bp a 1%(w/v) agarose gel was prepared in TAE (40 mM Tris/acetate pH 8.0, 1 mM EDTA). Ethidium bromide (5 mM) was included in both gel and TAE running buffer. The sample was mixed in a 5:1 ratio with loading buffer (0.25%(w/v) bromophenol blue, 0.25%(w/v) xylene cyanol FF and 15%(w/v) FICOLL. Giving a final concentration of 0.042% bromophenol blue, 0.042% xylene cyanol FF and 2.5% FICOLL). The sample was then loaded to a well at the cathode end of the gel. Electrophoresis was carried out at 100 volts for 45-90 minutes, depending on the size of the DNA fragments and the gel concentration. For DNA under 500 bp a 2%(w/v) agarose gel was used under the same conditions. The only other difference for DNA shorter than 500 bp being no xylene cyanol in the loading buffer. This was to aid visualisation of fragments running at the same level as the dye front.

2.10 Purification of DNA from agarose gel

2.10.1 Geneclean method

DNA fragments were cut from the agarose gel using a razor blade. The DNA was recovered from the gel using the Geneclean II kit (BIO 101, Anachem, UK) following the manufacturers instructions. The dissected agarose containing the DNA was melted at 55 °C in

2 volumes of saturated sodium iodide. 10 µl of Glass-milk was added to the mixture per 20 ng of DNA (a rough estimate of the quantity of DNA presented can be deduced by the intensity of the band compared to a known concentration band, usually in the 1Kb ladder). After mixing, the solution was incubated on ice for 1 hour with occasional agitation, to allow the DNA to bind the Glass-milk. The Glass-milk was pelleted by centrifugation at 13000 x *g* in a Sorvall MC 12V microfuge for 10 seconds and washed twice in 200 µl of pre-cooled New Wash solution (containing ethanol, NaCl and water). The pellet was resuspended in 100 µl of TE and incubated at 37 °C for 15 minutes. The Glass-milk was pelleted as before and the supernatant transferred to a fresh eppendorf tube. This was repeated giving 200 µl of recovered supernatant. The recovered DNA was cleaned using 200 µl phenol:chloroform:IAA (25:24:1) and precipitated with 2 volumes ethanol, 0.1 volume 3 M sodium acetate (pH 5.2) at -20 °C for at least 1 hour.

2.10.2 Spin-column method

The Qia-quick gel extraction kit (Qiagen, West Sussex, UK) was used according to the manufactures instructions. The appropriate band was excised from the gel as described previously (2.10.1). The DNA was purified from the gel fragment as described in the manufacturers instructions. The gel fragment was melted in QG (Solubilization and Binding Buffer, with pH indicator) buffer at 65 °C until completely dissolved (approximately 10 minutes). The DNA dissolved in QG buffer was then added to a spin column and centrifuged at 13000 x *g* in a Sorvall MC 12V microfuge for 30 seconds. The DNA, now bound to the column was washed using 700 µl PE (wash buffer) buffer and centrifuged for 30 seconds. The through-flow was removed and the column centrifuged again to ensure complete removal of PE buffer. The DNA was eluted from the column to a fresh tube using 30 or 50 µl EB buffer (elution buffer), depending on the desired final concentration.

2.10.3 Glass-wool method

DNA fragments were cut from the gel using a razor blade. The section of agarose gel containing the required DNA was placed on top of approximately 100 mg of glasswool (Fisher, UK) in the bottom half of an eppendorf tube with a small hole at the bottom. The DNA was removed from the agarose by centrifugation at 6000 x g in a Sorvall MC 12V microfuge for 1 minute. The TAE buffer containing the DNA was collected from a second tube underneath the

glasswool. The DNA was purified by phenol:chloroform:IAA (25:24:1) and precipitated with 2 volumes ethanol, 0.1 volume 3 M sodium acetate (pH 5.2) at -20°C for at least 1 hour.

2.11 DNA mutagenesis

2.11.1 DNA shuffling

DNA shuffling was carried out based on the method of Stemmer (1994). The process is described below.

2.11.1.1 DNaseI digest of DNA

The enzyme DNaseI was used to digest DNA strands to a range of smaller fragments. Due to the difficulty of purifying *RcAAP1* and *3*, Nev-N containing *RcAAP3* was used to optimise the digest conditions before continuing with *RcAAP1* and *RcAAP3.* 12 μg of DNA in a 10 μl reaction mix with 2 μl DNaseI (0.2 units/μl, final 0.04 units/μl) was placed in a water bath at 28 °C for 5-40 minutes. The reaction was stopped by the addition of 1 μl 0.5 M EDTA (pH 8). The reaction was run on a 2%(w/v) agarose gel to determine the level of digestion. Controls included tubes with; DNaseI and EDTA added together (effective time of 0 minutes), EDTA but no DNaseI added (ensuring EDTA had no digest effect) and 12 μg DNA in 10 μl H_2O.

Following these trials *RcAAP1* and *3* cDNA was digested with DNaseI in a similar manner. 100 ng of cDNA in a 10 μl reaction mix was digested using between 0.5 μl and 1.5 μl of DNaseI (0.2 units/μl) at 30 °C for 30 minutes. The amount of DNaseI in the reaction was varied depending on the purity of the cDNA sample used. Pure samples required less enzyme. The reaction was stopped by the addition of 1 μl 0.5 M EDTA (pH 8). The reaction was then run on a 2%(w/v) agarose gel to isolate the digested material.

In an attempt to optimise conditions, a modification was made to the digestion reaction. Following the method described in Lorimer and Pastan (1995), the DNaseI digest was performed in the presence of Mn^{2+}. Approximately 4.5 μg of either *RcAAP1* or*3* cDNA was suspended in 45 μl of H_2O. 5 μl 10x digestion buffer (500 mM Tris-HCl, 100 mM $MnCl_2$) was added. DNaseI (10-50 units/μl) was diluted 50000 fold in 1x digestion buffer to give a final activity of approximately $6x10^{-4}$ u/μl. Both mixtures were pre-equilibrated to 15 °C. 1.5 μl of the DNaseI mixture (final $1.8x10^{-5}$ units/μl) was then added to the DNA mixture and the reaction

incubated at 15 °C for staggered times between 30 seconds and 10 minutes. Heating at 90 °C for 10 minutes stopped the reaction. The resulting DNA was isolated from a 2%(w/v) agarose gel as previously described (see section 2.10) or using electroelution (2.11.1.2).

2.11.1.2 Electroelution of DNA from an agarose gel

DNA from the DNase digest was removed from the 2%(w/v) agarose gel following the manufacturer's instructions. The membrane cap was soaked in elution buffer for 1 hour at 60 °C prior to elution. The region of agarose gel containing the desired DNA was cut out under UV light and placed in the glass tube. The apparatus was set up as described in the manufacturer's instructions and 15 mA of current was supplied per tube for 1 hour. The polarity of the current was switched for 1 minute before disconnecting. Approximately 400 µl of elutant on the membrane cap was pipetted to a fresh eppendorf. The membrane cap was washed with 200 µl of elution buffer and this was added to the collected elutant. The total elutant was purified with phenol:chloroform:IAA (25:24:1) and overnight ethanol precipitation. The DNA collected was stored in 10 µl of TE at -20 °C until required.

2.11.1.3 Primerless PCR

A 10 µl reaction containing between 0.1 µl and 2 µl of DNaseI digested product, 0.1 µl Taq polymerase (10 units/µl), 0.1 µl dNTP mix (10 µM) and 1 µl 10x Taq polymerase buffer was prepared. The PCR conditions used are described in figure 2.2. Following PCR the products were diluted by a factor of 40 with sterile H_2O and stored at -20 °C until required.

Following a communication with Dr. Brande Wulff (Sainsbury laboratory, John Innes Centre, Norwich, UK), an alteration to the primerless PCR conditions was designed in an attempt to increase the efficiency of elongation. These conditions are described in figure 2.3. It was believed the step-wise increment in elongation time would encourage the production of shuffled products. The primary elongation time at 72 °C was for 5 seconds. Following this every subsequent step was 5 seconds longer.

2.11.1.4 Primered PCR

Primers were designed to the non-coding regions bordering *RcAAP1* (figure 2.4) and *RcAAP3* (figure 2.5). These primers produce products of the appropriate size (1.5 Kb for *RcAAP1* and 1.6 Kb for *RcAAP3*). Both sets of products were produced with EcoRI restriction

sites at either end. This was due to the design of the primers and intended for use in ligation. A 10µl reaction mix was prepared containing 0.25 µl of 40x diluted primerless PCR product, 0.1 µl Taq polymerase (10 units/µl), 0.25 µl of both forward and reverse *RcAAP 1* primers (100 pmol/µl), 1 µl 10x Taq polymerase buffer and 0.1 µl dNTP mix (10 µM). The PCR conditions followed for each set of primers are described in figure 2.6 (Sambrook *et al* 1989, Stemmer 1994). The product of this PCR was stored at -20 °C until required.

The EcoRI sites incorporated into the *RcAAP1* primers allows the PCR product to be ligated into the yeast shuttle vector Nev-E (figure 2.7) (Sauer and Stolz 1994). Nev-E is identical to Nev-N (figure 2.1), apart from the major cloning site.

2.11.2 Error prone PCR

Using the primers described in figures 8 and 9, *RcAAP1* and *3* cDNA was randomly mutated through slight variations in the components of the PCR mix (Goodman *et al* 1983, Martinez *et al* 1994, Fromant *et al* 1995, Vartanian *et al* 1996), following the PCR conditions described in figure 2.6. These changes increase the rate of errors made by the *Taq* DNA polymerase. This in turn produces random mutations in the resulting cDNA. The first change was the inclusion of manganese in the PCR mix (Goodman *et al* 1983). A 10 µl reaction mix was prepared containing 0.25 µl cDNA in Nev-N (approximately 5 ng), 0.1 µl *Taq* polymerase (10 units/µl), 0.25 µl of both forward and reverse primers (100 pmol/µl), 1 µl 10x *Taq* polymerase buffer (without Magnesium), 0.1 µl dNTP mix (10 µM) and 0.25, 0.5 or 2.0 µl $MnCl_2$ (25 mM) (giving final concentrations of 0.625, 1.25 and 5.0 mM). The second change was the depletion of one of the dNTPs in the PCR dNTP mix (Martinez *et al* 1994, Vartanian *et al* 1996). Both ATP and GTP were depleted separately by 10 fold. A 10 µl reaction mix was prepared containing 0.25 µl cDNA in Nev-N (approximately 5 ng), 0.1 µl *Taq* polymerase (10 units/µl), 0.25 µl of both forward and reverse primers (100 pmol/µl), 1µl 10x *Taq* polymerase buffer and 0.1 µl dNTP mix (10 µM except ATP or GTP at 1 µM). The products of these PCRs could then be cloned into the yeast shuttle vector Nev-E (figure 2.7) as the primers used produce EcoRI restriction sites at each end. All *Taq* polymerase and buffers were supplied by Hybaid (Middlesex, UK). dNTPs were supplied by Promega (Southampton, UK).

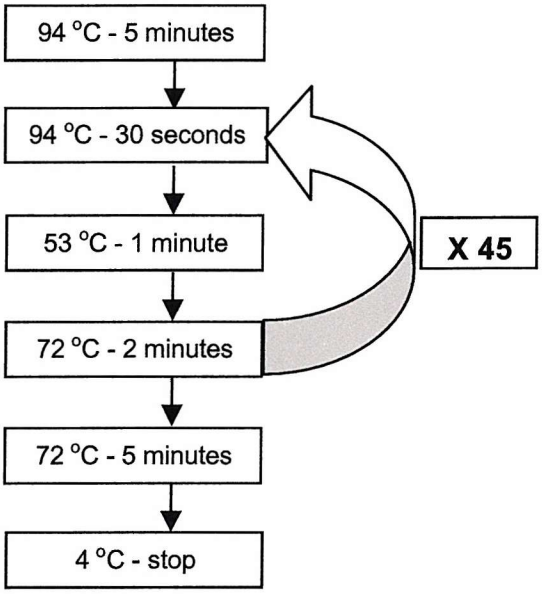

Figure 2.2 - Primerless PCR conditions for the DNA shuffling of *RcAAP1* and*3*.

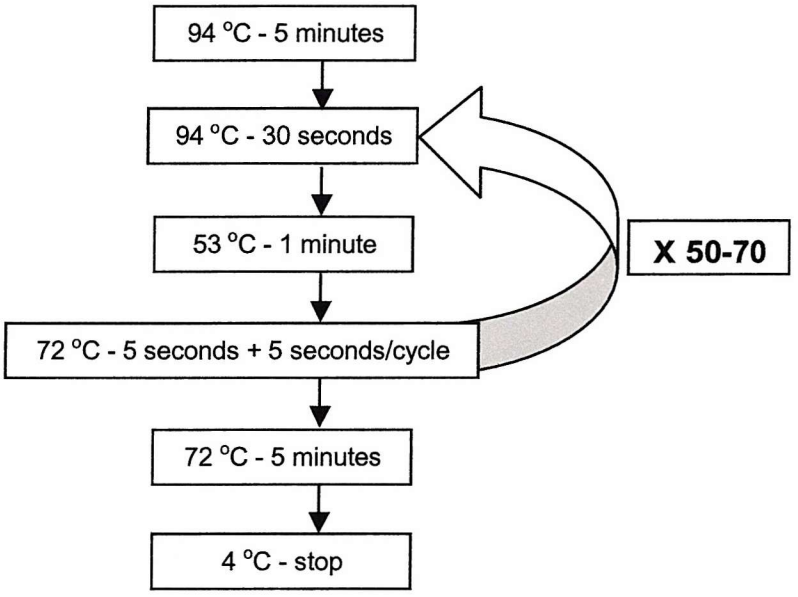

Figure 2.3 – Revised primerless PCR conditions for the DNA shuffling of *RcAAP1* and *RcAAP3*.

2.11.3 Chemical mutagenesis of yeast

Yeast were mutated following the method described by Curran *et al* (2000). Cultures were prepared of JT-16 and GAP yeast containing *RcAAP1* or *3* in the Nev-N shuttle vector, all in 5 ml YPD liquid media. The cultures were grown to log phase at 32 °C with vigorous shaking. 1 ml of culture was pelleted by centrifugation at 13000 x *g* in a Sorvall MC 12V microfuge for 30 seconds. The pellet was resuspended in 1 ml of 1%(v/v) (80.5 mM) EMS (Ethyl Methyl Sulphonate - $C_3H_8O_3S$) and incubated at room temperature for 30 or 60 minutes with gentle agitation every 5 minutes. The yeast was pelleted again by identical centrifugation and resuspended in 1 ml 5%(w/v) (316.3 mM) sodium thiosulphate ($Na_2S_2O_3$) wash solution. This centrifugation and washing steps were repeated 3 times and then the yeast were resuspended in 1 ml 5%(w/v) sodium thiosulphate and plated out onto selective media.

2.11.4 Conditions for isolating amino acid transport deficient yeast expressing 'useful' mutant transporters.

2.11.4.1 pH selection media

The pH levels of the previously specified yeast media (section 2.1) were altered using a citrate-phosphate buffer. 0.1 M citric acid and 0.2 M dibasic sodium phosphate were mixed in specific ratios and made up to a volume of 80 ml with water. The final pH was verified using a pH meter. This mixture was then added to 20 ml 10x media (appropriate for yeast used). This was filter sterilised and added to 100 ml molten 2x agar. 8-10 plates were poured from the resulting 200 ml media. Yeast cultures were transferred to each plate aseptically. To initially define selective conditions, plates with untransformed yeast, yeast transformed with Nev-N alone and yeast transformed with Nev-N containing WT *RcAAP1* and *3* were used. All plates were incubated at 30 °C and their growth recorded. The pH at which growth was dramatically reduced was considered to be selective and this condition was then used to select yeast expressing mutated transporters.

```
                    5'                              3'
RcAAP1 forward -    GGAATTCAACAAAGGGTGTGTGAAG

                    5'                              3'
RcAAP1 reverse -    GGAATTCCTGGGGTTCATCAGTAAG
```

Figure 2.4 - *RcAAP1* primers, yielding a 1.5Kb product. The EcoRI recognition sequence is shown in green, the annealing sequence is shown in red.

```
                    5'                              3'
RcAAP3 forward -    GGAATTCTTGACATGCCTCCTCAAG

                    5'                               3'
RcAAP3 reverse -    GGAATTCAACAGGACCACATAAAAGAG
```

Figure 2.5 – *RcAAP3* primers, yielding a 1.6Kb product. The EcoRI recognition sequence is shown in green, the annealing sequence is shown in red.

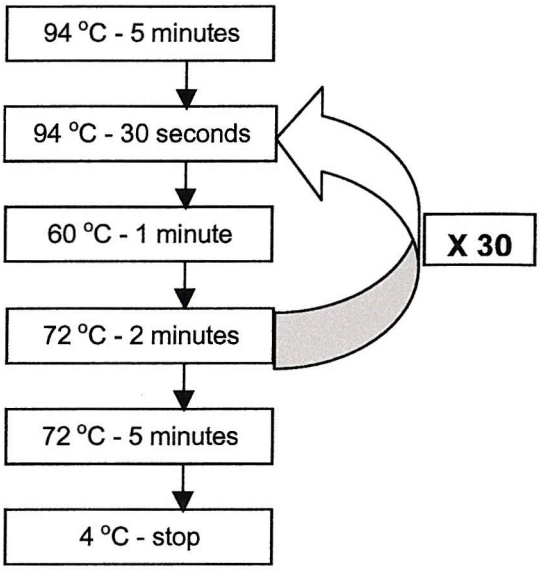

Figure 2.6 - Primered PCR conditions for *RcAAP1* and *3*.

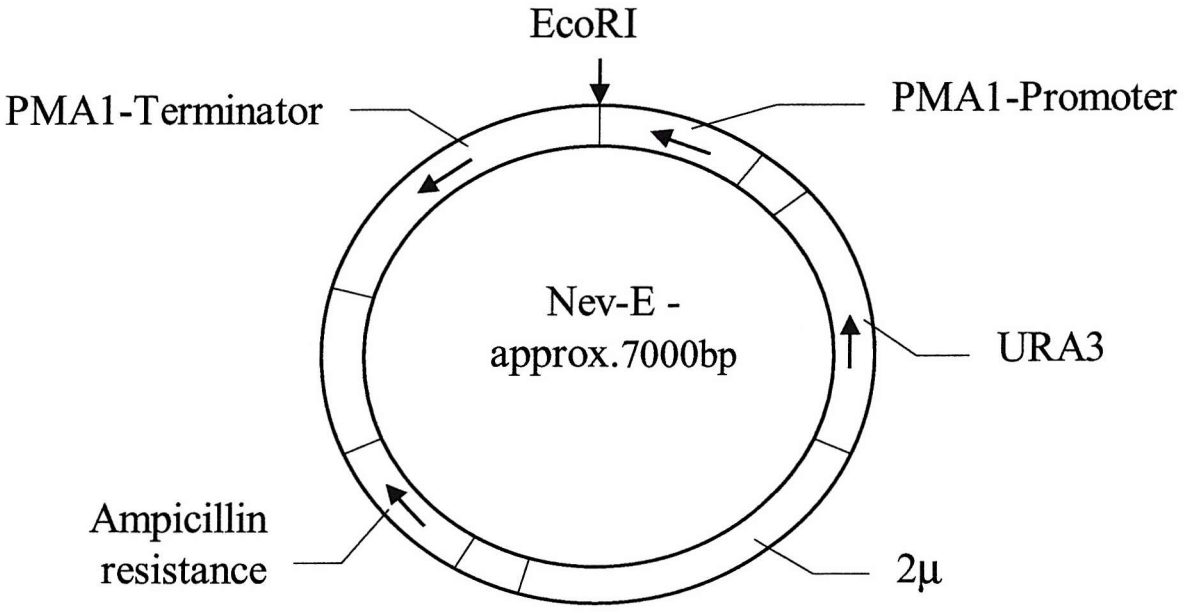

Figure 2.7 - Nev-E yeast shuttle vector (Sauer and Stolz 1994).

2.11.4.2 Canavanine selection media

Canavanine is a toxic analogue of arginine. Canavanine was added in varying concentrations (0.05 - 10.0 μg/ml) to the previously described yeast media (section 2.1). The canavanine was added to 20 ml 10x media (appropriate for yeast used, excluding arginine from JT-16 media) and 80 ml H_2O; this was filter sterilised and added to 100 ml molten 2x agar. 8-10 plates were poured from the resulting 200 ml media. Yeast cultures were transferred aseptically. To initially define selective conditions, plates with untransformed yeast, yeast transformed with Nev-N alone and yeast expressing WT *RcAAP1* and 3 were used. All plates were incubated at 30 °C and their growth recorded to decide on an appropriate time for selection. The concentration of canavanine at which growth of yeast expressing the *RcAAPs* was dramatically reduced was considered selective. These conditions were used to select yeast expressing mutated *RcAAPs*.

2.12 DNA sequencing

The 'BigDye' method (PE Biosytems, Cheshire, UK) was used to sequence WT and mutant *RcAAP1* and *3* on an ABI337 automated sequencer (Perkin Elmer, part number 4303149). The primers specific to *RcAAP1* and *3* previously mentioned were used (figures 2.4 and 2.5). On average 500 bp of sequence is accurately determined from each primer. With both *RcAAP1* and *RcAAP3* cDNAs being approximately 1600 bp it was necessary to design two more nested primers in order to obtain full-length sequence. Two primers were designed for each gene. These primers were designated '*RcAAP1* nested forward' (figure 2.8), '*RcAAP1* nested reverse' (figure 2.9), '*RcAAP3* nested forward' (figure 2.10) and '*RcAAP3* nested reverse' (figure 2.11). There approximate position on each gene and the rational behind sequencing is shown in figure 2.12. The 'BigDye' terminator reaction was made up containing 100-250 ng double-stranded template DNA, 4 μl terminator ready reaction mix, 1 μl forward primer (20 pmol), 1 μl reverse primer (20 pmol) and then made up to 10 μl with deionized sterile H_2O. The reaction was vortexed then centrifuged briefly to collect the contents at the bottom of the tube. PCR was used to produce material for sequencing. The conditions for PCR are illustrated in figure 2.13. This PCR follows the same basic principles as a normal PCR but incorporates chain-terminating fluorescent dNTPs. This produces fragments with a colour representing the chain-terminating base. This is translated by the gel reading equipment as red for T, green for A, blue for C and black for G. Once the thermal cycling was complete the reactions were precipitated.

5′ 3′

TTG GTG GAG CTA AGG TCA AGT TAT G

Figure 2.8 – '*RcAAP1* nested forward' primer for sequencing

5′ 3′

GTG AAG ACC ACA AAA AGT GTC CTC C

Figure 2.9 – '*RcAAP1* nested reverse' primer for sequencing

5′ 3′

GCG TTG CCA TTG GTT ACA CAA TAG

Figure 2.10 – '*RcAAP3* nested forward' primer for sequencing

5′ 3′

CAC AAA AAC AGT CCT CCA TAC CAT TC

Figure 2.11 – '*RcAAP3* nested reverse' primer for sequencing

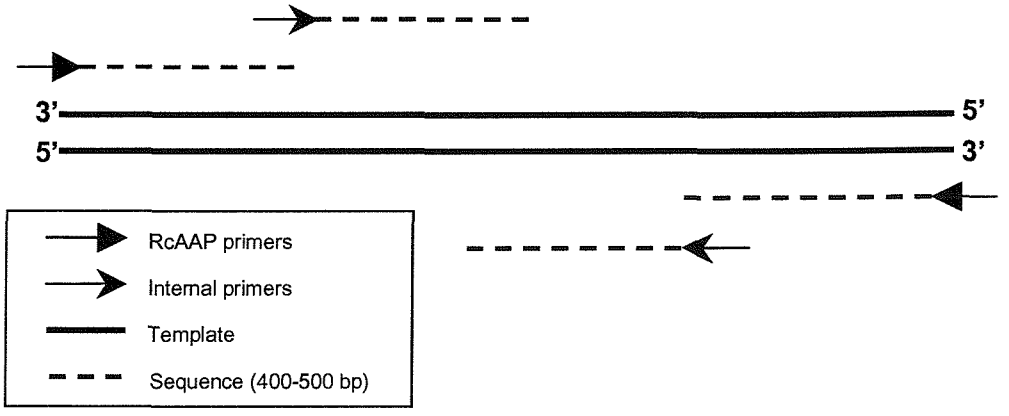

Figure 2.12 – Sequencing rationale. The whole 1.5-1.6 Kb gene will be sequenced in several 400-500 bp sections.

They were made up to 20 µl with sterile deionized H_2O, then 2 µl 3 M sodium acetate (pH 4.6) and 50 µl 95%(v/v) ethanol were added before incubation at room temperature for 1 hour. The sample was centrifuged at 13000 x *g* in a Sorvall MC 12V microfuge, 4 °C for 20 minutes to pellet the precipitate. The pellet was washed in 250 µl 70%(v/v) ethanol then re-pelleted by centrifugation at 13000 x *g* in a Sorvall MC 12V microfuge for 1 minute. The 70%(v/v) ethanol was removed with a pipette and the pellet dried in a heat block at 90 °C for 1 minute. The dried pellet was stored at -20 °C before being loaded onto the sequencing gel. The pellet was resuspended in 8 µl of a formamide: EDTA mix (5:1, de-ionised formamide and 25 mM EDTA pH 8 containing 50 mg/ml blue dextran). The sample was vortexed and briefly centrifuged. The samples were incubated at 95 °C for 2 minutes to denature the sample. The sample was stored on ice until it was loaded onto the gel (GENE PAGE plus 5%, 6 M urea (J437), Amresco, Solon, Ohio 44139, USA). The gel was run at 3000 volts for 2 hours. The position of the fragment on the gel will be relative to its length. This property correlated with the colour describes the sequence. The gel is read by the sequencer and translated by the program Chromas (version 1.45 (http://www.technelysium.com.au)) to give an initial sequence. This can be manually edited using Chromas to allow for mistakes in automated reading.

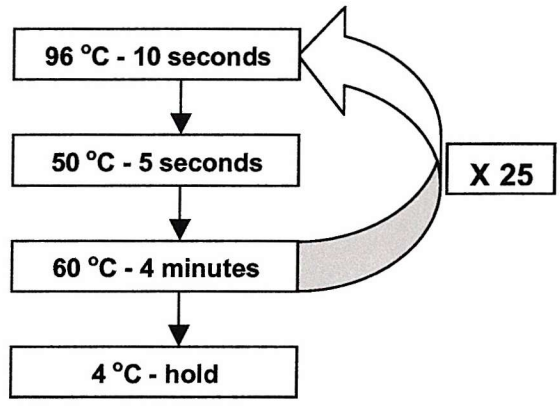

Figure 2.13 – Thermal cycling conditions for 'BigDye' DNA sequencing method

2.13 Sequence Analysis

Sequence analysis, alignments and protein translations were performed using software from the GCG package (Wisconsin Package) on the HGMP facility found at the telnet address – 'menu.hgmp.mrc.ac.uk'. EMBL/Genbank and EST sequence databases were searched using the BLAST package, found at the Internet address - http://www.ncbi.nlm.nih.gov/BLAST (Altschul *et al* 1990).

2.14 Expression in oocytes

2.14.1 *In vitro* transcription

cDNAs were cloned into the multiple cloning site of the *Xenopus* expression vector pXE2 (figure 2.14), following the ligation protocol previously described (section 2.4). DH-10 *E.coli* was transformed with the resulting ligated products. Once colonies had been identified which contained successfully ligated insert in the pXE2 vector, they were cultured overnight and plasmid DNA was prepared (section 2.6). Following purification of the plasmid DNA, it was linearised using one of the restriction enzymes specified in the linearisation site. This gave a template for transcription containing the T7 transcription promoter site, the gene of interest with a poly-A-tail and the termination site. The remainder of the vector lies before the T7 promoter and so was not involved in transcription. 2.5 ng of template DNA was used in a 50 µl transcription reaction mix containing 2.5 µl 10 mM ATP, 2.5 µl 10 mM CTP, 2.5 µl 10 mM UTP, 2.5 µl 1 mM GTP, 2.5 µl 10 mM GTP cap analogue (m^7G(5')ppp(5')G-Na salt – S1404S, New England Biolabs Ltd. Herts. UK), 5 µl 10x transcription buffer and 5 µl T7 polymerase plus RNase inhibitor (Boeringer Mannhiem, East Sussex, UK). The reaction was incubated at 37 °C for 1 hour and then 1 µl of DNaseI (10 units/µl) was added and the reaction left for a further hour in order to digest the template DNA. The mRNA produced was cleaned with 1 volume phenol:chloroform:IAA (25:24:1) and precipitated with 2 volumes ethanol and 0.1 volume 3 M sodium acetate at -20 °C for at least 2 hours. The mRNA was collected by centrifugation at 13000 x *g* in a Sorvall MC 12V microfuge for 20 minutes at 4 °C, then resuspended in 10 µl of distilled DEPC treated H_2O. This was stored at -70 °C until use.

Alternatively the 'mMESSAGE mMACHINE' *in vitro* transcription kit from Ambion (Cat. no. 1344, AMS Biotechnology, Oxfordshire, UK) was used according to the manufactures instructions. A 20 µl reaction was prepared containing 1 µg template DNA, 10 µl 2x T7

transcription buffer, 2 µl 10x dNTP mix and 2 µl 10x T7 enzyme mix. The reaction was made up to volume with nuclease free H_2O. The reaction was mixed and incubated at 37 °C for 2-3 hours. 1 µl DNaseI was added and the reaction incubated at 37 °C for a further 15 minutes to remove any remaining template DNA. The reaction was stopped by the addition of 115 µl nuclease free H_2O and 15 µl sodium acetate stop solution. The reaction was cleaned twice with 1 volume phenol:chloroform:IAA (25:24:1) and once with 1 volume chloroform. The reaction was precipitated with 1 volume isopropanol at -20 °C for at least 2 hours. Following precipitation, RNA was pelleted by centrifugation at 13000 x *g* in a Sorvall MC 12V microfuge, 4 °C for 30 minutes. As much isopropanol as possible was removed by pipetting. The remaining isopropanol was removed by vacuum drying for between 15-30 minutes. The RNA was resuspended in 10 µl nuclease free H_2O and stored at -80 °C until required.

2.14.2 Analysis of RNA on a denaturing agarose gel

Gel electrophoresis was carried out as described by Sambrook *et al* (1989). RNA was separated on a 1.2%(w/v) denaturing agarose gel containing 18%(v/v) formaldehyde and 20 mM MOPS buffer. The running buffer was 1x MOPS. Immediately before loading, the RNA was denatured at 65 °C for 15-20 minutes in 0.8 volumes formaldehyde, 2 volumes formamide and 0.4 volumes 10x MOPS buffer, and then snap cooled on ice. The RNA sample was mixed with loading buffer containing 0.25%(w/v) bromophenol blue, 0.25%(w/v) xylene cyanol FF, 15%(w/v) FICOLL and 20 µg ethidium bromide in a 5:1 ratio. Electrophoresis was carried out at 80 volts for 1-2 hours depending on the size of the fragments and gel. The gel was visualised under Ultra Violet light.

Alternatively, if only the presence and basic quality of RNA was to be checked, it was run on a 1%(w/v) agarose (non-denaturing) gel (as described in 2.10).

2.14.3 Surgical removal, stripping and storage of oocytes

The oocytes of a mature female *Xenopus laevis* were removed following the protocol described in Hames and Higgins (1984). The frog was immersed in a 0.1%(w/v) solution of ethyl *m*-aminobenzoate (also known as 3-aminobenzoic acid ethyl ester, tricaine and MS 2-2-2) until fully anaesthetised. This took between 30 and 50 minutes and could be continuously monitored by lack of reflex action. Reflex was measured by pinching the toe and observing

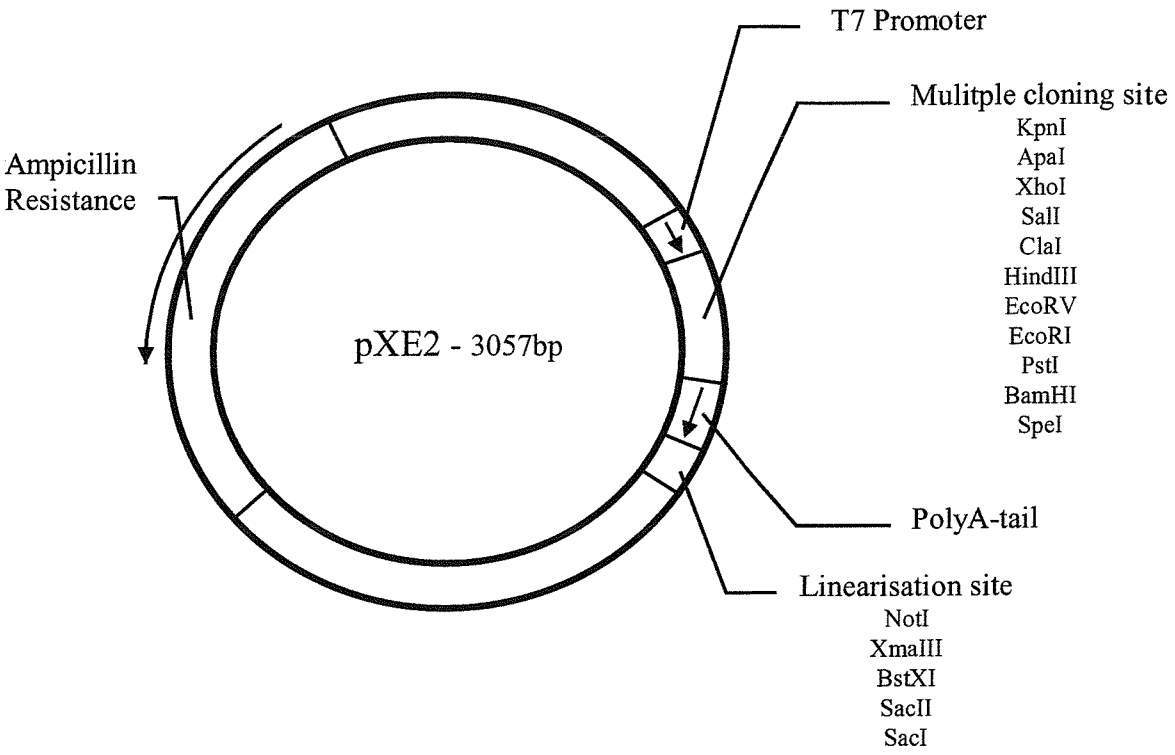

Figure 2.14 - The *Xenopus* expression vector, pXE2.

any leg movement and also by turning the frog and observing any righting action. The lack of both of these responses signified the frog was unconscious. A small (approximately 1 cm) incision was made through the loose skin and body wall in the posterior ventral side. Forceps were used to carefully tease out one lobe of the ovary and a ligature was tied at its base. The lobe was removed with scissors and transferred to modified Barths` saline (88 mM NaCl, 1 mM KCl, 2.4 mM $NaHCO_3$, 15 mM Hepes, 0.3 mM $CaNO_3$, 0.41 mM $CaCl_2$, 0.82 mM $MgSO_4$, 10 µg/ml sodium penicillin and 10 µg/ml streptomycin sulphate). The body wall and skin were sutured separately and the frog allowed to recover in shallow water containing 0.5%(w/v) NaCl. The frogs head was constantly checked to be above water until recovered. The frog was allowed to recover from the first removal, but was killed following the second removal by injection of a concentrated barbiturate (Sagital, Rhone Merieux, Athens GA. 30601, USA) to the brain. This method is in accordance with Home Office protocols. In the 'none recovery' removal it was possible to remove more lobes. The removed lobe/s were separated to give clumps of 10-30 mature oocytes. These were thoroughly washed in MBS and either stored at 4 °C in MBS or enzymatically stripped. The oocytes were stripped by gentle swirling at 18-24 °C in 2 mg/ml collagenase (Sigma, Type II) dissolved in calcium free MBS (88 mM NaCl, 1 mM KCl, 2.4 mM $NaHCO_3$, 15 mM Hepes, 0.82 mM $MgSO_4$, 10 µg/ml sodium penicillin and 10 µg/ml streptomycin sulphate. The oocytes were collagenased for 1 hour in two 30-minute periods. The oocytes could then easily be separated from each other. The oocytes were visually checked at this stage and individual health oocytes selected. Healthy oocytes appear smooth, relatively large, spherical and have a definite division between a dark brown/black animal pole and a white/cream vegetal pole (figure 2.15) The stripped oocytes were stored at 18 °C in MBS until required. Following the stripping, the oocytes could be kept for up to 7 days with twice daily washing in MBS and storage at 18 °C.

2.14.4 Micro-injection of oocytes with mRNA

50 ng of mRNA (approximately 1 ng/nl) was injected into each oocyte. The process was observed under a stereomicroscope and the liquid injected through a pulled borosilicate glass capillary (World Precision Instruments Inc. Sarasota, Florida 34240 USA) (figure 2.15C). The oocytes were transferred through a large diameter fire polished Pasteur pipette and held in position by a small ledge on the microscope table. After injection the oocytes were transferred to a dish containing MBS and incubated at 18 °C for 3-4 days before use. Control oocytes injected with 50 µl of nuclease free H_2O were prepared at the same time as non-injected oocytes.

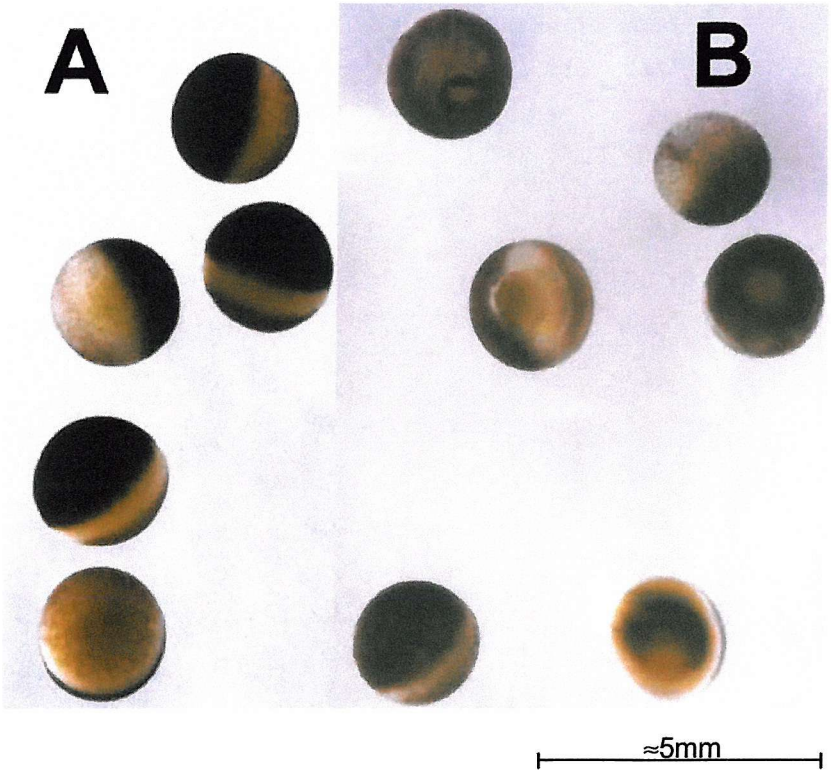

Figure 2.15 - Ooctyes obtained from a mature female *Xenopus laevis.* A) shows healthy oocytes, B) shows unhealthy oocytes, C) shows injection of a healthy oocyte with mRNA.

Oocytes were washed once a day with 18 °C MBS and any dead oocytes removed as these could poison surrounding oocytes (Hames and Higgins 1984).

2.14.5 Radiolabelled amino acid uptake assay

Following incubation at 18 °C for 3-4 days to allow for translation of mRNA and targeting of any protein produced, oocytes were incubated in uptake solution (100 mM choline chloride, 2 mM KCl, 1 mM CaCl, 1 mM MgCl, 5 mM MES, 10 µg/ml sodium penicillin and 10 µg/ml streptomycin sulphate) with a pH between 5 and 8 (pH with Tris or MES) for 30 minutes at room temperature. This allowed the oocytes to equilibrate to the new media. Seven to ten oocytes were then transferred to a single well in a 50 well plate containing 200 µl uptake solution (at appropriate pH), incorporating a mixture of non-labelled and radiolabelled L-[2,3-^{3}H]-histidine (stock 1.7 TBq/mmol) (NEN Life Science Products, Boston, USA) or L-[ureido-^{14}C]-citrulline (stock 2.083 GBq/mmol) (Amersham Pharmacia Biotech, Buckinghamshire, UK) at a final concentration of 100 µM. The oocytes were incubated in this labelled uptake solution for between 30 minutes and 2 hours in a water bath at 25 °C with regular gentle agitation. Following this incubation, oocytes were washed five times with ice-cold uptake solution. 5 ml of 5%(w/v) SDS was added to a scintillation vial with an individual oocyte and left for at least one hour to allow lysis. 4 ml of scintillation fluid was then added and the contents mixed thoroughly by shaking. Scintillations were counted in a Wallac 1209 Rackbeta liquid scintillation counter (Pharmacia, Turku, Finland).

2.14.6 Electrophysiological measurement

2.14.6.1 Dual electrode

The two-electrode voltage clamp technique was conducted as described by Miller and Zhou (2000). Single oocytes were transferred to the perfusion chamber using a fire polished Pasteur pipette, in MBS. The two electrodes were each connected to a pulled capillary needle back-filled with 3M KCl, mounted on Prior micromanipulators (Prior Scientific Instruments, Cambridge, UK). These were lowered into the bathing solution. The voltage clamp module (High voltage V Clamp DevTech, Twickenham, UK) was switched on and voltage display adjusted to 0 mV. Both needles impaled the cell and its membrane potential was allowed to recover to its initial resting value (usually -30 to -40 mV). The oocyte was perfused with choline solution (100 mM choline chloride, 2 mM KCl, 1 mM $CaCl_2$, 1 mM $MgCl_2$, 5 mM MES, 10 µg/ml

sodium penicillin and 10 μg/ml streptomycin sulphate) and its membrane potential and the value reported by the current electrode were monitored for approximately 5 minutes. Oocytes that did not recover their membrane potential to below -25 mV, or displayed large shifts on the current electrode were discarded. The voltage clamp was applied to set the membrane potential to -50 or -80 mV. Flow rate of the perfusion system was approximately 3.0 ml/min. The chamber volume was less than 0.5 ml. A chart recorder (model EPR-200A TOA Electronics Ltd., Tokyo, Japan) was employed to produce a paper record of each experiment. Once a steady base line had been established, an I-V curve was determined. Current-voltage (I-V) relations were obtained with a pulse protocol generated by a 486 computer via a Labmaster DMA A/D interface using the pCLAMP software 5.5 (Axon Instruments, Foster City, CA). The membrane was pulsed for 120 msec in a bipolar staircase to test potentials between -160 and 40 mV with 20 mV increments, followed by a 1-second interpulse interval at the holding potential (Zhou *et al* 1997). The perfusion solution was switched from choline solution to the test solution (containing amino acid) using a six-position teflon rotary valve with 0.8 mm bore (Rheodyne - Jones Chromatography, Mid Glamorgan, UK) and a second steady state established (usually less than 20 seconds). Any changes at this time could be observed on the chart recorder. A second I-V relationship was recorded at the peak of any response. The perfusion system was returned to choline solution and a third I-V relationship recorded once the current returned to baseline. This gave a total of 3 I-V relationship curves for each treatment, one during the treatment and one either side of the treatment.

2.14.6.2 Analysis of electrophysiological data

Membrane transport was described by applying classical enzyme kinetic analysis (Parent *et al* 1992). Using the three I-V curves collected for each treatment it was possible to calculate the change in current due to the application of substrate. The mean of the IV curves measured before and after treatment was subtracted from the IV curve measured during treatment. This change in current was measured at several different amino acid and proton (pH) concentrations. With an array of IV curves it was possible to fit equation **1** to the data. In this equation "substrate" refers to either amino acid or proton, as for amino acid symports they are both effectively substrates for transport. The plots were produced from equation **1** using the numerical analysis program Sigma Plot (version 6.00, SPSS science). The parameters i_{max} (V_{max}) and K_m ($K_{0.5}$) in equation **1** were adjusted for each stepping voltage by the program in order to fit the data.

$$i = \frac{i_{max}\,[substrate]}{K_{0.5} + [substrate]}$$

Equation 1 - for calculating i_{max} (nA) and K_m (mM/μM) from the current (i) (nA) produced by the addition of substrate (mM/μM). Where i_{max} (or V_{max}) and K_m (or $K_{0.5}$) are parameters which are adjusted to fit the collected data.

K_m (also referred to as $K_{0.5}$) is the concentration of amino acid or protons required for the expressed protein to operate at half its maximum rate. This represents the affinity of the protein for the amino acid or protons, the lower the K_m the higher the affinity. I_{max} (also referred to as V_{max}) is the maximum current exerted due to the amino acid or protons applied. This describes the transport rate of the protein. The higher the i_{max} the higher the amount of amino acid and proton transported. The i_{max} value is also an indication of the concentration of transporter protein in the plasma membrane of the oocyte. The higher the i_{max} the higher the expression level of the protein.

By plotting K_m and i_{max} against the membrane voltage it was possible to see if these properties alter with potential. Dependence of I_{max} on pH and voltage indicates electrogenic proton cotransport.

Membrane transporters can only work at a finite rate. Once this rate is reached the transporter is described as saturated. By comparing the i_{max} measurements relative to amino acid concentration and proton concentration it is possible to deduce the coupling ratio of the protein. That is the ratio of amino acid to proton transported by the protein. If, for example, four protons are required to provide a sufficient driving force to move two amino acid molecules across the membrane via the protein, the coupling ratio would be 2:1 (proton:amino acid). This would be represented by the i_{max} for protons being twice that for the co-substrate at saturation. However, from these values alone it would not be possible to deduce how many protons and amino acid molecules move across the membrane in one cycle of the protein, just the ratio.

In order to determine the actual number of protons and amino acid molecules transported per cycle it is necessary to calculate the Hill coefficient of the protein. Using a variant of the formula for producing a substrate concentration against current plot (equation **1**) a further variable (n) is introduced which represents the Hill coefficient (equation **2**). The Hill coefficient will give an approximation of the actual number of molecules transported per cycle of

a protein (Parent *et al* 1992). This number must be an integer, but the difficulty in getting an accurate value, as well as the possibility that the transport characteristics of a protein may alter under different conditions; means that this value should be used in conjunction with the coupling ratio. By using the two values, an accurate estimation of the stoichiometry of the transporter can be formed.

The cooperativity of a protein is a representation of the alteration in binding characteristics toward a substrate upon the binding of another substrate (the same substrate or an alternate one). If the Hill coefficient is 1 then there is no cooperativity. If the Hill coefficient is below 1 then the protein displays negative cooperativity; the affinity for a second substrate molecule decreases upon binding the first substrate molecule. If the Hill coefficient is over 1 the protein displays positive cooperativity; the affinity for a second substrate increases upon binding a first substrate.

$$i = \frac{i_{max}[substrate]^n}{(K_{0.5})^n + [substrate]^n}$$

Equation 2 - for calculating i_{max} (nA), K_m (mM / μM) and the Hill coefficient (n) from the current (i) (nA) produced by the addition of substrate (mM / μM). Where i_{max} (or V_{max}), K_m (or $K_{0.5}$) and n are parameters which are adjusted to fit the collected data.

The cooperativity of a system can also be investigated by rearranging the electrophysiological data to correlate substrate concentration to co-substrate K_m. If affinity for each substrate increases as the co-substrate concentration increases this is a sign of positive cooperativity. In a similar way if affinity decreased as co-substrate concentration increased this would be a sign of negative cooperativity. This same correlation can also show if binding of substrates to a protein is random or ordered. In an ordered system one substrate must bind before another can. This would give two different K_m versus co-substrate concentration plots with the affinity for the first substrate being primarily much higher than the second substrate. In a random system, the substrates bind independently from one another (Jauch and Läuger 1986).

2.15 Structure elucidation

Computer programs were used in order to produce a 2-dimensional model of the transmembrane proteins RcAAP1 and RcAAP3. The amino acid residue sequence of each protein was supplied to two separate programs.

2.15.1 TMHMM (Sonnhammer *et al* 1998)

The TMHMM program was found at the Internet address 'http//:www.cbs.dtu.dk/services/TMHMM-1.0". The amino acid sequence under analysis was supplied to the program. From known properties of the individual residues and specific parameters of all transmembrane proteins the probability of any part of the sequence being intracellular, extracellular, helix cap (both sides), helix core or globular was determined. This was then displayed as a graph of probability for the sequence being intracellular, extracellular or transmembrane. The TMHMM package also produced a designation to every individual residue supplied. The designations used were i (inside), o (outside) and m (membranous). From these two outputs the topology of a protein relative to the plasma membrane can be approximated.

2.15.2 Seqnet (Wisconsin Package)

The seqnet program was found at the telnet address 'seqnet.dl.ac.uk'. The sequence under analysis was supplied to a program called peplot. This program applied a hydrophobic value to each residue. The hydrophobicity of the entire sequence was displayed following analysis at a defined window size. The length of hydrophobic regions under analysis defines the window size used. In the case of putative transmembrane regions a window size of 15-21 residues is recommended. The usual range of transmembrane α-helices being 15-21 residues (Rose *et al* 1985). The program also displayed the hydrophobic moment of the sequence under analysis. The hydrophobic moment was used to determine the symmetry of hydrophobicity of α-helical sections. This was to identify any possible membrane seeking α-helical sections or globular α-helices. Both of these structures tend to be hydrophobic on one surface and hydrophilic on the other. Any areas of the protein with a high hydrophobicity value and high hydrophobic moment could have one of these configurations.

2.16 Chemicals

Unless otherwise stated chemicals were supplied by Fisher Scientific Ltd. (Loughborough, Leicestershire, UK), GibcoBRL Life Technologies Ltd. (Paisley, Scotland, UK) and Sigma-Aldrich Co. Ltd. (Poole, Dorset, UK). Molecular biological enzymes were supplied by Hybaid Ltd. (Ashford, Middlesex, UK), Promega (Southampton, Hampshire, UK) and Stratagene Ltd. (Cambridge, Cambridgeshire, UK). Radiolabelled chemicals were supplied by Amersham Life Science Ltd. (Buckinghamshire, UK). *Xenopus laevis* were supplied by Blades Biologicals (Cowden, Edenbridge, Kent, UK).

Chapter 3 Complementation of yeast mutants and design of selection conditions for the isolation of mutated plant amino acid transporters.

3.1 Introduction

Complementation of specific yeast mutants has become a powerful tool for isolating and biochemically characterising a range of plant membrane transporters (Frommer and Ninnemann 1995, Dreyer *et al* 1999). Heterologous expression in yeast can also be used to study the transport properties of mutated transporters (Bush *et al* 1996, Ichida *et al* 1999). A number of amino acid transporters have been identified and studied using yeast complementation. These include: AtAAP1 - 6, AtLHT1, AtProT1 and 2 and AtCAT1 from *Arabidopsis thaliana* (Frommer *et al* 1993, Hsu *et al* 1993, Kwart *et al* 1993, Fischer *et al* 1995, Rentsch *et al* 1996, Chen and Bush 1997); RcAAP1 and RcAAP3 from *Ricinus communis* (Marvier *et al* 1998, Neelam *et al* 1999); VfAAP2 from *Vicia faba* (broad bean) (Montamat *et al* 1999); PsAAP1 from *Pisum sativum* (pea) (Tegeder *et al* 2000) and LeProT1 from *Lycopersicon esculentum* (tomato) (Schwacke *et al* 1999).

The technique of yeast complementation usually involves using a yeast mutant strain with specific exploitable deficiencies. An example of this would be a strain that is deficient in the uptake of a particular amino acid that can be used as a nitrogen source for growth. Consequently, such a mutant would be unable to grow on a selective medium containing low concentrations of this substrate. The yeast mutant is then transformed with a cDNA library or a particular cloned transporter. Successful complementation is observed when the expression of either a cDNA from the library or the cloned transporter allows the yeast to take up the particular substrate more efficiently from the selective medium and use it for growth.

RcAAP1 from *Ricinus communis* was isolated by yeast complementation using a yeast strain defective in the general amino acid permease (a, *gap, ura3-52*; referred to here as GAP mutants). Yeast cells defective in the *GAP* gene are unable to efficiently transport the amino acid citrulline and hence grow very slowly on low concentrations of this amino acid (Grenson *et al* 1970). In this example, the yeast GAP mutant (a, *gap, ura3-52*) was also defective in the *URA3* gene encoding the enzyme orotidine-5-phosphate decarboxylase, which is required for uracil synthesis. Thus this mutant also required uracil to be supplied for growth, a property which was exploited in the selection of transformants (Marvier *et al* 1998). The GAP mutant was transformed with a cDNA library from *Ricinus communis* in the Nev-N shuttle vector (figure

2.1). This vector contains the *URA3* gene as a selectable marker and confers on transformants the ability to grow without uracil. Transformants, selected on medium lacking uracil, were then transferred to a medium containing citrulline as the sole nitrogen source. One of the clones growing on this selective medium was found to contain the full-length 1.5Kb cDNA of *RcAAP1*. Although *RcAAP1* was able to rescue the growth of the mutant yeast on the citrulline-selective medium, no appreciable uptake of radiolabelled citrulline could be detected in the *RcAAP1* GAP transformants (Marvier *et al.* 1998). This is possibly because RcAAP1 has a low affinity for citrulline and although sufficient was taken up to rescue growth, it was insufficient for detection of radiolabelled citrulline uptake (Marvier *et al* 1998). In an attempt to measure uptake, Marvier *et al* (1998) used an alternative yeast mutant strain, JT-16 (*Mat-a, hip1-614, his4-401, can1, ino1, ura3-52*), that is defective in histidine transport (Tanaka and Fink 1985). *RcAAP1* was able to complement this strain and rescue growth on low-histidine medium (Marvier *et al* 1998). RcAAP1 was shown to transport radiolabelled histidine (Marvier *et al* 1998) and competition analysis indicated that the basic amino acids (histidine, lysine and arginine) showed strongest inhibition of histidine uptake, while the acidic amino acids competed less effectively (Marvier *et al* 1998). Of the neutral amino acids tested, alanine was the most effective inhibitor of histidine uptake, while others showed only moderate inhibition. Glycine, proline and citrulline caused slight stimulation (Marvier *et al* 1998).

Another amino acid transporter cDNA, *RcAAP3*, has also been cloned from *Ricinus*. It was characterised following expression in the GAP yeast mutant, using L-[^{14}C]-citrulline (Neelam *et al* 1999). This appears to encode a broad-substrate permease that can efficiently transport neutral and basic amino acids, with a lower affinity for acidic amino acids (Neelam *et al* 1999).

Information about structure/function relationships of transport proteins can be gained by comparing the functional properties of mutated transporters to those of the WT. Differences in properties, found using heterologous expression systems, can then be attributed to the region(s) of the protein that has been mutated (Bush *et al* 1996, Ichida *et al* 1999). The aim of the work in this chapter was to design suitable strategies for selecting mutated amino acid transporters from *Ricinus*, using yeast as the system for heterologous expression. At the start of this study, *RcAAP1* was already available in both *GAP* and JT-16 yeast mutants (Marvier *et al* 1998) while *RcAAP3* was only available in *GAP* mutants (Neelam *et al.* 1999). The first part of the work in this chapter describes experiments carried out to functionally complement JT-16 with *RcAAP3*. This, together with the other available yeast transformants, was subsequently used to develop suitable mutant-selection procedures. Conditions were designed to select for amino acid transporters with altered transport characteristics. Two selection strategies are

described in this chapter, which were used subsequently in the mutant selection procedure (chapter 4), to provide information on structure/function relationships.

3.2 Results

3.2.1 Complementation of JT16 with *RcAAP3*

The yeast mutant, JT-16, lacks the endogenous high-affinity histidine-uptake system; therefore, it cannot grow on histidine as a nitrogen source when this amino acid is supplied at low concentrations. This yeast mutant also lacks the ability to produce uracil. These characteristics were exploited in the selection procedure for functional complementation with *RcAAP3.*

The Nev-N/*RcAAP3* construct was purified from a DH-10 *E.coli* culture previously transformed with the construct and held in stock. Competent JT-16 yeast was transformed with the purified construct using the method of Dohmen *et al* (1991) (section 2.2). Transformants were selected on a selective medium lacking uracil but containing 3.68mM histidine (high-histidine medium). The Nev-N vector contains the *URA3* gene as a selectable marker and confers on transformants the ability to grow without uracil. The transformation rate was 5.6 x 10^3 transformants/μg DNA and 509 colonies were isolated. These were washed from the plates with distilled water and plated on the same medium but containing 0.13mM histidine (low-histidine medium). Colonies were observed following growth for 3 days at 30°C. Control JT-16 transformed with the Nev-N vector alone were unable to grow on low-histidine medium (figure 3.1) suggesting that growth was conferred by the expression of *RcAAP3*. Ten colonies were selected from five plates and transferred to 5ml liquid cultures containing the same selective medium. JT-16 yeast transformed with Nev-N alone fail to grow on this medium while all ten colonies selected from the plates showed good growth after two days (results not shown). Plasmid DNA was collected from each liquid culture and two restriction digests carried out to confirm the presence of *RcAAP3*. *RcAAP3* had been cloned into the Not I restriction site of the Nev-N shuttle vector. The cloned *RcAAP3* cDNA sequence contains Sal I endonuclease restriction sites on either side of the coding region, within the Not I restriction sites. A representative example of a restriction digest from one of the plasmids is shown in figure 3.2. A Not I restriction digest removed the inserted 1.6Kb *RcAAP3* cDNA and linearised the 7Kb vector (figure 3.2 lane 3). A Sal I restriction digest (figure 3.2 lane 4) removed the 1.6kb

RcAAP3 cDNA insert and cut the 7Kb plasmid into a 1.3Kb and a 5.7 Kb fragment at the vectors Sal I site.

Complementation of JT-16 on low-histidine medium, together with the demonstration of the construct in the transformed yeast, suggests that the transformation of JT-16 with *RcAAP3* has been successful. To confirm that the protein has been successfully expressed and targeted, direct uptake of radiolabelled histidine was measured.

3.2.2 Uptake of radiolabelled histidine following heterologous expression of *RcAAP3* in JT-16

Following the transformation of JT-16 with the *RcAAP 3* / Nev-N construct, the transport properties of RcAAP 3 were investigated by measuring uptake of radiolabelled histidine. Yeast cells transformed with *RcAAP 3* showed time-dependent uptake (figure 3.3). This experiment was repeated for another isolate with a similar profile (results not shown).

3.2.3 The effect of pH on the growth of various JT-16 and GAP transformants

There is evidence that the amino acid permeases under study are proton symports (see introduction, Marvier *et al* 1998, Neelam *et al* 1999). Mutations in the proton-binding site could therefore have an effect on the activity of the amino acid transporters. Preliminary experiments were conducted to determine the effect of pH on the growth of non-transformed JT-16 and GAP mutants and also mutants transformed with a range of constructs to determine whether selection at a particular pH may be a useful strategy for the subsequent isolation of mutated amino acid permeases. Figure 3.4 shows the effect of pH on the growth of non-transformed JT-16 cells and also JT-16 transformed with the Nev-N vector alone, the Nev-N/*RcAAP1* construct and finally the Nev-N/*RcAAP3* construct. In all cases a record of growth was kept on an arbitrary scale of 0 (no growth) to 5 (maximum growth). The growth of non-transformed cells and the transformants was relatively constant between pH 3 and 6. At higher pH, growth was reduced. There was a rapid reduction in growth between pH 7 and 8 for the *RcAAP1* and *RcAAP3* / JT-16 transformants. A slightly different profile was observed for the corresponding GAP transformants (figure 3.5). Non-transformed cells and vector-alone transformants showed a similar level of growth between pH 3 and 7 with growth being reduced at pH 8. The growth of *RcAAP1* and *RcAAP3* transformants appeared to peak between pH4 and 5. Growth was reduced above pH 5, falling to its lowest value at pH 8. The more rapid reduction in growth at high pH observed for the JT-16 transformants suggests that this yeast mutant when grown on

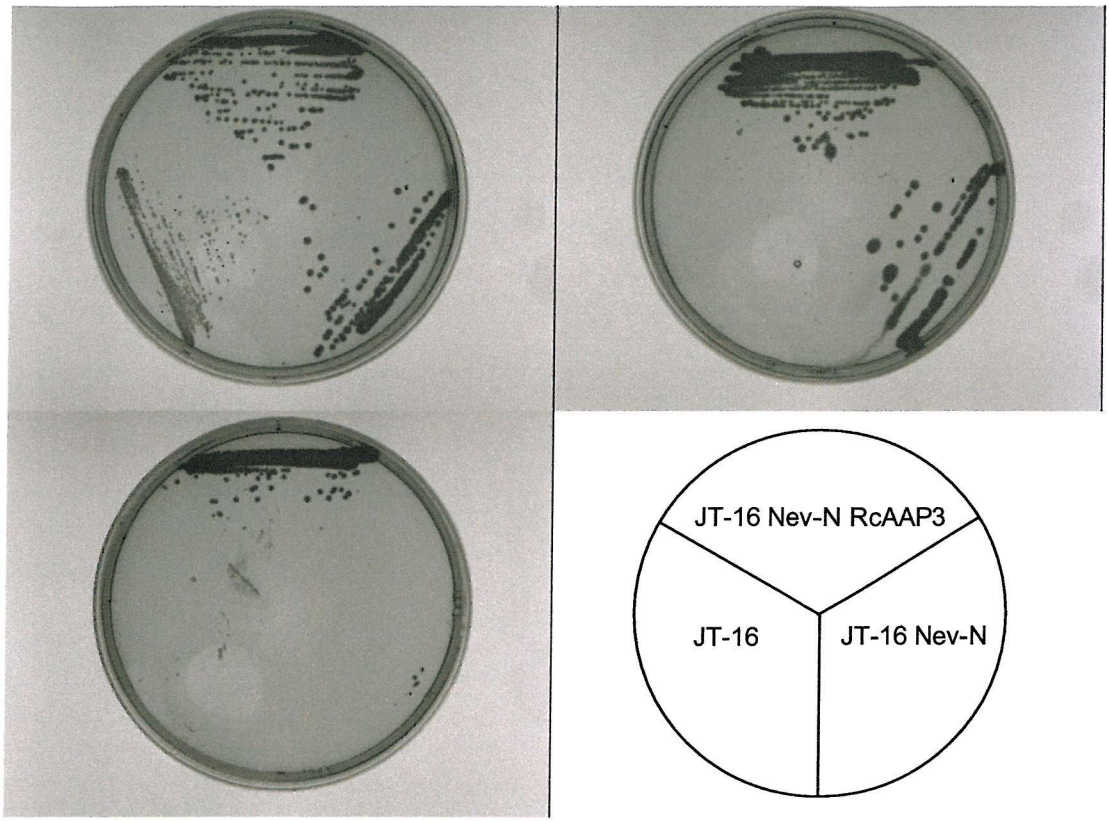

Figure 3.1– Growth of non-transformed JT-16, JT-16 transformed with Nev-N alone and JT-16 transformed with the Nev-N / *RcAAP3* construct on various selective media. The media contain: 3.86 mM histidine plus uracil (top left); 3.86 mM histidine without uracil (top right); 0.13 mM histidine without uracil (bottom left). The key (bottom right) indicates the position of JT-16 and transformants.

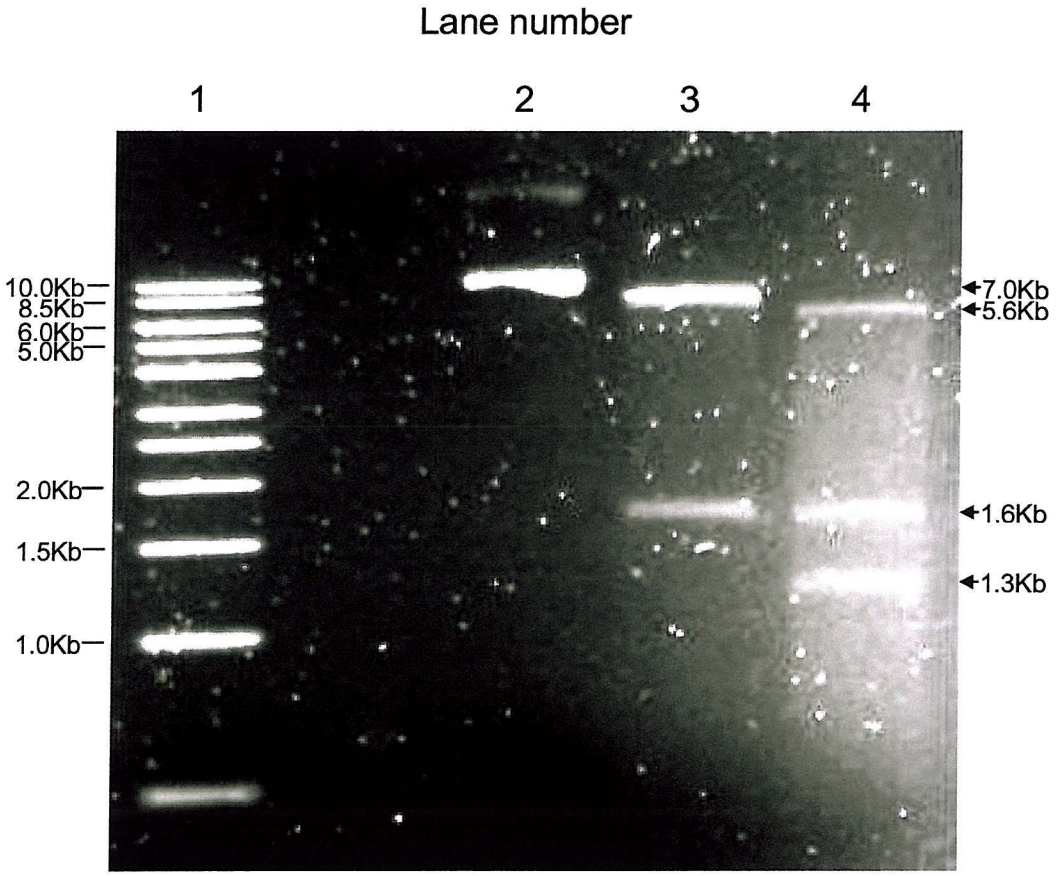

Figure 3.2 – Restriction digest of plasmid DNA isolated from one of the *RcAAP3*/Nev-N JT-16 transformants. 1% agarose gel showing 1Kb Ladder (1), Non-digested *RcAAP3* / Nev-N (2), Not I endonuclease restriction digested *RcAAP3* / Nev-N (3) and Sal I endonuclease restriction digested *RcAAP3* / Nev-N (4)

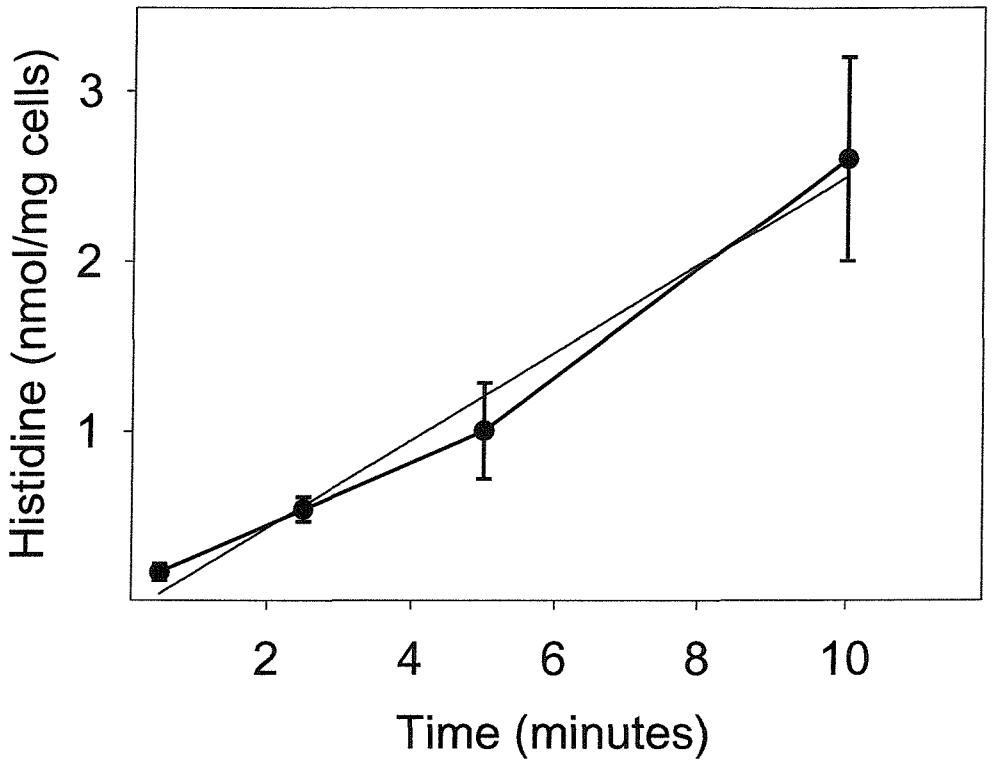

Figure 3.3 – Time-dependent uptake of histidine (50μM) into Nev-N/*RcAAP3* transformed JT16. The rate of uptake, signified by the slope of the line of best fit, is 258.2 (±26.2) pmol histidine/mg cells/minute (R^2=0.98). Results shown are the mean ± S.E obtained from four replicates. Background measured in controls using yeast transformed with vector alone has been deducted.

selective medium at pH 8 may be more useful for selection of mutated transporters affected in their proton binding-properties.

3.2.4 The effect of canavanine on the growth of various JT-16 and GAP transformants

Canavanine is a toxic analogue of arginine. Therefore, the growth of yeast mutants transformed with amino acid permeases that have an affinity for arginine may be inhibited in the presence of canavanine. Alleviation of the canavanine susceptibility could be used as a strategy to isolate mutated transporters with altered affinity for this amino acid. This could reveal information about the substrate-binding site of these permeases. The effect of different concentrations of canavanine on the growth of various GAP and JT-16 transformants is shown in figures 3.6 and 3.7. For experiments with GAP mutants, the previously described +citrulline medium (section 2.1) was used with various concentrations of canavanine. For experiments with JT-16 transformants, arginine was omitted from low-histidine medium (section 2.1). If arginine and canavanine were both available in the medium, arginine may be taken up preferentially and this may necessitate a higher concentration of canavanine in the medium for inhibition. Also arginine itself at high enough concentration in a medium can be toxic. The additive effect of canavanine and arginine could have been toxic purely on a concentration basis.

GAP cells expressing *RcAAP1* and *RcAAP3* grew well after 5 days at 30 °C in canavanine concentrations as high as 0.1 μg/ml (figure 3.6). It should be noted that GAP transformed with the Nev-N vector alone on canavanine-containing media (figure 3.6) failed to grow. The lack of growth is not necessarily associated with the canavanine on these plates but the inability of the yeast to take up sufficient citrulline to support growth (due to the lack of transport system). Growth of GAP expressing *RcAAP1* or *3* was substantially reduced at canavanine concentrations of 0.5 μg/ml and 1.0 μg/ml. JT-16 expressing *RcAAP1* and *RcAAP3* grew well after 3 days at 30 °C with canavanine concentrations of 0.5 μg/ml and 1.0 μg/ml. At higher concentrations (5 and 10 μg/ml) growth was substantially reduced. Growth of JT-16 expressing *RcAAP3* appeared to be slightly less susceptible than cells expressing *RcAAP1*. These results show that on canavanine-containing medium, GAP transformants are susceptible to lower concentrations of canavanine than JT-16 transformants. Approximately ten times higher concentrations of canavanine are required to inhibit growth of JT-16 successfully. These results suggest that for the selection of mutated transporters, the GAP cells at a canavanine concentration of 1.0 μg/ml may provide the best option.

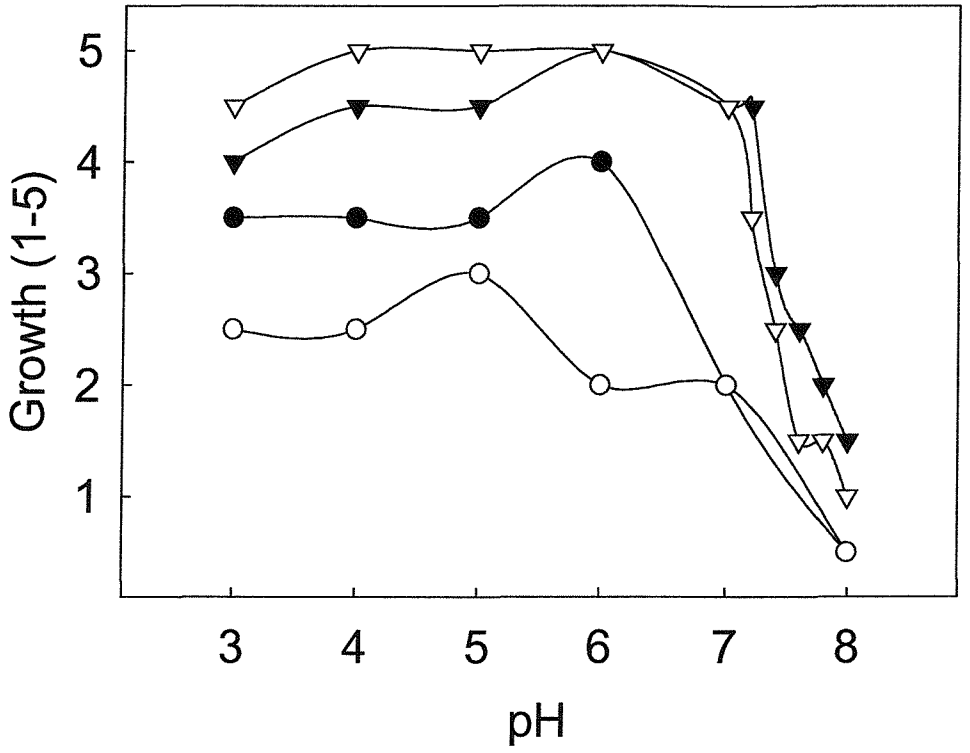

Figure 3.4 – pH-dependent growth of various JT-16 yeast mutants. Non-transformed JT-16 on high-histidine medium (3.86 mM) containing uracil (●), JT-16 transformed with Nev-N on high-histidine medium (3.86 mM) without uracil (○), JT-16 transformed with Nev-N / *RcAAP1* on low-histidine medium (0.13 mM) without uracil (▲), JT-16 transformed with Nev-N / *RcAAP3* on low-histidine medium (0.13 mM) without uracil (△). Growth was determined on plates after 88 hours at 30 °C. The profile is from one representative experiment (using two replicates) repeated twice.

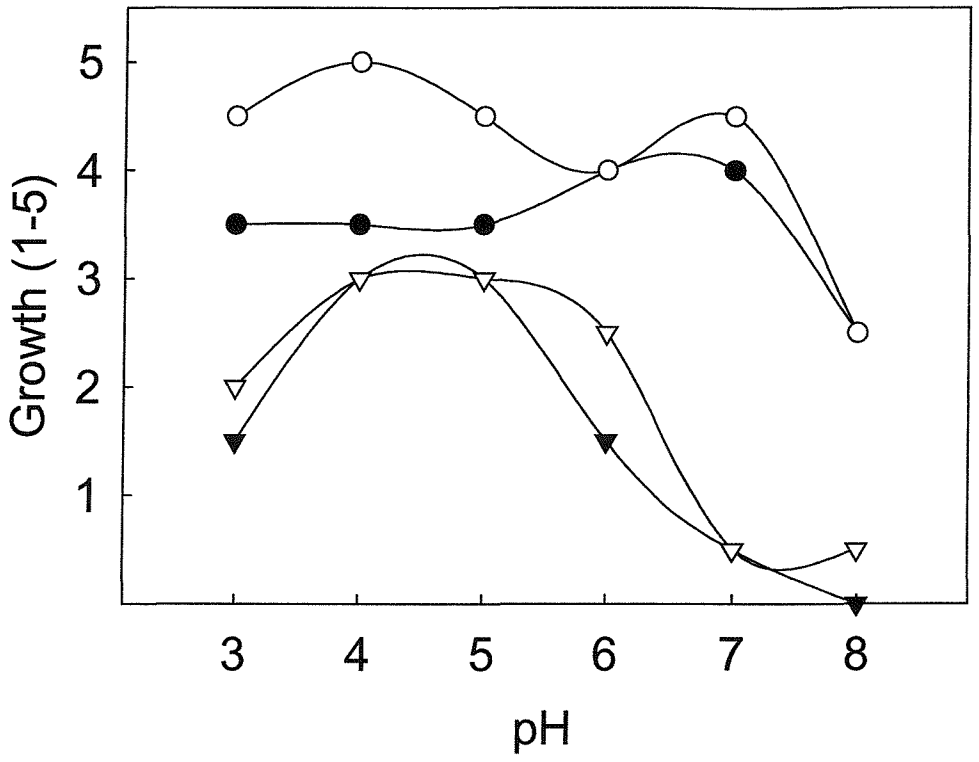

Figure 3.5 – pH-dependent growth of various GAP mutants. Non-transformed GAP on simple dextrose + uracil medium (section 2.1) (●), GAP transformed with Nev-N on simple dextrose medium (○), GAP transformed with Nev-N / *RcAAP1* on +citrulline medium (section 2.1) (▲), GAP transformed with Nev-N / *RcAAP3* on +citrulline medium (△). Growth is after 140 hours at 30 °C. The profile is from one representative experiment (with two replicates) repeated twice.

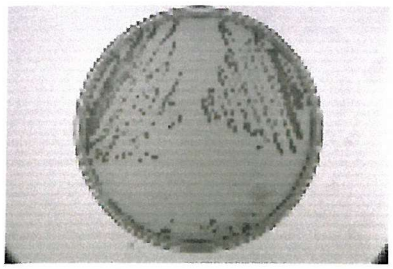

0 µg/ml

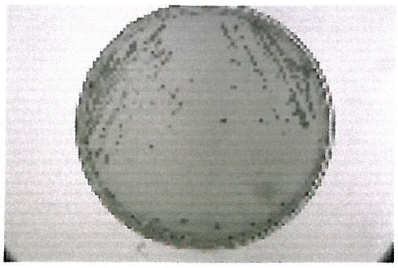

0.05 µg/ml

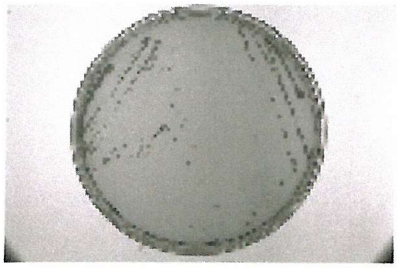

0.10 µg/ml

0.50 µg/ml

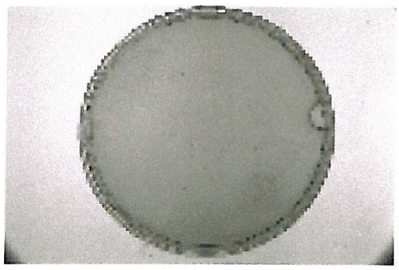

1.00 µg/ml

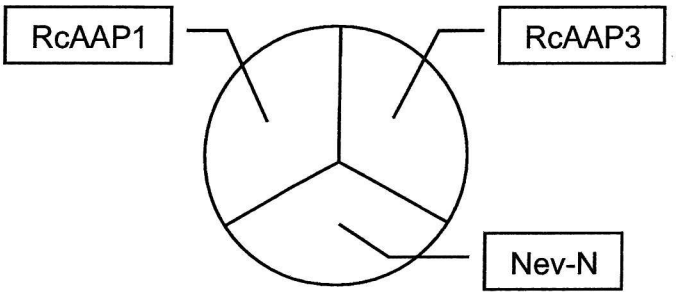

Figure 3.6 – Growth of GAP transformants on increasing concentrations of canavanine. GAP mutant yeast transformed with Nev-N, *RcAAP1* and *RcAAP3*, on citrulline-containing medium (section 2.1) containing various concentrations of canavanine. Growth is shown after 5 days at 30 °C. The plates shown are representative plates from two replicates; the experiment was repeated and a similar result obtained.

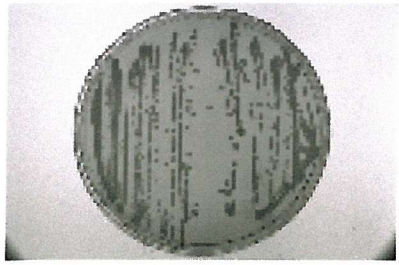

0.0 µg/ml

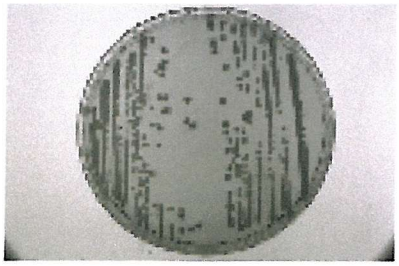

0.5 µg/ml

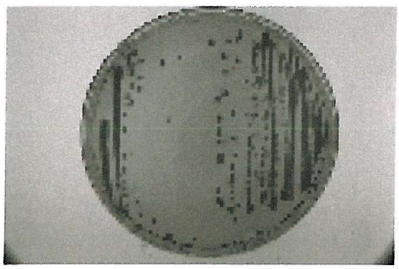

1.0 µg/ml

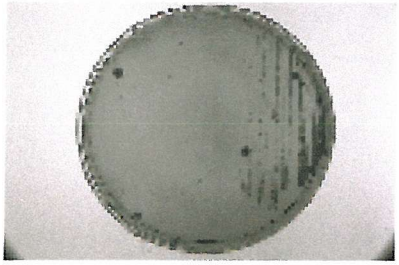

5.0 µg/ml

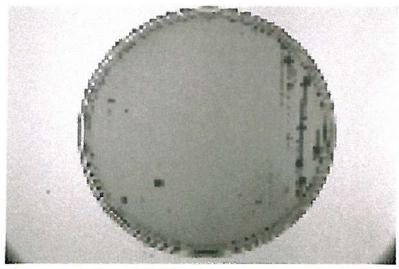

10.0 µg/ml

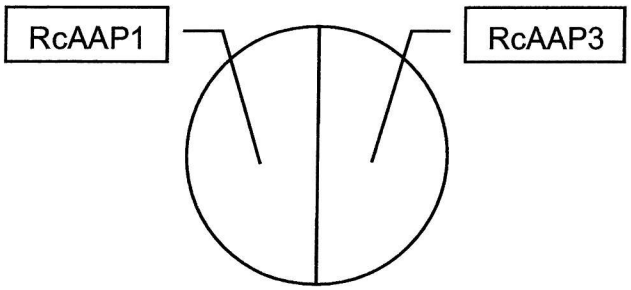

Figure 3.7 – Growth of JT-16 mutants on increasing concentrations of canavanine. JT-16 transformants expressing *RcAAP1* and *RcAAP3*, on low-histidine (0.13 mM) medium (with no arginine) (section 2.1), containing various concentrations of canavanine. Growth is shown after 3 days at 30 °C. This experiment was repeated and a similar result obtained.

3.3 Discussion

The JT-16 mutant can be grown on a high-histidine (3.86 mM), uracil-containing medium but growth does not occur at low histidine concentrations (0.13 mM) or without uracil. This is due to a lack of the high-affinity histidine-uptake system and the lack of uracil production respectively (Jauniaux *et al* 1987). The *URA3* gene is present in the Nev-N shuttle vector and can be used as a selectable marker to select for vector transformants. Growth of JT-16 on low-histidine medium was restored previously by transformation with the Nev-N/*RcAAP1* construct (Marvier *et al* 1998). In the present study, *RcAAP3* was used to complement JT-16 cells, restoring their ability to grow on low-histidine medium. Cells transformed with vector alone failed to restore growth. The *RcAAP3* JT-16 transformants showed time-dependent uptake of radiolabelled histidine with an average rate of 258.2 (±26.2) pmol histidine/mg cells/minute in the presence of 50 μM histidine. This was similar to the rate observed in *RcAAP1* transformants (318 pmol/mg cells/second; Marvier *et al* 1998).

The growth of both JT-16 and GAP yeast mutants is complemented on specific media through the expression of *RcAAP1* or *RcAAP3* (Marvier *et al* 1998, Neelam *et al* 1999, this study). This system can be used further to select for mutated amino acid permeases, by extending selective conditions just beyond those where the WT permeases will complement the mutant phenotype of the yeast. Two different sets of conditions were investigated for their potential to select for mutated transporters. The first investigated the effect of pH (proton concentration) on the growth of transformants, while the second investigated the effects of canavanine, the toxic arginine analogue.

RcAAP1 and RcAAP3 may function as proton symports (Marvier *et al* 1998, Neelam *et al* 1999). Mutations in the proton-binding site could therefore have an effect on the activity of the amino acid transporters. The use of high pH on JT-16 cells grown on low-histidine medium appears to be a suitable selection option for isolating mutated transporters. A dramatic reduction in the growth of JT-16 expressing WT *RcAAP1* and *3* was observed between pH 7 and 8. This appeared to be much more marked than for the GAP transformants over the same pH range. Since the evidence to date suggests that AAPs are proton symports (see introduction) this may imply that at high pH (low proton concentration), growth is impaired due to the inability of the RcAAPs to transport amino acids efficiently for use as a source of nitrogen. Indeed it has been demonstrated previously, using radiolabelled uptake analysis in yeast, that the uptake of histidine is markedly reduced as the pH rises above 5, with transport being nearly completely obliterated at pH 7.5 (Marvier *et al* 1998). Mutated transporters, which are able to complement JT-16 when grown at high pH, may have an altered ability to bind

protons. This could be due to an increased affinity for protons (decrease in K_m) or an increased transport rate. However, if the mutated expressed transporter could transport histidine more efficiently, possibly due to a mutation in the amino acid binding site, then this mutated transporter may also be able to complement growth at high pH. Sufficient levels of amino acid may be transported even at low proton concentrations. These possibilities could be investigated by studying the kinetic characteristics of the mutated transporters.

pH appears to have an effect on the general growth of yeast cells independent of the activity of any expressed transporter. It was found that in the non-transformed and vector-alone transformed cells, there was an impairment of growth at high pH. It is not certain by which mechanism histidine, when supplied at high concentration, is taken up into these cells, but it is possible that endogenous yeast transporters are also affected under these conditions. However the selection procedure is designed to select for mutated plant transporters that will restore growth by allowing amino acid uptake under otherwise unfavourable pH conditions.

Canavanine was found to inhibit the growth of JT-16 and GAP expressing *RcAAP1* and *3*. Much lower concentrations of canavanine were required for the inhibition of GAP. The reason for this is not clear, but it may indicate that canavanine can enter GAP cells more readily than JT-16 cells under the selective conditions used. The GAP cells will be used in subsequent mutant selection experiments. Results from radiolabelled uptake analysis for *RcAAP1* and *RcAAP3* transformants (Marvier *et al* 1998, Neelam *et al* 1999, respectively) have already shown that these permeases are likely to transport arginine and, therefore, canavanine into GAP. Selective conditions will be employed that have sufficiently high canavanine concentrations to be toxic to yeast expressing WT *RcAAP1* and *3*. Mutated transporters, which are still able to function in supplying GAP cells with sufficient nitrogen levels (citrulline from medium), but have reduced levels of canavanine transport/recognition, could be isolated by this method. This altered characteristic could indicate a mutation in the amino acid-binding region of the permease. The two different yeast mutants (GAP and JT-16), although expressing the same amino acid transporters, responded slightly differently to the selection conditions. This could be due, in part, to the difference in selective media used with different mutants. Even with this consideration, the difference in the canavanine concentration, required for inhibition of JT-16 cells expressing *RcAAP3,* was substantially higher than that of GAP expressing the same transporter. JT-16 expressing *RcAAP3* grew at canavanine concentrations as high as 10.0 µg/ml. GAP expressing the same permease was unable to grow at 0.5 µg/ml canavanine. This represents at least a 20-fold difference in canavanine tolerance between the two yeast mutants. The reason for this is not clear but the participation of different endogenous yeast transporters in the transport of canavanine in the two strains could be an explanation. This also

serves to illustrate one of the problems of using yeast in subsequent kinetic measurements. It is often preferable to derive kinetic parameters following expression in *Xenopus* oocytes, which have little background interference (Miller *et al* 1994, Miller and Zhou 2000, see chapter 5).

Chapter 4 Isolation of mutated amino acid permeases using random mutagenesis and selection in yeast.

4.1 Introduction

Random mutagenesis combined with a suitable selection procedure is a useful technique for isolating mutants with desired traits e.g. altered substrate specificity or affinity (Ortiz-Lopez *et al* 2000). It is a powerful technique for obtaining more information about structure/function relationships and has several advantages over site-directed mutagenesis. Primarily, there is no need to have prior detailed knowledge of the gene under mutagenesis. With site-directed mutagenesis, individual amino acids (or small groups) are targeted in order to reveal their functional role. These sites are chosen either with knowledge of their importance or a high probability of some function being assigned to them. However, with random mutagenesis, effectively every amino acid can be mutated and, providing an effective selection is in place, the functionally interesting mutations can be identified. This means that there is no bias toward particular nucleotides as with point mutagenesis. Nucleotides that would have been overlooked by point mutagenesis may be mutagenised and investigated.

Various random mutagenesis procedures have been used to produce random mutations in genes. The procedures tested in this study included DNA shuffling (Stemmer 1994, Crameri *et al* 1996, Crameri *et al* 1997, Crameri *et al* 1998, Ichida *et al* 1999), error-prone PCR (Vartanian *et al* 1996), and chemical mutagenesis using EMS (Curran *et al* 2000). DNA Shuffling is a technique for *in vitro* recombination of pools of homologous genes (Crameri *et al* 1996). In this PCR-based technique, the pool of genes is randomly digested giving products of between 50 and 200 bp. These small DNA products are purified and subjected to multiple rounds of primerless PCR. The theory behind this step is that the small fragments act as a form of primer on each other. After dilution, the resulting products are put through multiple rounds of primered PCR using primers designed to amplify the entire gene. Products of this final PCR step, which are the same size as the initial gene, can then be ligated into a suitable vector and cloned. When used in conjunction with a yeast complementation approach, the 'shuffled' pool would be used to transform a particular yeast mutant and selection conditions would be used to screen for mutants that would confer on the yeast the ability to grow. Selection conditions applied would be unfavourable to yeast not expressing mutagenised proteins e.g. extreme pH, different substrate or altered substrate levels. This would then allow for selection of particular traits. This technique has already been used to investigate structure/function relationships of a plant K^+ -transporter (Ichida *et al* 1999). Random mutations were generated in the *Arabidopsis thaliana* inward-

rectifying K^+ channel, *KAT1* (Ichida *et al* 1999). The mutated cDNA pool was then expressed in a K^+-uptake deficient yeast mutant and the selection carried out on medium containing the alkali metal caesium (Cs^+). Normally Cs^+ blocks KAT1 function and so yeast expressing WT *KAT1* were unable to grow on this medium. The isolated mutants were considered to be insensitive to the effects of Cs^+. Further analysis and sequencing of the mutated K^+ channels revealed that this insensitivity was due mainly to the mutation of two key residues.

Error-prone PCR is a PCR-based protocol using altered reaction components, designed to introduce errors in amplified products. The DNA polymerase used in standard PCR, *Taq* polymerase (from the archeobacterial thermophile *Thermus aquaticus*) has no proof-reading ability and so a low level of errors occurs even under conditions of optimal fidelity. However, by altering the ratio of one dNTP in relation to the remaining three (Vartanian *et al* 1996, Giver *et al* 1998, Ichida *et al* 1999) or by including Mn^{2+} in the reaction (Goodman *et al* 1983, Fromant *et al* 1995), it is possible to increase the rate at which errors occur. Under normal conditions the presence of the divalent cation Mg^{2+} is required in order for the polymerase to operate. The addition of $MnCl_2$ to the standard PCR mix alters the way in which the divalent-cation-dependent DNA polymerase operates. This has been attributed to the fact that nucleotides bind in a distorted manner at the active sites of the polymerase in the presence of Mn^{2+} (Goodman *et al* 1983). By depleting the concentration of one dNTP in the standard PCR mix, the error rate is increased. This is believed to be due to a bias characteristic of the *Taq* polymerase. Under certain dNTP concentrations, bases are substituted incorrectly, with dNTPs at higher concentrations sporadically replacing those at lower concentrations. This mismatching would be repaired by a proof-reading polymerase but is left incorrect by *Taq* polymerase.

Random mutagenesis involving chemical treatment with EMS has been used successfully to mutate *ACA2*, a calmodulin-activated Ca^{2+}-pump (Curran *et al* 2000). Following the expression of *ACA2* in a yeast deficient in two endogenous Ca^{2+}-pumps (K616), chemical mutagenesis was achieved using EMS. The yeast was selected on a Ca^{2+} -deficient medium, which did not support growth of this yeast expressing the WT pump. Plasmid DNA was isolated from yeast colonies that successfully grew on this medium, in order to sequence any expressed *ACA2* derivatives. Useful information was obtained in this study in identifying regions playing a role in auto-inhibition (Curran *et al* 2000).

The aims of the work described in this chapter were firstly to introduce random mutations into the *Ricinus communis* amino acid transporter cDNAs, *RcAAP1* and *3*. Secondly, to use the selection procedures developed for the yeast mutants, JT-16 and GAP (described in chapter 3) to isolate transporters with altered transport characteristics that would confer on the yeast mutants the ability to grow under selective conditions. Finally, to

sequence the mutated transporters and, by comparison with the WT transporters, provide information regarding functionally important residues.

4.2 Results

Three different procedures were investigated for their potential in generating mutant amino acid permeases: DNA shuffling, error-prone PCR and chemical mutagenesis of yeast expressing WT permeases.

4.2.1 DNA Shuffling

The initial step in DNA shuffling is the random fragmentation of the genes of interest. Due to the difficulties experienced in obtaining large and pure quantities of *RcAAP1* and *RcAAP3*, initial experiments in random fragmentation were performed using *RcAAP3* cloned in the yeast shuttle vector, Nev-N. The construct was digested using DNase I at a final concentration of 0.04 units/µl over a range of time points at 28 °C. When the digests were viewed on a 2% agarose gel (figure 4.1) progressive fragmentation was observed. The final lane (10), representing a 40-minute digest, contained an approximate average length of DNA of 100 bp. The recommended for DNA shuffling being 50-200 bp. This preliminary experiment provided an approximation of the experimental conditions required for successful digestion with DNase I.

RcAAP1 was digested from Nev-N using a Not I restriction enzyme and purified (results not shown). This material was then randomly digested with DNase I. Digest conditions were modified from that described previously as initial attempts to digest *RcAAP* cDNA with 0.04 units/µl DNase for 40 minutes resulted in low levels of digestion. Results in which 100ng of cDNA in a 10µl reaction mix was digested using between 0.02 and 0.2 units/µl of DNase I for 30 minutes at 30°C are shown in figure 4.2. Digested products were run on a 2% agarose gel against an undigested *RcAAP1* control (figure 4.2). The section of the agarose gel containing the smear corresponding to DNA of approximately 50-200 bp was excised. The digested nucleic acid was purified from the agarose gel using electroelution (section 2.11.1.2). The yield of DNA retrieved from agarose gels using this method was approximately 10% (using the 134 bp and 75 bp fragments from Gibco 1Kb ladder). This is a relatively low yield as compared to the retrieval of larger fragments by this and alternative methods. The small size of the fragments makes retrieval more difficult (Electro-eluter model 422 manual. Bio-Rad laboratories Ltd., Hemel Hempstead, Hertfordshire, UK). After purification the small base pair products were subjected to primerless PCR, which was followed by primered PCR, using primers designed to amplify

the entire gene (figure 2.4). A sample of the product was run on a 1% agarose gel, against an *RcAAP1* control (figure. 4.3). The resulting product from the shuffling process was observed to be the same size (approximately 1500 bp) as the control. However, the yield of this product was generally very low in comparison to control PCR reactions run alongside the shuffled products. On average, 5-20 ng/µl of shuffled product would be constructed compared to 150-200 ng/µl from a control PCR under standard conditions. This is possibly due to poor reconstruction of small base pair products in the primerless PCR step. In an attempt to increase yield, the DNase I digest was done in the presence of manganese (section 2.11.1.1) (Lorimer and Pastan 1995). The Mn^{2+} ions increase the activity of the enzyme and also alter the way in which it cuts. A final DNase I concentration of $1.8x10^{-5}$ units/µl was used which is over a thousand times less than in the absence of manganese). DNase I creates double stranded breaks when in the presence of Mn^{2+}, as opposed to single stranded nicks when in the presence of Mg^{2+}. The digested fragments created in this way should act as more effective primers in the primerless PCR step. Additionally Mn^{2+} makes the enzyme less effective at cutting DNA smaller than 50 bp, making it more difficult to over-digest the template (Lorimer and Pastan 1995). The main advantage of this method is that there is no requirement for purification of the digested material using electrophoresis as the resulting products can be used directly in primerless PCR. However, in this study the use of digested product obtained in the presence of Mn^{2+} had no noticeable effect on overall yields (result not shown).

Following the primered-PCR step to produce shuffled products, a restriction digest was performed using EcoRI. The *RcAAP1* primers, which had been used, incorporate an EcoRI site onto the ends of the products (figure 2.4). The digestion creates 'sticky ends' on the shuffled products, facilitating ligation into the yeast shuttle vector Nev-E. However, several problems were encountered with the experimental procedure up to this stage. A major problem was that a background DNase I activity appeared to be constantly present in the pools of shuffled product. This meant any products produced through this method degraded over a relatively short time. Additionally the amplification of products of the correct size was extremely difficult. Often no products of the correct size would be produced at all. The mixture of products produced following the primered PCR step of the protocol were often visualized on a 1% gel as a smear, generally smaller than the desired size of product (figure 4.4). The difficulty in producing shuffled product from a single gene was seen to an even larger degree when *RcAAP1* and *RcAAP3* were shuffled together. DNA shuffling can be used to mix two genes together by using a DNase I digested pool from both genes and primers from both genes. In this way it is thought that properties from each gene can be incorporated into the one product (Stemmer 1994, Crameri *et al* 1996, Crameri *et al* 1997, Crameri *et al* 1998, Ichida *et al* 1999). Only smears were produced following primered PCR

with a variety of mixtures of the four relevant primers (results not shown). These smears would rarely show any products over 1Kb.

These factors made incorporation into a yeast shuttle vector and subsequent transformation of bacteria very difficult. Ligation of the product into the yeast shuttle vector was attempted at least ten times, using various shuffled products; however, no transformants with a successfully ligated insert were constructed. Considering these combined problems, other methods were investigated to produce a library of randomly mutated products.

4.2.2 Error-Prone PCR

Initially, PCR of *RcAAP1* and *RcAAP3* was performed with the inclusion of $MnCl_2$ in the standard PCR mix. This markedly reduced the yield from PCR reactions regardless of the three Mn^{2+} concentrations used (results not shown). To counteract this, the annealing temperature was reduced and the elongation time lengthened. This increased yield to a certain extent but at the same time reduced the specificity of the amplification. Products of the correct size were often not visible from this procedure on an agarose gel (figure 4.5). The average yield from PCR including $MnCl_2$ would be 1-10 ng/µl, compared to 150-200 ng/µl from a control PCR under standard conditions.

PCR with a dNTP bias was then performed. A depleted concentration of dATP and dGTP were used separately with the aim of causing mis-incorporations. As with the previously described error-prone PCR method, yield was decreased and again this was counteracted by decreasing annealing temperature and increasing elongation time. This gave a very slight increase in yield but still left the efficiency of the PCR substantially depleted (figure 4.5 and 4.6). The average yield from the PCR with a depleted dNTP would be 5-20 ng/µl, compared to 150-200 ng/µl from a control PCR under standard conditions. A slight reduction in yield was expected from the depleted-dNTP PCR (Martinez *et al* 1994, Vartanian *et al* 1996), but not to the extent observed in this study. It has been reported that the inclusion of $MnCl_2$ in a PCR has had no significant effect on yield at low concentrations (such as 0.625mM used in this study) (Fromant *et al* 1995), but that the yield does decrease rapidly as the concentration increases (Fromant *et al* 1995, Vartanian *et al* 1996). The consistent problems of obtaining adequate yield meant that this method was also not suitable for production of a library of randomly mutated transporters.

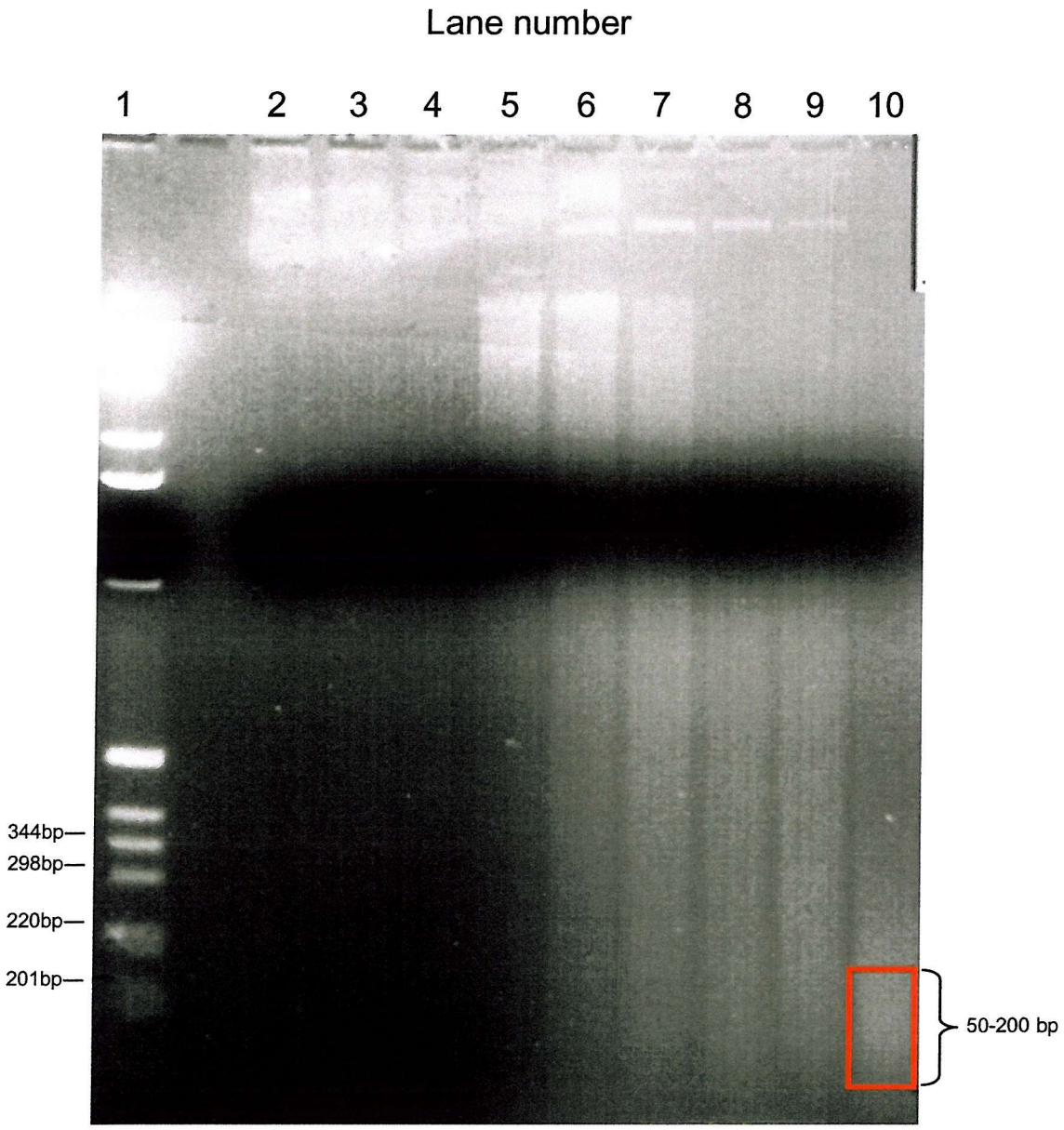

Figure 4.1 – DNase I digest of *RcAAP3* / Nev-N over time. DNase (0.04 units/µl) digest of *RcAAP3* / Nev-N on a 2% agarose gel. 1Kb ladder (1), *RcAAP3* / Nev-N (2), *RcAAP3* / Nev-N + EDTA (3), *RcAAP3* / Nev-N + 0 min DNase I (4), 5 min DNase I (5), 10 min DNase I (6), 15 min DNase I (7), 20 min DNase I (8), 30 min DNase I (9), 40 min DNase I (10).

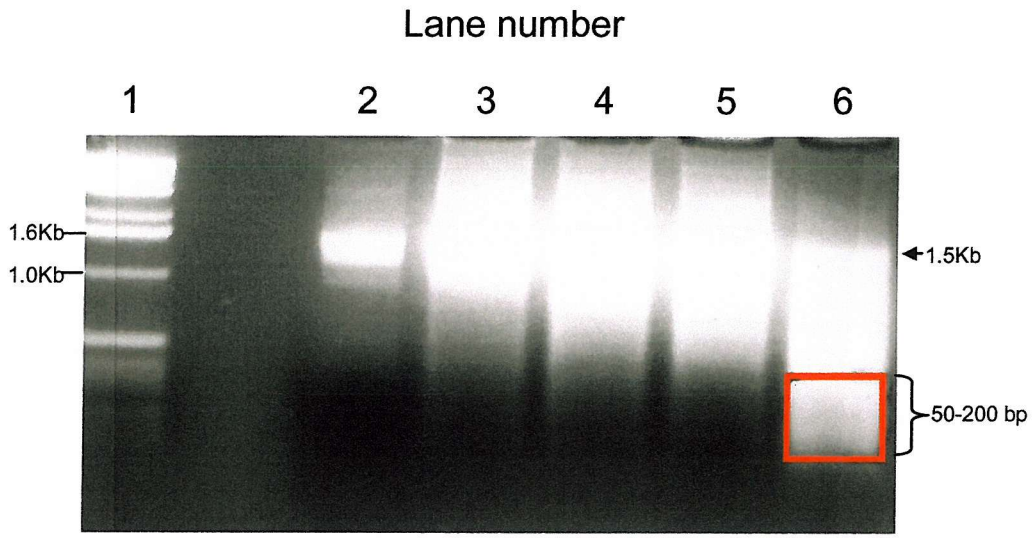

Figure 4.2 – 30 minute digests of *RcAAP1* cDNA with a range of DNase I concentrations. 2% agarose gel containing 1Kb ladder (1), *RcAAP1* cDNA (2), DNase I digested *RcAAP1* using 0.02 units/µl (3), 0.05 units/µl (4). 0.1 units/µl (5) and 0.2 units/µl (6) in a 10µl reaction. All samples contain approximately 1µg DNA. The area in lane 7 representing approximately 50-200 bp was excised.

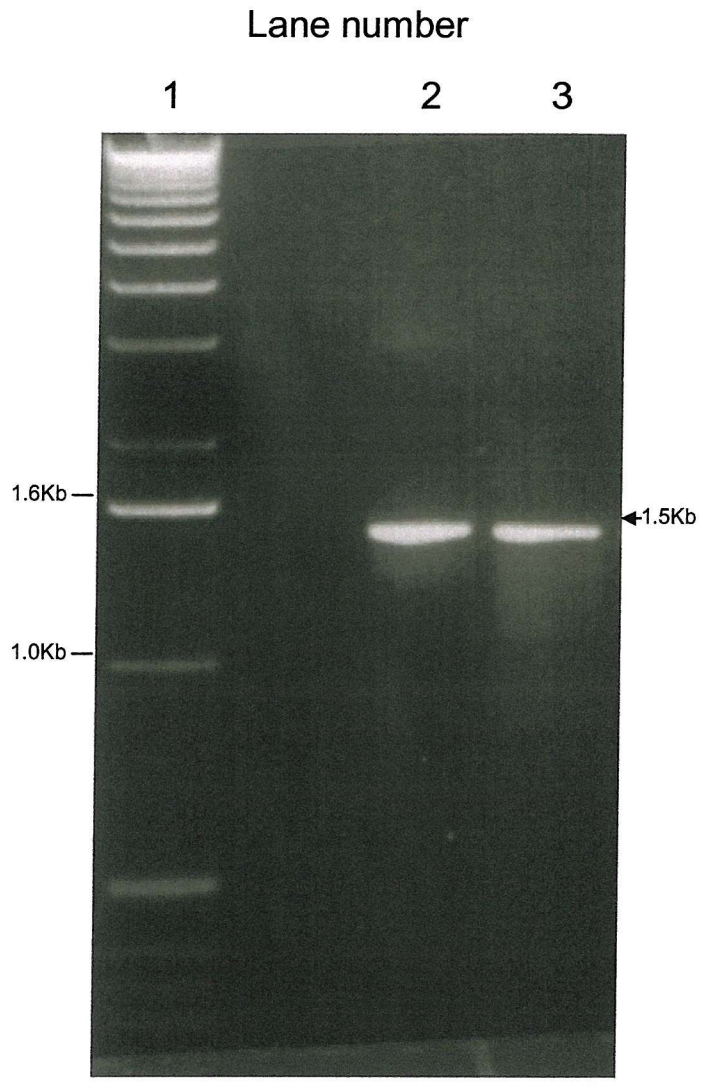

Figure 4.3 - Shuffled *RcAAP1* product compared to WT *RcAAP1* cDNA. 1% agarose gel containing 1Kb ladder (1), WT *RcAAP1* cDNA (2), DNA shuffled *RcAAP1* product (primered-PCR product) (3).

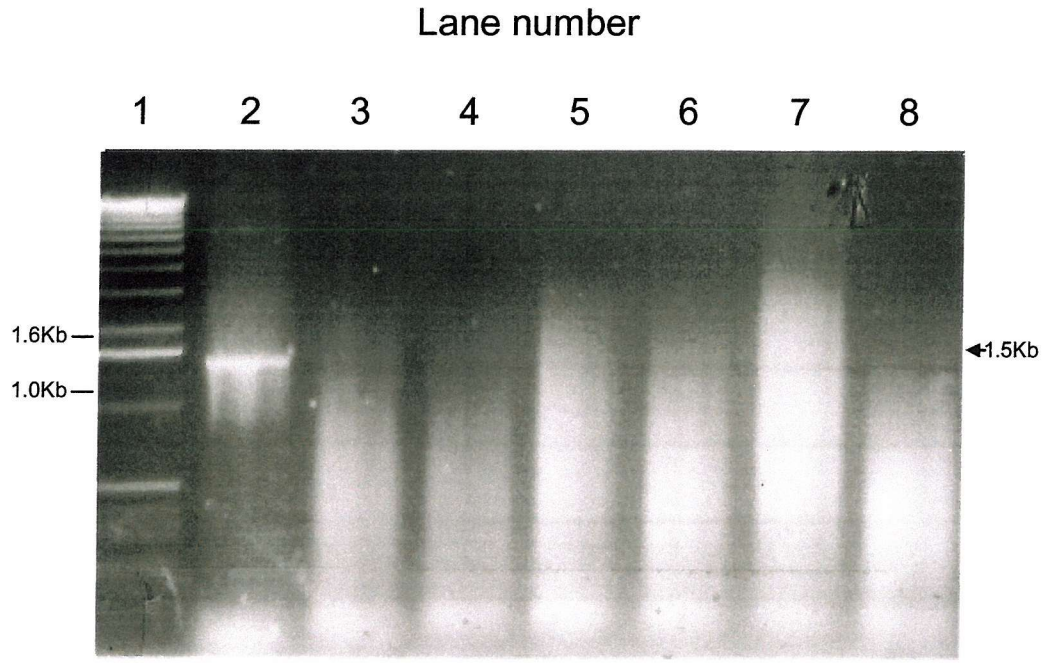

Figure 4.4 – Non-specific products generated from DNA-shuffling. 1% Agarose gel containing 1Kb ladder (1), *RcAAP1* cDNA (2), DNA shuffled *RcAAP1* product from 0.25ml (3), 1.0ml (4) and 2.0ml (5) primerless PCR product (derived from DNase I digested *RcAAP1* material). DNA shuffled *RcAAP3* product from 0.25 ml (6), 1.0 ml (7) and 2.0 ml (8) primerless PCR product (derived from DNase I digested *RcAAP3* material). This is representative of the majority of results from the DNA-shuffling technique.

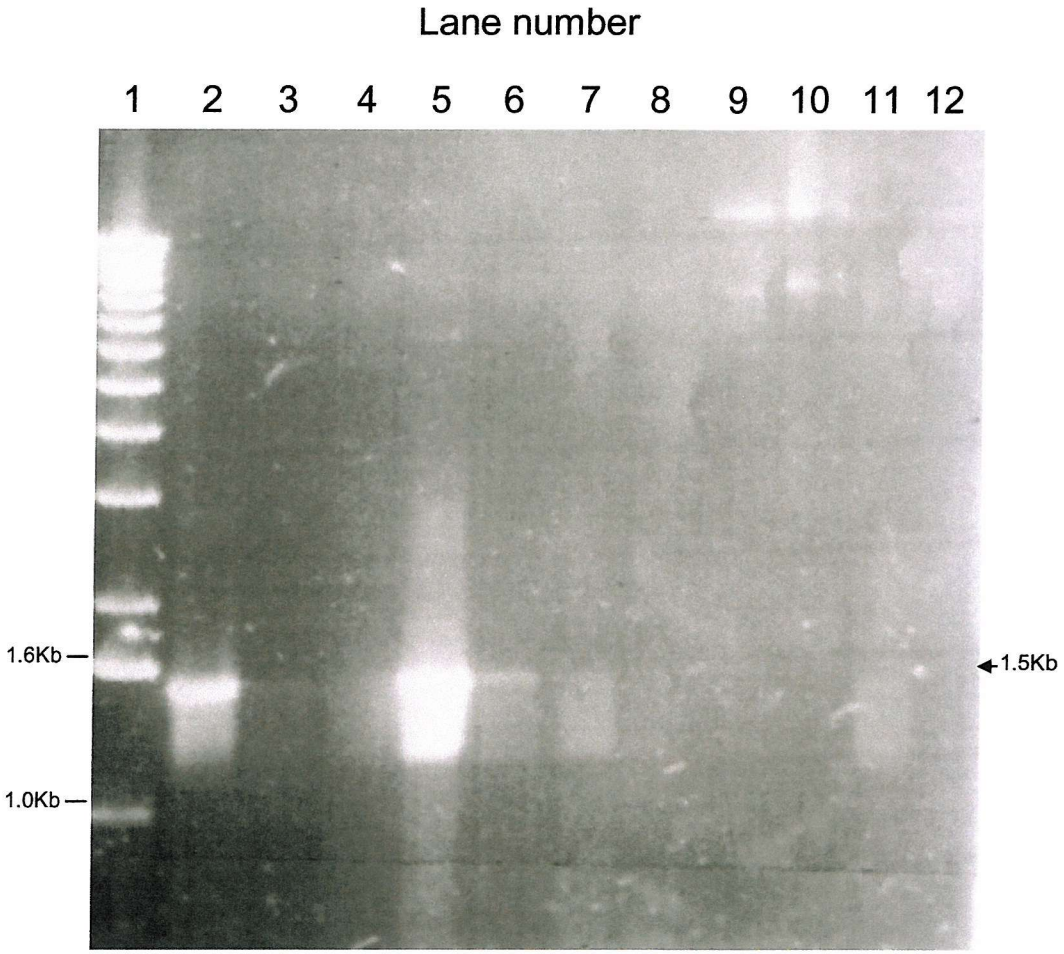

Figure 4.5 – Products obtained from error-prone PCR. 1% agarose gel containing 1Kb ladder (1), *RcAAP1* cDNA from standard PCR conditions (2), *RcAAP1* PCRs with depleted GTP (3) and ATP (4). *RcAAP3* cDNA from standard PCR conditions (5), *RcAAP3* PCRs with depleted GTP (6) and ATP (7). *RcAAP1* PCRs with 0.625mM $MnCl_2$ (8), 1.25mM $MnCl_2$ (9) and 5.0mM $MnCl_2$ (10). *RcAAP3* PCRs with, 0.625mM $MnCl_2$ (11) and 1.25mM $MnCl_2$ (12). This is representative of the majority of results from error-prone PCR.

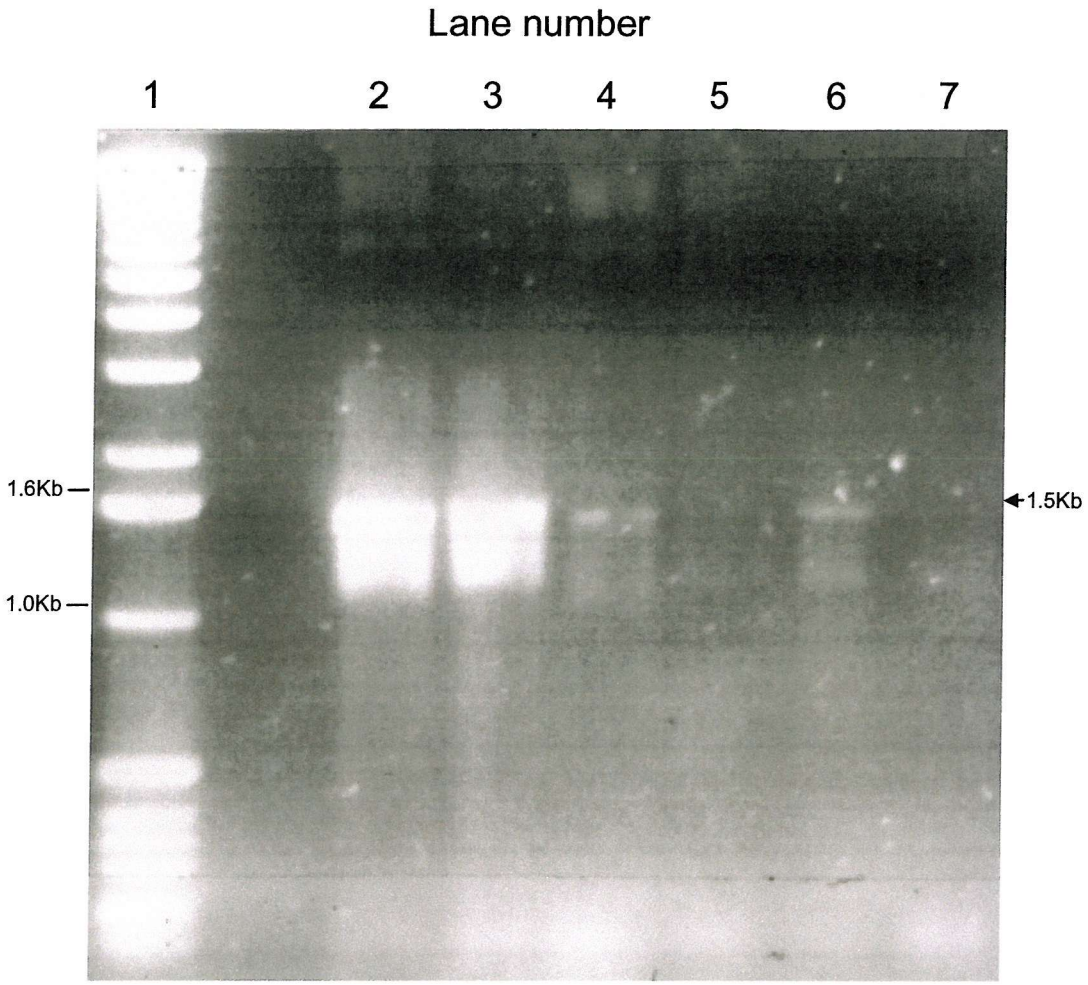

Figure 4.6 – Products obtained from error-prone PCR with depleted dNTP. 1% agarose gel containing 1kb ladder (1), *RcAAP1* cDNA from standard PCR conditions (2), *RcAAP3* cDNA from standard PCR conditions (3), *RcAAP1* PCRs using depleted GTP (4) and depleted ATP (5), *RcAAP3* PCRs using depleted GTP (6) and depleted ATP (7). This is representative of the majority of results from depleted dNTP error-prone PCR.

4.2.3 Chemical Mutagenesis

4.2.3.1 Mutagenesis and Selection

JT-16 and GAP yeast mutants expressing *RcAAP1* or *RcAAP3* were mutagenised using EMS for both 30 and 60 minutes. Following washing, yeast were plated on a range of selective media with either a raised pH or containing canavanine (see chapter 3). Due to time constraints raised pH selection was not done using *RcAAP3*-expressing yeast. The selection conditions used were designed to give an optimum range for selection. The raised pH selective medium for each yeast strain were set between pH 7.2 and pH 8.1. Canavanine concentrations were set between 0 and 10 μg/ml. JT-16 and GAP yeast expressing WT *RcAAP1* were plated as the controls. These controls were not subjected to EMS but were washed in an identical manner to the mutagenised samples. JT-16 expressing WT *RcAAP1* had been shown to have dramatically reduced growth at pH ranges over 7.0 (chapter 3). Growth was nearly completely obliterated at pH 8.0 after 88 hours at 30 °C (figure 3.7). Therefore, the plates containing the mutagenised and control yeast were assessed after 48 hours of growth at 30 °C. Distinct colonies were apparent on the plates containing the mutagenised yeast, and the colonies were progressively more distinct the higher the pH of the medium. On the control plates, growth was visible at pH 7.2 but reduced rapidly as the pH increased, with no growth visible at pH 8.1 (figure 4.7). After a similar time, no colonies were apparent in the mutagenised GAP yeast expressing *RcAAP1* and *3*. These were placed back in the incubator and observed every 24 hours for a further 72 hours. After 120 hours of growth there were no colonies visible on the plates containing either the mutated or the control yeast (figure 4.8). This chemical mutagenesis of GAP / *RcAAP1*, GAP / *RcAAP3* and JT-16 / *RcAAP1* was repeated and similar results were observed.

Twelve colonies from the experiment with JT-16 (figure 4.7) were removed from each of the 30 minute and 60 minute pH 8.1 selective plates. These were labelled A-L (30 minute mutation) and M-X (60 minute mutation). The growth of JT-16 expressing each of the twenty-four mutants was compared to that of JT-16 expressing WT *RcAAP1* on low-histidine concentration (0.13 mM) liquid medium at pH 7.5 (LHpH7.5). The growth of the majority of yeast expressing mutagenised permeases (15 out of 24) was faster than that of yeast expressing WT *RcAAP1* after 25 hrs (figure 4.9) (appendix 1). This would explain why these colonies had been visible on the selective plates before any non-mutagenised controls. It was also observed that yeast expressing mutagenised transporters would start to lyse after approximately 40 hours of growth on LHpH7.5. Yeast expressing WT *RcAAP1* did not lyse and growth continued beyond 40 hours (appendix 1). The reason for the lysis is unclear. When a similar experiment was carried out at pH 8.1 the mutagenised yeast grew

initially but lysed after only 24 hours (results not shown). The time to lysis thus appears to decrease with the increase in pH. Because of the lysis in liquid-selective medium, the isolates and non-mutagenised JT-16 expressing *RcAAP1* were grown in YPD liquid medium and then spread on plates containing low-histidine selective medium at pH 8.1 (LHpH8.1). Non-mutagenised JT-16 showed no growth after 96 hours. All the mutagenised isolates grew successfully on the selective medium after 48 hours. A representative result from the experiment is shown in figure 4.10.

Previously, GAP expressing WT *RcAAP1* and *RcAAP3* did not grow on selective medium with canavanine concentrations above 0.1μg/ml (chapter 3). However, in subsequent experiments (figure 4.11), a background lawn of growth was observed for mutagenised and non-mutagenised GAP expressing *RcAAP1* and *RcAAP3* at canavanine concentrations as high as 10 μg/ml. Growth of larger distinct colonies was visible for mutagenised yeast, the colonies being more distinct at the higher canavanine concentrations (figure 4.11). The results from this selection were not as distinct as the previous experiments with raised pH, which had shown much less background growth. Six of the colonies from the canavanine-containing selective medium (three expressing *RcAAP1* and three expressing *RcAAP3*) were isolated and cultured on the same selective medium in the absence of canavanine. The growth of these six isolates was very slow compared to that of non-mutagenised GAP expressing WT *RcAAP1*. Growth of Non-mutagenised yeast was observed on selective medium after 7 days whereas mutagenised isolates showed very weak growth even after 9 days. The difficulty in growing these isolates, their less clear-cut selection and time restraints meant that only the isolates from the raised pH selection were investigated further.

4.2.3.2 Isolation of potential mutated cDNAs and transformation of yeast

It was necessary to test whether the mutagenised yeast could grow on pH 8.1 selective medium due to mutations in *RcAAP1* rather than an alteration of the yeast genome. This was performed by preparing plasmid DNA from the mutagenised isolates and transforming fresh competent JT-16. If this yeast was then able to grow on pH 8.1 selective medium it would suggest that this ability would have been conferred by a *RcAAP1* mutant. Plasmid DNA was retrieved from the twenty four isolates; however initial experiments did not provide sufficient amounts of good quality DNA to carry out yeast transformation. Also it was found that this material could not be used successfully for bacterial transformations. This may have been due to low quality DNA or mutations in the ampicillin resistance region of the Nev-E plasmid. As an alternative strategy, PCR was used to amplify the insert to obtain sufficient amounts, which could then be ligated into Nev-E, cloned in bacteria and used for yeast transformation. In the majority of cases it was necessary to use lower

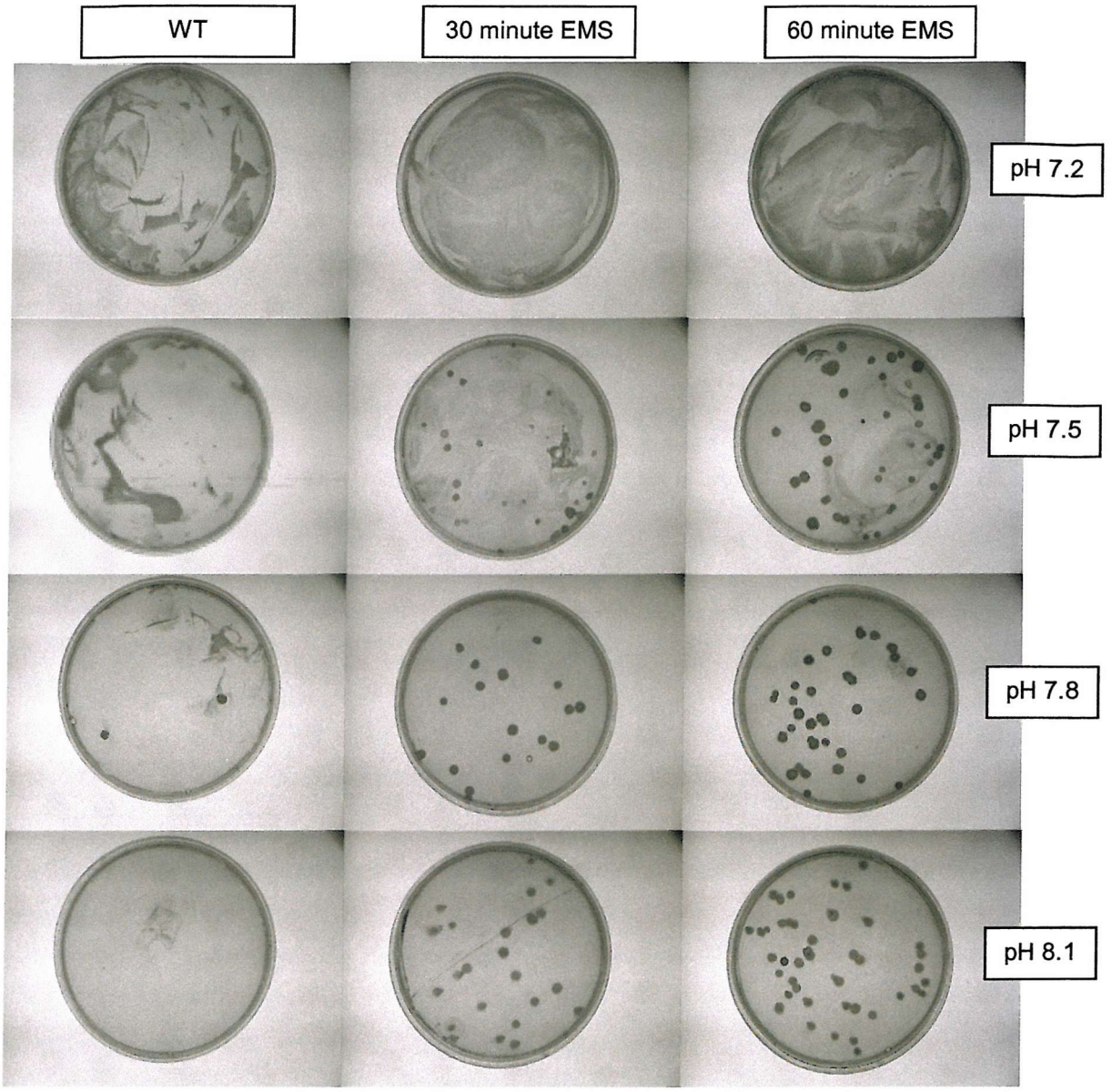

Figure 4.7 – Growth of EMS mutagenised JT-16 expressing *RcAAP1* on raised pH medium. A range of raised pH, low-histidine selective plates with non-mutagenised (left), 30 minute EMS mutagenised (middle) and 60 minute EMS mutagenised (right) JT-16 expressing *RcAAP1*. Incubation was for 48 hours at 30 °C. This is a representative experiment, repeated twice.

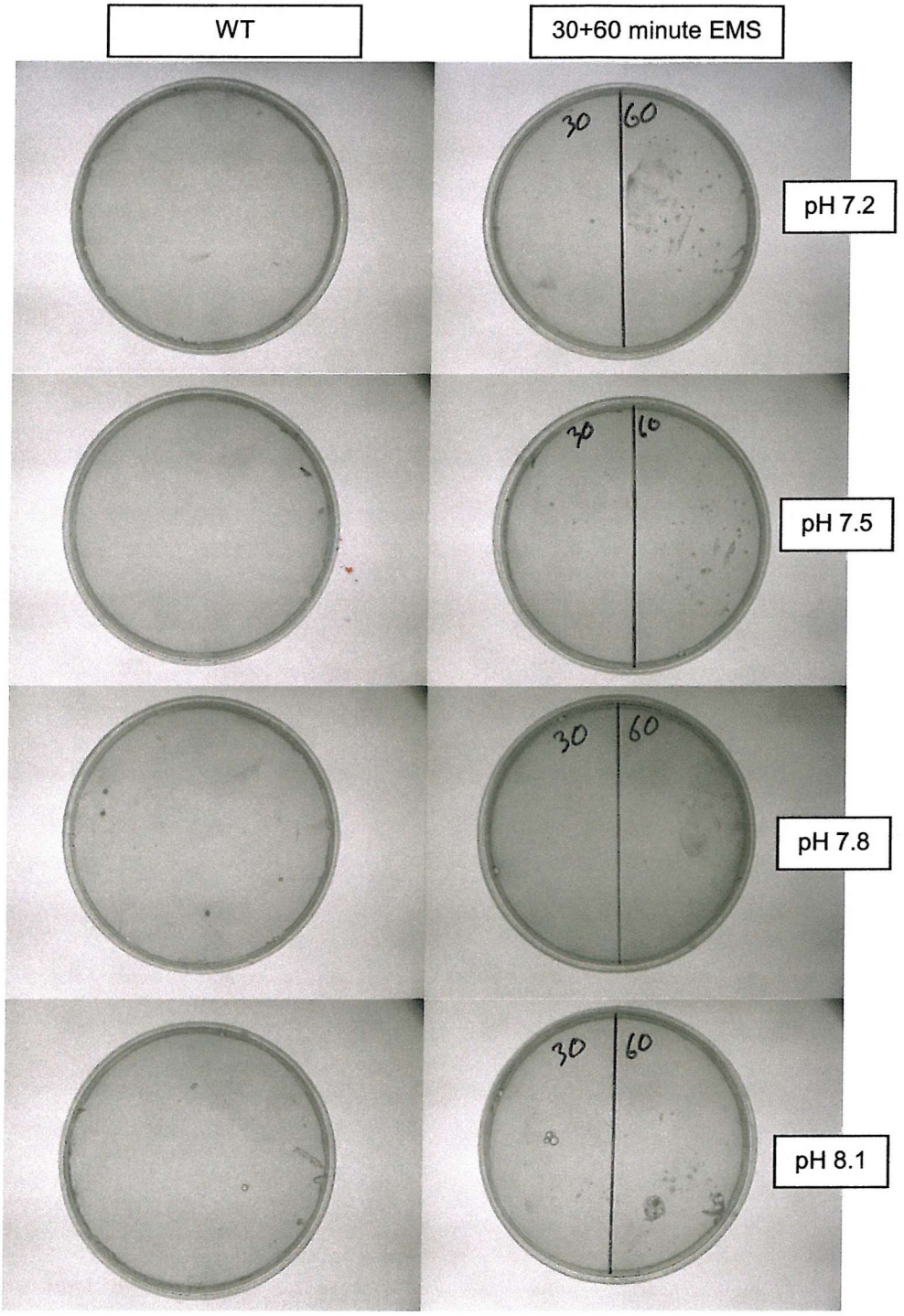

Figure 4.8 – Growth of EMS mutagenised GAP expressing *RcAAP1* on raised pH medium. Raised pH +citrulline selective medium plates with non-mutagenised (left), 30 minute and 60 minute EMS mutagenised (right) GAP expressing *RcAAP1*. Incubation was for 48 hours at 30 °C. This is a representative experiment, repeated twice.

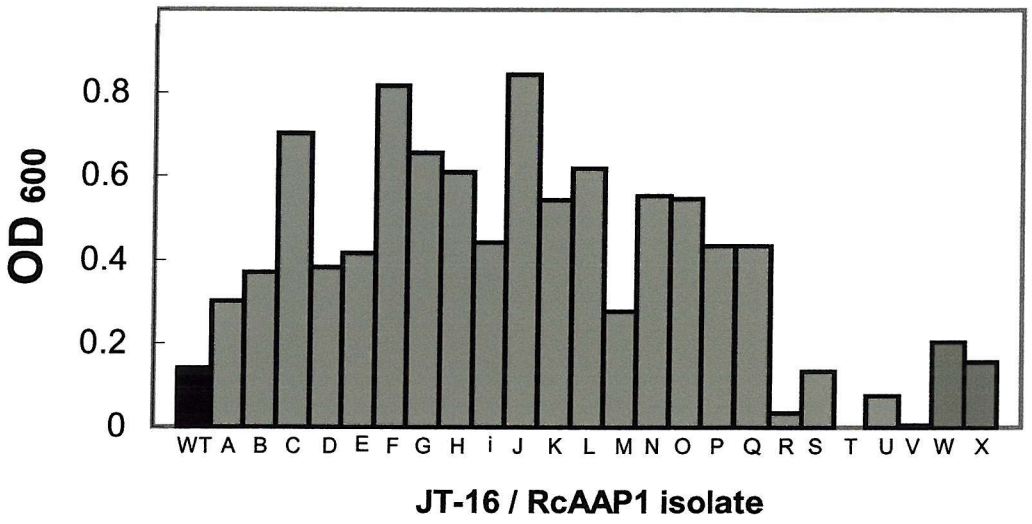

Figure 4.9 – Growth of mutagenised JT-16 / *RcAAP1* isolates (A-X) compared to non-mutagenised JT-16 / *RcAAP1* (WT). OD_{600} of JT-16 expressing WT *RcAAP1* (WT) against the OD_{600} of twenty mutagenised JT-16 isolates (A-X) on pH 7.5 low-histidine selective medium after 25 hours at 30 °C. This growth analysis was repeated under identical conditions and gave a similar result. Growth on this selective medium beyond 40 hours resulted in lysis for mutagenised isolates but sustained growth for the WT expressing yeast (OD against growth is shown in appendix 1).

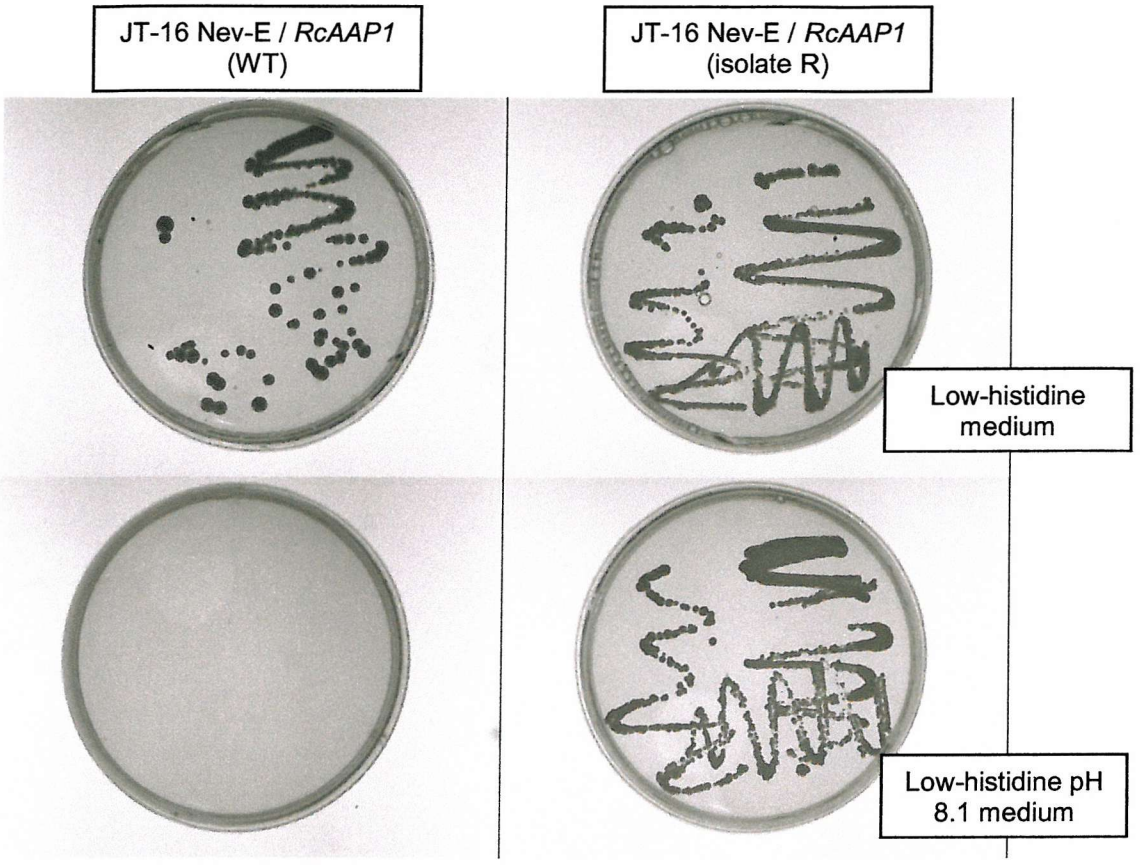

Figure 4.10 – Growth of JT-16 expressing WT *RcAAP1* (left) and the mutagenised isolate R (right) on low-histidine selective medium (top) and pH 8.1 low histidine selective medium (bottom). The growth of this yeast is representative of all the isolates on these selective media. Incubation was for 96 hours at 30 °C.

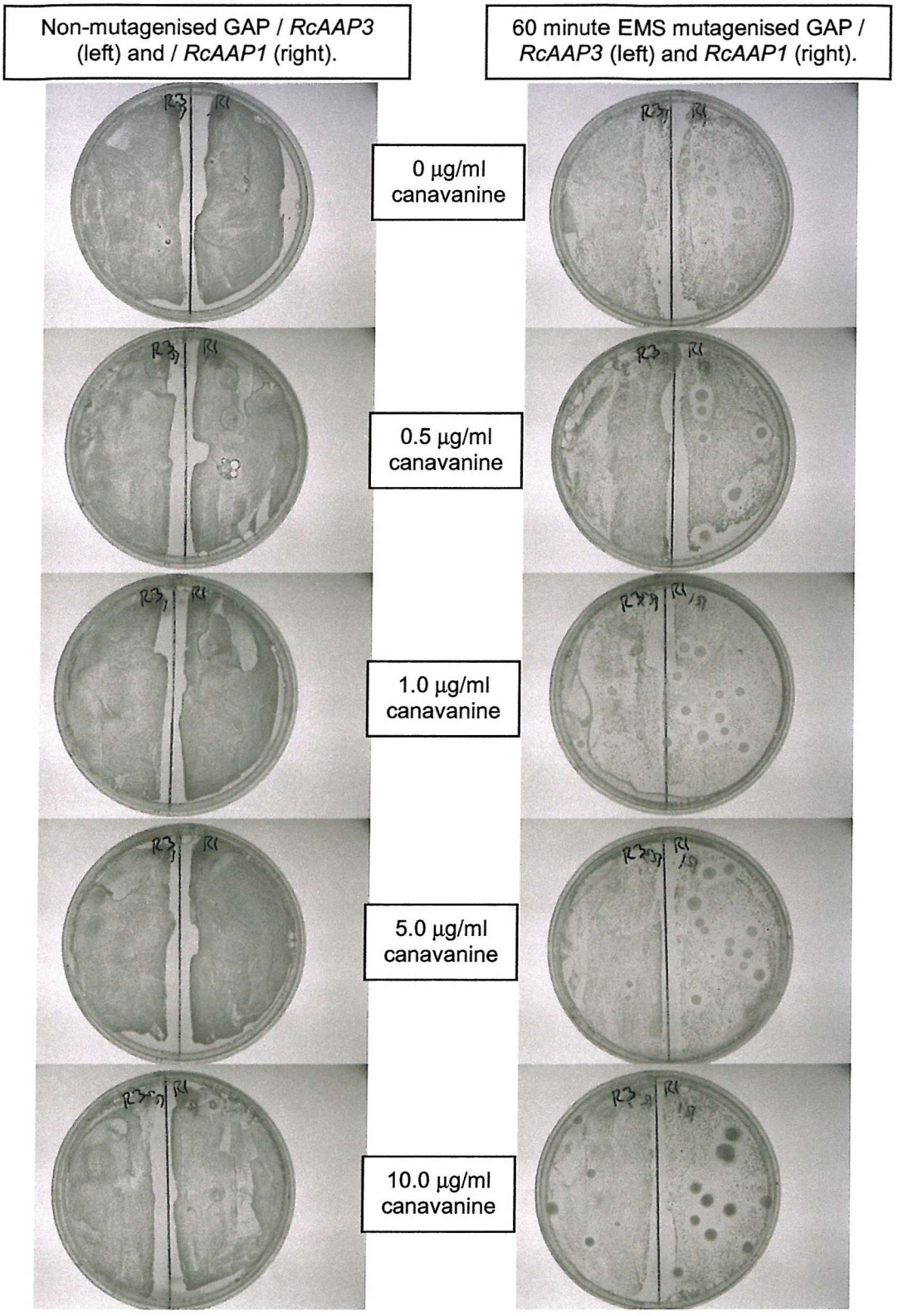

Figure 4.11 – Growth of EMS mutagenised GAP expressing *RcAAP1* and *RcAAP 3* on canavanine-containing medium. Non-mutagenised (left) and 60 minute EMS mutagenised (right) GAP expressing *RcAAP1* and *RcAAP3* on +citrulline selective medium over a range of canavanine concentrations after 72 hours growth at 30 °C. This was repeated under identical mutagenesis and selection conditions and gave similar results.

annealing temperatures to give optimal yield for this PCR amplification than previously used for the WT *RcAAP1*. This may be due to altered annealing regions of the template through mutagenesis. PCR products were obtained from eleven of the isolates from the raised pH selection. These were from isolates C, G, I, N, O, R, S, T, U, W and X. Of these products, those from C, G, N, O, R, S, T, W and X were successfully ligated into Nev-E and used to transform competent bacteria. Subsequently, plasmids isolated from these bacteria were used to transform competent, non-mutagenised JT-16. All were able to confer growth of the transformed yeast on LHpH8.1. Yeast transformed with non-mutagenised *RcAAP*1 / Nev-E was not able to grow on this raised pH selective medium (figure 4.12). This indicates that it was an alteration in *RcAAP1* cDNA that allowed complementation of JT-16 on the raised pH selective medium and not mutagenesis of the yeast genome.

4.2.4 Sequencing of mutated transporters

Plasmids from isolates C, G, N, O, R, S, T, W and X were sequenced and compared to that of WT *RcAAP1* in order to identify any mutated bases. These mutations were then translated in order to observe the amino acid sequence of the protein. Of the isolates used to successfully complement non-mutagenised JT-16 on raised pH selective medium (figure 4.12), all four sections of isolates G, O, R, S, T, W and X were fully sequenced at least three times. This is referred to a three full sequence runs. For the majority of sequences, mutations were only found once. Only when alterations in sequence were consistently present in all three of sequence runs were the mutations considered genuine. In isolate G, six separate mutation positions were discovered. Of these six, only one mutation was found consistently in all three sequence runs (table 4.1). This mutation and its subsequent effect on protein sequence are shown in figure 4.13. The single base change of a guanine to a thymine at position 204 changes the codon from CAG, coding for glutamine, to CAT, coding for histidine. The altered amino acid is at position 68. In isolate S two separate mutation positions were discovered. Of these two only one mutation was found consistently in all three sequence runs (table 4.1). The mutation and its subsequent effect on the protein sequence are shown in figure 4.13. The single base that is altered is the same as that discovered in isolate G. However, in isolate S, the guanine at position 204 has been replaced by a cytosine. The codon is changed from CAG, coding for glutamine, to CAC, again coding for histidine. Although the sequence mutation is different from isolate G, the resulting amino acid sequence change is identical in both isolates. In isolate W, four separate mutation positions were discovered in the three sequence runs, but only one occurred consistently (table 4.1). The mutation and its subsequent effect on the protein sequence are shown in figure 4.13. The single base change at position 855 is from adenine

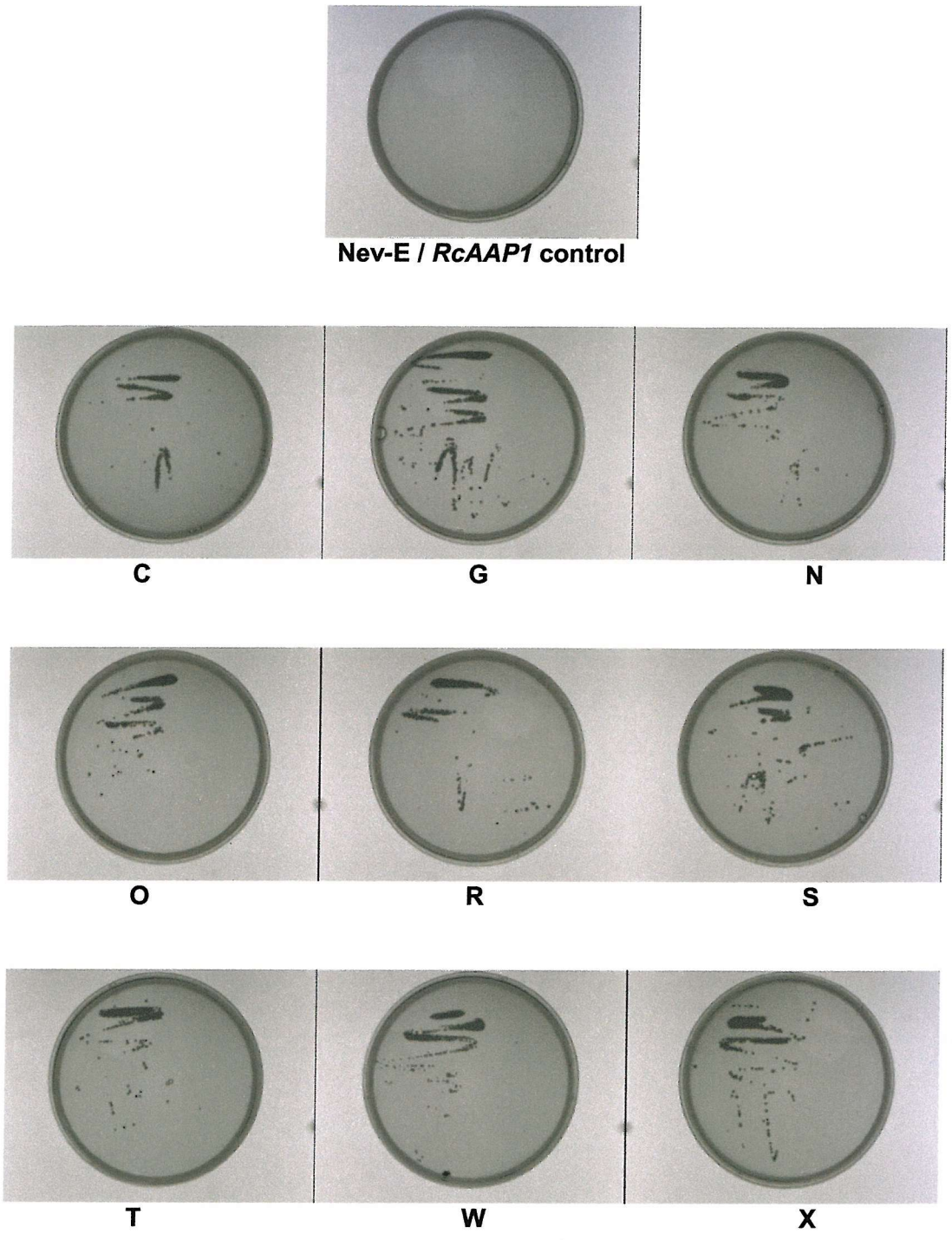

Figure 4.12 – Growth of JT-16 transformed with *RcAAP1* / Nev-E obtained from mutagenised isolates. JT-16 transformed at the same time with WT RcAAP1 is a control (top). Yeast from liquid low histidine concentration selective medium cultures, streaked onto pH 8.1 low histidine concentration selective medium. Incubation was for 96 hours at 30 °C.

to cytosine. Although the codon changes from GCA to GCC, there is no effect on the protein sequence as both of these codons code for an alanine residue at position 285. Isolate O had three separate mutations, isolate R had one mutation, isolate T had two separate mutations and isolate X also had two separate mutations. However none of these mutations were consistently present in all three sequence runs and so were not considered to be true mutations. Certain difficulties were experienced during sequencing which meant sequence was often of low quality. This is discussed in more detail in section 4.3.

4.2.5 Membrane topology and position of mutations

Two-dimensional topological representations of RcAAP1 and 3 were produced from the solved amino acid sequences in order to map the mutations. The two programs used to analyse the sequence were seqnet (Wisconsin Package) (section 2.15.2) and TMHMM (section 2.15.1). Both programs interpret properties of membrane protein amino acid sequences to determine which sections are likely to be buried in the lipid bilayer (hydrophobic), and which are likely to be exposed to either the cytoplasm of the cell or the extracellular environment (hydrophilic).

4.2.5.1 Seqnet (Wisconsin Package)

A hydrophobicity plot and a hydrophobic moment plot were produced with this program for each transporter (figure 4.14). From these plots it can be seen that both proteins have very similar profiles. The two hydrophobicity plots for each protein ('Goldman *et al*' (Rose *et al* 1985) in green and 'Kyte and Doolittle' (Kyte and Doolittle 1982) in black) have between nine and eleven significant peaks, suggesting that the proteins pass through the membrane between nine and eleven times. The two hydrophobic moment plots for each protein (α-helical sections in red and β-sheet sections in blue) show that the hydrophobic peak at approximately position 420 represents an α-helical region with a high hydrophobic moment. This could be due to the proximity of another α-helical region, or contact with the environment outside the membrane, either due to a pore formation in the protein or the section in question being a membrane seeking α-helix.

4.2.5.2 TMHMM

A graphical representation of each protein describing sections as inside (intracellular), outside (extracellular) or trans-membrane (α-helical membrane spanning section) was produced with this program (figure 4.15). From this output it appears clear that

both proteins have nine membrane-spanning domains with an intracellular N-terminal region and an extracellular C-terminal region.

4.2.5.3 Topological models

Using the data from both analysis packages a nine trans-membrane domain model with an intracellular N-terminal region and an extracellular C-terminal region was produced for both RcAAP1 (figure 4.16) and RcAAP3 (figure 4.17). Indicated on these models are the positions of the mutations from isolates G, S and W. However, there is experimental evidence from *Arabidopsis thaliana*, suggesting that members of the AAP family have eleven trans-membrane domains, an intracellular N-terminal region and an extracellular C-terminal region (Chang and Bush 1997) (discussed in section 1.5.2.1.1). Two members of this family (AtAAP1 and 2) were examined with the TMHMM analysis packaged used to build the nine trans-membrane domain models for RcAAP1 and 3. The output from AtAAP1 (figure 4.18 A) shows nine definite trans-membrane domains and two areas of low probability trans-membrane domain (at approximately positions 175 and 250). These same areas of low probability are visible on the TMHMM output for RcAAP1 (figure 4.15 A) and AtAAP2 (figure 4.18 B). Only the second low probability domain can be seen on the TMHMM output for RcAAP3 (figure 4.15 B). Using these positions predicted by TMHMM as a guide, the previously constructed RcAAP1 and 3 models (figures 4.16 and 4.17) and the strict rule of eleven trans-membrane domains, two new models for RcAAP1 (figure 4.19) and RcAAP3 (figure 4.20) were constructed. The key features of these models are eleven trans-membrane domains, an intracellular N-terminal region and an extracellular C-terminal region. The positions of the mutations discovered in the isolates G, S and W are shown on the eleven trans-membrane domain model of RcAAP1 (figure 4.19). On this model it can be seen that Gln68, the mutation position in isolates G and S, is on the extracellular edge of the first predicted trans-membrane domain. Ala285, the mutation position in isolate W, is on the intracellular edge of the seventh predicted trans-membrane domain. It can be seen from the eleven trans-membrane domain model of RcAAP3 (figure 4.20), that the mutated positions Gln68 and Ala285 from the RcAAP1 mutated isolates G and S, have comparable residue in RcAAP3. By aligning the amino acid sequences of RcAAP1, RcAAP3 and AtAAP1-10 (figure 4.21), it can be seen that the Gln68 and Ala285 positions from RcAAP1 are also conserved throughout the majority of the *Arabidopsis thaliana* AAP family. The exceptions being AtAAP9 and 10 for both positions and AtAAP7 for Gln68.

Table 4.1 – Details of the alterations in sequence gathered for isolates G, S and W. Three complete sequence runs were completed for each isolate. Differences from the WT sequence are marked in bold. Reoccurring alterations, considered to be genuine mutations are marked in red.

Isolate	Run	Position of mutation	Detail of alteration
G	1	137	CG**N**ACC
		204	CTCA**T**CTT
		250	TG**G**CCC
		454	A**A**TAT
		750	CT**T**CAA
	2	143/147/149	CCAA**N**AGA**G**C**N**
		204	CTCA**N**CTT
		265/270	TGT**N**CTTG**C**TC
		415	TTG**N**TCA
	3	216	TTTA**A**C
		194/197/198/204	**N**AT**TC**CTCA**T**CTT
		415	TTG**N**TCA
		753	TCCA**N**CCC
S	1	204	CTCA**C**CTT
		756	CC**A**AGA
	2	204/207/209	CA**C**CTA**G**G
	3	204	CTA**N**CTT
		747-751	TG**TC-TT**A
W	1	855	AGC**C**ACT
		1095	TT**A**AAAAA
		1131	GGA**A**TCA
	2	855	AGC**N**ACT
		1129	GTG**G**ATT
		1257/1259	TTC**A**T**A**AA
	3	855	AGC**C**ACT
		1098-1104/1109	AA**TTAACAA**GTGC**N**
		1261	TTTA**C**CGA

Isolate G

```
WT-GCA ATC GCT CAG CTT GGG        DNA
   Ala Ile Ala Gln Leu Gly        Protein

Mut-GCA ATC GCT CAT CTT GGG       DNA
   Ala Ile Ala His Leu Gly        Protein
```

Isolate S

```
WT-GCA ATC GCT CAG CTT GGG        DNA
   Ala Ile Ala Gln Leu Gly        Protein

Mut-GCA ATC GCT CAC CTT GGG       DNA
   Ala Ile Ala His Leu Gly        Protein
```

Isolate W

```
WT-ATG AAG AAA GCA ACT CTG        DNA
   Met Lys Lys Ala Thr Leu        Protein

Mut-ATG AAG AAA GCC ACT CTG       DNA
   Met Lys Lys Ala Thr Leu        Protein
```

Figure 4.13 – Sequence and amino acid translation of mutated isolates G, S and W compared to WT RcAAP1. Mutated bases are shown in red, altered codons are shown in bold.

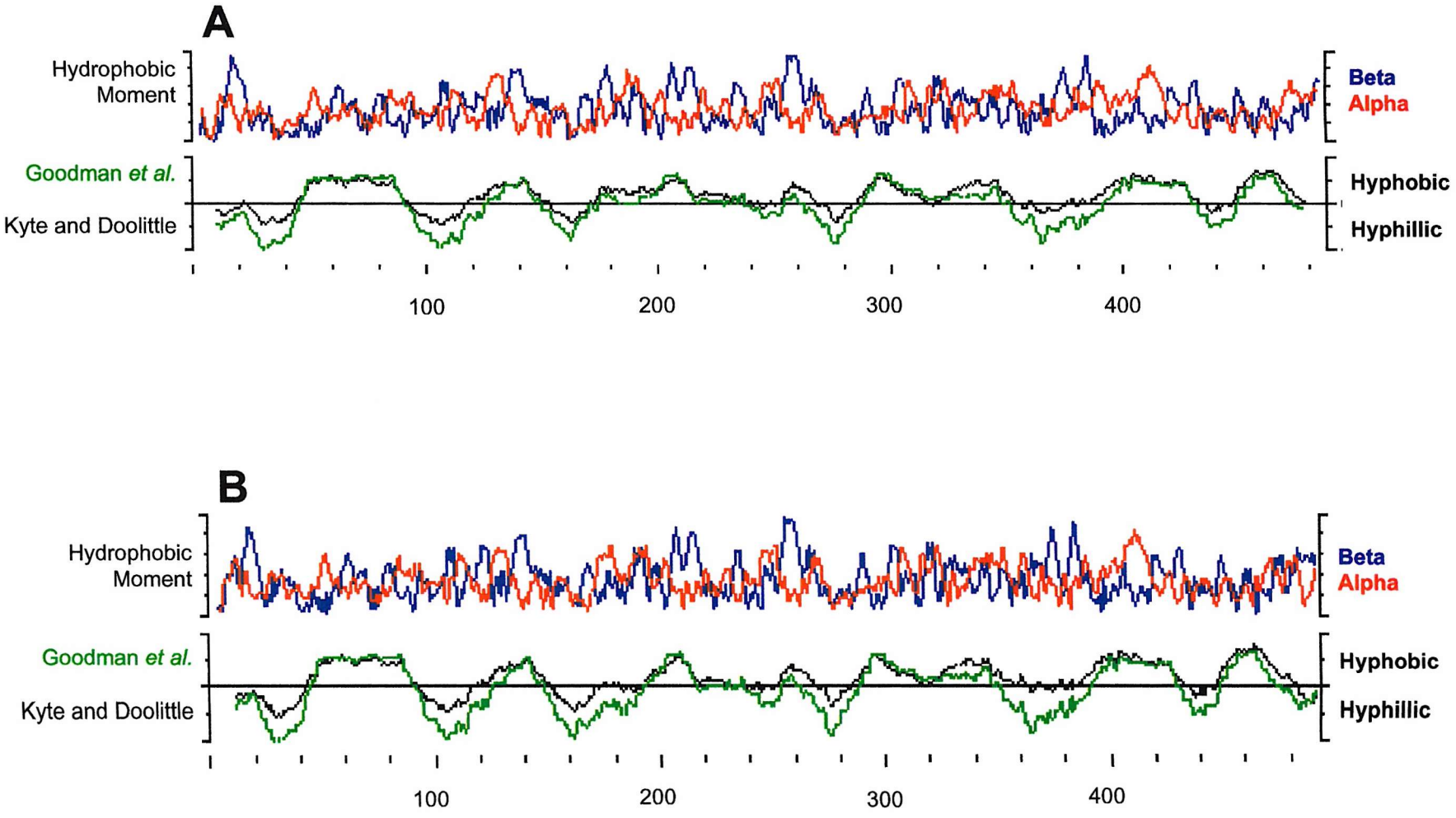

Figure 4.14 - Hydrophobic moment and hydrophobicity plots from the amino acid sequence of RcAAP1 (A) and RcAAP3 (B) using the peplot package from seqnet (Wisconsin package). The hydrophobic moment plot shows a blue plot for beta sheet regions and a red plot for α-helical regions. The hydrophobicity plot shows a green plot for the Goodman *et al* method (Rose *et al* 1985) and a black plot for the Kyte and Doolittle method (Kyte and Doolittle 1982).

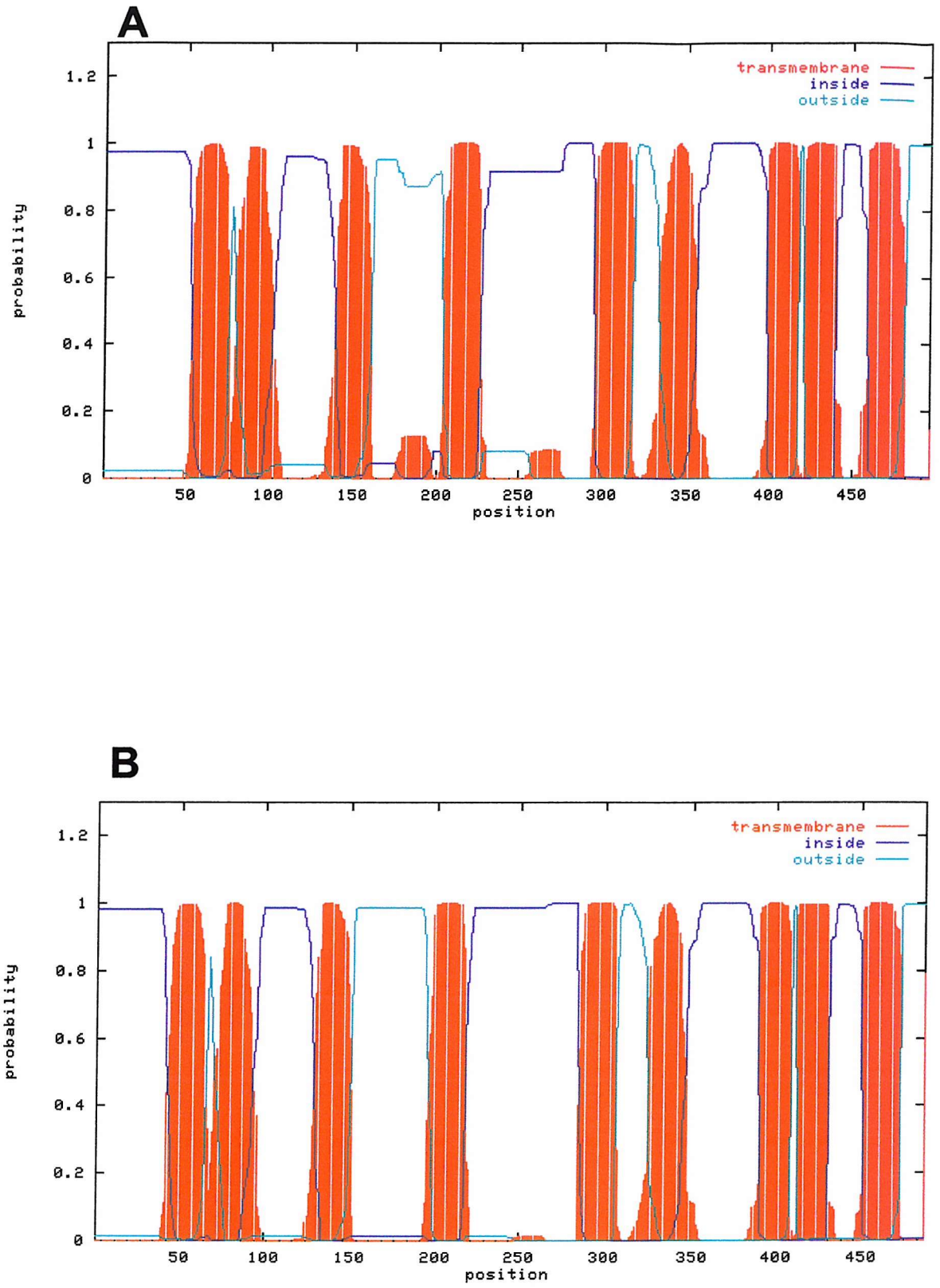

Figure 4.15 – TMHMM output for RcAAP1 (A) and RcAAP3 (B). Describing the length of the protein sequence as intracellular (inside, blue), extracellular (outside, green) or trans-membrane (α-helical membrane spanning section, red).

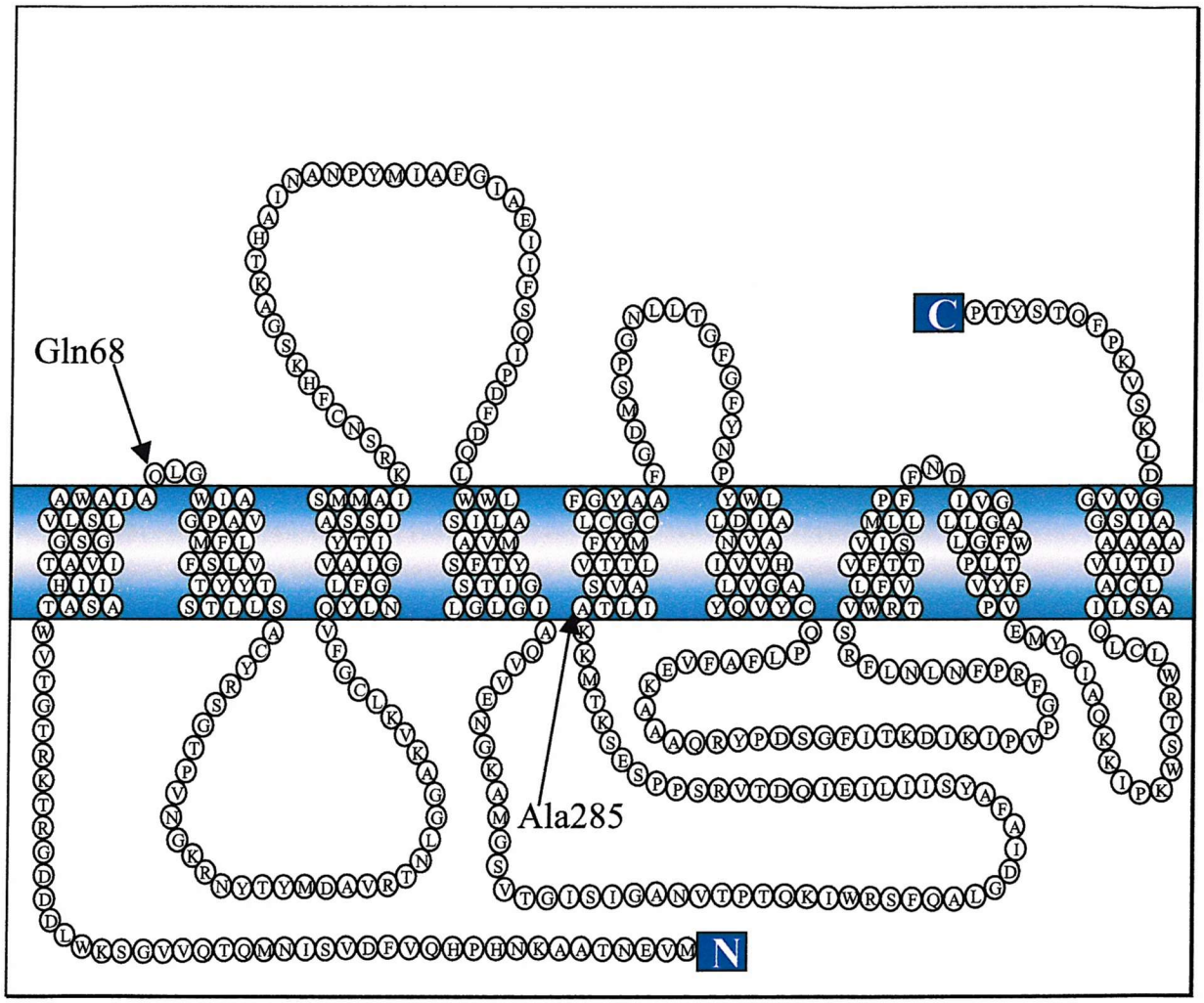

Figure 4.16 - Two-dimensional trans-membrane topology representation of RcAAP1 from the combined seqnet and TMHMM graphical outputs. The key features of this model are nine trans-membrane domains, an intracellular N-terminal region and an extracellular C-terminal region. Also indicated on this model are the positions of the mutations found from sequencing isolates G, S and W.

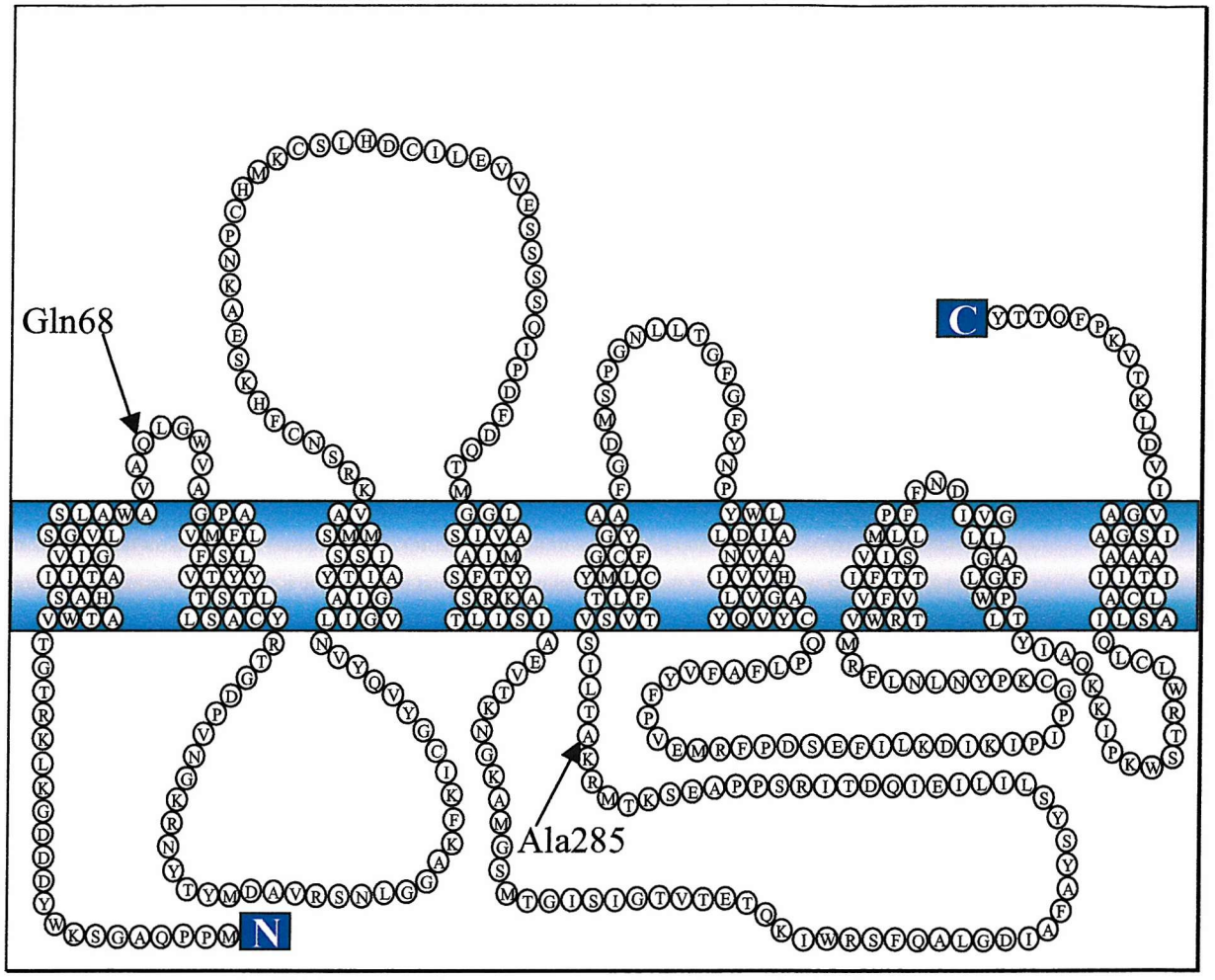

Figure 4.17 Two-dimensional trans-membrane topology representation of RcAAP3 from the combined seqnet and TMHMM graphical outputs. The key features of this model are nine trans-membrane domains, an intracellular N-terminal region and an extracellular C-terminal region. Also indicated on this model are the relative positions of the mutations found from sequencing isolates G, S and W.

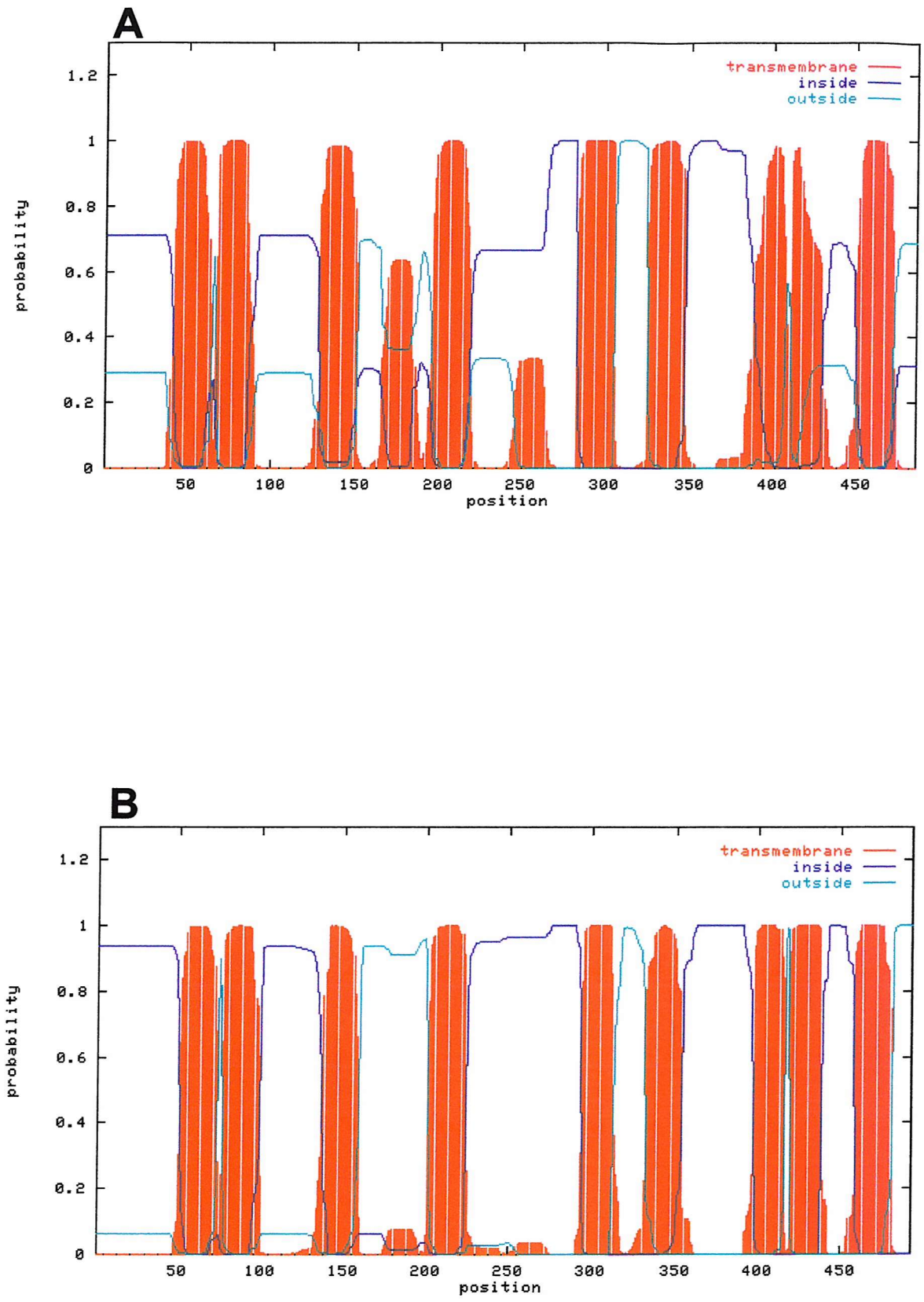

Figure 4.18 - TMHMM output for AtAAP1 (A) and AtAAP2 (B). Describing the length of the protein sequence as intracellular (inside, blue), extracellular (outside, green) or trans-membrane (α-helical membrane spanning section, red).

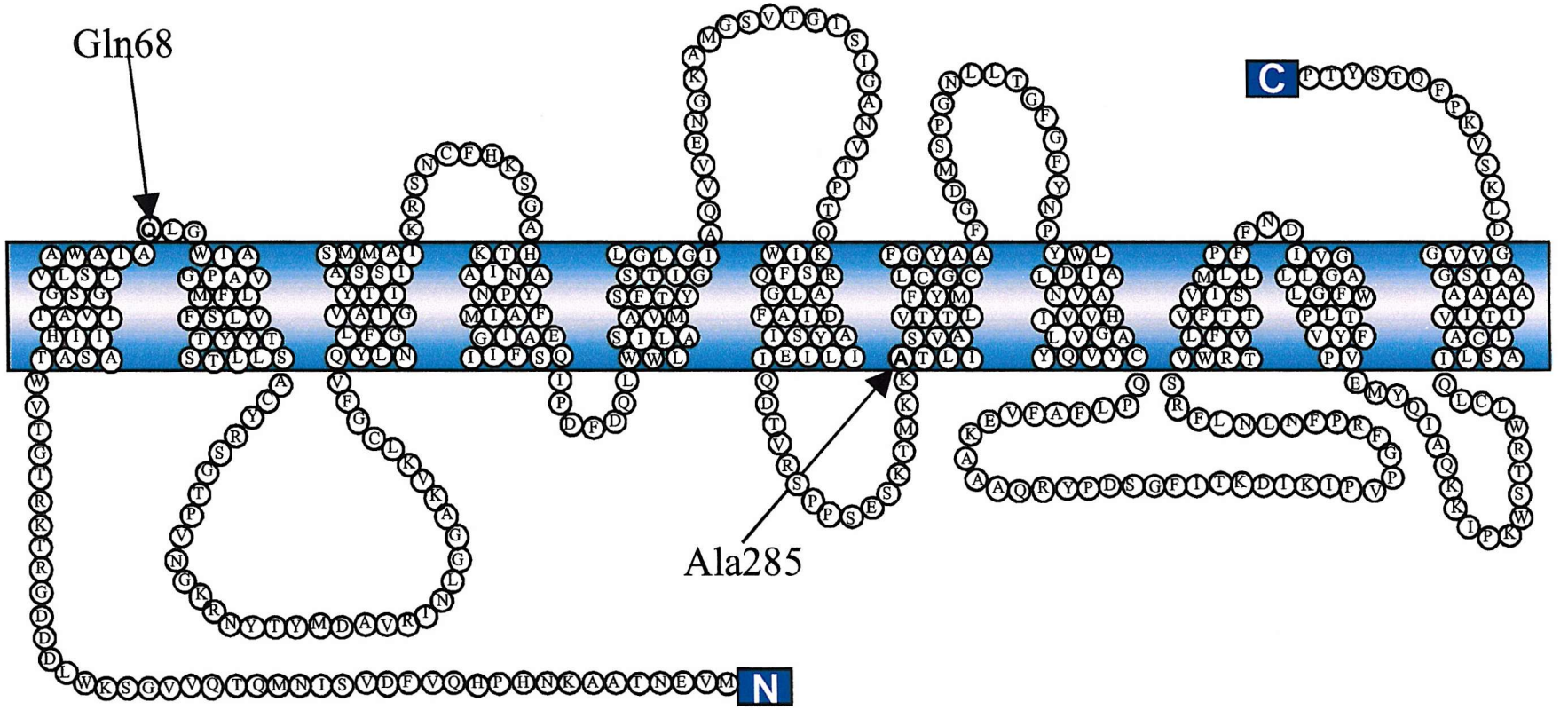

Figure 4.19 - 2-dimensional trans-membrane topology representation of RcAAP1 from the combined seqnet and TMHMM graphical outputs, following the strict rule of eleven trans-membrane domains. The positions of the mutations found from sequencing of isolates G, S and W are indicated.

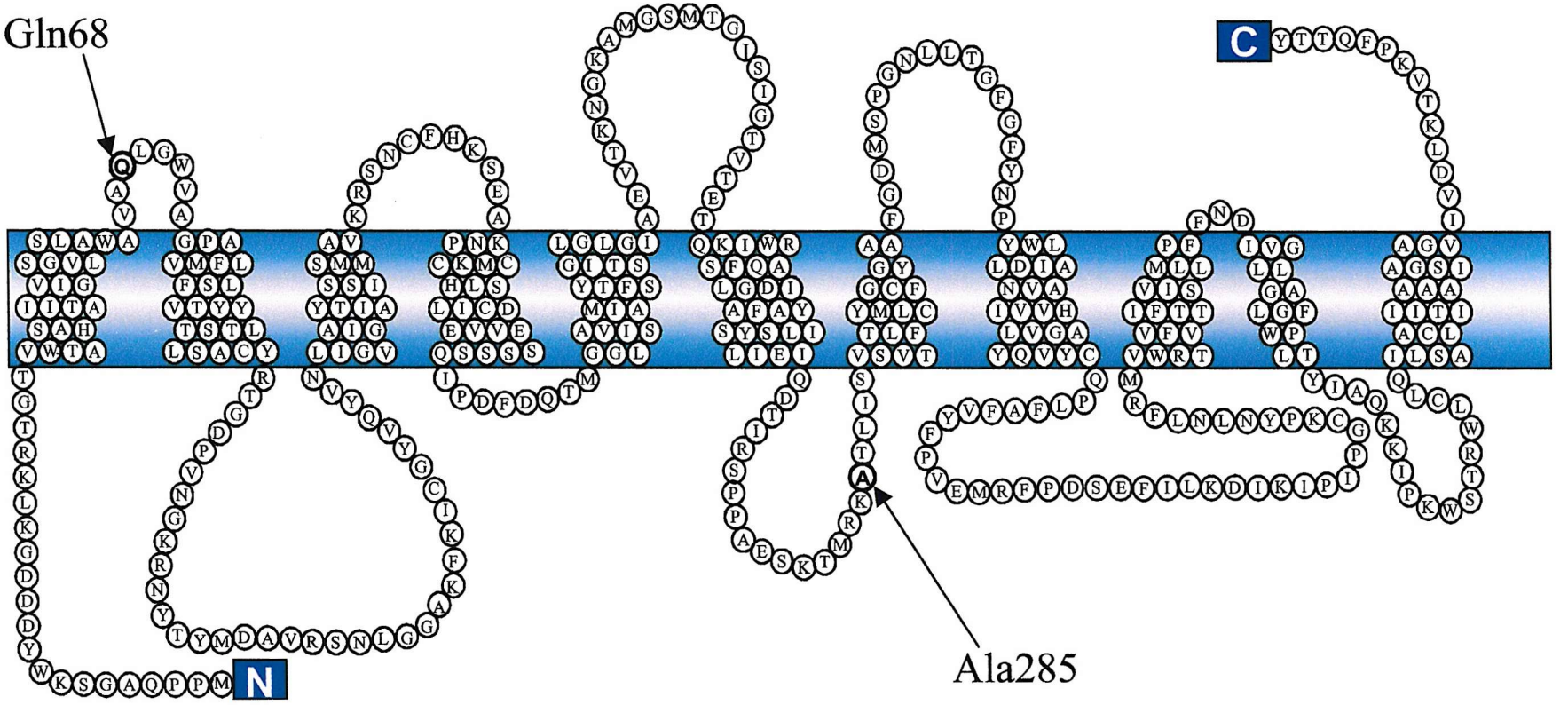

Figure 4.20 - 2-dimensional trans-membrane topology representation of RcAAP3 from the combined seqnet and TMHMM graphical outputs, following the strict rule of eleven trans-membrane domains. The relative positions of the mutations found from sequencing isolates G, S and W are indicated.

```
          44                                                      93

 RcAAP1   WTASAHIITA VIGSGVLSLA WAIAQLGWIA GPAVMFLFSL VTYYTSTLLS
 RcAAP3   WTASAHIITA VIGSGVLSLA WAVAQLGWVA GPAVMFLFSL VTYYTSTLLS
 AtAAP1   LTASAHIITA VIGSGVLSLA WAIAQLGWIA GTSILLIFSF ITYFTSTMLA
 AtAAP2   WTASAHIITA VIGSGVLSLA WAIAQLGWIA GPAVMLLFSL VTLYSSTLLS
 AtAAP3   WTASAHIITA VIGSGVLSLA WATAQLGWLA GPVVMLLFSA VTYFTSSLLA
 AtAAP4   WTASAHIITA VIGSGVLSLA WAIGQLGWIA GPTVMLLFSF VTYYSSTLLS
 AtAAP5   WTASAHIITA VIGSGVLSLA WAVAQIGWIG GPVAMLLFSF VTFYTSTLLC
 AtAAP6   MTGSAHIITA VIGSGVLSLA WAIAQLGWVA GPAVLMAFSF ITYFTSTMLA
 AtAAP7   WTAVAHIITG VIGAGVLSLA WATAELGWIA GPAALIAFAG VTLLSAFLLS
 AtAAP8   WTASAHIITA VIGSGVLSLA WAIAQLGWVA GTTVLVAFAI ITYYTSTLLA
 AtAAP9   RPDPFPVTRL DSDAGAL... FVLQSKGWWL GFVCLTTMGL VTFYAYYLMS
AtAAP10   SGDGEKRGEE VVDAGSL... FVLKSKGWAA GISCLVGGAA VTFYSYTLLS

          263                                                     311

 RcAAP1   IILIEIQDTV RS.PPSESKT MKKATLISVA VTTLFYMLCG CFGYAAFGDM
 RcAAP3   LILIEIQDTI RS.PPAESKT MRKATLISVS VTTLFYMLCG CFGYAAFGDM
 AtAAP1   TVLIEIQDTL RSSPA.ENKA MKRASLVGVS TTTFFYILCG CIGYAAFGNN
 AtAAP2   VVLIEIQDTV RS.PPAESKT MKKATKISIA VTTIFYMLCG SMGYAAFGDA
 AtAAP3   IILIEIQDTV KS.PPSEEKT MKKATLVSVS VTTMFYMLCG CMGYAAFGDL
 AtAAP4   VVLIEIQDTV RS.PPAESKT MKIATRISIA VTTTFYMLCG CMGYAAFGDK
 AtAAP5   MILIEIQDTV KS.PPAEVNT MRKATFVSVA VTTVFYMLCG CVGYAAFGDN
 AtAAP6   TVLIEIQDTL KAGPPSENKA MKRASLVGVS TTTFFYMLCG CVGYAAFGND
 AtAAP7   IILLEIQDTL RS.PPAEKQT MKKASTVAVF IQTFFFFCCG CFGYAAFGDS
 AtAAP8   TILIEIQDTL RSSPP.ENKV MKRASLVGVS TTTVFYILCG CIGYAAFGNQ
 AtAAP9   .ILPEIQATL A..PPATGKM LKGLLLCYSV IFFTFYSAA. ISGYWVFGNN
AtAAP10   .IIPEIQATI S..APVKGKM MKGLCMCYLV VIMTFFTVA. ITGYWAFGKK
```

Figure 4.21 – Amino acid sequence alignments of RcAAP1, RcAAP3 and AtAAP1-10. Residues 44 to 93 and 263 to 311 for RcAAP1. Gln68 and Ala285 from RcAAP1 are highlighted in bold, as are the comparable residues in the other displayed sequences. The alignment was done using the multiple sequence alignment with hierarchical clustering program (Corpet 1988), found at 'http://protein.toulouse.inra.fr/multalin/multalin.html'.

4.3 Discussion

Two selection conditions were designed (chapter 3) with the aim of obtaining mutated transporters with altered proton- and amino acid- binding characteristics. The first involved screening JT-16 on selective medium with a raised pH. The low level of protons available in this medium means that JT-16 expressing WT *RcAAP1* and *3* are unable to grow, or show reduced levels of growth (chapter 3). The WT transporters are unable to operate to a sufficient level to supply the yeast with a nitrogen source essential for growth. Through random mutagenesis, the aim was to produce a transporter that would be able to operate under these depleted proton conditions. The second selection condition involved the inclusion of canavanine in the selective medium. This analogue of arginine was shown to be toxic to GAP (a, *gap, ura3-52*) yeast expressing *RcAAP1* and 3 on selective medium at concentrations above 0.1 μg/ml (chapter 3). Presumably WT RcAAP1 and 3 transport canavanine into the yeast and cause toxic effects. Through random mutagenesis, the aim was to produce transporters with altered amino acid recognition. When expressed in GAP, mutated transporters that were not able to transport canavanine, but were still able to supply citrulline from the medium as a nitrogen source, would in theory complement the growth of the yeast mutant.

Two PCR-based methods (DNA shuffling and error-prone PCR) were initially tried with the aim of producing mutated libraries of *RcAAP1* and *RcAAP3* for transformation into yeast mutants. Unfortunately neither of these methods consistently produced DNA in sufficient yield or of adequate quality for ligation and subsequent transformation. With DNA shuffling, the progressive digestion of *RcAAP3* / Nev-N showed that the production of small base pair DNA products was possible using DNase I. The subsequent digestion of *RcAAP1* cDNA with DNase I provided suitable genetic material, of approximately 10-50 bp, for the DNA shuffling protocol. Multiple rounds of primerless and primered PCR reconstructed this material to produce a library of randomly mutated cDNA approximately the same size as the original *RcAAP1* cDNA. This material was however not stable enough to be used in cloning, possibly due to degradation by residual DNase I activity. Production of good quality shuffled product in sufficient quantity was rarely repeatable. Due to these problems, DNA shuffling was discontinued as a method of random mutagenesis.

Error-prone PCR involving the depletion of dGTP and dATP concentrations and the inclusion of Mn^{2+}, both produced very low yields of product. This method did not produce the quality or quantity of cDNA required for the production of a randomly mutated library. Although some product was collected, there was insufficient to make ligation and transformation feasible. This method was therefore not pursued for the production of a randomly mutated library.

The use of EMS to mutagenise transporter cDNA following transformation in a yeast mutant appeared to be successful in producing colonies able to grow on the raised pH and canavanine-containing selective medium. Twenty four isolates (A-X) were obtained from the raised pH selection conditions and the majority of the isolates displayed much faster growth on the pH 7.5 selective liquid medium than yeast expressing WT *RcAAP1*. This verifies their differences to the WT RcAAP1-expressing yeast but does not demonstrate whether the mutation is in the expressed transporter or the yeast genome. Lysis of mutagenised isolates on this liquid medium again distinguishes them from WT *RcAAP1*-expressing yeast. Subsequent growth of these isolates in non-selective liquid medium (e.g. YPD) and normal pH selective medium did not result in lysis. This suggests that there is some property of the raised pH selective liquid medium that causes the lysis, possibly the extreme of pH. The twenty four isolates were also compared with non-mutagenised yeast on pH 8.1 selective medium plates. Growth was observed for all the isolates while the non-mutagenised yeast did not grow. Once again this verifies the difference between mutagenised isolates and non-mutagenised yeast, but does not show if it is mutagenesis of the *RcAAP1* cDNA or of the yeast genome.

Selection on canavanine-containing medium, for chemically mutagenised GAP expressing *RcAAP1* and *RcAAP3* was not as distinct as on raised pH medium as background growth was observed. This less stringent selection, difficulties in culturing and time restraints meant that work on these isolates was discontinued in favour of concentrating on the isolates from the raised pH experiments.

Problems were encountered when removing inserts from the isolated plasmid DNA with restriction enzymes and transforming bacteria with plasmid purified directly from yeast isolates. To overcome this, PCR was performed on plasmid DNA removed from mutagenised yeast isolates, selected on raised pH medium. This showed that an *RcAAP1* derivative was present in the yeast, although for the efficient production of PCR products, the annealing temperatures were lowered for each isolate, suggesting that the primer-annealing sequence of the transporter may have been altered.

The PCR products from isolates C, G, N, O, R, S, T, W and X were ligated into Nev-E, cloned into bacteria and used to complement new JT-16 competent cells. These conferred on the JT-16 the ability to grow at high pH, suggesting that this property was due to the mutation of the transporter cDNA rather than the yeast genome. To confirm whether mutations were present, the cDNAs were isolated and sequenced.

Sequencing was carried out on all of the full-length *RcAAP1* derivative from isolates G, O, R, S, T, W and X. However problems were encountered in obtaining good quality sequence data from these reactions. This could be linked to the problems encountered when previously attempting to carry out PCR on these isolates (section 4.2.3.2). This involved the use of the same primers as for sequencing. If mutations were present in the

primer annealing sites, reaction efficiency would be reduced when using primers designed to the WT sequence. Sequence reactions were repeated until at least three acceptable full-length sequences were obtained. With the difficulties mentioned this was only achieved for isolates G, O, R, S, T, W and X. There was evidence of mutations in the sequences from all of the isolates but only in three instances were these mutations apparent in all three sequence data sets. Of the three definite mutations discovered, two were in the same position. Although these mutations were different at the DNA level, they each produced a codon that subsequently formed an identical mutation at the amino acid level (Gln68 to His68). From the eleven trans-membrane domain model produced for RcAAP1 (figure 4.19), this mutation is predicted to be on the extracellular side of the plasma membrane at the top of the first trans-membrane domain. Being positioned on the external surface of the cell could imply that this residue plays a role in proton binding. However more intensive studies of this residue and its surrounding area would be required to verify this. It is an interesting point that on both the nine and eleven trans-membrane domain models the loop between the first and second trans-membrane domain (on which Gln68 is positioned) is a different size in RcAAP1 and RcAAP3, even though the residues in this section are very similar. Only future experimental evidence of the membrane topology will reveal the accuracy of these predicted models.

The other definite mutation identified was in isolate W. The substitution of an adenine with cytosine was observed, but in this case the resulting triplet still coded for the same amino acid, alanine (Ala285). As no protein alteration has occurred the advantage this particular isolate has over yeast expressing the WT transporter cannot be explained by an alteration in transport capability. An alternative possibility is one of codon bias in yeast. If the codon in the mutant represents a tRNA that is more readily available in the yeast then this could mean that the mRNA is translated more rapidly. Consequently, more of the transporter would be produced and so more would be present in the plasma membrane. If WT RcAAP1 can still transport amino acids at this higher pH but at a much reduced efficiency then it is possible that with more of the transporters active in the plasma membrane the yeast could acquire sufficient levels of amino acid from the medium to sustain growth. According to the codon usage database (Nakamura *et al* 2000) (found at 'http://www.kazusa.or.jp/codon') the triplet GCA is used at a higher frequency (16.2 per 1000 codons) than GCC (12.6 per 1000 codons) to code for alanine. The most common triplet for this amino acid being GCU (21.1 per 1000 codons) and the least common being GCG (6.1 per 1000 codons). As the mutant from isolate W is using the lower frequency triplet it is possible that the production of this protein would be slightly decreased rather than increased, however the difference in the codon use is minimal and so would probably not make any significant change. It is also possible that the mutant codon allows for more 'wobble' that the WT codon. This would mean that as well as the tRNA carrying the exact

anti-codon being able to bind, other tRNAs with an alternate wobble base could also bind. This possibility could also increase the amount of protein produced. A further possible explanation concerns mRNA stability. It has been shown that the stability of an mRNA construct can be altered by the use of alternative codons, coding for the same amino acid (Seffens and Digby 1999). This work has not investigated the effect of a single codon change, as is the case for the mutant permease from isolate W, but if the mRNA produced was more stable it could give rise to an increased level of transporters in the yeast. Further investigation into the levels of protein present in isolate W, compared to WT may show if these explanations are feasible. A final possibility is that another mutation exists in the transporter from isolate W that has not been detected in sequencing.

The chemical random mutagenesis and selection method employed in this study yielded three positively identified mutations from seven successfully sequenced isolates. This represents an efficiency of 43%. The other isolates therefore appeared to contain non-mutated transporters (although further sequencing runs should be carried out to confirm this). Since all of the sequences obtained from these isolates (mutated and non-mutated) conferred on fresh JT-16 the ability to grow at high pH, it may suggest that the selection procedure used was not stringent enough. The effect of the three positively identified mutations should be investigated in more detail before concluding that these mutations are indeed changing the functioning of the transporter. The efficiency of the chemical mutagenesis method used in this study was also investigated by Curran *et al* (2000) during their study of the auto-inhibitory region of the *Arabidopsis thaliana* Ca^{2+} ATPase ACA2. They reported that 20% of the selected colonies expressed an ACA2 derivative. Removal of plasmid DNA and the use of PCR on isolates from the raised pH media in this study showed that 100% of these expressed an RcAAP1 derivative. This suggests that the selection for plasmid DNA in this study was more stringent that the ACA2 study. Following multiple selection procedures over 50% of the ACA2 final survivors were found to contain mutated versions of ACA2 with alterations in their auto-inhibitory characteristics. From eighty one identified mutants, seven positions of point mutations were discovered. The efficiencies of 43% (this study) and over 50% (Curran *et al* 2000) of finally selected colonies containing mutated permeases, suggests that the mutation selection protocols (high pH) employed in this study could have been more stringent in order to isolate only mutants.

Chapter 5 Oocyte Expression

5.1 Introduction

Oocytes from mature female *Xenopus laevis* (South African Clawed Toad) contain proteins and organelles such as histones, nucleoplasmin, RNA polymerases, tRNAs and ribosomes, which are a reserve to be used for early embryonic development. The use of this store is normally triggered by fertilisation but it can also be used to translate foreign genetic material introduced by micro-injection. This method of using the oocyte to express foreign DNA has been likened to hijacking the resources of a fully equipped factory (Miller and Zhou 2000). Membrane proteins from yeast, bacteria and plants have been expressed in oocytes and there has been success in expressing all types of transporters including pumps, channels and carriers (for a list see Miller and Zhou 2000). Only two higher plant amino acid permeases (AtAAP1, AtAAP5), both from *Arabidopsis*, have so far been expressed and characterised in oocytes (Boorer *et al* 1996, Boorer and Fischer 1997). The work to date on *Ricinus* transporters in oocytes has involved the injection of purified mRNA from roots (Schobert *et al* 1997). This work showed that several transporters with different specificities and transport rates for neutral amino acids are present in *Ricinus* roots. However, no individual transporters were characterised by this method. *Ricinus* amino acid permeases have also been characterised in yeast cells and plasma membrane vesicles. Analysis of substrate specificity was determined by measuring the inhibition of amino acid transport activity by various substrates (Marvier *et al* 1999, Neelam *et al* 1999). However, although these experiments yielded information on substrates that interact with amino acid transporters they could not distinguish between competition for transport and inhibition due to binding. Unlike work in oocytes, the membrane voltage could not be controlled in yeast. This important parameter is a key driving force and can regulate transporter kinetics.

The oocyte expression system also has advantages over the yeast system, as there is thought to be less interference with endogenous transport activity (Miller *et al* 1994, Theodoulou and Miller 1995, Boorer *et al* 1996,). Other major advantages of the oocyte system are linked to their size (approximately 1 mm diameter). This makes the handling of individual cells relatively easy, which in turn with the ability to control the membrane potential of oocytes makes electrophysiological kinetic measurements possible. The main disadvantage of this system is that the expression is transient and the oocyte normally dies 2-3 weeks after removal

from the frog (Miller and Zhou 2000). Also, the delicate nature of oocytes means that much greater care must be taken in handling than required when dealing with yeast and bacteria.

5.1.1 mRNA production and micro-injection

In vitro transcription is used to produce mRNA for micro-injection into oocytes. Micro-injection of double-stranded cDNA into the nucleus can also be performed but this is technically difficult and more likely to damage the oocyte. Certain modifications and additions are made to the mRNA in order to improve its stability and consequently level of translation. Within the oocyte, endogenous enzymes will actively degrade mRNA, especially from the 3' end. This is a normal function in the cell that exists in order to control levels of protein production. By introducing a 'poly-A-tail' (a string of usually between 20 and 100 adenine residues) to the 3' end of the mRNA it is possible to protect the coding region for an increased amount of time (Munroe and Jacobson 1990, Miller *et al* 1994, Cao *et al* 1995, Theodoulou *et al* 1995, Miller and Zhou 2000). The addition of a poly-A-tail also appears to aid the stability of mRNA in other ways but these have not yet been explained (Cao *et al* 1995). An oocyte expression vector can be used to incorporate the poly-A-tail into mRNA. The vector used in this study, pXE2 (plasmid *Xenopus* Expression) (figure 2.14 - section 2.14.1), contains a poly-A-region after the cloning site and before the linearisation site. This incorporates a poly-A-tail into any mRNA produced from this vector. mRNA can also be capped (capped mRNA) by using a modified G base ($m^7G(5')ppp(5')G$) (see section 2.14.1). This is known as a cap analogue and it increases the stability of the mRNA by making it less accessible to degradation. It has been shown that on average uncapped mRNA will be translation viable for 15 minutes after injection into an oocyte, compared with up to 2 days by capped mRNA (Krieg and Melton 1984). Incorporating this modified base has been shown to reduce transcription levels but this is comparatively insignificant compared to the increase in translation levels (Ambion mMessage mMachine *in vitro* transcription kit instruction manual, catalogue number 1344, AMS Biotechnology, Oxfordshire, UK).

5.1.2 Analysis following expression in oocytes

Following heterologous expression in oocytes, transporters can be assayed in two main ways. The first involves measuring the uptake of a radiolabelled substrate whereas the second involves electrophysiological methods (when the transport is electrogenic). Both methods have

been used in analysis of the amino acid permeases AtAAP1 and 5 from *Arabidopsis*. (Boorer *et al* 1996, Boorer and Fischer 1997).

The radiolabelled substrate-uptake method will give an idea of uptake capability relative to other transporters expressed in oocytes. It can be used to provide information about specificity and pH dependence but for detailed characterisation, electrophysiological methods are preferable. Dual electrode electrophysiological analysis has been used to characterise many membrane transporters, including plant proteins. The *Arabidopsis thaliana* permease, AtAAP1, was characterised in this manner and a kinetic model was presented to explain the data obtained (Boorer *et al* 1996). In this model, two amino acid molecules and two protons were taken up in a single cycle of the protein. The binding of these molecules was thought to be positively co-operative; the affinity for proton or amino acid increasing upon the binding of their co-substrate. This was deduced from the drop in K_m observed as the concentration of co-substrate increased. This K_m profile also suggested that binding to the transporter was random not ordered and translocation happened simultaneously rather than sequentially (Boorer *et al* 1996). AtAAP1 transports neutral, basic, and acidic amino acids, and the study showed that glutamine, histidine and glutamate were transported in their zwitterionic form by a similar mechanism (Boorer *et al* 1996). The stoichiometry for AtAAP5, characterised in oocytes, was one proton per amino acid (Boorer and Fischer 1997). For this permease, lysine was transported in its cationic form whereas histidine and glutamate were transported as neutral species.

5.1.3 Aims

The initial aim of this project was to characterise the transport properties of WT and mutated RcAAP1 and 3 following heterologous expression in *Xenopus* oocytes. Due to time constraints, only work with the WT transporters was achieved.

Oocytes injected with mRNA of *RcAAP1* and *3* were examined by two experimental procedures. Firstly, the uptake of a radiolabelled amino acid was measured in oocytes to demonstrate expression and targeting to the plasma membrane and obtain an approximation of the uptake rate for an expressing oocyte. Following this, electrophysiological methods were used to characterise the permeases in more detail.

5.2 Results

5.2.1 mRNA production and micro-injection

To produce mRNA for *RcAAP1* and *3* for oocyte injection, it was necessary to clone the cDNAs into an oocyte expression vector. The aim was to clone the cDNAs in both the sense and anti-sense orientations. The pXE2 *Xenopus* expression vector was used (figure 2.14) which has Sal I cloning sites and also Sac I and BamHI restriction sites, which can be used to check the orientation of the insert. The resulting banding pattern expected with these restriction enzymes on the vector and insert (insert cloned in sense and anti-sense orientations) is shown in figure 5.1.

RcAAP1 and *RcAAP3* cDNAs were successfully cloned into the pXE2 *Xenopus* expression vector, at the Sal I cloning site. Digestion with Sal I shows the 1.7 Kb and 1.5 Kb inserts for *RcAAP3 and 1* together with the 3.0 Kb linearised vector (figure 5.2). A restriction digest with Sac I revealed *RcAAP1* had been cloned in the sense orientation (figure 5.2; approximate 4500 bp fragment). A BamHI restriction digest revealed that *RcAAP3* had been cloned in both sense (figure 5.2; approximate 4000 bp fragment and 600 bp fragment -not visible on reproduction of gel) and anti-sense (figure 5.2; approximate 3500 bp fragment and 1400 bp fragment) orientations. Repeated attempts to clone *RcAAP1* in the anti-sense orientation resulted in failure; the reason for this is not clear.

Using pXE2/*RcAAP* constructs, mRNA was produced for *RcAAP1* (sense orientation) and *RcAAP3* (sense and anti-sense orientations). Low concentrations of poor quality *RcAAP3*-sense mRNA was produced using the first method described (section 2.14.1). Spectrophotometer readings indicated concentrations of approximately 0.3 µg/µl and average purity readings of 1.7 (section 2.8). Samples of this mRNA run on a 1.2% denaturing gel showed no signal (results not shown). The 'mMessenger mMachine' *in vitro* transcription kit from Ambion (AMS Biotechnology, Oxfordshire, UK) (section 2.14.1) produced better quality mRNA at usable concentrations (figure 5.3). From known concentrations of the 1Kb ladder (figure 5.3 – 1600 bp band approximately 25 ng/µl) the concentration of mRNAs were calculated to be approximately 100 ng/µl *RcAAP1*-sense mRNA, 100 ng/µl *RcAAP3*-sense mRNA and 50 ng/µl *RcAAP3*-anti-sense mRNA. The samples show 2 or 3 bands on the agarose gel but there is in fact only one product present. This is because the gel is a non-denaturing gel. mRNA will have several conformations and so move to different positions on the gel. The specificity of the procedure and the use of DNase ensures the authenticity of the products.

50ng of mRNA was typically injected into healthy oocytes. A visual check of oocytes was made after surgical removal to determine their general health. Healthy oocytes appear smooth, relatively large, spherical and have a definite division between a dark brown/black animal pole and a white/cream vegetal pole (figure 2.15 section 2.14.3). Individual healthy oocytes were selected and incubated at 18 °C in MBS for at least an hour before injection. Radiolabelled amino acid uptake experiments were initially conducted to determine whether *RcAAP1* and *3* had been expressed and showed functional activity in oocytes.

5.2.2 Radiolabelled amino acid uptake

For radiolabelled amino acid uptake experiments in oocytes expressing *RcAAP1* and *3*, L-[^{3}H]-histidine and L-[C^{14}]-citrulline were chosen. From radiolabelled uptake analysis in yeast expressing the permeases it was shown that RcAAP1 could directly take up L-[^{3}H]-histidine and this uptake would be approximately 10% stimulated by L-citrulline (Marvier *et al* 1998). It was likewise shown that RcAAP3 could take up L-[C^{14}]-citrulline directly and this uptake would be approximately 70% inhibited by L-histidine (Neelam *et al* 1999). From these results it was expected that RcAAP1 and 3 would show uptake of L-[^{3}H]-histidine while RcAAP3 only would show uptake of L-[C^{14}]-citrulline .

Water injected controls indicated how much of the uptake of radiolabel was background due to the activity of endogenous transport and incomplete washing of the radiiolabelled molecule from the oocyte. This residual radiolabel signal was minimised by washing the oocyte thoroughly with ice-cold buffer. The buffer sometimes contained either histidine or citrulline at the same concentration as in the uptake medium to see if this made any difference to the quality of wash off. Three types of control oocytes were used: non-injected, water injected and anti-sense injected. Non-injected oocytes showed the amount of endogenous uptake and how much radiolabel signal was not washed from the surface of a healthy oocyte. Oocytes injected with 50 nl sterile nucleotide free water show how much radiolabel signal was not washed from oocytes that had experienced the trauma of micro-injection. Micro-injection can cause significant damage to oocytes and a significant membrane leakage can occur during or following injection (Theodoulou and Miller 1995). Oocytes injected with anti-sense mRNA show how much radiolabel signal is not washed from oocytes that have experienced micro-injection trauma and have experienced the introduction of mRNA to their cytoplasm. It is believed that micro-injection of foreign mRNA into the cytoplasm of oocytes may trigger the activation of endogenous proteins or the activation of endogenous genes (Miller and Zhou 2000).

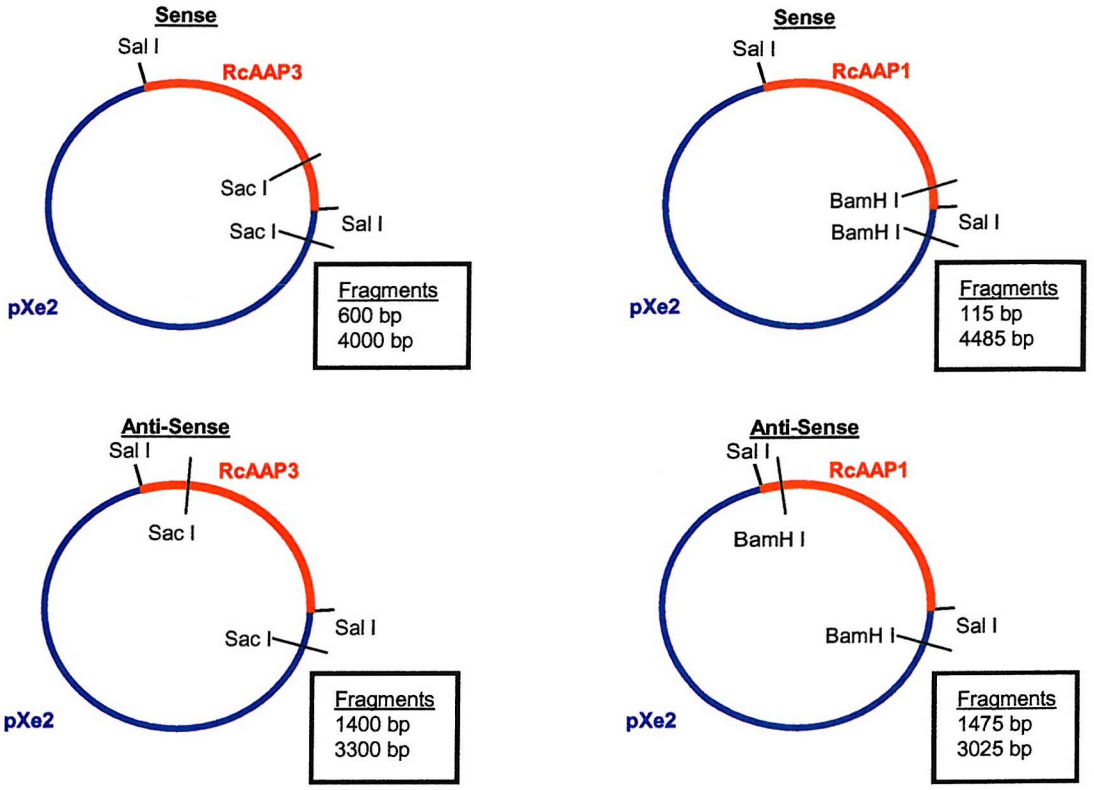

Figure 5.1 – Predicted size of fragments following restriction digests of pXe2/*RcAAP1* and pXe2/*RcAAP3* constructs cloned into the Sal I site in sense and anti-sense orientations.

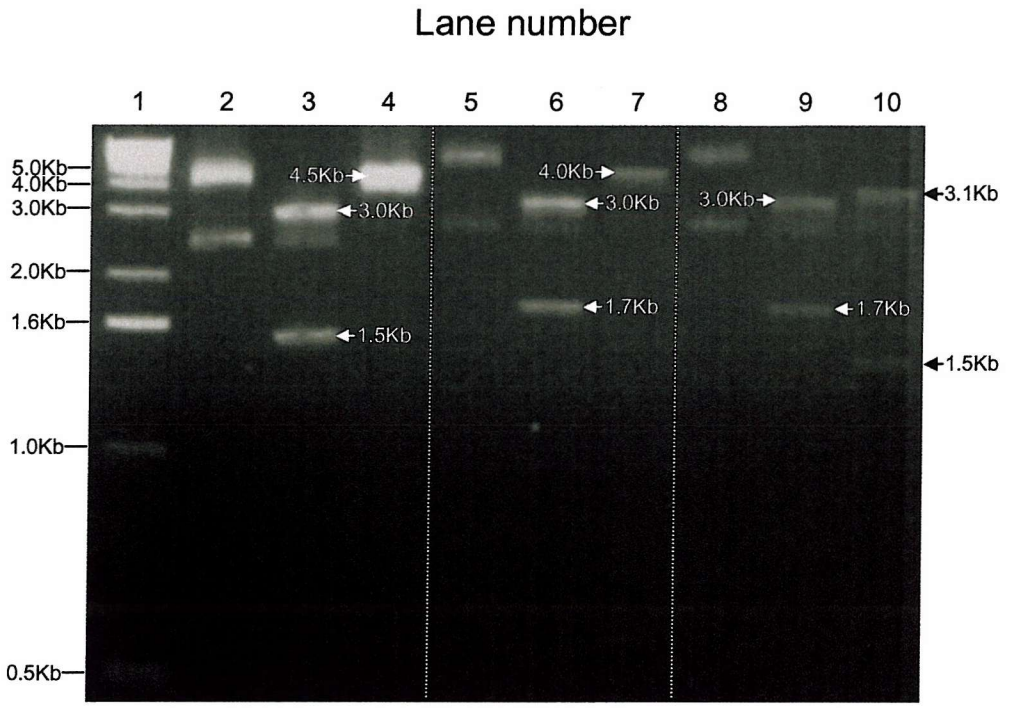

Figure 5.2 - 1% agarose gel showing restriction digests of *pXe2/RcAAP* constructs. 1kb ladder (1), pXe2/*RcAAP1* (2), pXe2/*RcAAP1* Sal I digest (3), pXe2/*RcAAP1* (sense) BamH I digest (4), pXe2/*RcAAP3* (5), pXe2/*RcAAP3* Sal I digest (6), pXe2/*RcAAP3* (sense) Sac I digest (7), pXe2/*RcAAP3* (8), pXe2/*RcAAP3* Sal I digest (9), pXe2/*RcAAP3* (anti-sense) Sac I digest (10).

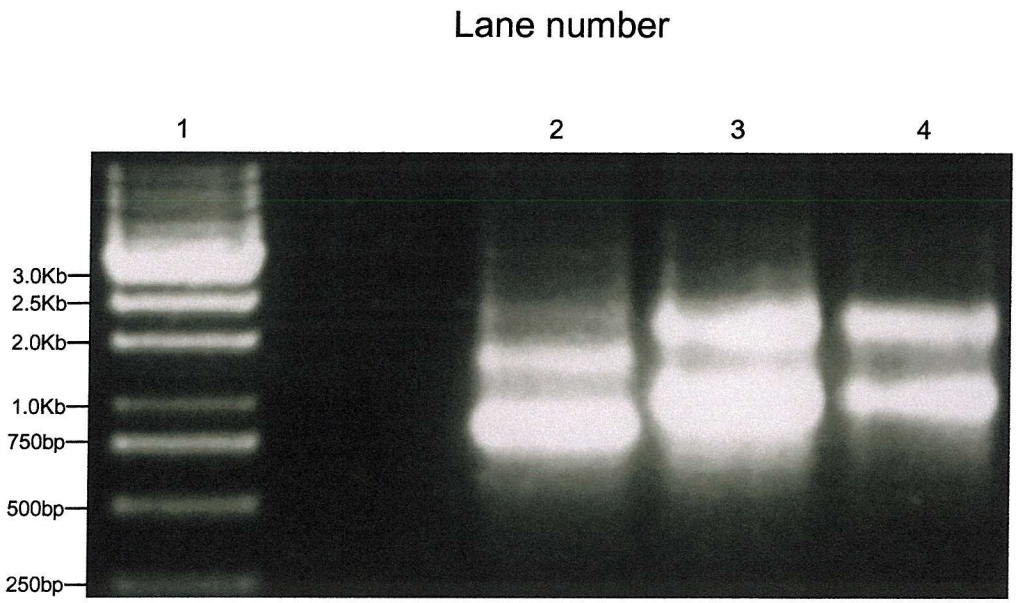

Figure 5.3 - mRNA produced from pXE2/*RcAAP* constructs. 1Kb ladder (1), *RcAAP1*-sense mRNA (2), *RcAAP3*-sense mRNA (3), *RcAAP3*-anti-sense mRNA (4).

The best control available to identify this possible problem should be the injection of anti-sense mRNA, but even this might not be an ideal control as this alternate orientation of mRNA could activate different endogenous genes and/or proteins. The most commonly used control is water-injected oocytes (Miller and Zhou 2000). These controls are easily repeatable and give a relatively consistent reading. Uptake was measured at pH 5.5 and 7.5 as described in materials and methods (section 2.14.5).

At pH5.5, levels of citrulline uptake for *RcAAP1*-sense mRNA injected oocytes were not significantly higher than those for water or non-injected oocytes (figure 5.4A) indicating that either RcAAP1 does not transport citrulline or that *RcAAP1* has not been expressed and targeted to the plasma membrane in oocytes. In contrast, uptake of citrulline into *RcAAP3* sense mRNA injected oocytes at pH 5.5 was significantly higher than non-injected, water-injected and *RcAAP3* anti-sense mRNA injected oocytes. This indicates that RcAAP3 does transport citrulline (figure 5.4A). The uptake values with the background water-injected control values subtracted are shown in figure 5.4C and give a value of 50.3 pmol/oocyte/hour ±5.3 for *RcAAP3* sense mRNA injected oocytes at pH5.5.

At pH7.5 a similar profile for citrulline uptake is observed although all the values are lower (figure 5.4B and D). Once again citrulline uptake for *RcAAP3*-sense mRNA injected oocytes is significantly higher than the non-injected, water injected, *RcAAP1*-sense mRNA injected and *RcAAP3*-anti-sense mRNA injected oocytes (figure 5.4B). The uptake values with the background water- injected control values subtracted are shown in figure 5.4D and give a value of 33.6 pmol/oocyte/hour ± 6.6 for *RcAAP3* sense mRNA injected oocytes at pH 7.5. Thus there is a reduction in the value at pH7.5 compared to pH5.5.

The same experiment was carried out using histidine. A similar result was indicated at pH5.5, in that only the *RcAAP3*-sense mRNA injected oocytes showed a significant uptake (figure 5.5A). With the water-injected controls subtracted (figure 5.5C) an uptake value of 14.91 pmol/oocyte/hour ±3.7 was determined at pH5.5. The corresponding value at pH7.5 was zero. These preliminary experiments show that RcAAP3 appears to mediate the uptake of histidine and citrulline and uptake is higher at pH5.5 than pH7.5. Suggesting a dependence on pH (proton concentration). No significant uptake was observed for RcAAP1.

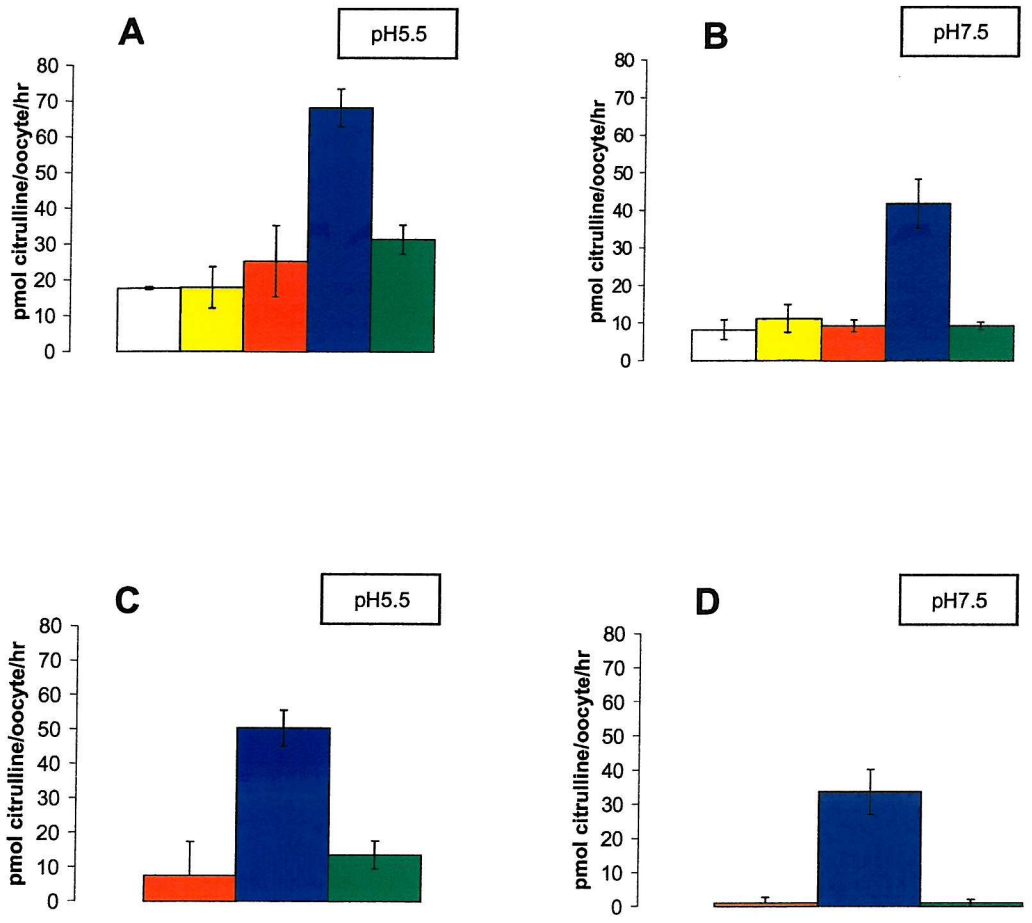

Figure 5.4 – Uptake of radiolabelled L-citrulline (100 µM) into oocytes at pH5.5 (A, C) and pH7.5 (C, D). White, non-injected; yellow, water injected; red, *RcAAP1*-sense mRNA injected; blue, *RcAAP3*-sense mRNA injected; green, *RcAAP3*-anti-sense mRNA injected. The results shown in C and D are the uptake values following deduction of the water-injected control values. The results are from a representative experiment (carried out twice) and are the means ±S.E. of 7-10 oocytes.

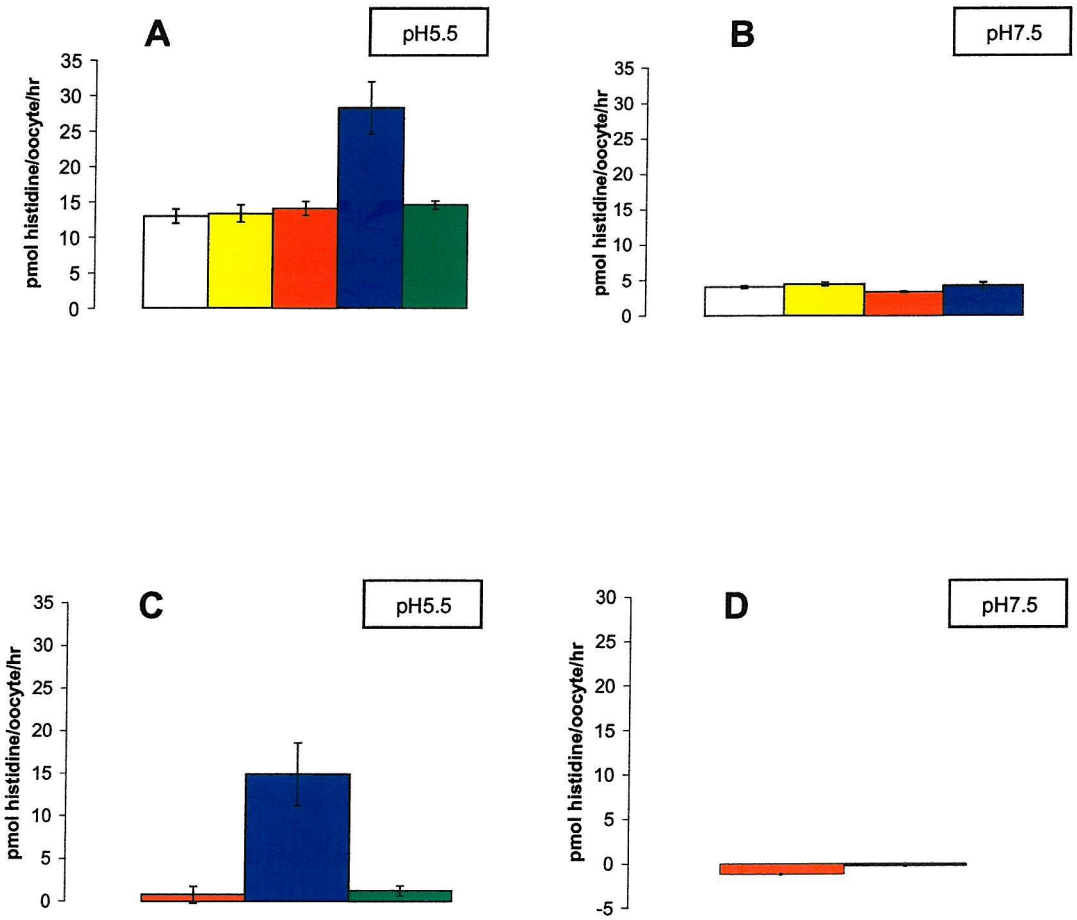

Figure 5.5 – Uptake of radiolabelled L-histidine (100μM) into oocytes at pH5.5 (A, C) and pH7.5 (C, D). White, non-injected; yellow, water injected; red, *RcAAP1*-sense mRNA injected; blue, *RcAAP3*-sense mRNA injected; green, *RcAAP3*-anti-sense mRNA injected. The results shown in C and D are the uptake values following deduction of the water-injected control values. The results are from a representative experiment (carried out twice) and are the means ±S.E. of 7-10 oocytes.

5.2.3 Electrophysiological determinations – dual electrode measurements

Oocytes injected with *RcAAP1*-sense mRNA, *RcAAP3*-sense mRNA, *RcAAP3*-anti-sense mRNA and water were incubated for 3 days at 18 °C in MBS. A dual electrode approach was adopted where steady-state amino acid-induced currents were measured as a function of membrane voltage (see section 2.14.6.1). IV curves were produced for oocytes injected with *RcAAP1* and *3*-sense mRNA under various conditions involving alterations in the amino acid substrate, its concentration and the pH (appendix 2). For all these conditions, the three types of control oocyte (non-injected oocytes, water-injected oocytes and *RcAAP3*-anti-sense injected oocytes) all showed a zero or negligible response to treatments (figure 5.6). The largest change in current upon addition of amino acid for RcAAP3 anti-sense mRNA injected oocytes was -2 nA. This indicates that any measured response beyond this is due to the action of an expressed membrane protein.

RcAAP1-sense mRNA injected oocytes consistently gave no response to histidine, citrulline, isoleucine and glutamine at concentrations between 0.5 mM and 14 mM and pHs between pH 6.8 and pH 5.5. This concurs with the result shown for radiolabelled uptake, where *RcAAP1*-sense mRNA injected oocytes did not give a signal significantly larger than that of the controls. The possible reasons for this will be discussed later (section 5.3).

RcAAP3-sense mRNA injected oocytes gave measurable responses for a range of amino acids. The amino acids citrulline (neutral), isoleucine (neutral hydrophobic), histidine (basic) and glutamine (neutral hydrophilic) all gave measurable currents. The other amino acids tested: valine (neutral hydrophobic), alanine (neutral hydrophobic) and aspartic acid (acidic), did not give measurable responses.

Measurements made for isoleucine and citrulline were obtained over a wide enough range of concentrations and pH conditions for kinetic parameters to be determined. The average IV response from measurements taken before and after treatment with isoleucine and citrulline were deducted from the IV measurement during treatment (at the peak of response). This is then the IV response due to RcAAP3. Insufficient determinations were made for histidine and glutamine to calculate IV curves. The data representing transport of citrulline by RcAAP3 at a variety of pH conditions is shown in figure 5.7. The plots of citrulline concentration against induced current are shown on the left of this figure. Curves were fitted to these plots using equation **1** (section 2.14.6.2). Once these curves were produced, the constants in the equation, K_m and i_{max}, were plotted against membrane potential. These plots are shown to the right of the corresponding concentration versus current plot (figure 5.7), and they show if the K_m and i_{max} alter with changes in the membrane potential. One point to remember when looking at

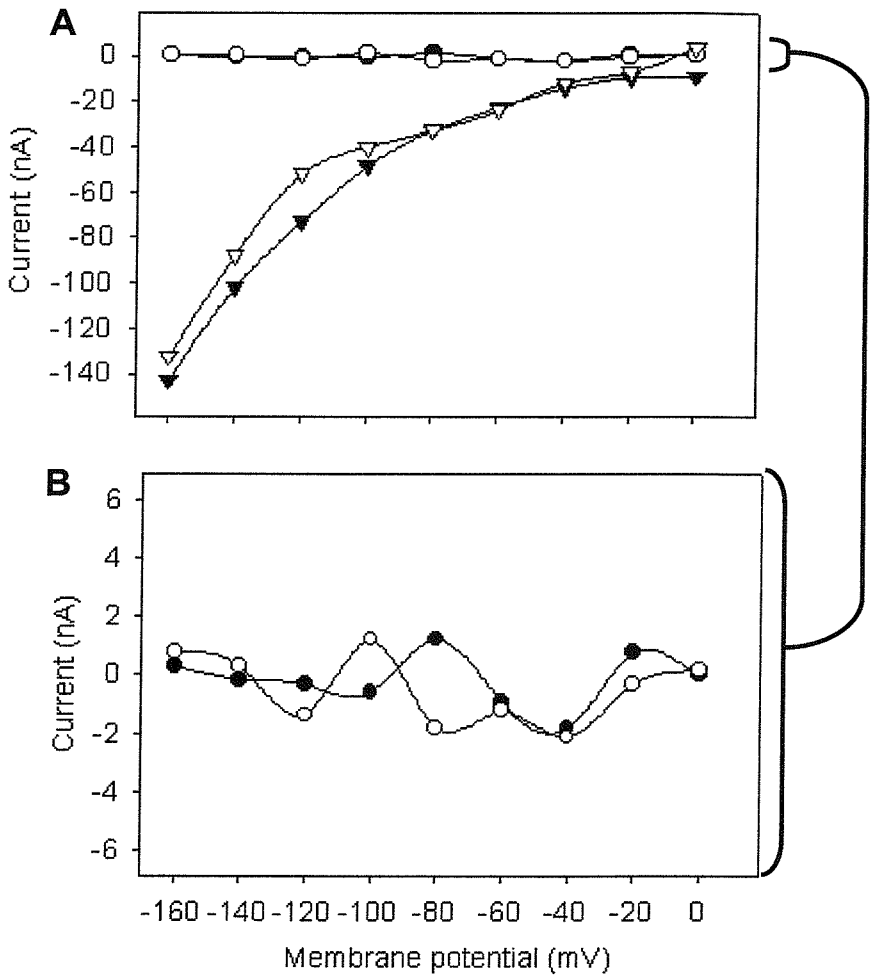

Figure 5.6 – Membrane potential against current (IV) curves comparing the response from *RcAAP3* sense and anti-sense mRNA injected oocytes. *RcAAP3* sense mRNA injected in 10 mM histidine (▼), *RcAAP3* sense mRNA injected in 10 mM citrulline (▽), *RcAAP3* anti-sense mRNA injected in 10 mM histidine (●), *RcAAP3* anti-sense mRNA injected in 10 mM citrulline (○). All curves were produced at pH 5.5 in choline chloride solution and are representative of repeated experiments with different mRNA and oocytes. **B** is the control plots from **A** with a smaller scale y-axis to improve resolution.

this relationship is that the membrane potentials applied across the plasma membrane of the oocytes (40 mV to -160 mV) are not as negative as the membrane potentials found in plants (-100 mV and -200 mV, Miller and Zhou 2000). If K_m values depend on the size of the membrane potential then this result could explain variation in the estimates of this kinetic property of the transporter in the plant. The same calculations were performed with isoleucine as a substrate (figure 5.8). Isoleucine, like citrulline is a non-polar amino acid. Again curves were fitted to the concentration versus current plots and the subsequent K_m and i_{max} constants plotted against potential. This shows how the K_m and i_{max} of RcAAP3 alter at different membrane potentials when taking up isoleucine. Comparing the K_m and i_{max} profiles for citrulline and isoleucine it can be seen that for both sets of data the i_{max} is voltage dependant, becoming more negative as the membrane potential becomes more negative. Also in both sets of data the i_{max} is not as negative at higher pH (lower proton concentrations). The K_m for both citrulline and isoleucine appears to be relatively independent of potential (this is investigated in further detail later). The average K_m for citrulline is consistently lower than that for isoleucine under all pH conditions. This result suggests that RcAAP3 has a higher affinity for citrulline than isoleucine. The K_m measurements for both isoleucine and citrulline generally increase at higher external pH, suggesting that the affinity of RcAAP3 for amino acid is reduced as the proton concentration decreases (this will be investigated in more detail later).

The data collected for isoleucine and citrulline with *RcAAP3*-expressing oocytes (figure 5.7 and 5.8) were used to calculate the K_m and i_{max} values for protons. The induced current was plotted against the proton concentration for a range of citrulline concentrations. These plots were then used to produce curves using equation **1** (section 2.14.6.2). The subsequent constants, K_m and i_{max}, were plotted against membrane potential to reveal any correlation (figures 5.9 and 5.10). Again it is important to remember that the membrane potentials used in oocytes (40 mV to -160 mV) are not as negative as the membrane potential in plants; on average -100 mV to -200 mV (Miller and Zhou 2000). The membrane potential is an essential factor in the kinetics of membrane transport. From these plots of K_m and i_{max} against potential it can be seen that at all citrulline concentrations i_{max} is dependent on membrane potential, becoming more negative as the potential becomes more negative. There is also a general decrease in K_m as the citrulline concentration decreases, although this is not as pronounced as the i_{max} change for citrulline over a pH range (figure 5.9). The K_m for protons remains relatively constant throughout the range of potentials. There is variation in average K_m between citrulline concentrations but there is no definite pattern (this is investigated in more detail later).

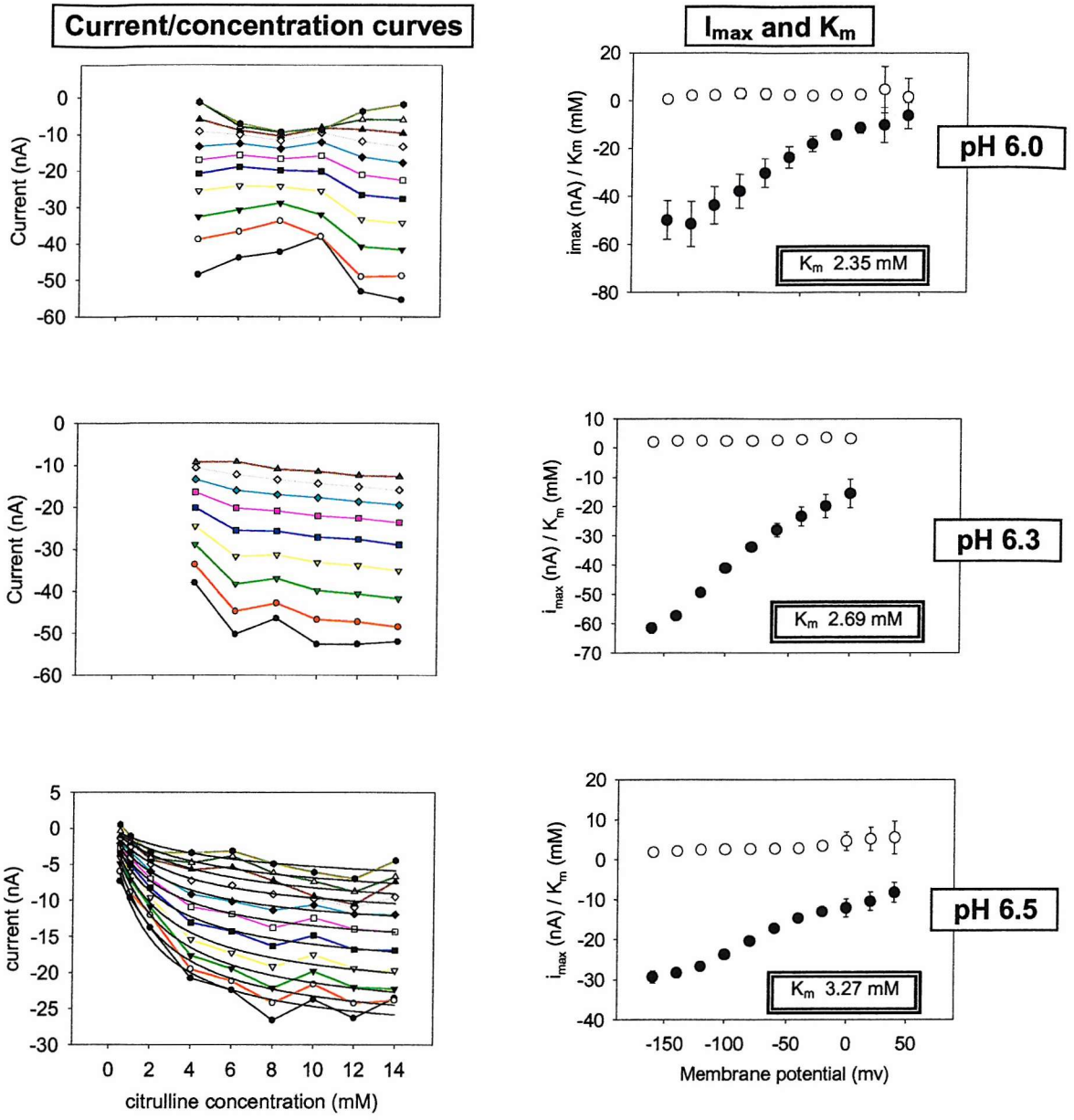

Figure 5.7 – Currents measured from voltage clamped oocytes expressing RcAAP3, in response to the addition of citrulline. Plots of current against citrulline concentration for voltages between -160 mV and +40 mV (colour scale – key below) at different pHs (left). Calculated K_m(○) and i_{max}(●) constants of RcAAP3 for citrulline with standard error (right). An example of the best fit lines used to estimate the constants K_m and i_{max} are shown for pH 6.5 (bottom left).

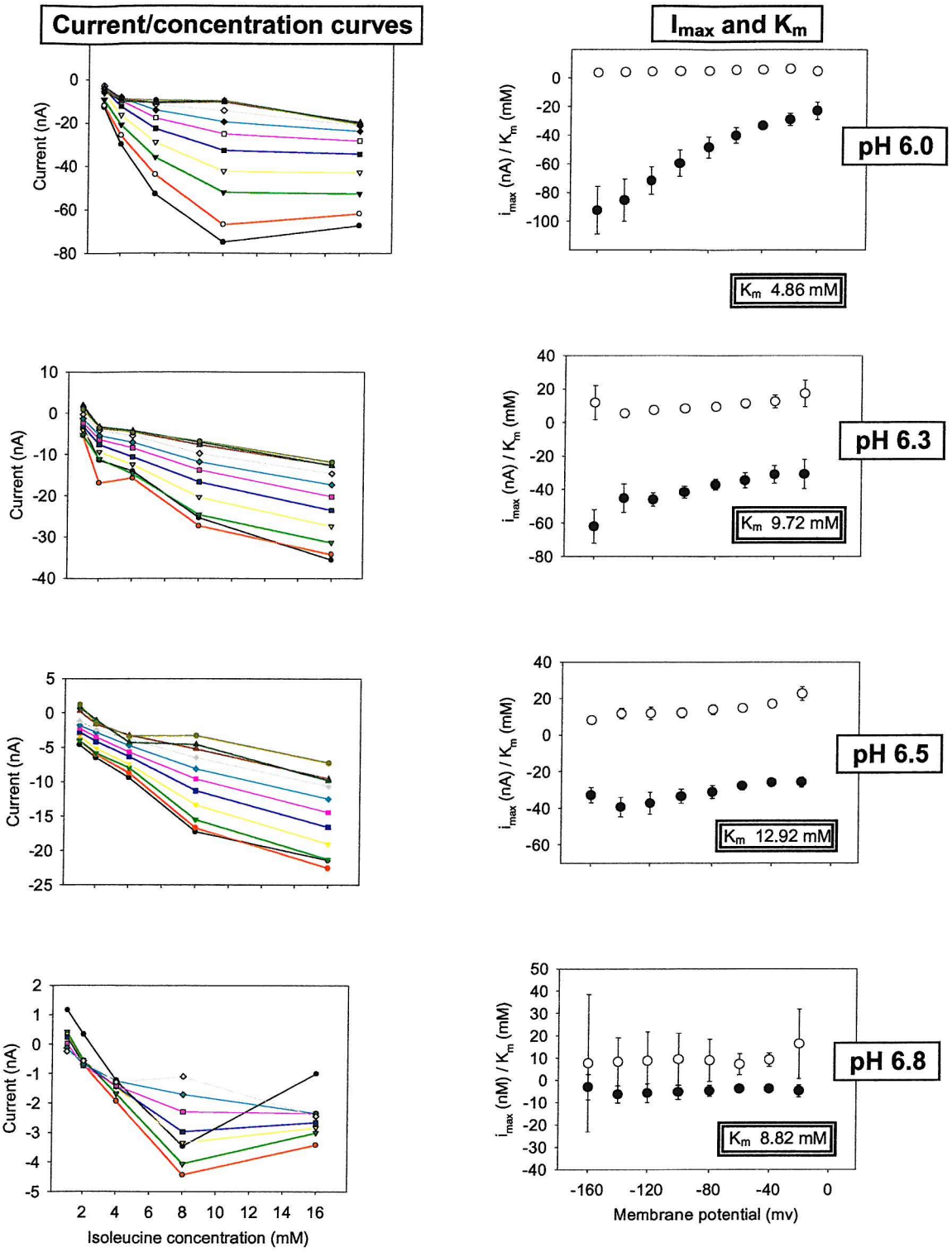

Figure 5.8 – Currents measured from voltage clamped oocytes expressing RcAAP3, in response to the addition of isoleucine. Plots of current against isoleucine concentration for voltages between -160 mV and +40 mV (colour scale - key bottom of figure 5.7) at different pHs (left). Calculated K_m(○) and i_{max}(●) constants of RcAAP3 for isoleucine with standard error (right).

The data for protons in the presence of isoleucine was similarly rearranged, but the resultant standard errors during curve fitting to equation **1** (section 2.14.6.2) made the data unusable. This may be because the current against concentration plots did not sufficiently approach an asymptote (figure 5.10). This may suggest that saturation of isoleucine uptake for RcAAP3 occurs at a more acidic pH (higher proton concentration) than for citrulline. Although the standard errors do not allow for accurate translation of the results for K_m and i_{max} for protons in the presence of isoleucine, it appears that the i_{max} for protons is dependent on potential in the same way as it was in the presence of citrulline. The i_{max} becomes more negative as the potential becomes more negative. The K_m is also dependent on potential but only at potentials more negative than -100mV (figure 5.10).

The data was re-plotted to show the K_m values for citrulline and isoleucine at four different pH values (figure 5.11A and C). In addition, the K_m for protons at a range of citrulline and isoleucine concentrations was re-plotted in more detail (figure 5.11B and D). By plotting the K_m values without showing i_{max} values, removing standard error bars for clarity and incorporating several plots onto the same axis it was possible to observe the following. The K_m for citrulline is dependent on membrane potential, decreasing as the potential becomes more negative (figure 5.11A). However, there was no marked shift in K_m between different pH values. The K_m plots for citrulline at pH 6.0, pH 6.3 and pH 6.5 all appear to follow the same pattern over the range of potentials. The K_m for isoleucine is also dependent on potential (figure 5.11C), similarly decreasing at more negative potentials. Unlike the K_m for citrulline, the K_m for isoleucine does have some dependence on pH. The K_m for isoleucine increases (decreasing affinity) as pH increases (decreasing proton concentration), up until pH 6.8 where the K_m drops again. The K_m for protons in the presence of isoleucine was not measurable with satisfactory confidence (figure 5.11D); as mentioned before, this may be because the concentration against current plot did not saturate, reaching an asymptote (figure 5.10). The K_m for protons in the presence of isoleucine did appear to increase at potentials more negative than –100mV, but this result is not significant. The K_m for protons in the presence of citrulline is dependent on potential, but in the opposite manner to the K_m for isoleucine and citrulline (figure 5.11B). The K_m for protons increases (affinity decreases) as the potential becomes more negative, this is the same pattern as the K_m in the presence of isoleucine. There was some variation in K_m for protons over the citrulline concentration range, although there was no discernible pattern to this data (figure 5.11B).

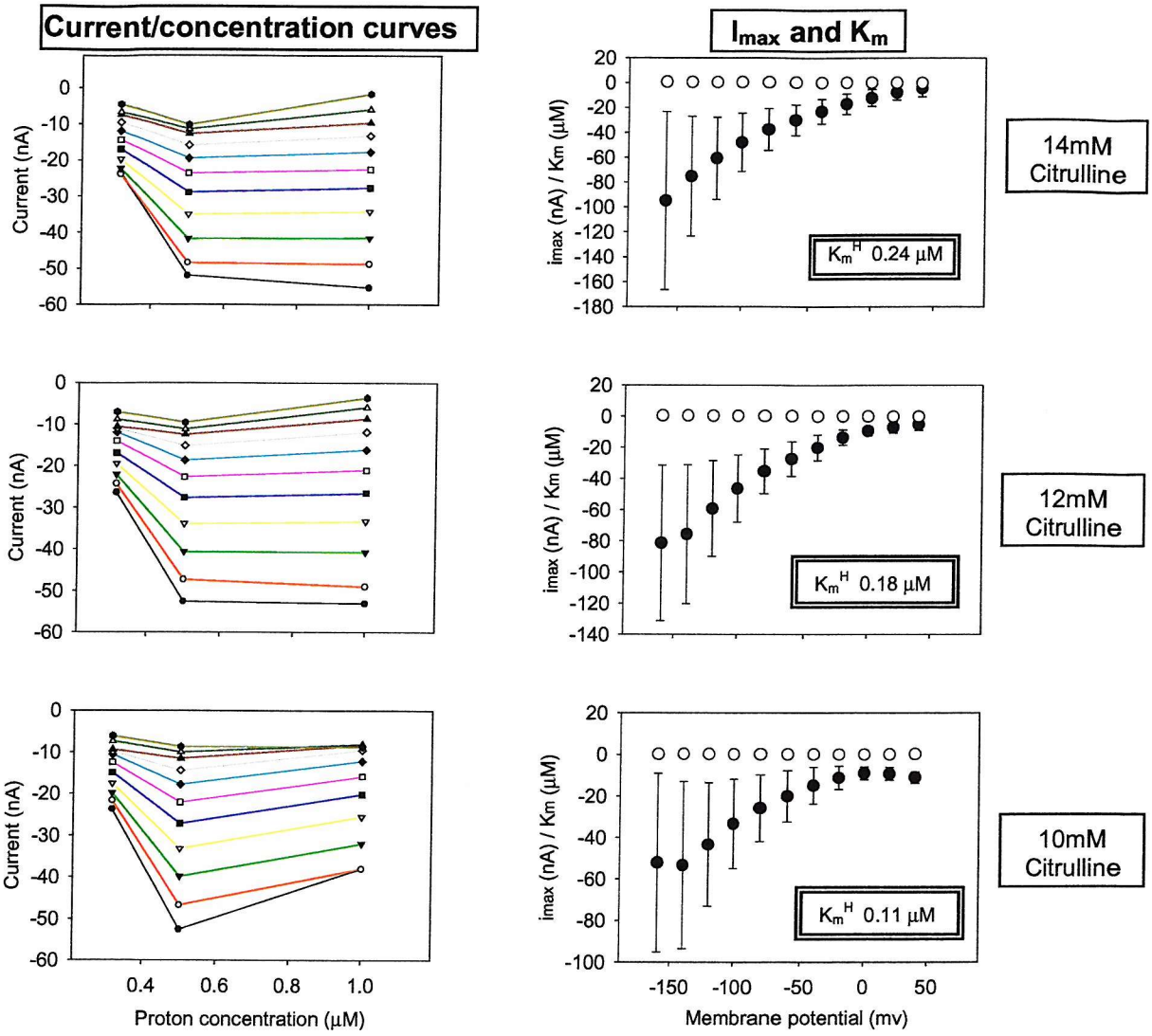

Figure 5.9 – Relationship between current and proton concentration for *RcAAP3*-expressing oocytes, determined from the rearrangement of the data in figure 5.7. Plots of current against proton concentration for voltages between -160 mV and +40 (colour scale – key below) mV at different citrulline concentrations (left). Calculated K_m(○) and i_{max}(●) constants of RcAAP3 for protons with standard error (right).

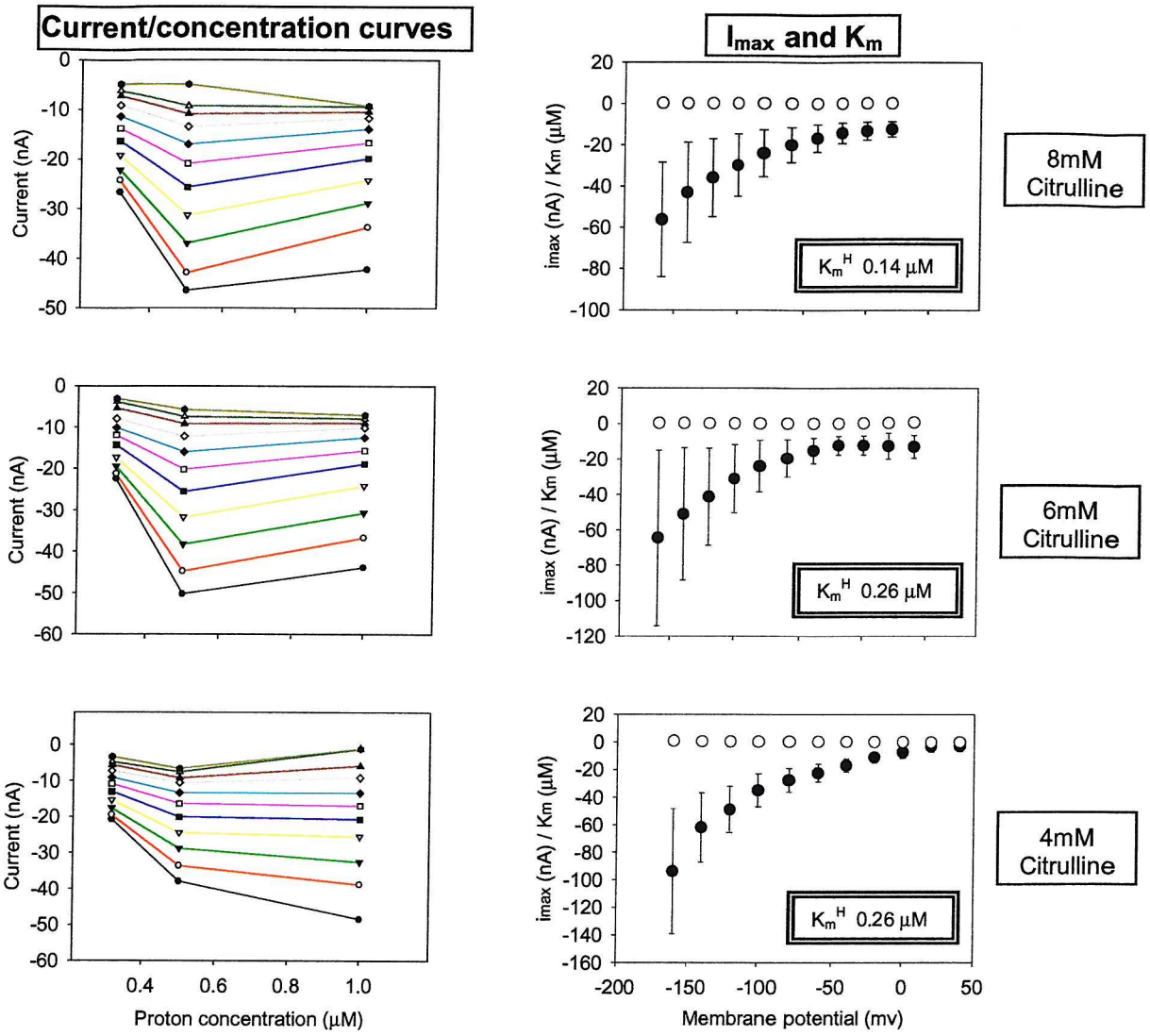

Figure 5.9 (continued)– Relationship between current and proton concentration for *RcAAP3*-expressing oocytes, determined from the rearrangement of the data in figure 5.7. Plots of current against proton concentration for voltages between -160 mV and +40 mV (colour scale – key below) at different citrulline concentrations (left). Calculated K_m(○) and i_{max}(●) constants of RcAAP3 for protons with standard error (right).

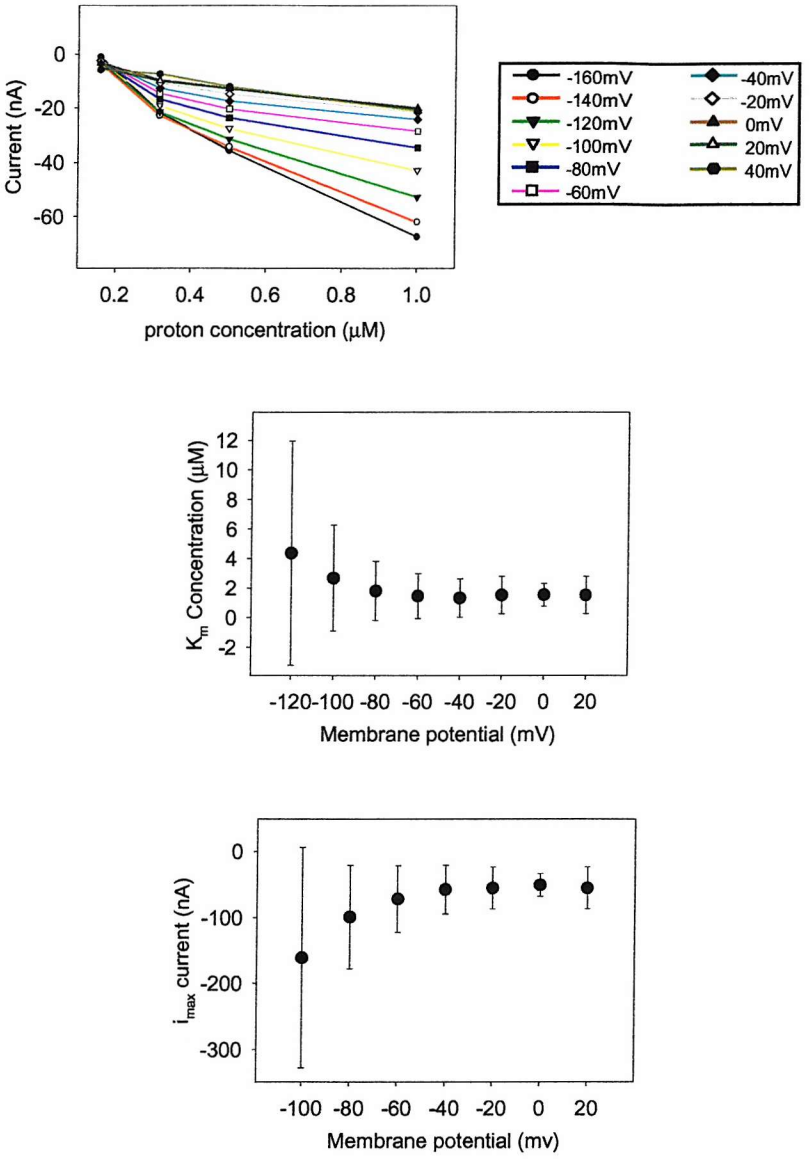

Figure 5.10 - Relationship between current and proton concentration for *RcAAP3*-expressing oocytes, determined from the rearrangement of the data in figure 5.8. Plots of current against proton concentration for voltages between -160 mV and +40 mV (colour scale – key top) at 16 mM isoleucine (top). Calculated K_m (middle) and i_{max} (bottom) constants of RcAAP3 for protons with S.E.

The data was rearranged to show K_m and i_{max} for protons, isoleucine and citrulline against the concentration of their co-substrate (figure 5.12 and 5.13). The K_m for protons against citrulline concentration at three membrane potentials (figure 5.12A) shows that the K_m for protons decreases (affinity increases) as citrulline concentration increases. This pattern is followed until 10 mM citrulline. Beyond this concentration the K_m increases again (affinity decreases). At 10 mM citrulline and higher, RcAAP3 is approaching saturation. This is demonstrated in figure 5.7, where plots approach an asymptote on the current axis (y-axis) at citrulline concentrations over 10 mM (x-axis). The K_m for citrulline against proton concentration (figure 5.12B) shows that K_m decreases (affinity increases) as the proton concentration increases. This indicates that as the concentration of either protons or citrulline increases, the affinity of RcAAP3 for the co-substrate is likewise increased. The i_{max} for both citrulline and protons is shown to be dependent on membrane potential (figure 5.12C and D). At more negative membrane potentials the i_{max} for each is more negative. The i_{max} is also more negative at higher concentrations of each co-substrate. These results show that as proton and citrulline concentrations increase, so the affinity and transport for the corresponding co-substrate increases.

Data for isoleucine K_m and i_{max} was similarly rearranged to show the variation against proton concentration (figure 5.13). The rearrangement to show proton K_m and i_{max} against isoleucine concentration has not been displayed here as the errors previously mentioned for this data made the results unusable. As with citrulline K_m, isoleucine K_m decreases (affinity increases) as the proton concentration increases (figure 5.13, top). The i_{max} of isoleucine against proton concentration also follows the same pattern as that for citrulline. As the proton concentration increases, the i_{max} for isoleucine becomes more negative (figure 5.13, bottom). The i_{max} for isoleucine also becomes more negative at more negative membrane potentials. These results concur with the results for citrulline i_{max} and K_m against proton concentration (figure 5.12B and D). The affinity for isoleucine increases as proton concentration increases and the i_{max} becomes more negative as proton concentration increases.

The original current against concentration data (used in figures 5.7, 5.8 and 5.9) was applied to equation **2** (section 2.14.6.2) in order to calculate the Hill coefficient for isoleucine, citrulline and protons for RcAAP3. The resulting Hill coefficient was plotted against potential (figure 5.14). The Hill coefficient plot for isoleucine at three different pH shows two different values (figure 5.14A). At pH 6.5 and pH 6.3 the Hill coefficient is approximately 1 through the range of potentials. For the higher proton concentration (pH 6.0) the Hill coefficient is approximately 2 through the range of potentials. The Hill coefficient plot for citrulline at three different pH values (figure 5.14B) again shows pH-dependence. There is a Hill coefficient of

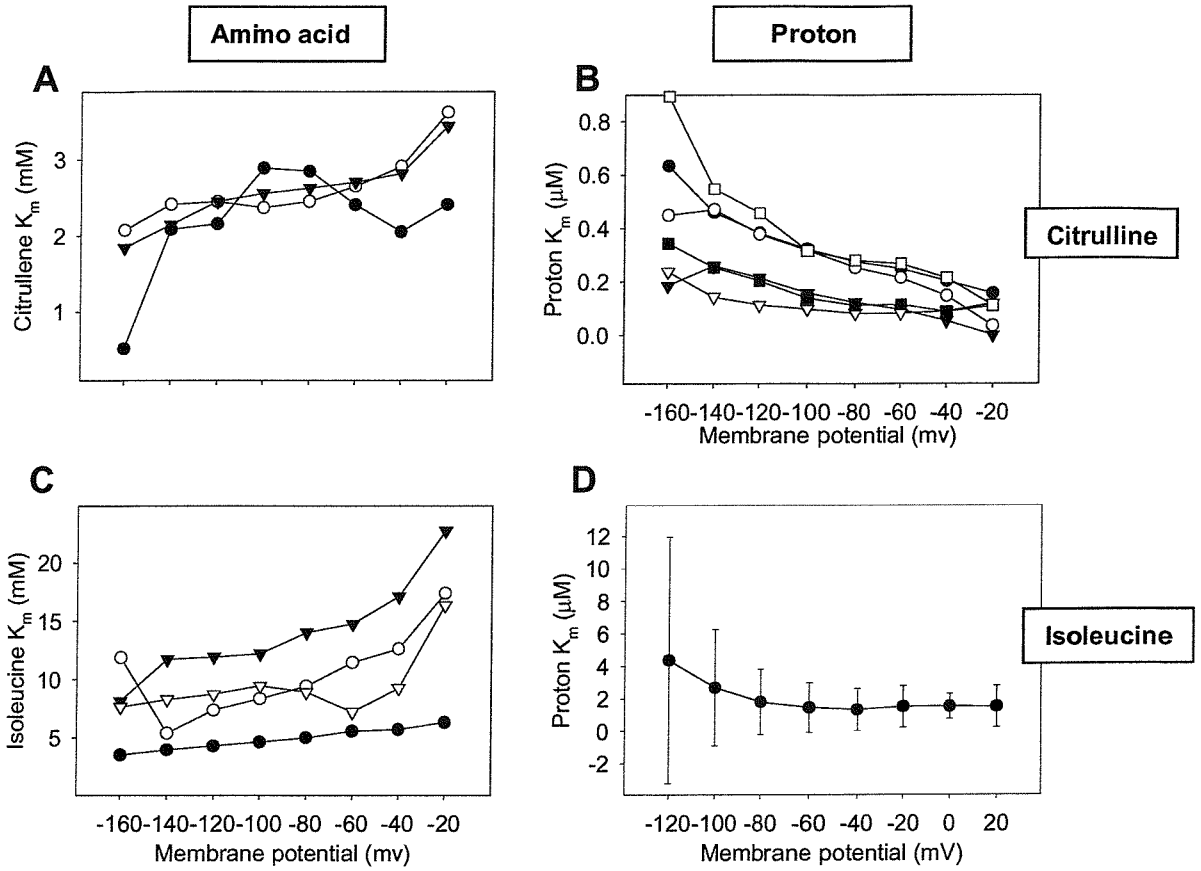

Figure 5.11 – Relationship of K_m to potential calculated for RcAAP3-expressing oocytes for: citrulline (A), isoleucine (C), and protons in the presence of citrulline (B) or isoleucine (D). Error bars have been omitted for clarity (except for bottom right). In A and C, pH 6.0 (●), pH 6.3 (○), pH 6.5 (▼), pH 6.8 (▽). In B citrulline concentrations; 14 mM (●), 12 mM (○), 10 mM (▼), 8 mM (▽), 6 mM (■), 4 mM (□). In D 16 mM isoleucine (●).

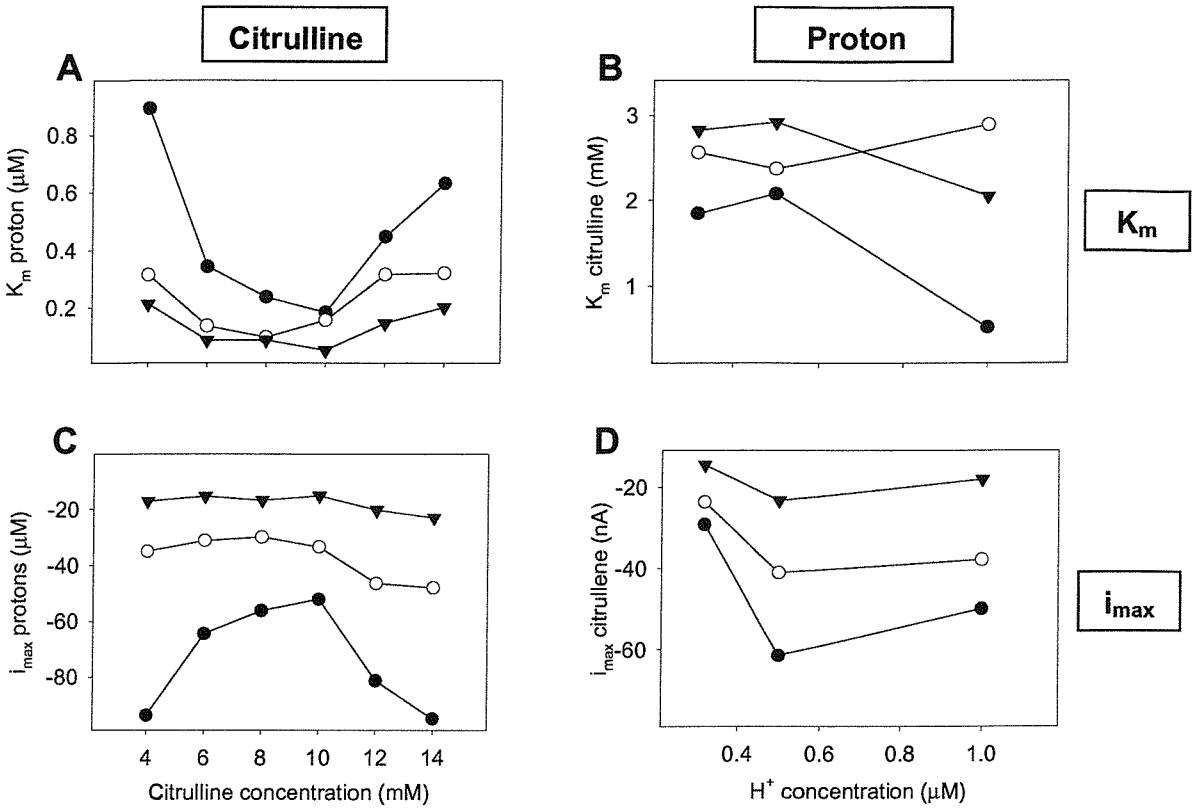

Figure 5.12 – Plots showing the K_m and i_{max} relationships between the co-substrates citrulline and protons in RcAAP3-expressing oocytes. K_m for protons against citrulline concentration (**A**). K_m for citrulline against proton concentration (**B**). i_{max} for protons against citrulline concentrations (**C**). i_{max} for citrulline against proton concentrations (**D**). Error bars have been omitted and only three potentials have been included for clarity. These three potential are representative of the full range of potentials between -160mV and +40 mV. -160 mV (●), -100 mV (○), -40 mV (▼).

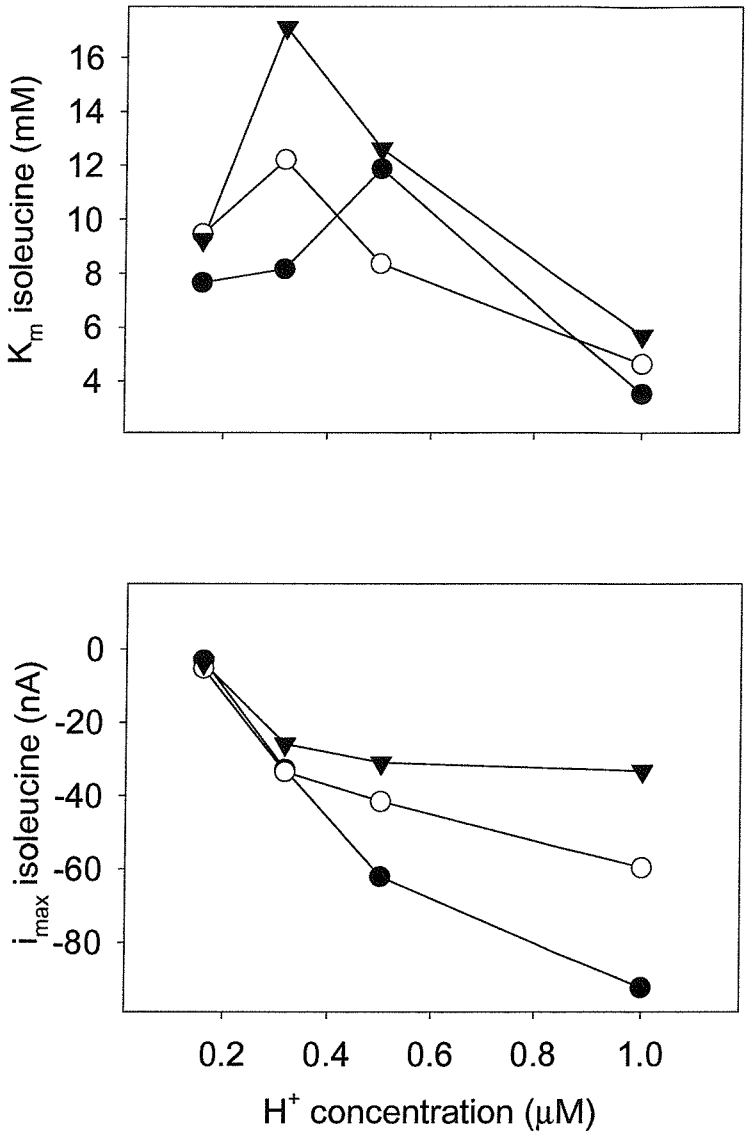

Figure 5.13 – Plots showing the K_m and i_{max} relationships between the co-substrates isoleucine and protons in RcAAP3-expressing oocytes. Error bars have been omitted and three potentials are shown for clarity. These three potentials are representative of the full range of potentials between -160 mV and +40 mV. -160 mV (●), -100 mV (○), -40 mV (▼).

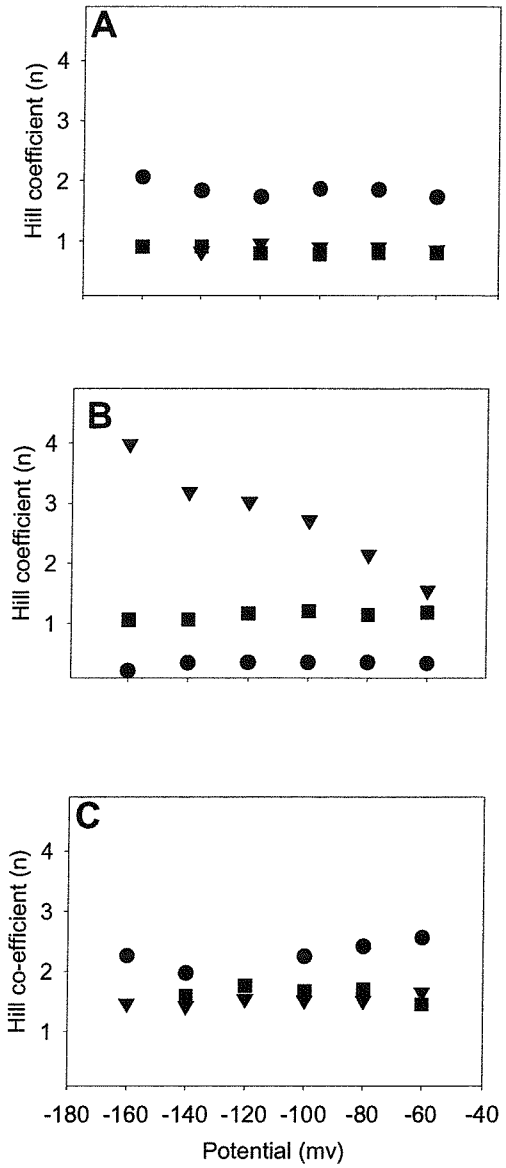

Figure 5.14 – Plots showing Hill coefficient against potential for RcAAP3-expressing oocytes. Hill coefficient with respect to isoleucine at three different pHs (A). Hill coefficient with respect to citrulline at three different pHs (B). In A and B pH 6.0 (●), pH 6.3 (▼), pH 6.5(■). Hill coefficient with respect to protons at three different isoleucine concentrations (C). In C isoleucine concentrations 16 mM (●), 8 mM (▼), 4 mM (■).

below 1 at pH 6.0, approximately 1 at pH 6.5 and at pH 6.3 the Hill coefficient appears to have a dependence on potential, going from 1.5 to 4 between the potentials of –60 mV and –160 mV. The Hill coefficient for protons in the presence of citrulline has not been included, as the current against concentration data for this result would not successfully fit to equation **2** (section 2.14.6.2). This is probably due to the fact that only three proton concentrations were plotted for citrulline. This was sufficient to give K_m and i_{max} values for this data from equation **1** (section 2.14.6.2), but not sufficient to fit equation **2** (section 2.14.6.2) with its extra variable (n – Hill coefficient). The Hill coefficient plot for protons at 3 different isoleucine concentrations (figure 5.14C) shows less voltage-dependence than the other two plots (figure 5.14A and B). At 4 mM and 8 mM isoleucine, the Hill coefficient is approximately 1.5 through the range of potentials. At 16 mM isoleucine, the Hill coefficient is approximately 2.5 through the range of potentials. The mean of these three plots would indicate a Hill coefficient of 2 for protons.

5.3 Discussion

The responses measured from oocytes injected with *RcAAP3*-sense mRNA, in both radiolabelled uptake and electrophysiological experiments indicate that *RcAAP3* has been correctly translated and targeted to the plasma membrane by the oocyte. Oocytes injected with *RcAAP1* mRNA have consistently shown no significant response compared to control oocytes. Results from competition analysis in yeast indicated that RcAAP1 should be able to transport citrulline, histidine and isoleucine (Marvier *at al* 1998). The lack of any response, even from the sensitive dual electrode method under pH 5.5, 14 mM histidine, 14 mM citrulline and 16 mM isoleucine conditions, shows no transport activity of *RcAAP1* in oocytes. There are a number of possible reasons for this disappointing result. The mRNA injected may not have been translated by the oocyte, or only at very undetectable low levels. Although possible, this reason seems unlikely as the *RcAAP3* mRNA was prepared using the same method of transcription from an insert in the same vector. The results from section 5.2.1 clearly show that the *RcAAP1* cDNA insert has been successfully incorporated into the pXE2 oocyte expression vector in the sense orientation. Furthermore *RcAAP1* sense mRNA is produced during *in vitro* transcription, and this has been visualised on an agarose gel running at the correct size relative to *RcAAP3* mRNA (figure 5.3). It is not possible however, to show the fate of this mRNA within the oocyte. The *Arabidopsis* K^+ channels AtAKT1 and AtKAT1 were successfully isolated by yeast complementation (Sentenac *et al* 1992, Anderson *et al* 1992, consecutively), but only AtKAT1 was successfully expressed in oocytes (Schachtman *et al* 1992, Miller *et al* 1994). Although

these sequences both share high homology, as with *RcAAP1* and *3* (85% identity at the amino acid level), AtAKT1 has a hydrophilic C-terminus believed to be involved in protein: protein interactions and also believed to interfere with translation. However, this kind of structural variance is not apparent between RcAAP1 and 3 and so there may be another reason for the apparent lack of *RcAAP1* expression in oocytes. A possible problem may be in targeting of the protein. It is possible that *RcAAP1* is being successfully translated but not successfully targeted to the plasma membrane. In oocytes the plasma membrane is the default target for proteins carrying no targeting signal so mis-targeting would involve a targeting sequence being present on the clone RcAAP1 cDNA. This is extremely unlikely as any targeting sequence from the plant would not be in the cloned cDNA sequence, meaning a sequence would have to be present in the cDNA transcript which was recognised as a targeting signal in the oocyte. Incorrect targeting is still a possibility, and could be tested by fusing the gene to an antigenic sequence e.g. c-myc epitope tag. This tag could then be used to show the membrane location of the protein in oocytes and other expression systems. A further possibility is that the RcAAP1 protein is not functional in the oocyte system because of a particular sensitivity to this lipid or ionic environment.

From the radiolabelled uptake results, it can be seen that oocytes expressing *RcAAP3* are able to take up L-[^{3}H]-histidine and L-[^{14}C]-citrulline. Transport of these two amino acids at two different conditions of pH are summarised in table 5.1. The table suggests two key things about RcAAP3. Firstly, the transport of amino acids is dependent on proton concentration. Uptake is reduced or completely obliterated in oocytes expressing *RcAAP3* at pH 7.5 (39.8 nM protons), compared to the uptake measured at pH 5.5 (3162.3 nM protons). Secondly these results suggest a preference of RcAAP3 for citrulline over histidine. At pH 5.5, histidine predominantly exists in its basic form (only 24% zwitterionic) whereas citrulline is predominantly in its zwitterionic form at this pH (see figure 5.15, A and B). Presuming histidine is transported in its zwitterionic form, this difference could be the reason that citrulline appears to be preferentially transported by RcAAP3. From yeast competition analysis, the uptake of radiolabelled L-citrulline was 70% inhibited by a 10x concentration of L-histidine at pH4.5 (Neelam *et al* 1999). This does not give any inference as to any level of preference for transport by RcAAP3, only that RcAAP3 competitively binds L-histidine. In *Arabidopsis*, the permease most similar to RcAAP3 (in terms of sequence identity) is AtAAP3 (Fischer *et al* 1995) with an identity of 77.4%. In yeast competition analysis, RcAAP3 (Neelam *et al* 1999) like AtAAP3 (Fischer *et al* 1995) has been shown to bind and transport a wide range of amino acids, including acidic, basic and neutral molecules. Competition analysis of radiolabelled proline has shown that AtAAP3 binds citrulline. Direct radiolabelled uptake measurements have shown that

AtAAP3 transports L-[^{14}C]-citrulline more effectively than L-[^{14}C]-histidine. Although these properties of AtAAP3 follow those for RcAAP3 is does not necessarily mean they are closely functionally linked. RcAAP1 has a much higher identity to RcAAP3 of 85 %, yet this has been shown to preferentially transport basic and neutral amino acids when expressed in yeast (Marvier *et al* 1998). Some part of this high identity may be due to the permeases coming from the same organism, yet this clearly demonstrates how a small change to these proteins at the amino acid level can significantly change their function. The *Arabidopsis* permease, AtAAP5 is the closest related permease to RcAAP3 (68% identity at the amino acid level) that has been analysed using the *Xenopus* oocyte expression system (Boorer and Fischer 1997). AtAAP5, like AtAAP3 and RcAAP3, is a broad range amino acid permease, and shares 71% homology to AtAAP3. Again this is not a sign of functional similarity, as AtAAP1 has a 76% homology to AtAAP5 yet preferentially transports neutral amino acids (Boorer *et al* 1996). AtAAP5 was shown to transport acidic, basic and neutral amino acids. Uptake was driven by proton co-transport and through simultaneous electrophysiological and radiolabelled measurement a ratio of 1 amino acid to 1 proton was proposed. The data described in the AtAAP5 characterisation (Boorer and Fischer 1997) was not subjected to Hill coefficient calculation and so the exact transport mechanism could not be revealed. Oocyte expression analysis did, however, reveal a mechanism for AtAAP1 co-transport (Boorer *et al* 1995). Comparison of i_{max} values for AtAAP1 transporting protons and alanine at saturating co-substrate concentrations were similar, indicating a coupling ratio of 1 proton to 1 amino acid. The Hill coefficient for alanine over three pH conditions was shown to be consistently over 1. In respect to protons, over three alanine concentrations, the Hill coefficient was shown to be approximately 2. This lead to a proposed transport model of 2 protons to 2 amino acids. The model for AtAAP1 transport also included a random-binding step and a simultaneous translocation step. This was proposed from two observations: the affinity and i_{max} for co-substrate increased as substrate concentration increased; and the Hill coefficient was over unity suggesting a positively co-operative system. Positive co-operatively is where the affinity for a second substrate is increased upon binding of a first substrate.

The transport kinetics of RcAAP3 were investigated in detail using the amino acids isoleucine and citrulline at a variety of concentrations in conjunction with a variety of proton concentrations (pH). From these experiments, the affinity of RcAAP3 for citrulline and isoleucine was found to be dependent on pH and membrane potential, increasing at more acidic pH (higher proton concentration) and more negative membrane potential. For citrulline, the average K_m over the potential range measured (40 mV to -160 mV) varied from 2.36 mM at

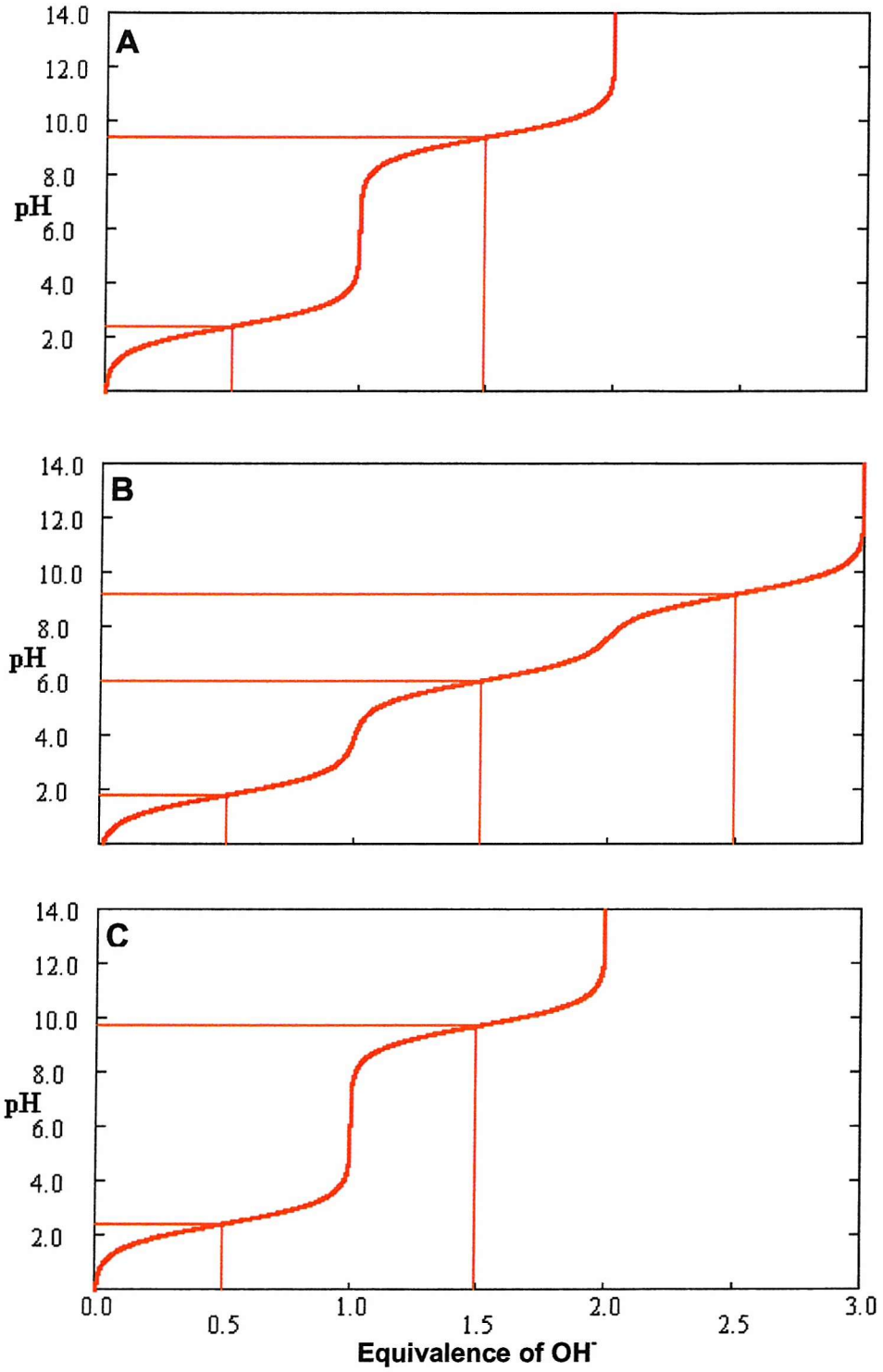

Figure 5.15 - Titration curves for citrulline (pKa 2.4 and 9.40) A, Histidine (pKa 1.8, 6.0 and 9.2) B and Isoleucine (pKa 2.4 and 9.7) C. These curves describe the ratio of forms each amino acid takes at a particular pH.

pH 6.0 to 3.27 mM at pH 6.5. In comparative analyses, AtAAP1 was found to have K_m values ranging from 0.6 mM for alanine at pH5.0 to 10.4 mM for histidine at pH5.5 (Boorer *et al* 1996). AtAAP5 was found to have a K_m over 1 mM toward citrulline and K_m values for other amino acids ranged from approximately 0.1 mM to over 100 mM (Boorer *et al* 1997). In yeast radiolabelled uptake experiments, RcAAP3 showed a K_m of 0.4 mM for citrulline (Neelam *et al* 1999). This K_m is considerably lower than that measured in oocytes, suggesting a higher affinity. However, it must be remembered that this was carried out at pH 4.5 and that yeast generally have a membrane potential of -170mV to -160mV. Taking this difference in membrane voltage into consideration, the K_m calculated in yeast seems in reasonable agreement with the oocyte K_m determinations. The RcAAP3 K_m measurements for citrulline in yeast and oocytes are displayed over a pH range in figure 5.16. This correlation of K_m over pH from oocytes to yeast has an R^2 of 0.989, suggesting a good correlation. The correlation is tentative however, as these two expression systems are different physiologically and experimentally (Miller and Zhou 2000). Also, the transport characterisation in these two systems was done using different media. In oocytes a choline chloride based medium was used (section 2.14.5) to remove any interference due to Na^+ binding. In yeast, transport characterisation was done in a 50mM potassium phosphate buffer (Neelam *et al* 1999), the oocyte work uses other added buffers and MBS has a high background of concentration of NaCl (section 2.14.3) The K_m for isoleucine in oocytes varies from 4.9 mM at pH 6.0 to 12.9 mM at pH 6.5. In yeast competition experiments (Neelam *et al* 1999) isoleucine was shown to inhibit the uptake of radiolabelled citrulline by 75% when applied in 10-fold excess. This reduction in affinity measured in oocyte experiments for isoleucine compared to citrulline indicates a preference (higher affinity) of RcAAP3 for citrulline over isoleucine.

The i_{max} values for citrulline and protons can be compared to deduce the binding ratio of RcAAP3. Table 5.2 shows the i_{max} values for citrulline at pH 6.0 and protons at 14 mM citrulline over three membrane potentials (-160 mV was not used in this table as in citrulline uptake at pH 6.0 the plot did not appear to fit as well to the data as at other potentials (figure 5.7, top left). From the i_{max} comparisons in table 5.2 it can be seen that the average H^+ i_{max}:citrulline i_{max} ratio is 0.79. This suggests a binding ratio of 1 proton to 1 amino acid. To deduce the actual numbers of protons and amino acids binding during the transport cycle of the protein, the Hill coefficient was calculated for RcAAP3 binding to citrulline, isoleucine and protons (in the presence of isoleucine) (figure 5.14). The Hill coefficient indicates how many molecules are bound to the protein during a single translocation. For isoleucine, the Hill coefficient was approximately 1 over the displayed potential range (-60mV to -160mV) at pH 6.3 and pH 6.5. At pH 6.0 however, the Hill coefficient was approximately 2 (figure 5.14A). For citrulline over a

potential range (-60 mV to -160 mV) the Hill coefficient was below 1 at pH 6.0, approximately 1 at pH 6.5 and at pH 6.3 the Hill coefficient was not constant, going from 1.5 to 4 over the potential range (figure 5.14B). For protons, the Hill coefficient was approximately 2 through the range of potentials (-60 mV to -160 mV) and isoleucine concentrations (figure 5.14B). These results display a high degree of variation, with 3 plots displaying a constant Hill coefficient of approximately 1, and 4 plots displaying a constant Hill coefficient of approximately 2. Because the citrulline measurements were so variable, they have been ignored whilst constructing a model of RcAAP3 transport. The fact that at 3 different isoleucine concentrations the Hill coefficient result for protons was consistently approximately 2 was a strong influence on the model. The plot concerning proton transport at 3 isoleucine concentrations (5.13C) gave a Hill coefficient of approximately 2 at the highest proton concentration. At this proton concentration (pH 6.0) the current against concentration plots for transport of isoleucine were closer to asymptotic than at lower proton concentrations (figure 5.8), an essential component of accurate fitting to equation **2**. Following this reasoning and combining the i_{max} ratio findings (table 5.2) these results support a model for RcAAP3 where 2 amino acid molecules are translocated with 2 protons.

This model can be taken further by observing the relationship between K_m and co-substrate concentration. In the case of both isoleucine (figure 5.13, top) and citrulline (figure 5.12B) the affinity for amino acid increased as the proton concentration increased. This observation combined with a Hill coefficient over 1 suggests positive co-operativity. When a proton binds to RcAAP3 the affinity for an amino acid increases. In the case of protons only data from citrulline uptake was usable (figure 5.12A). The relationship here is not as well defined as that for amino acids. Although there is a general trend of increased affinity for protons at lower citrulline concentrations, the correlation becomes slightly reversed at saturating amino acid concentrations (above 10 mM). When looking at the co-operativity of binding, the characteristics prior to saturation are of interest and so again a case of positive co-operativity is evident.

In a similar way to the AtAAP1 model of transport (Boorer *et al* 1996), the characteristics observed here suggest random binding of proton and amino acid as opposed to ordered binding (Jauch and Läuger 1986). If one substrate had to bind first, before the other could bind (ordered binding) the K_m against co-substrate profiles would be different from one another. The second binding component would not increase the affinity of the transporter (decrease K_m) for the first binding component. The first binding component however, probably would increase the affinity of the transporter for the second component. The resultant K_m against co-substrate concentration plots would therefore show a decrease in K_m for one

component but not the other as co-substrate concentrations increased. Also suggested by the kinetics of RcAAP3 is simultaneous translocation as opposed to sequential translocation of the two protons and two amino acid molecules across the plasma membrane. As there is positive co-operativity shown in this system by a Hill coefficient over 1, it can be assumed that protons and amino acid molecules must all be bound before translocation (Jauch and Läuger 1986). This implies that the protons and amino acid molecules move across the membrane as a complex.

A further experiment carried out on oocytes expressing AtAAP1 (Boorer *et al* 1996) was freeze fracture electron microscopy observations. This revealed that particle levels at the plasma membrane of oocytes injected with *AtAAP1* sense mRNA was 5 fold higher than that of water injected controls. The authors did not comment on what these particles in the plasma membrane may be, but it was assumed that the extra particles were the expressed protein (Boorer *et al* 1996). By using this measurement in conjunction with kinetic properties and an estimate of the oocytes surface area, it was possible to estimate the turnover of AtAAP1 to be 350 to 800 s^{-1}. This was commented on as being higher than other proton cotransport proteins (Boorer *et al* 1996), but is still considerably lower than the turnover of ion channels (typically 10^7 s^{-1}) (Dreyer *et al* 1999). This makes electrophysiological measurements relatively more difficult to make. This low turnover in oocytes may not represent the actual ability of AtAAP1 when expressed in *Arabidopsis*. Again it must be remembered that membrane potentials in plants are much more negative than in oocytes and the pH would most probably be lower than has been used in oocytes (Miller and Zhou 2000).

To summarise, it has been shown that RcAAP3 is able to transport a range of neutral amino acids and the basic amino acid histidine. It has yet to be verified that RcAAP3 can transport acidic amino acids since no measurable response was observed when aspartic acid was supplied. The transport stoichiometry is 2 protons to 2 amino acid molecules, with binding being positively co-operative and random. Translocation of 2 protons and 2 amino acid molecules across the plasma membrane happens simultaneously as a complex (figure 5.17). RcAAP3 has a higher affinity for citrulline than isoleucine. RcAAP3 has a higher transport rate for citrulline than isoleucine and possibly histidine. However, it must be remembered that at the pH tested only a proportion of the histidine was in its zwitterionic form.

Table 5.1 – Calculated radiolabelled amino acid uptake by oocytes expressing *RcAAP3*. Uptake is in the presence of 100μM amino acid at pH 7.5 and pH 5.5

	Uptake into oocytes expressing *RcAAP3* (p mol of amino acids/ oocyte / hour)	
Amino acid [initial]	**[zwitterion] pH 5.5**	**[zwitterion] pH 7.5**
L-histidine [100μM]	[24μM] 14.9 ±3.7	[97μM] n/a
L-citrulline [100μM]	[100μM] 50.3 ±5.3	[100μM] 33.6 ±6.6

Table 5.2 – RcAAP3 i_{max} ratios at three membrane potentials for transporting citrulline at pH6.0 and protons at 14 mM citrulline. The average indicates the binding ratio of amino acid molecules to protons for RcAAP3 transport.

Membrane potential (mV)	I_{max} citrulline, pH6 (nA)	I_{max} H^+, 14 mM citrulline (nA)	Ratio H^+ i_{max} to citrulline i_{max}
-140	-51.5811	-75.2872	0.69
-100	-37.8879	-47.9894	0.79
-40	-18.0474	-20.1205	0.90
			Average 0.79

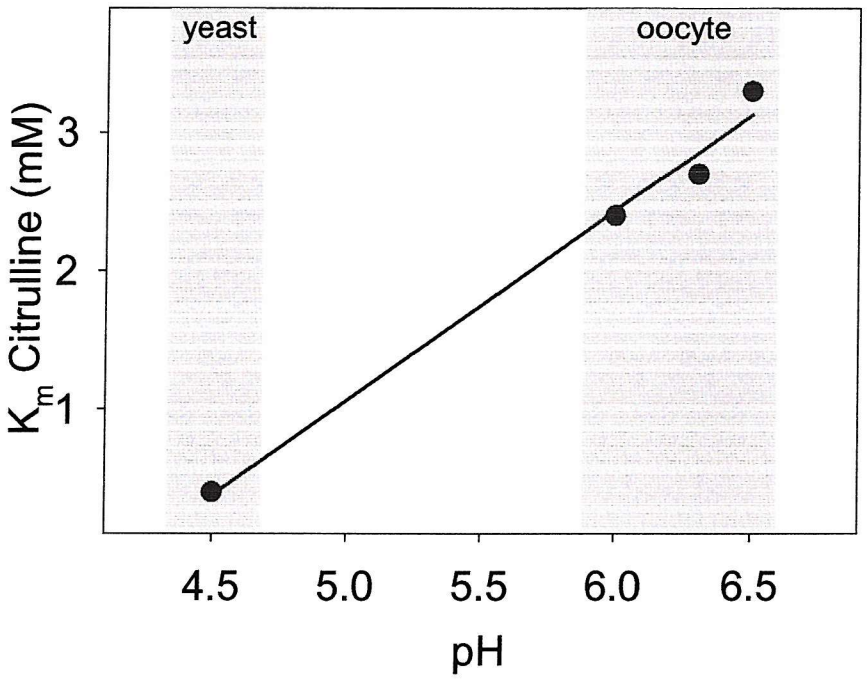

Figure 5.16 – Relationship of K_m to pH for RcAAP3 transporting citrulline over a pH range. The values at pH6.0, pH6.3 and pH6.5 are taken from oocyte measurements in this study. The value at pH4.5 is from yeast radiolabelled uptake taken from Neelam *et al* (1999). The line of best fit is **y=1.36x-5.77** (R^2 = 0.989).

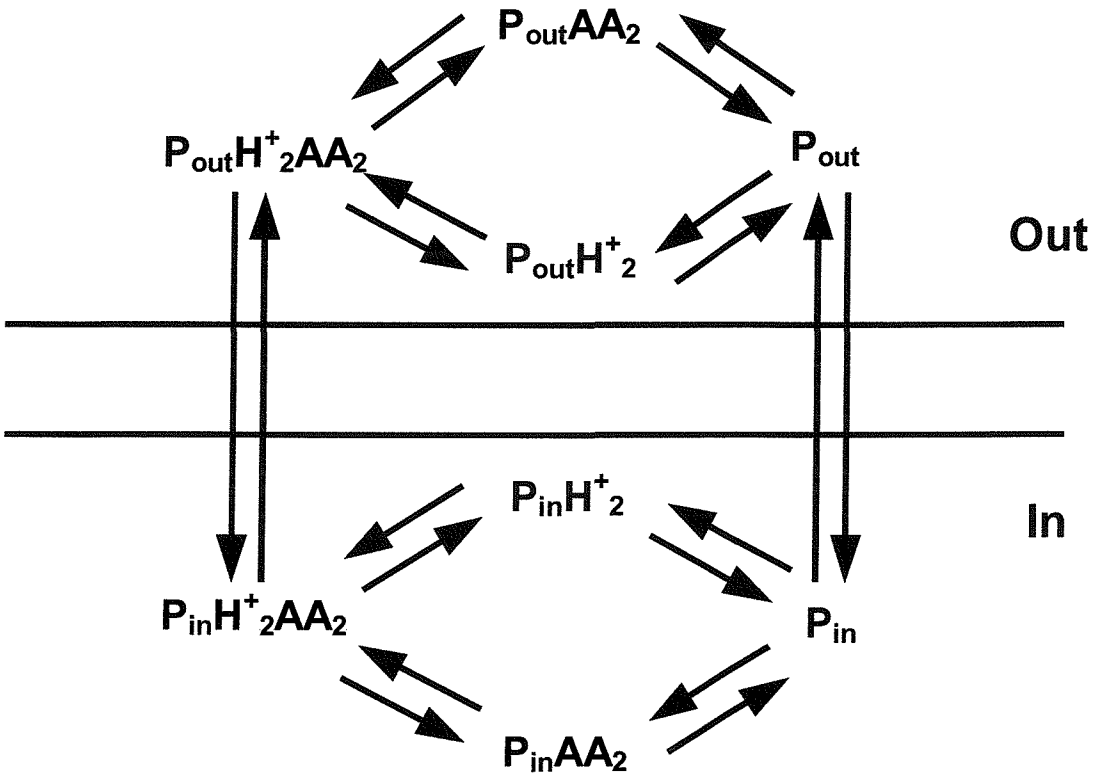

Figure 5.17 – Proposed random simultaneous model for the translocation of neutral amino acid and protons across the plasma membrane by RcAAP3. Two amino acid molecules (AA_2) or two protons (H^+_2) bind to the empty permease (P_{out}) to form $P_{out}AA_2$ or $P_{out}H^+_2$ respectively. The relative co-substrate is then bound to form the complex $P_{out}H^+_2AA_2$, which is transported across the membrane ($P_{in}H^+_2AA_2$). The amino acid and protons dissociate and the permease returns to its empty form (P_{in})

Chapter 6 General Discussion

The acquisition and allocation of nitrogenous compounds are essential processes in plant growth (Williams and Miller 2001). Inorganic nitrogen is assimilated in the roots and leaves and reduced nitrogen, mainly in the form of amino acids, amides and ureides, is transported around the plant in the vascular system. Amino acids can also be taken up directly from the soil and it is believed that this can become an important source of nitrogen for some species growing in mineral-poor soils (Kielland 1994). Amino acid transporters are thought to play a fundamental role in these processes and thus represent physiologically important proteins in the plant. The aim of this work was to investigate the structure/function relationships of plasma membrane amino acid permeases from higher plants. The amino acid permeases, RcAAP1 and RcAAP3, from *Ricinus communis* were used in this project. These are members of the AAP family of plant transporters, a sub-family of the AAAP superfamily, which has representatives in a wide range of eukaryotes including plants, animals, yeast and fungi.

6.1 Transport characterisation following expression in oocytes

The results from chapter 5 indicate that RcAAP3 has been correctly translated and targeted to the oocyte plasma membrane. Radiolabelled amino acid uptake analysis using mRNA-injected oocytes has verified certain findings from yeast expression studies with RcAAP3 (Neelam *et al* 1999). The permease transports citrulline (neutral amino acid) and also histidine (basic amino acid) in a proton-dependent manner as indicated by the higher uptake at acidic pH. However, these experiments do not rule out a pH effect on the transport protein independent of the driving force (pH gradient). The electrophysiological measurements made for RcAAP3 concur with the findings from the radiolabelled amino acid uptake and also expand upon the results obtained in yeast expression studies (Neelam *et al* 1999). The results show that RcAAP3 is able to transport neutral amino acids (citrulline, isoleucine, and glutamine) and also the basic amino acid, histidine. The neutral amino acids, citrulline and isoleucine appear to be taken up by a proton:amino acid symport system. Yeast expression studies also showed transport of acidic amino acids by RcAAP3 (Neelam *et al* 1999). This should be investigated in more detail using the oocyte expression system in the future, as preliminary data from this study indicated no detectable currents from the application of aspartic acid. It will also be important to test glutamic acid, as this gave a higher level of inhibition of citrulline uptake than aspartic acid when used as a competitor in yeast expressing *RcAAP3* (Neelam *et al* 1999). A single transport cycle of

RcAAP3, as proposed by a model derived from neutral amino acid transport (section 5.3), involves the random binding of 2 protons and 2 amino acid molecules to the extracellular side of the protein in a positively co-operative manner. Following translocation as a single complex all four molecules are released on the intracellular side of the protein, again in a random manner (summarised in figure 5.17). The only other model of this kind for an amino acid permease describes an identical model of action for AtAAP1 (Boorer *et al* 1996). AtAAP5 was also expressed in oocytes and investigated using electrophysiological methods (Boorer and Fischer 1997). In this case an overall transport model was not described. However a transport ratio of 1 proton: 1 amino acid was reported. This concurs with the findings for AtAAP1 and RcAAP3. AtAAP5 was shown to transport the zwitterionic but not the cationic form of histidine. However, for lysine the ratio of net inward charge measured for a positively charged lysine molecule was shown to be 2:1. This suggests that lysine is transported at a ratio of 1 amino acid: 1 proton but that it is only taken up in its protonated form. Further studies of this kind with the full range of amino acids are necessary for RcAAP3 to build up an accurate description of the its substrate specificity and mechanism of transport. These measurements would show if the uptake of acidic amino acids via RcAAP3 (as suggested from competition studies in yeast) were authentic, if the transport of charged amino acids was possible by RcAAP3 and if the stoichiometry of RcAAP3 remained at 2 amino acids: 2 protons for all amino acids and conditions.

The functional expression of *RcAAP1* in oocytes could not be achieved. The reason for this is not clear, as an equal quantity of *RcAAP1* sense mRNA with similar apparent quality to that of *RcAAP3* sense mRNA (figure 5.3, section 5.2.1) was injected into healthy oocytes. The cDNA used as template for this mRNA had previously been successfully used in yeast expression. However whereas the *RcAAP3* mRNA injected oocytes gave measurable radiolabelled uptake and electrophysiological responses the *RcAAP1* mRNA injected oocytes showed no response on multiple occasions. This may indicate that the flaw in *RcAAP1* oocyte expression most likely occurs post-oocyte injection.

It is possible that the expression levels of RcAAP1 were too low for detectable measurements to be made. Comparing the figures for i_{max} during RcAAP3 electrophysiological measurements (-140 nA, 10mM histidine at pH 5.5; figure 5.6 section 5.2.3) with those for AtAAP1 (-900 nA, 10mM alanine at pH 5.6; Boorer *et al* 1996) it appears that the expression level of RcAAP3 was far lower than that of AtAAP1. It could be possible that the expression level of RcAAP1 was even lower than this and so currents could not be detected above background during testing. By increasing the expression level of RcAAP1 in oocytes it may therefore be possible to make accurate electrophysiological and radiolabelled measurements. There are several ways in which this may be achieved. The amount of mRNA injected into the oocyte could be increased. This would give the oocyte more template with which to produce protein. However, increasing the volume of

liquid injected or concentrating RNA samples can lead to further damage or contamination of the oocyte. Alternatively, improving the stability of the injected mRNA can increase the production of protein. The mRNA used in this study already incorporates the GTP cap analogue ($m^7G(5')ppp(5')G$-Na salt) to protect the mRNA from degradation. However the poly-A-tail incorporated from the pXE-2 plasmid is only of minimal length (33bases) compared to that incorporated by alternative *Xenopus* expression plasmids. The plasmid used in the electrophysiological characterisation of AtAAP1 for example, pKJB1 (Boorer et al 1996), incorporates a 70 base poly-A-tail. The translation of injected mRNA can also be improved by incorporating the 3' and 5' untranslated regions of a Xenopus β-globin gene (Miller and Zhou 2000). For expression of a mammalian potassium channel in oocytes, the inclusion of the Xenopus β-globin gene sections flanking the coding region of the inserted cDNA increased currents by 200 fold (Liman *et al* 1992). By using such a system with RcAAP1 it may be possible to record electrophysiological and radiolabelled measurements in oocytes. Also by using such an improved system with future *RcAAP3* oocyte expression it should be possible to make measurements after less incubation time. Another reason for the lack of RcAAP1 expression in oocytes could be that the mRNA is not accurately translated in oocytes. Certain post-transcriptional modifications, necessary for subsequent efficient translation in the oocyte, may not occur when mRNA is produced through *in vitro* transcription. However, the similarity of the successfully expressed *RcAAP3* and the fact that the *RcAAP1* cDNA was successfully expressed in yeast makes this unlikely. This possible problem could be overcome by using direct introduction of cDNA to the oocyte nucleus. The problem with this technique is the inherent technical difficulty of injecting such a tiny organelle and the increased trauma to the oocyte.

Following expression of *AtAAP1* in oocytes (Boorer *et al* 1996), freeze fracture images were gathered. This analysis was used to estimate the expression level of foreign material in the oocytes, as well as verifying the membrane localisation of the expressed transporter. This technique may not work with RcAAP3 in oocytes, as the expression levels are so much lower than those for AtAAP1. The methods of obtaining improved expression levels described for RcAAP1 may help this situation, but it would be useful to track the targeting of RcAAP3 and RcAAP1 in oocytes and other systems as well. By producing a fusion gene of RcAAP1 and 3 this type of tracking would be possible. A c-myc epitope was successfully fused separately to the N and C terminal regions of AtAAP1 in order to determine the position of the terminal regions in relation to the membrane when expressed in microsomal membranes (Ortiz-Lopez *et al* 2000). Each of these fusion products was able to rescue the growth of an amino acid transport deficient yeast, in the same way as WT AtAAP1. This suggests that the addition of the epitope did not affect the targeting or function of the protein. If a similar fusion product were made with RcAAP1 and 3 then it may be possible to look at the expression pattern of each protein at the cellular level in *Ricinus*,

yeast and oocytes. It would also be possible to observe the position, relative to the membrane, of each terminal region. According to the topological models produced for RcAAP1 and 3 the C terminal epitope would be exposed to the extracellular environment, while the N terminal epitope would be intracellular. The fusion products would make it possible to determine the level of protein expression in oocytes, and in the case of RcAAP1 they would provide a highly sensitive method for determining if any product was being expressed at the plasma membrane, or anywhere else in the oocyte. The level of oocyte expression in conjunction with electrophysiological analysis could be used to estimate the transport rate of the expressed protein. This would be comparable to the freeze fracture technique used for AtAAP1 (Boorer *et al* 1996) with the added benefit that any epitope labelled product observed would represent the specific protein, rather than just general product in the membrane as was concluded from freeze fracture observations (Boorer et al 1996).

6.2 Isolation of amino acid permease mutants

Random mutagenesis combined with a suitable selection procedure is a useful technique for isolating mutants with desired functional properties. Three random mutagenesis protocols were investigated in this project with the aim of isolating mutated amino acid permeases: DNA shuffling, error-prone PCR, and chemical mutagenesis of yeast expressing wild-type transporters. The first two procedures failed to produce DNA in sufficient yield or of sufficient quality for ligation and subsequent transformation into yeast. The third procedure, involving EMS mutagenesis of yeast expressing RcAAP1, was the most successful in terms of isolating potential mutants. Two selection procedures were designed for selecting RcAAP mutants in yeast: the first involved selection on high pH-selective medium while the second used the toxic amino acid canavanine. The growth of JT-16 expressing WT *RcAAP1* and *3* on low-histidine selective medium is markedly reduced above pH 7.0. Following EMS mutagenesis of JT-16 expressing WT *RcAAP1*, colonies were selected that could grow at pH 8.1. The ability to transport protons and amino acid at low proton (high pH) concentrations could indicate that the mutated permeases have an increased affinity for protons, or can transport amino acids in the absence of proton transport. Another possibility is that selected mutated transporters have an increased affinity for the amino acid available in the medium (histidine) or an altered amino acid translocation mechanism compared to the WT. With an increased amino acid affinity or altered translocation mechanism, a mutant permease could still take up sufficient amounts of histidine at pH 8.1 for growth to continue. This could be investigated by characterising the kinetic properties of these mutants following heterologous expression in oocytes, as has

been achieved with WT RcAAP3 in this study (chapter 5). Using electrophysiological analysis, the i_{max} and K_m values for mutants could be compared to the data collected for WT permeases. This would accurately show the functional differences between the WT and mutant permeases and would indicate whether mutants were affected in proton or amino acid binding and translocation.

The second selection strategy was based on the use of the toxic arginine analogue, canavanine. If the WT permease can transport this amino acid then a media containing canavanine would be toxic to yeast expressing that permease. By mutating the permease it may be possible to alter the affinity for this amino acid so that it is no longer transported, or transported at a depleted level. Thus media containing canavanine would no longer be toxic to the yeast. Several yeast isolates were obtained from this selection procedure, although these were not sequenced due to time constraints. This selection procedure has the potential to isolate mutated transporters with altered amino acid recognition sites. Such mutated transporters would still recognise citrulline (the supplied nitrogen source) but would no longer efficiently bind and translocate canavanine. It is possible that this selection procedure could just isolate mutants with a lower translocation rate. In this situation, insufficient transport rates of canavanine may occur in order to be toxic to the yeast, but the permease would still transported sufficient concentrations of citrulline to sustain growth. Selection on canavanine-containing medium was not as stringent as that for raised pH media, as background growth was observed. One possibility to increase the chances of isolating mutants with altered amino acid binding sites would be to reduce the citrulline concentration in the selection medium; this may lead to the isolation of mutants with higher affinity for this amino acid. As with the isolates obtained from the high pH selection experiments, it will be important to further characterise those obtained from this selection. The amino acid recognition characteristics and translocation rate of the potential mutants could be determined following heterologous expression in oocytes using electrophysiological methods.

There are only a few reports giving information about structure/function relationships of plant amino acid permeases using a mutagenesis approach. *AtAAP1* was randomly mutated and selection procedures were implemented using yeast expression (Ortiz-Lopez *et al* 2000). Characterisation in yeast suggested that two residues (Asp252 and Ala254) were important for function (discussed as unpublished results in Ortiz-Lopez *et al* 2000). Mutation of these residues, located on the predicted sixth trans-membrane domain, reportedly altered the apparent K_ms for histidine and alanine. It is possible that the products of the canavanine-medium selection could be altered at or near these residues, as this selection could isolate permeases with altered amino acid interactions. His65 from the *Arabidopsis* proton/sucrose symport AtSUC1, is in a comparable position to Gln68 from RcAAP1 in this study (extracellular loop between the predicted first and second trans-

membrane domains). His65 was replaced with an array of amino acids by point mutagenesis (Lu and Bush 1998). Replacing His65 with cysteine resulted in a complete loss of transport activity, while replacement with glutamine did not significantly alter activity from that of the WT. This could suggest that glutamine and histidine can play an analogous role in proteins. Interestingly, replacement of His65 with lysine or arginine increased transport rates by a significant amount. This could suggest possible point mutation ideas for Gln68 in RcAAP1.

6.2.1 Structure/Function correlations

A mutation (Gln68 → His) was identified in this study that could have an effect on proton binding or translocation in RcAAP1. Gln68 is located at the extracellular edge of the predicted first trans-membrane domain of RcAAP1. It is a conserved residue in all the members of the AAP family sequenced to date except AtAAP7, 9 and 10 and NsAAP1 (figure 6.1). Interestingly, in the phylogenetic tree presented in the section 1.5.2.2 (figure 1.7), which contains all of the plant amino acid transporters sequences to date, AtAAP9 and 10 are clustered away from the main AAP group and are more closely associated with the ProT family. NsAAP1 also falls out of the AAP cluster, being more closely associated with the LHT family. This suggests that they should not be considered part of the AAP family. It will be interesting to see if the phylogenetic prediction of the close relationship of these transporters to the ProT and LHT families, is also reflected in their functional properties AtAAP7 is in an AAP sub-cluster along with VfAAPc, away from the main two sub-clusters containing the remainder of the sequenced AAPs. Further investigation of residue Gln68 will be necessary to interpret the role this residue plays in transport and proton interaction. Primarily the mutation of Gln68 to a histidine residue should be done under controlled point mutagenesis conditions and the resulting mutant expressed in JT-16 yeast to see whether it confers growth on high pH media. Isolates G and S containing this mutation in *RcAAP1* should be studied alongside the point mutagenised product to check the similarity in growth rate and characteristics. Following this, Gln68 should be mutagenised through point mutagenesis into an array of different residues. This could suggest whether the residue is involved in direct or indirect interactions with the substrates (proton or amino acid). The mutation that occurs in isolates G and S is from glutamine (neutral) to histidine (basic). It may be significant that the substitution is from a neutral to basic amino acid, or that histidine has an aromatic side chain. It is also possible that Gln68 plays a role in the structural aspect of a functional domain of the protein, or in insertion of the protein into the plasma membrane. Residues at the ends of trans-membrane domains can play a key role in positioning the α-helical sections in the plasma membrane, with charged residues often being found at the ends of trans-membrane regions as an 'anchor' (Ulmschneider and

```
          43                                                  92
 RcAAP1   VWTASAHIIT AVIGSGVLSL AWAIAQLGWI AGPAVMFLFS LVTYYTSTLL
 RcAAP2   .......... .......... ..AIAQLGWV AGPVILMAFS FITFFTSTLL
 RcAAP3   VWTASAHIIT AVIGSGVLSL AWAVAQLGWV AGPAVMFLFS LVTYYTSTLL
 AtAAP1   WLTASAHIIT AVIGSGVLSL AWAIAQLGWI AGTSILLIFS FITYFTSTML
 AtAAP2   VWTASAHIIT AVIGSGVLSL AWAIAQLGWI AGPAVMLLFS LVTLYSSTLL
 AtAAP3   VWTASAHIIT AVIGSGVLSL AWATAQLGWL AGPVVMLLFS AVTYFTSSLL
 AtAAP4   VWTASAHIIT AVIGSGVLSL AWAIGQLGWI AGPTVMLLFS FVTYYSSTLL
 AtAAP5   VWTASAHIIT AVIGSGVLSL AWAVAQIGWI GGPVAMLLFS FVTFYTSTLL
 AtAAP6   WMTGSAHIIT AVIGSGVLSL AWAIAQLGWV AGPAVLMAFS FITYFTSTML
 AtAAP7   LWTAVAHIIT GVIGAGVLSL AWATAELGWI AGPAALIAFA GVTLLSAFLL
 AtAAP8   FWTASAHIIT AVIGSGVLSL AWAIAQLGWV AGTTVLVAFA IITYYTSTLL
 AtAAP9   PRPDPFPVTR LDSDAGAL.. .FVLQSKGWW LGFVCLTTMG LVTFYAYYLM
AtAAP10   RSGDGEKRGE EVVDAGSL.. .FVLKSKGWA AGISCLVGGA AVTFYSYTLL
 PsAAP1   SWTASAHVIT AVIGSGVLSL AWAIAQLGWI AGPVVMILFA WVTYYTSVLL
 PsAAP2   VWTTSSHIIT AVVGSGVLSL AWAIAQLGWV IGPSVMLFFS LITWYTSSLL
 NaAAP1   .......... AVIGSGVLSL AWAIAQLGWV AGPAVLIAFS AITYFTSTML
 NaAAP2   .......... AVIGSGVLSL AWAIAQLGWI AGPAVMLLFS FVIYYTSILL
 NaAAP3   .......... AVIGSGVLSL AWATAQLGWI AGPTAMLLFS FITFYTSRLL
 NsAAP1   GGYSAFHNVT AMVGAGVLGL PYAMSELGWG PGVTVMVVSW VITLYTLWQM
 StAAP1   ......HIIT AVIGSGVLSL AWAIAQLGWV AGPAVLFAFS FITYFTSTLL
 StAAP2   ......HIIT AVIGSGVLSL AWATAQLGWV AGPTVLLLFF FVTYYTSALL
 VfAAPa   .....AHIIT AVIGSGVLSL AWAIAQMGWV AGPAVLLAFS LITYFTSTLL
 VfAAPb   .....AHIIT AVIGSGVLSL AWAIAQLGWI AGPSMMLLFS FVTYYTSTLL
 VfAAPc   .....AHIIT AVIGSGVLSL AWSTAQLGWI GGPVALLCCA IVTYVSSFLL

          263                                                 310
 RcAAP1   IILIEIQDTV RSPP..SESK TMKKATLISV AVTTLFYMLC GCFGYAAFGD
 RcAAP2   TVLIEIQDTI KSGP..PENK AMKKASFVGI VTTTMFYILC GCIGYAAFGN
 RcAAP3   LILIEIQDTI RSPP..AESK TMRKATLISV SVTTLFYMLC GCFGYAAFGD
 AtAAP1   TVLIEIQDTL RSSPA..ENK AMKRASLVGV STTTFFYILC GCIGYAAFGN
 AtAAP2   VVLIEIQDTV RSPP..AESK TMKKATKISI AVTTIFYMLC GSMGYAAFGD
 AtAAP3   IILIEIQDTV KSPP..SEEK TMKKATLVSV SVTTMFYMLC GCMGYAAFGD
 AtAAP4   VVLIEIQDTV RSPP..AESK TMKIATRISI AVTTTFYMLC GCMGYAAFGD
 AtAAP5   MILIEIQDTV KSPP..AEVN TMRKATFVSV AVTTVFYMLC GCVGYAAFGD
 AtAAP6   TVLIEIQDTL KAGPP.SENK AMKRASLVGV STTTFFYMLC GCVGYAAFGN
 AtAAP7   IILLEIQDTL RSPP..AEKQ TMKKASTVAV FIQTFFFFCC GCFGYAAFGD
 AtAAP8   TILIEIQDTL RSSPP..ENK VMKRASLVGV STTTVFYILC GCIGYAAFGN
 AtAAP9   GILPEIQATL AP....PATG KMLKGLLLCY SVIFFTFYSA AISGYWVFGN
AtAAP10   GIIPEIQATI SA....PVKG KMMKGLCMCY LVVIMTFFTV AITGYWAFGK
 NaAAP1   NVLVEIQDTL KSSP..PENK VMRRASLIGG RPPHSFYVLC GCMGYAAFVY
 NaAAP2   IILIEIQDTV KSPP..SEAK TMKKASLISI VVTTAFYMLC GCMGYAAFGD
 NaAAP3   LVLVEIQDTI KSPP..SEIK TMKKATVMSI AVTTLIYLLC GCMGYAAFGD
 NsAAP1   NVVLEIQATI PSTPEKPSKG PMWKGVLVAY IIVALCYFPV AIIGYWIFGN
 PsAAP1   MILIEIQDTV KAPPP.SESK TMKKATLISV IVTTFFYMLC GCLGYAAFGN
 PsAAP2   QILIEIQDTI KNPP..SEVK TMKQATRISI GVTTIFYMLC GGMGYAAFGD
 StAAP1   VMKRASLAGV TVLIEIQDTL KSSP..SESK STTTLFYVLC GTIGYAAFGN
 StAAP2   LILIEIQDTL KSPP..AEAK TMKRATLISV AVTTVFYMLC GCFGYAAFGD
 VfAAPb   MILIEIQDTI KSPP..SESK TMKAATLISV VVTTIFYMLC GCLGYAAFG.
 VfAAPa   NVLIEIQDTL KSSP..PENQ VMKRASLIGV LTTSMFYMLC GCLGYAAFG.
 VfAAPc   ILLLEIQDTL ESPP..PENQ TMKKASMVAI FITTFFYLCC GCFGYAAFG.
```

Figure 6.1 – Amino acid sequence alignments of all of the AAP family members sequenced to date. Residues 43 to 92 and 263 to 310 for RcAAP1. Gln68 and Ala285 from RcAAP1, and His47 from AtAAP1 (Ortiz-Lopez *et al* 2000) are highlighted in bold as are the comparable residues in the other displayed sequences. The alignment was done using the multiple sequence alignment with hierarchical clustering program (Corpet 1988), found at 'http://protein.toulouse.inra.fr/multalin/multalin.html'.

Sansom 2001). Altering the position of the domain relative to the membrane or to the rest of the protein could have major effects on transport. It would also be interesting to see how substituting different amino acids alters the ability of the permease to complement yeast at raised pH. For example, could certain substitution allow yeast to survive under even higher pH conditions?

The other mutation identified in this study was at Ala285, detected in isolate W. The advantage that this mutation gives the protein at high pH over the WT cannot be one of function as the DNA mutation gives rise to an alternative triplet coding for the same amino acid as the WT. Instead the possibility of increased protein production was considered, through codon bias or increased mRNA stability (chapter 4).It is also possible that this mutation identified in isolate W was not the only mutation, and so not the reason that the mutant from isolate W conveyed the ability to grow on high pH medium. This is a definite possibility as isolates O, R, T, and X were all used to successfully complement the growth of JT-16 on high pH medium but subsequent sequencing showed no definite mutations. This would suggest that further sequencing of all isolates needs to be undertaken to see if the mutations discovered in isolates G, S and W are the only ones and also if other isolates contain any other mutations.

Preliminary data reported for site-directed mutagenesis of *AtAAP1* (Bush *et al* 1996) indicated that there are two essential histidine residues, positioned on predicted trans-membrane α-helical sections. His337, on the predicted eighth trans-membrane α-helix was replaced with leucine, proline, cysteine, phenylalanine, tyrosine, tryptophan, arginine and glutamine. All of these mutated carriers, although only altered by one amino acid, failed to complement amino acid transport deficient yeast, previously complemented by the WT At*AAP1*. This suggests a loss of function of the permease, although no information was given as to whether this mutation affected targeting to the plasma membrane. His47, on the predicted first trans-membrane α-helix was replaced in a similar way but the consequences of this mutagenesis have not yet been published (discussed as unpublished results in Ortiz-Lopez *et al* 2000). The His47 residue from this mutagenesis work in AtAAP1 is conserved throughout the majority of the AAP family and is predicted to be on the same trans-membrane domain as Gln68 (figure 6.1), identified in this study. It will be interesting to see if the effects of the mutagenesis of His47 are in any way related to the altered proton interactions speculated for the mutant permeases from isolates G and S in this study. The residues identified in AtAAP1 by random mutation and selection, Asp252 and Ala254 (discussed as unpublished results in Ortiz-Lopez *et al* 2000) are on the sixth predicted trans-membrane domain. Mutation of these residues was reported to alter apparent K_ms for alanine and histidine (Ortiz-Lopez *et al* 2000). It will be interesting to see where these residues are in comparison to the conserved Gln68 from RcAAP1. At the tertiary structure level it is possible that these two areas may be positioned in close proximity to one another.

Without further characterisation, it is also impossible to rule out the possibility that the ability of isolates G and S to grow on raised pH selective media is unrelated to the mutations detected. This remains a possibility as no mutations were consistently detected in plasmids from four of the seven isolates sequenced in this project (isolates. O, R, T and X).

6.3 Future Considerations

In order to explain the exact nature of the mutants produced in this study, further sequencing, electrophysiological analysis and extended mutagenesis programs must be undertaken. The isolates identified from high pH selection which did not show mutations in RcAAP1, must be altered in some way in order to have an increased tolerance to low proton concentrations. Also, sequencing of plasmids in the isolates identified in the canavanine selection protocol may yield further key residues involved in translocation. The Gln68 residue altered to histidine in two separate isolates could well play a role in influencing proton binding. Electrophysiological analysis in oocytes and an extended mutation program would increase our knowledge of the nature of this mutation. Also, an extended mutation program and analysis of RNA stability could explain the nature of the codon change at Ala285 in isolate W.

The production of tagged RcAAPs, with no alteration in targeting and function, would reveal a great deal of information about the expression of the proteins, as well as their membrane topology. This may also indicate where the flaw in RcAAP1 expression in oocytes occurs. With the inclusion of β-globin flanking sequences however, the expression of RcAAP1 in oocytes may become measurable.

By solving the crystal structure of these amino acid permeases the full implications of mutations at the tertiary structure level will be appreciated. By thoroughly defining which domains of a transporter are involved in which individual elements of translocation it will eventually be possible to continue into a more targeted mutagenesis protocol. This could then potentially produce transporters with positively altered transport capabilities. In the long term, transporters with the ability to operate at depleted proton concentrations, or operate more efficiently than the WT at identical proton concentrations might offer improved amino acid redistribution *in vivo*. The production of transgenic plants with specifically mutated transporters is then a feasible expansion of this area that could lead to improved nitrogen redistribution and ultimately crop yield.

The AAPs are expressed in a wide range of tissues throughout the plant and have been implicated in many physiologically important processes. As the AAP family members generally show high sequence homology, the results from this study, investigating structure/function relationships will contribute to the further understanding of these amino

acid permeases. The AAPs transport a variety of amino acids and there is now evidence of a proton:amino acid symport mechanism for at least two members (AtAAP1-Boorer *et al* 1996, RcAAP3-this study). There is also new evidence suggesting that members of the family vary in their transport mechanism for certain amino acids (Boorer *et al* 1997).

Chapter 7 References

Altschul. S.F., Fish. W., Miller. W., Myers. E.W., Lipman. D., (1990).
Basic local alignment search tool. *Journal of Molecular Biology*. **215**: 403-410.

Anderson. J.A., Huprikar. S.S., Kochian. L.V., Lucas. W.J., Gaber. R.F., (1992).
Functional expression of a probable *Arabidopsis thaliana* potassium channel in Saccharomyces cerevisiae. *Proceedings of the National Academy of Sciences USA*. **89**: 3736-3740.

Bennett. M.J., Marchant. A., Green. H.G., May. S.T., Ward. S.P., Millner. P.A., Walker. A.R., Schulz. B., Feldmann. K.A., (1996).
Arabidopsis AUX1 gene: A permease-like regulator of root gravitropism. *Science*. **273**: 948-950.

Bick. J.A., Neelam. A., Hall. J.L., Williams. L.E., (1998).
Amino acid carriers of Ricinus communis expressed during seedling development: molecular cloning and expression analysis of two putative amino acid transporters, RcAAP1 and RcAAP2. *Plant Molecular Biology*. **36**: 377-385

Bonnemain. J.L., Delrot. S., Lucas. W.J., Dainty. J., (1991).
Recent advances in phloem transport and assimilate compartmentation. *(Quest Editions)*.

Boorer. K.J., Frommer. W.B., Bush. D.R., Kreman. M., Loo. D.D.F., Wright. E.M., (1996).
Kinetics and specificity of a H+ amino acid transporter from *Arabidopsis thaliana*. *Journal of Biological Chemistry*. **271**: 2213-2220.

Boorer. K. and **Fischer. W.**, (1997).
Specificity and stoichiometry of the *Arabidopsis* H+/ amino acid transporter AAP5. *Journal of Biological Chemistry*. **272**: 13040-46.

Borstlap. A.C. and **Schuurmans. J.**, (1988).
Kinetics of L-valine uptake in tobacco leaf-disks – comparison of wild-type, the digenic mutant Val^r-2, and its monogenic derivatives. *Planta*. **176**: 42-50.

Bourgin. J.P., (1978).

Valine-resistant plants from in vitro selected tobacco cells. *Molecular and General Genetics*. **161**: 225-230.

Breitkreuz. K.E., Shelp. B.J., Fischer. W.N., Schwacke. R., Rentsch. D., (1999).

Identification and characterization of GABA, proline and quaternary ammonium compound transporters from *Arabidopsis thaliana. FEBS Letters.* **450**: 280-284.

Bright. S.W.J., Kueh. J.S.H., Rognes. S.E., (1983).

Lysine transport in 2 barley mutants with altered uptake of basic-amino-acids in the root. *Plant Physiology*. **72**: 821-824.

Bush. D., Chiou. T., Chen. L., (1996).

Molecular analysis of plant sugar and amino acid transporters. *Journal of Experimental Botany*. **47**: 1205-10.

Bush. D., (1993).

Proton-coupled sugar and amino acid transporters in plants. *Annual Review of Plant Physiology and Plant Molecular Biology.* **44**: 513-42.

Canny. M.J., (1988).

Bundle sheath tissue of legume leaves as a site of recovery of solutes from the transpiration stream. *Physiologia Plantarum.* **73**: 457-464.

Cao. Y., Ward. J.M., Kelly. W.B., Ichida. A.M., Gaber. R.F., Anderson. J.A., Uozumi. N., Schroeder. J.I., Crawford. N.M., (1995).

Multiple genes, tissue specificity, and expression-dependent modulation contribute to the functional diversity of potassium channels in *Arabidopsis thaliana. Plant Physiology.* **109**: 1093-1106.

Caspari. W. and **Tanner. T.**, (1996).

Membrane transport carriers. *Annual Review of Plant Physiology and Plant Molecular Biology.* **47**: 595-626.

Chang. H. and **Bush. D.**, (1997).

Topology of NAT2, a prototypical example of a new family of amino acid transporters. *The Journal of Biological Chemistry.* **272**: 30552-30557.

Chen. L. and **Bush. D.**, (1997).
LHT1, a lysine and histidine specific amino acid transporter in *Arabidopsis. Plant Physiology*. **115**: 1127-1134.

Chen. L., Ortiz-Lopez. A., Jung. A., Bush. D.R., (2001).
ANT1, an aromatic and neutral amino acid transporter in *Arabidopsis. Plant Physiology*. **125**: 1813-1820.

Christensen. H. N., (1990).
Role of amino-acid-transport and countertransport in nutrition and metabolism. *Physiological Reviews*. **70**: 43-77.

Cooper. H.D. and **Clarkson. D.T.**, (1989).
Cycling of amino-nitrogen and other nutrients between shoots and roots in cereals – a possible mechanism integrating shoot and root in the regulation of nutrient uptake. *The Journal of Experimental Botany*. **40**: 753-762.

Corpet. F., (1988).
Multiple sequence alignment with hierarchical-clustering. *Nucleic Acids Research.* **16**: 10881-10890.

Coruzzi. G. and **Bush. D.R.**, (2001).
Nitrogen and carbon nutrient and metabolite signaling in plants. *Plant Physiology*. **125**: 61-64.

Coruzzi. G. and **Last. R.**, (2000).
Chapter 8, Buchanan. B.B., Gruissem. W., Jones. R.L., (2000).
Biochemistry and molecular biology of plants. American Society of Plant Physiologists, Rockville, Maryland.

Crameri. A., Whitehorn. E. A., Tate. E., Stemmer. W. P. C., (1996).
Improved green fluorescent protein by molecular evolution using DNA shuffling. *Nature Biotechnology*. **14**: 315-319.

Crameri. A., Glenn. D., Rodriguez. E., Silver. S., Stemmer. W. P. C., (1997).
Molecular evolution of an arsenate detoxification pathway by DNA shuffling, *Nature Biotechnology*. **15**: 436-438.

Crameri. A., Raillard. S., Bermudez. E., Stemmer. W. P. C., (1998).
DNA shuffling of a family of genes from diverse species accelerates directed evolution. *Nature*. **391**: 288-291.

Crawford. M.C., Grace. P.R., Oades. J.M., (2000a).
Allocation of carbon to shoots, roots, soil and rhizosphere respiration by barrel medic (*Medicago truncatula*) before and after defoliation. *Plant and Soil*. **227**: 67-75.

Crawford. N.M., Kahn. M.L., Leustek. T., Long. S.R., (2000b)
Chapter 16, Buchanan. B.B., Gruissem. W., Jones. R.L., (2000).
Biochemistry and molecular biology of plants. American society of plant physiologists, Rockville, Maryland.

Curran. A. C., Hwang. I., Corbin. J., Martinez. S., Rayle. D., Sze. H., Harper. J. F., (2000).
Autoinhibition of a calmodulin-dependent calcium pump involves a structure in the stalk that connects the transmembrane domain to the ATPase catalytic domain. *Journal of Biological Chemistry*. **275**: 30301-30308.

DeBoer. A.H., (1989).
Xylem transport. *Methods in Enzymology*. **174**:277-287.

Delauney. A.J. and **Verma. D.P.S.**, (1993).
Proline biosynthesis and osmoregulation in plants. *The Plant Journal*. **4**: 215-223.

Delrot. S and **Bonnemain. J.L.**, (1985).
Mechanism and control of phloem transport. *Physiologie Vegetale*. **23**: 199-220.

Delrot. S., (1987).
Phloem loading: apoplastic or symplastic?. *Plant Physiology and Biochemistry*. **25**: 667-76.

Didion. T., Regenberg. B., Jorgensen. M.U., Kielland-Brandt. M.C., Andersen. H.A., (1998).
The permease homologue Ssy1p controls the expression of amino acid and peptide transporter genes in *Saccharomyces cerevisiae*. *Molecular Microbiology*. **27**: 643-650.

Dohmen. R.J., Strasser. A.W.M., Honer. C.B., Hollenberg. C.P., (1991).
An efficient transformation procedure enabling long-term storage of competent cells of various yeast genera. *Yeast*. **7**: 691-692.

Evert. R.F. and **Russin. W.A.**, (1993).
Structurally, phloem unloading in the maize leaf cannot be symplastic. *American Journal of Botany*. **80**: 1310-1317.

Fieuw. S. and **Willenbrink. J.**, (1990).
Sugar-transport and sugar-metabolizing enzymes in sugar-beet storage roots (*Beta vulgaris* SSP altissima). *Journal of Plant Physiology*. **137**: 216-223.

Fischer. W., Kwart. M., Hummel. S., Frommer. W., (1995).
Substrate specificity and expression profile of amino acid transporters (AAP's) in *Arabidopsis. The Journal of Biological Chemistry*. **270**: 16315-20.

Fischer. W., Andre. B., Rentsch. D., Krolkiewicz. S., Tegeder. M., Breitkreuz. K., Frommer. W., (1998).
Amino acid transport in plants. *Trends in Plant Science.* **3**: 118-195.

Fisher. D.B. and **Oparka. K.J.**, (1996).
Post-phloem transport: principles and problems. *Journal of Experimental Botany*. **47**: 1141-1154.

Fisher. D.B. and **Cash-Clark. C.E.**, (2000).
Sieve tube unloading and post-phloem transport of fluorescent tracers and proteins injected into sieve tubes via severed aphid stylets. *Plant Physiology*. **123**: 125-137.

Frenzel. B., (1960).
Zur åtiologie per anreicherung von aminosauren und amiden in wurzelraum von *Helianthus annus* L. *Planta*. **55**: 169-207.

Fromant. M., Blanquet. S., Plateau. P., (1995).
Direct random mutagenesis of gene sized DNA fragments using polymerase chain reaction. *Analytical Biochemistry*. **224**: 347-353.

Frommer. W., Hummel. S., Riesmeier. J., (1993).
Expression cloning in yeast of a cDNA encoding a broad specificity amino acid permease from *Arabidopsis thaliana*. *Proceedings of the National Academy of Scientists USA*. **90**: 5944-48.

Frommer. W., Hummel. S., Unsled. M., Ninnemann. O., (1995).
Seed and vascular expression of a high-affinity transporter for cationic amino acid in *Arabidopsis*. *Proceedings of the National Academy of Scientists USA*. **92**: 12036-40.

Frommer. W., Kwart. M., Hirner. B., Fischer. W., Hummel. S., Ninnemann. O., (1994).
Transporters for nitrogenous compounds in plants. *Plant Molecular Biology.* **26**:1651-70.

Frommer. W.B. and **Ninnemann. O.**, (1995).
Heterologous expression of genes in bacterial, fungal, animal and plant-cells. *Annual Review of Plant Physiology and Plant Molecular Biology.* **46** 419-444.

Giver. L., Gershenson. A., Freskgard. P-O., Arnold. F. H., (1998).
Directed evolution of a thermostable esterase. *Proceedings of the National Academy of Scientists USA*. **95** 12809-13.

Goodman. M. F., Keener. S., Guidotti. S., Branscomb. E.W., (1983).
On the enzymatic basis for mutagenesis by manganese. *Journal of Biological Chemistry*. **258**, 3469-6475.

Grant. M. and **Bevan. M.W.**, (1994).
Asparaginase gene-expression is regulated in a complex spatial and temporal pattern in nitrogen-sink tissues. *Plant Journal*. **5**: 695-704.

Grenson. M., Hou. C., Crabell. M., (1970)
Multiplicity of the amino acid permease in *Saccharomyces ceravisiae*. I. Evidence for a general amino acid permease. *Journal of Bacteriology*. **103**: 770-777.

Hames. B.D. and **Higgins. S.J.**, - editors (1984).
Transcription and translation: a practical approach. IRL press Oxford, Washington DC. (practical approach series).

Haupt. S., Duncan. G.H., Holzberg. S., Oparka. K.J., (2001).
Evidence for symplastic phloem unloading in sink leaves of barley. *Plant Physiology*. **125**: 209-218.

Heremans. B., Borstlap. A.C., Jacobs. M., (1997).
The *rlt11* and *raec1* mutants of *Arabidopsis thaliana* lack the activity of a basic-amino-acid transporter. *Planta*. **201**: 219-226.

Heremans.B. and **Jacobs. M.**, (1994).
Selection of *Arabidopsis-thaliana* (L) *heynh* mutants resistant to aspartate-derived amino-acids and analogs. *Plants Science*. **101**: 151-162.

Hirner. B., Fischer. W., Rentsch. D., Kwart. M., Frommer. W., (1998).
Developmental control of H+ amino acid permease gene expression during seed development of *Arabidopsis*. *The Plant Journal*. **14**: 535-544.

Hsu. L., Chiou. T., Chen. L., Bush.D., (1993).
Cloning a plant amino acid transporter by functional complementation of a yeast amino acid transport mutant. *Proceedings of the National Academy of Scientists USA*. **90**: 7441-7445.

Ichida. A.M., Baizabal-Aguirre. V.M., Schroeder. J.I., (1999).
Genetic selection of inward-rectifying K^+ channel mutants with reduced Cs^+ sensitivity by random recombinant DNA shuffling mutagenesis and mutant selection in yeast. *Journal of Experimental Botany*. **50**: 967-978.

Iraqui. I., Vissers. S., Bernard. F., De Craene. J.O., Boles. E., Urrestarazu. A., Andre. B., (1999).
Amino acid signaling in *Saccharomyces cerevisiae*: a permease-like sensor of external amino acids and F-box protein Grr1p are required for transcriptional induction of the AGP1 gene, which encodes a broad-specificity amino acid permease. *Molecular and Cellular Biology*.**19**: 989-1001.

Israel. D.I., (1993).
A PCR based method for the high stringency screening of DNA libraries. *Nucleic Acids Research*. **21**: 2627-2631.

Jauch. P. and **Läuger. P.**, (1986).

Electrogenic properties of the sodium-alanine cotransporter in pancreatic acinar-cells .2. Comparison with transport models. *Journal of Membrane Biology*. **94**: 117-127.

Jauniaux. J.C., Vandenbol. M., Vissers. S., Broman. K., Grenson. M., (1987).

Nitrogen catabolite regulation of proline permease in *Saccharomyces ceravisiae* cloning of the PUT4 gene and study of PUT4 RNA levels in wild-type and mutant strains. *European Journal of Biochemistry*. **164**: 301-606.

Johannes. E. and **Felle. H.**, (1985).

Transport of basic amino-acids in *Riccia fluitans* – evidence for a 2nd binding-site. *Planta*. **166**: 244-251.

Kinraide. T.B. and **Etherton. B.**, (1980).

Electrical evidence for different mechanisms of uptake for basic, neutral, and acidic amino acids in oat coleoptiles. *Plant Physiology*. **65**: 1085-1089.

Kirkby. E.A. and **Armstrong. M.J.**, (1980).

Nitrate uptake by roots is regulated by nitrate assimilation in the shoot of castor bean plants. *Plant Physiology*. **65**: 286-290.

Komor. E., (1977).

Sucrose uptake by cotyledons of *Ricinus communis* L. characteristics, mechanism and regulation. *Planta*. **137**: 119-131.

Kriedeman. P. and **Beevers. H.**, (1967).

Sugar uptake and transpiration in the castor bean seedling. *Plant Physiology*. **42**: 161-173.

Krieg. P.A. and **Melton. D.A.**, (1984).

Functional messenger RNAs are produced by SP6 in vitro transcription of cloned cDNAs. *Nucleic Acids Resarch*. **12**: 7057-7070.

Kuhn. C., Franceschi. V.R., Schulz. A., Lemoine. R., Frommer. W.B., (1997).

Macromolecular trafficking indicated by localization and turnover of sucrose transporters in enucleate sieve elements. *Science*. **275**: 1298-1300.

Kwart. M., Hirner. B., Hummel. S., Frommer. W., (1993).
Differential expression of two related amino acid transporters with differing substrate specificity in *Arabidopsis thaliana. The Plant Journal.* **4**: 993-1002.

Kyte. J. and **Doolittle. R.F.**, (1982).
A simple method for displaying the hydropathic character of a protein. *Journal of Molecular Biology* **157**: 105-132.

Lam. H.M, Chiu. J., Hsieh. M., Meisel. L., Oliveria. I., Shin. M., Coruzzi. G., (1998).
Glutamate-receptor genes in plants. *Nature.* **396**: 125-126.

Larsson. C.M., Larsson. M., Purves. J.V., Clarkson. D.T., (1991).
Translocation and cycling through roots of recently absorbed nitrogen and sulpher in wheat (*Triticum aestivum*) during vegative and generative growth. *Physiologia Plantarum.* **82**: 345-352.

Li. Z.C. and **Bush. D.R.**, (1990).
Delta-pH-dependent amino-acid-transport into plasma-membrane vesicles isolated from sugar-beet leaves .1. Evidence for carrier-mediated, electrogenic flux through multiple transport-systems. *Plant Physiology.* **94**: 268-277.

Li. Z.C. and **Bush. D.R.**, (1991).
Delta-pH-dependent amino-acid-transport into plasma-membrane vesicles isolated from sugar-beet (*Beta-vulgaris L*) leaves .2. Evidence for multiple aliphatic, neutral amino-acid symports. *Plant Physiology.* **96**: 1338-1344.

Li. Z.C. and **Bush. D.R.**, (1992).
Structural determinants in substrate recognition by proton amino acid symports in plasma membrane vesicles isolated from sugar beet leaves. *Archives of Biochemistry and Biophysics.* **294**: 519-526.

Liman. E.R., Tygat. J., Hess. P., (1992).
Subunit stoichiometry of a mammalian K^+ channel determined by construction of multimeric cDNAs. *Neuron.* **9**: 861-871.

Lin. G., Cai. X., Johnstone. R., (1997).

Expression cloning of a mammalian amino acid transporter or modifier by complementation of a yeast transporter mutant. *Journal of Cellular Physiology*. **173**: 351-360.

Lohaus. G. and **Moellers. C.**, (2000).

Phloem transport of amino acids in two *Brassica napus* L. genotype and one *B. carinata* genotype in relation to their seed protein content. *Planta*. **211**: 833-840.

Lorimer, I.A.J. and **Pastan, I.**, (1995).

Random recombination of antibody single-chain FV sequences after fragmentation with DNaseI in the presence of $Mn2^{+}$. *Nucleic Acids Research*. **23**: 3067-3068.

Lu. J.M.-Y. and **Bush. D.R.**, (1998).

His-65 in the proton-sucrose symport is an essential amino acid whose modification with site-directed mutagenesis increases transport activity. *Proceedings of the National Academy of Scientists USA*. **95**: 9025-9030.

Lucas. W. J., (1999).

Plasmodesmata and the cell-to-cell transport of proteins and nucleoprotein complexes. *Journal of Experimental Botany*. **50**: 979-987.

Lundborg. T., Sandelius. A.S., Widell. S., Larsson. C., Liljenberg. C., Kylin,. A., (1983).

Characterization of root plasma membranes prepared by partition in an aqueous polymer two-phase system. In Wintermans, J.F.G.M. and Kuiper, P.C. J. (eds) *Biochemistry and Metabolism of Plant Lipids*. Proceedings from a conference held in Groningen, The Netherlands, June 7-10 1982. Elsevier, Amsterdam pp 183-186.

Maher. E.P. and **Martindale. S.J.B.**, (1980).

Mutants of *Arabidopsis thaliana* with altered response to auxins and gravity. *Biochemical Genetics*. **18**: 1041-1053.

Marchant. A., Kargul. J., May. S. T., Muller. P., Delbarre. A., Perrot-Rechenmann. C., Bennett. M. J., (1999).

AUX1 regulates root gravitropism in *Arabidopsis* by facilitating auxin uptake within root apical tissues. *EMBO Journal*. **18**: 2066-2073.

Marionpoll. A., Missonier. C., Goujaud. J., Caboche. M., (1998).
Isolation and characterization of valine-resistant mutants of *Nicotiana-plumbaginifolia*. *Theoretical and Applied Genetics*. **75**: 272-277.

Marschner. H., (1995).
Mineral Nutrition of higher plants (2nd edition). London, San Diego; Academic Press.

Marschner. H., Kirkby. E.A., Engels. C., (1997).
Importance of cycling and recycling of mineral nutrients within plants for growth and development. *Botanica Acta*. **110**: 265-273.

Martinez. M. A., Vartanian. J-P., Wain-Hobson. S., (1994).
Hypermutagenesis of RNA using immunodeficiency virus type 1 reverse transcriptase and bias dNTP concentrations. *Evolution*. **91**: 11787-11791.

Marvier. A., Neelam. A., Bick. J., Hall. J., Williams. L., (1998).
Cloning of a cDNA coding for an amino acid carrier from *Ricinus communis* (RcAAP1) by functional complementation in yeast: kinetic analysis, inhibitor sensitivity and substrate specificity. *Biochemica et Biophysica Acta-Biomembranes.* **1373**: 321-331.

McGrath. R.B. and **Coruzzi. G.M.**, (1991).
A gene network controlling glutamine and asparagine biosynthesis in plants. *The Plant Journal*. **1**: 275-280.

Miller. A.J., Smith. S.J., Theodoulou. F.L., (1994).
The Heterologous expression of H^+-coupled transporters in *Xenopus* oocytes, in: Blatt. M.R., Leight. R.A. and Sanders. D. (Eds.), Membrane Transport in Plants and Fungi: Molecular Mechanisms and Control, Company of Biologists, 1994, 167-177.

Miller, A.J. and **Zhou. J.J.**, (2000).
Xenopus oocytes as an expression system for plant transporters. *Biochimica et Biophysica Acta-Biomembranes*. **1465**: 343-358.

Mizuno. A., Kojima. H., Katou. K., Okamoto. H., (1885).
The Electrogenic proton pumping from parenchyma symplast into xylem direct demonstration by xylem perfusion. *Plant Cell and Environment*. **8**: 525-529.

Montamat. F., Maurousset. L., Tegeder. M., Frommer. W., Delrot. S., (1999).
Cloning and expression of amino acid transporters from broad bean. *Plant Molecular Biology* **41**:259-268.

Morsomme. P. and **Boutry. M.**, (2000).
The plant plasma membrane H^+-ATPase: structure, function and regulation. *Biochimica et Biophysica Acta-Biomembranes*. **1465**: 1-16.

Muller. B. and **Touraine. B.**, (1992).
Inhibition of NO_3^- uptake by various phloem-translocated amino-acids in soybean seedlings. *Journal of Experimental Botany*. **43**: 617-623.

Munroe. D. and **Jacobson. A.**, (1990).
Messenger-RNA poly(A) tail, a 3' enhancer of translational initiation. *Molecular and Cellular Biology*. **10**: 3441-3455.

Nakamura. Y., Gojobori. T., Ikemura. T., (2000).
Codon usage tabulated from the international DNA sequence databases: status for the year 2000. *Nucleic Acids Research*. **28**: 292-292.

Neelam. A., Marvier. A.C., Hall. J.L., Williams. L.E., (1999).
Functional characterization and expression analysis of the amino acid permease RcAAP3 from castor bean. *Plant Physiology*. **120**: 1049-1056.

Oparka. K.J. and **Cruz. S.S.**, (2000).
The great escape: Phloem transport and unloading of macromolecules. *Annual Review of Plant Physiology and Plant Molecular Biology*. **51**: 323-347.

Ortiz-Lopez. A., Chang. H. C., Bush. D. R., (2000).
Amino acid transporters in plants. *Biochimica et Biopysica Acta-Biomembranes*. **1465**: 275-280.

Ozcan. S., Dover. J., Johnston. M., (1998).
Glucose sensing and signaling by two glucose receptors in the yeast *Saccharomyces cerevisiae*. *EMBO Journal*. **17**: 2566-2573.

Ozcan. S., Dover. J., Rosenwald. A.G., Wolfl. S., Johnston. M., (1996).
Two glucose transporters in Saccharomyces cerevisiae are glucose sensors that generate a signal for induction of gene expression. *Proceedings of the National Academy of Sciences USA*. **93**: 12428-12432.

Page. R.D.M., (1996).
TREEVIEW: An application to display phylogenetic trees on personal computers. *Computer Applications in the Biosciences.* **12**: 357-358.

Parent. L., Supplisson. S., Loo. D.D.F., Wright. E.M., (1992).
Electrogenic properties of the cloned Na^+/glucose cotransporter: I. Voltage-clamp studies. *The Journal of Membrane Biology*. **125**: 49-62.

Patrick. J.W. and **Offler. C.E.**, (1996).
Post-sieve element transport of photoassimilates in sink regions. *Journal of Experimental Botany*. **47**: 1165-1177.

Palacin. M., Estevez. R., Bertran. J., Zorzano. A., (1998).
Molecular biology of mammalian plasma membrane amino acid transporters. *Physiological Reviews*. **78**: 969-1054.

Pilon. M. and **Borstlap. A.C.**, (1987).
Kinetics of L-valine uptake in suspension-cultured cells and protoplast-derived cells of tobacco - comparison of wild-type and the Val^r-2 mutant. *Plant Physiology*. **84**: 737-742.

Ramos. S. and **Kaback. H.R.**, (1977a).
The electrochemical proton gradient in *Escherichia coli* membrane vesicles. *Biochemistry* **16**, 848-854.

Ramos. S. and **Kaback. H.R.**, (1977b).
The relationship between the electrochemical proton gradient and active transport in *Escherichia coli* membrane vesicles. *Biochemistry* **16**, 854-859.

Rawat. S.R., Silim. S.N., Kronzucker. H.J., Siddiqi. M.Y., Glass. A.D.M., (1999).
AtAMT1 gene expression and NH4+ uptake in roots of *Arabidopsis thaliana*: evidence for regulation by root glutamine levels. *The Plant Journal*. **19**: 143-152.

Rentsch. D., Hiner. B., Schmelzer. E., Frommer. W., (1996).

Salt stress-induced proline transporters and salt stress-repressed broad specificity amino acid permeases identified by suppression of a yeast amino acid permease-targeting mutant. *The Plant Cell.* **8**: 1437-46.

Rentsch. D., Boorer. K. J., Frommer. W., (1998).

Structure and function of plasma membrane amino acid, oligopeptide and sucrose transporters from higher plants. *Journal of Membrane Biology.* **162**: 177-190.

Rentsch. D., and **Frommer. W.**, (1996).

Molecular approaches towards an understanding of loading and unloading of assimilates in higher plants. *The Journal of Experimental Botany.* **47**: 1199-1204.

Robards. A. and **Lucas. W.**, (1990).

Plasmodesmata. *Annual Review of Plant Physiology and Plant Molecular Biology.* **41**: 369-419.

Robinson. S.P. and **Beevers. H.**, (1981a).

Evidence for amino-acid-proton cotransport in *Ricinus* cotyledons. *Planta.* **152**: 527-533.

Robinson. S.P. and **Beevers. H.**, (1981b).

Amino-acid-transport in germinating castor bean seedlings. *Plant Physiology.* **68**: 560-566.

Robinson. D. and **Benos. D.**, (1991).

Glucose-metabolism in the trophectoderm and inner cell mass of the rabbit embryo. *Journal of Reproduction and Fertility.* **91**: 493-499.

Rose. G. D., Geselowitz. A. R., Lesser. G. J., Lee. R. H., Zehfus. M. H., (1985).

Hydrophobicity of amino acid residues in globular proteins. *Science.* **229**: 834-838.

Sambrook. J., Fritsch. E. F., Maniatis. T., (1989).

Molecular cloning: a laboratory manual. Cold spring harbour, NY: Cold spring harbour laboratory press.

Sauer. N. and **Stolz. J.**, (1994).

SUC1 and SUC2 – 2 sucrose transporters from *Arabidopsis-thaliana* - expression and characterization in bakers yeast and identification of the histidine-tagged protein. *The Plant Journal.* **6**: 67-77.

Schachtman. D.P., Schroeder. J.I., Lucas. W.J., Anderson. J.A., Gaber. R.F., (1992).

Expression of an inward-rectifying potassium channel by the *Arabidopsis KAT1* cDNA. *Science.* **258**: 1654-1657.

Schobert. C. and **Komor. E.**, (1987).

Amino acid uptake by *Ricinus communis* roots: characterisation and physiological significance. *Plant, Cell and Environment.* **10**: 493-500.

Schobert. C. and **Komor. E.**, (1989).

The Differential transport of amino acids into the phloem of *Ricinus communis* L seedlings as shown by the analysis of sieve-tube sap. *Planta.* **177**: 342-349.

Schobert. C. and **Komor. E.**, (1990).

Transfer of amino acid and nitrate from the roots into xylem of *Ricinus communis* seedlings. *Planta.* **181**: 85-90.

Schobert. C., Mitsusada. N., Aoshima. H., (1997).

Diverse transporters for neutral amino acids in *Ricinus communis* L seedlings. *Biologia Plantarum.* **39**: 187-196.

Schwacke. R., Grallath. S., Breitkreuz. K.E., Stransky. E., Stransky. H., Frommer. W.B., Rentsch. D., (1999).

LeProT1, a transporter for proline, glycine betaine, and gamma-amino butyric acid in tomato pollen. *Plant Cell.* **11**: 377-391.

Seffens. W. and **Digby. D.**, (1999).

mRNAs have greater negative folding free energies than shuffled or codon choice randomized sequences. *Nucleic Acids Research.* **27**: 1578-1584.

Setenac. H., Bonneaud. N., Minet. M., Lacroute. F., Salmon. J.-M., Gaymard. F., Grignon. C., (1992).

Cloning and expression in yeast of a plant potassium ion transport system. *Science.* **256**: 663-665.

Smith. G.P., (1994).

Applied evolution – the progeny of sexual PCR. *Nature*. **370**: 324-325.

Sonnhammer. E.L.L., von Heijne. G., Krough. A., (1998).

A hidden Markov model for predicting transmembrane helices in protein sequences. *Proceedings of the Sixth International Conference on Intelligent Systems for Molecular Biology*. AAAI Press. 175-182.

Stemmer. W., (1994).

Rapid evolution of a protein *in vitro* by DNA shuffling. *Nature*. **370**: 389-91.

Stewart. C.R. and **Beevers. H.**, (1967).

Gluconeogenesis from amino acids in germinating castor bean endosperm and its role in transport to the embryo. *Plant Physiology* **42**, 157-161.

Sze. H., (1985).

H^+-translocating ATPases – Advances using membrane-vesicles. *Annual Review of Plant Physiology and Plant Molecular Biology*. **36**: 175-208.

Tamura. S., Nelson. H., Tamura. A., Nelson. N., (1995).

Short external loops as potential substrate binding site of γ-aminobutyric acid transporters. *The Journal of Biological Chemistry*. **48**: 28712-15.

Tanaka. J. and **Fink. G.R.**, (1985).

The histidine permease gene (HIP1) of *Saccharomyces cerevisiae*. *Gene*. **38**: 205-214.

Theodoulou. F.L. and **Miller. A.J.**, (1995).

Xenopus oocytes as a heterologous expression system for plant proteins. *Molecular Biotechnology*. **3**: 101-115.

Tillard. P., Passama. L., Gojon. A., (1998).

Are phloem amino acids involved in the shoot to root control of NO_3- uptake in *Ricinus communis* plants? *Journal of Experimental Botany*. **49**: 1371-1379.

Turgeon. R. and **Beebe. D.U.**, (1991).

The evidence for symplastic phloem loading. *Plant Physiology*. **96**: 349-54.

Ulmschneider. M.B. and **Sansom. M.S.P.**, (2001).
Amino acid distributions in integral membrane protein structures. *Biochimica et Biophysica Acta-Biomembranes*. **1512**: 1-14.

Urquhart. A.A. and **Joy. K.W.**, (1981).
Use of phloem exudate technique in the study of amino-acid-transport in pea plants. *Plant Physiology*. **68**: 750-754.

Vartanian. J.P., Henry. M., WainHobson. S., (1996).
Hypermutagenic PCR involving all four transitions and a sizable proportion of transversions. *Nucleic Acids Research*. **24**: 2627-2631.

Van Bel. A.J.E., (1993).
Strategies of phloem loading. *Annual Review of Plant Physiology and Plant Molecular Biology*. **44**: 253-281.

Van Beusichem. M.L., Baas. R., Kirkby. E.A., Nelemans. J.A., (1985).
Intracellular pH regulation during NO_3 assimilation in shoot and roots of *Ricinus communis*. *Plant Physiology*. **78**: 768-773.

Verbruggen. N., Borstlap. A.C., Jacobs. M., VanMontagu. M., Messens. E., (1996).
The *raz1* mutant of *Arabidopsis thaliana* lacks the activity of a high-affinity amino acid transporter. *Planta*. **200**: 247-253.

Viola. R., Roberts. A.G., Haupt. S., Gazzani. S., Hancock. R.D., Marmiroli. N., Machray. G.C., Oparka. K.J., (2001).
Tuberization in potato involves a switch from apoplastic to symplastic phloem unloading. *The Plant Cell*. **13**: 385-398.

Von Wiren. N., Lauter. F.R., Ninnemann. O., Gillissen. B., Walch-Liu. P., Engels. C., Jost. W., Frommer. W.B., (2000).
Differential regulation of three functional ammonium transporter genes by nitrogen in root hairs and by light in leaves of tomato. *Plant Journal*. **21**: 167-175.

Ward, A.C., (1990).
Single-step purification of shuttle vectors from yeast for high-frequency back-transformation into *Escherichia coli*. *Nucleic Acids Research*. **18**: 5319-5319.

Wegner. L.H. and **Raschke. K.**, (1994).

Ion channels in the xylem parenchyma of barley roots - A procedure to isolate protoplasts from this tissue and a patch-clamp exploration of salt passageways into xylem vessels. *Plant Physiology*. **105**: 799-813.

Weston. K., Hall. J., Williams. L., (1994).

Characterisation of a glutamine/proton cotransporter from *Ricinus communis* roots using isolated plasma membrane vesicles. *Physiologia Plantarum*. **91**: 623-30.

Weston. K., Hall. J., Williams. L., (1995).

Characterisation of amino acid transport in *Ricinus communis* roots using isolated membrane vesicles. *Planta*. **196**: 166-73.

Williams. L.E., Nelson, S,J., Hall. J.L., (1992).

Charcterisation of solute cotransport in plasma-membrane vesicles from *Ricinus* cotyledons, and a comparison with other tissues. *Planta*. **184**: 541-550.

Williams. L., Bick. J., Neelam. A., Weston. K., Hall. J., (1996).

Biochemical and molecular characterisation of sucrose and amino acid carriers in *Ricinus communis*. *The Journal of Experimental Biology*. **47**: 1211-16.

Williams. L.E. and **Miller. A.J.**, (2001).

Transporters responsible for the uptake and partitioning of nitrogenous solutes. *Annual Review of Plant Physiology and Plant Molecular Biology*. **52**: 659-688.

Williams. L., Nelson. S., Hall. J., (1990a).

Characterisation of solute transport in plasma membrane vesicles isolated from cotyledons of *Ricinus communis* L. 1. Adenosine-triphosphatase and pyrophosphatase activities associated with a plasma-membrane fraction isolated by phase partitioning *Planta*. **182**: 532-39.

Williams. L., Nelson. S., Hall. J., (1990b).

Characterisation of solute transport in plasma membrane vesicles isolated from cotyledons of *Ricinus communis* L. 2 Evidence for a proton-coupled mechanism for sucrose and amino-acid-uptake. *Planta*. **182**: 540-45.

(Wisconsin Package).

Program manual for the Wisconsin package, version 8, September 1994, Genetics Computer Group, 575 Science Drive, Madison, Wisconsin, USA 53711.

Wyse. R.E. and **Komor. E.**, (1984).

Mechanism of amino-acid uptake by sugarcane suspension cells. *Plant Physiology*. **76**: 865-870.

Young. G.B., Jack. D.L., Smith. D.W., Saier Jr. M.H., (1999).

The amino acid/auxin:proton symport permease family. *Biochimica et Biophysica Acta-Biomembranes*. **1415**: 306-322.

Zhou. J.-J., Theodoulou. F., Sauer. N., Sanders. D., Miller. A.J., (1997).

A kinetic model with ordered cytoplasmic dissociation for SUC1, an *Arabidopsis* H^+/sucrose cotransporter expressed in *Xenopus* oocytes. *The Journal of Membrane Biology*. **159**: 113-125.

Appendix 1

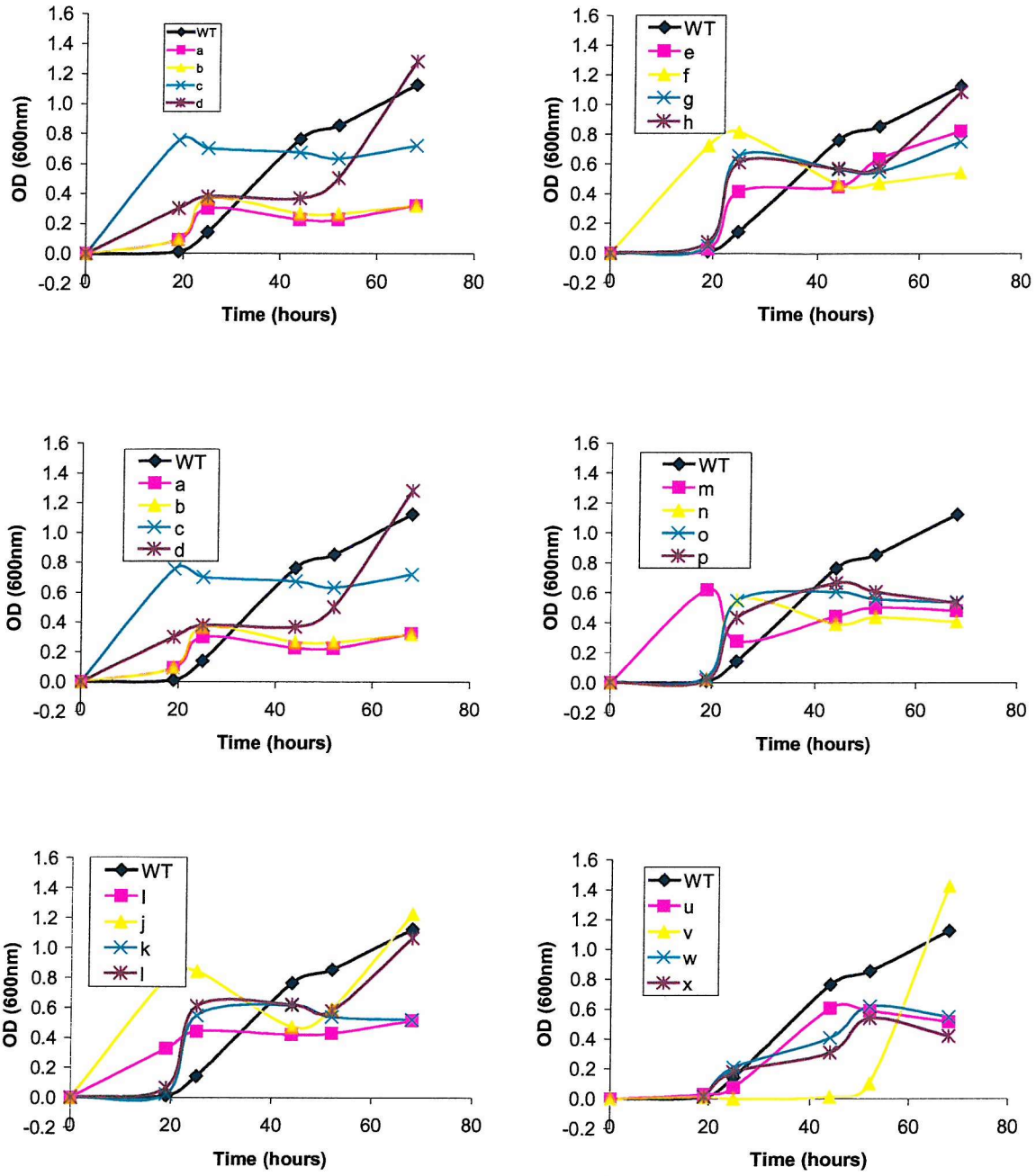

Figure A1.1 – Growth of mutagenised JT-16/RcAAP1 isolates (A-X) compared in each graph to non-mutagenised JT-16/RcAAP1 (WT). Graphs carry individual keys but all show WT growth. OD_{600} of JT-16 isolates on pH 7.5 low-histidine selective medium over 68 hours at 30°C. The growth analysis was repeated under identical conditions and a similar result was recorded. Growth on this selective medium beyond 40 hours resulted in lysis for the majority of mutagenised isolates but sustained growth of the WT expressing yeast.

Appendix 2

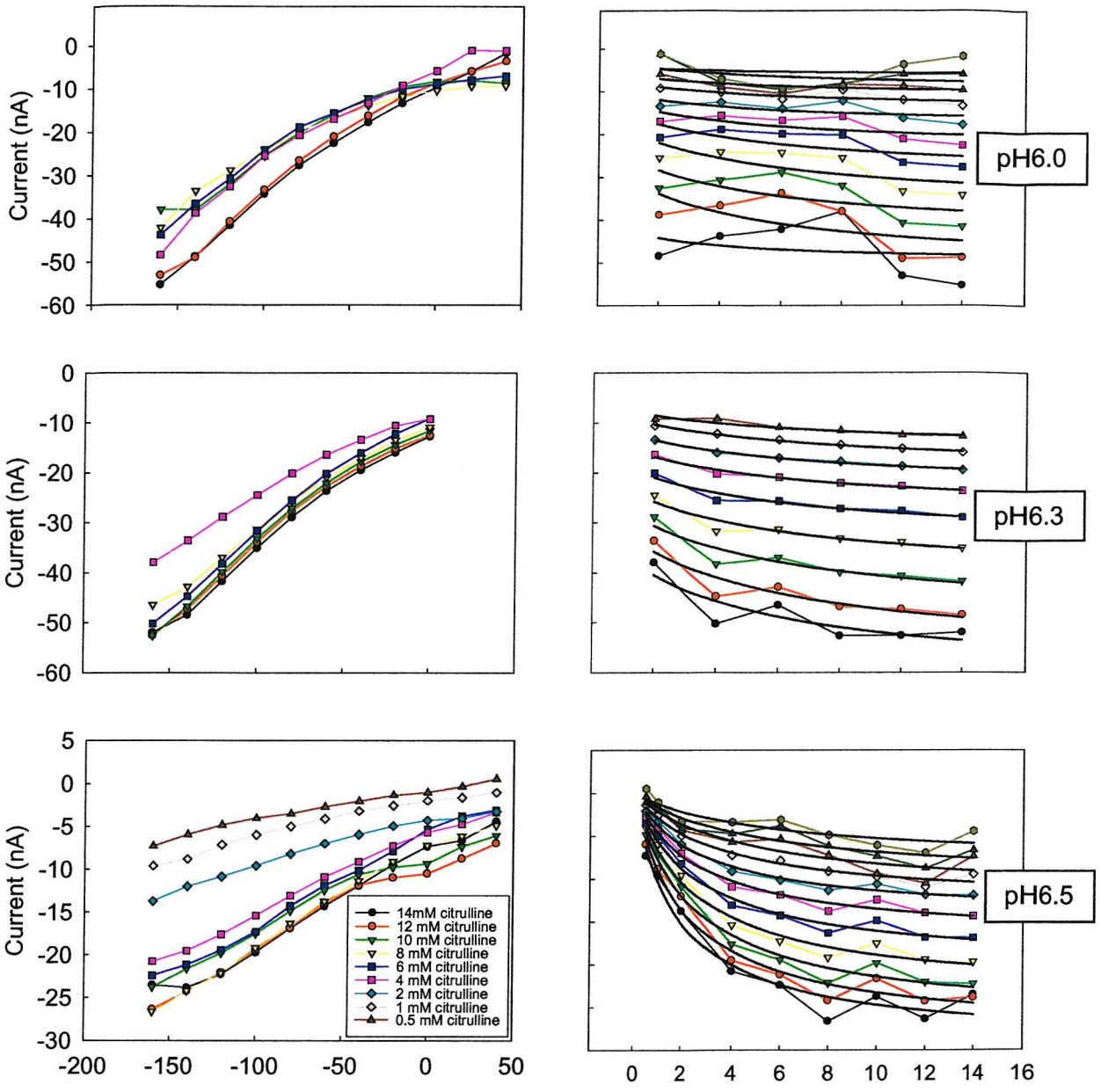

Figure A2.1 - Currents measured from voltage clamped oocytes expressing RcAAP3, in response to the addition of citrulline at 3 different pHs. Plots of current against membrane potential with a range of citrulline concentration (left), key on pH6.5 graph. Subsequent plots of current against citrulline concentration for voltages between -160 mV and +40 mV (right) (colour scale – key below). Calculated fits to these data are included (black lines with no symbols).

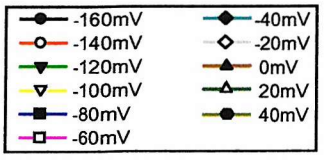

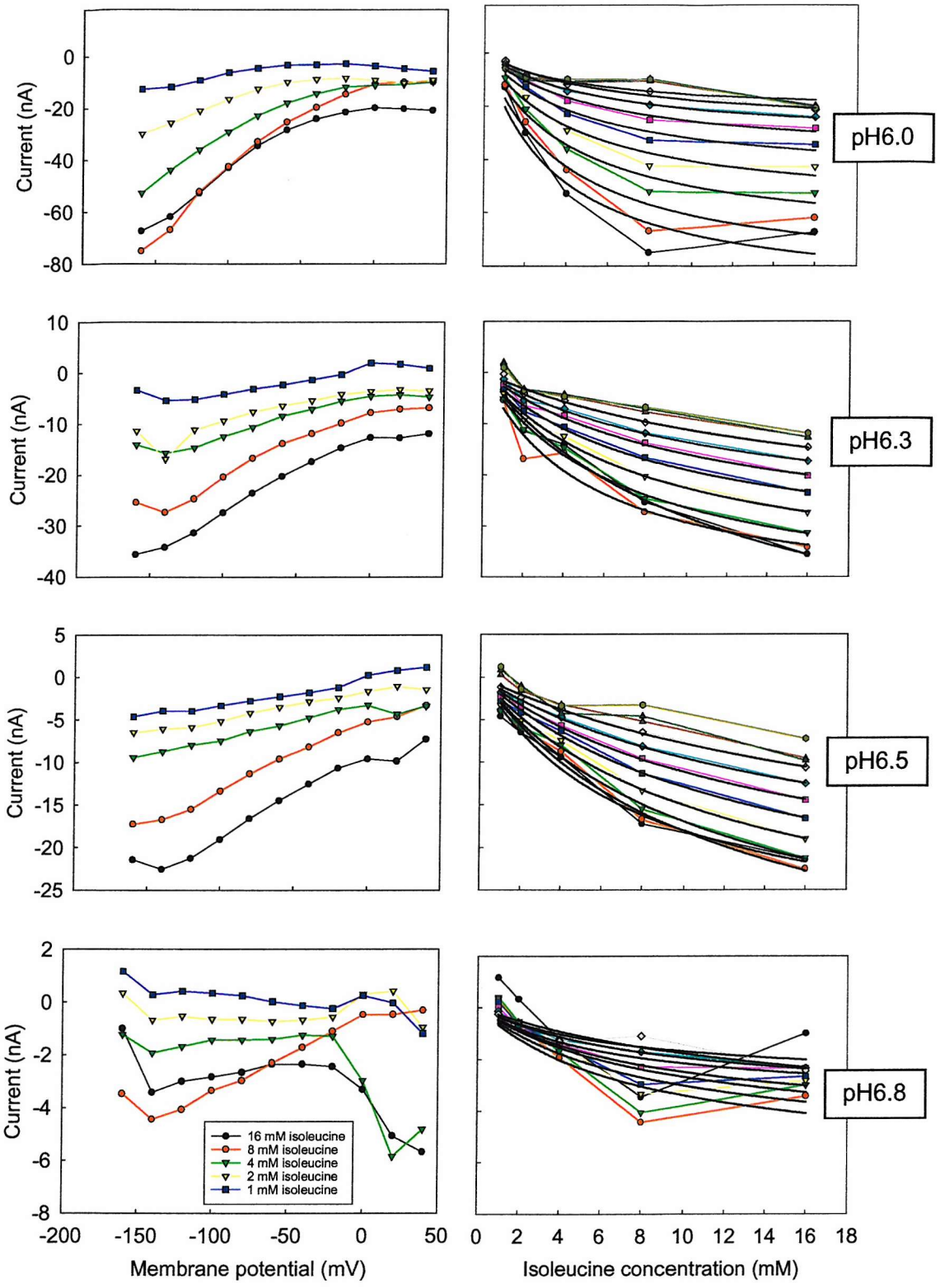

Figure A2.2 - Currents measured from voltage clamped oocytes expressing RcAAP3, in response to the addition of isoleucine at 3 different pHs. Plots of current against membrane potential with a range of isoleucine concentration (left), key on pH6.8 graph. Subsequent plots of current against isoleucine concentration for voltages between -160 mV and +40 mV (right) (colour scale – key figure A2.1). Calculated fits to these data are included (black lines with no symbols).

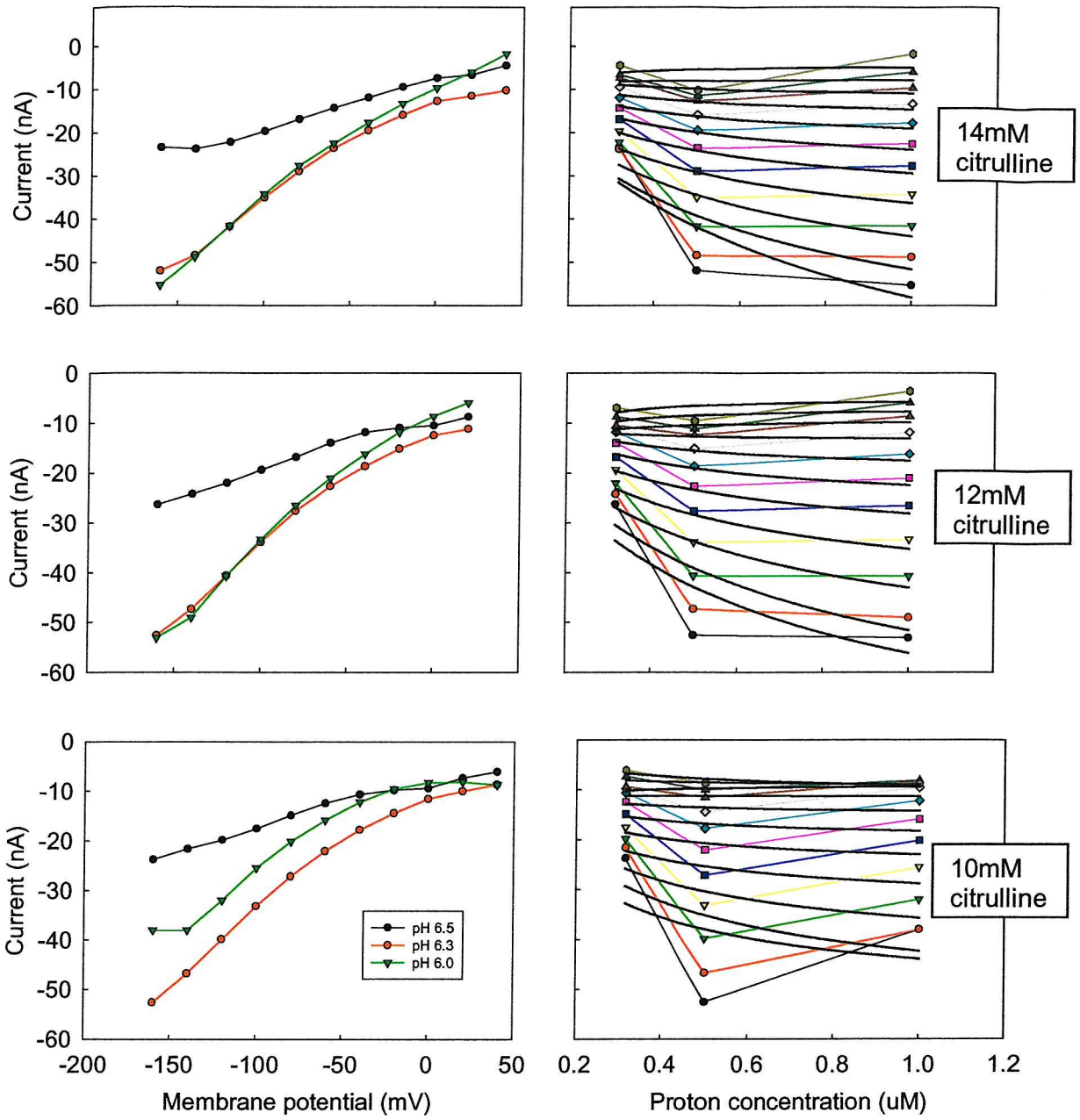

Figure A2.3 - Relationship between current and proton concentration for *RcAAP3*-expressing oocytes, determined from the rearrangement of the data in figure A2.1 at three citrulline concentration. Plots of current against membrane potential over a range of pH (proton concentration) (left), key on 10mM citrulline graph. Subsequent plots of current against proton concentration for voltages between -160 mV and +40 mV (right) (colour scale – key below). Calculated fits to these data are included (black lines with no symbols).

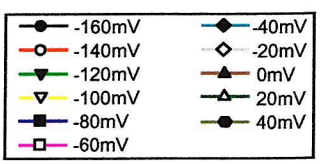

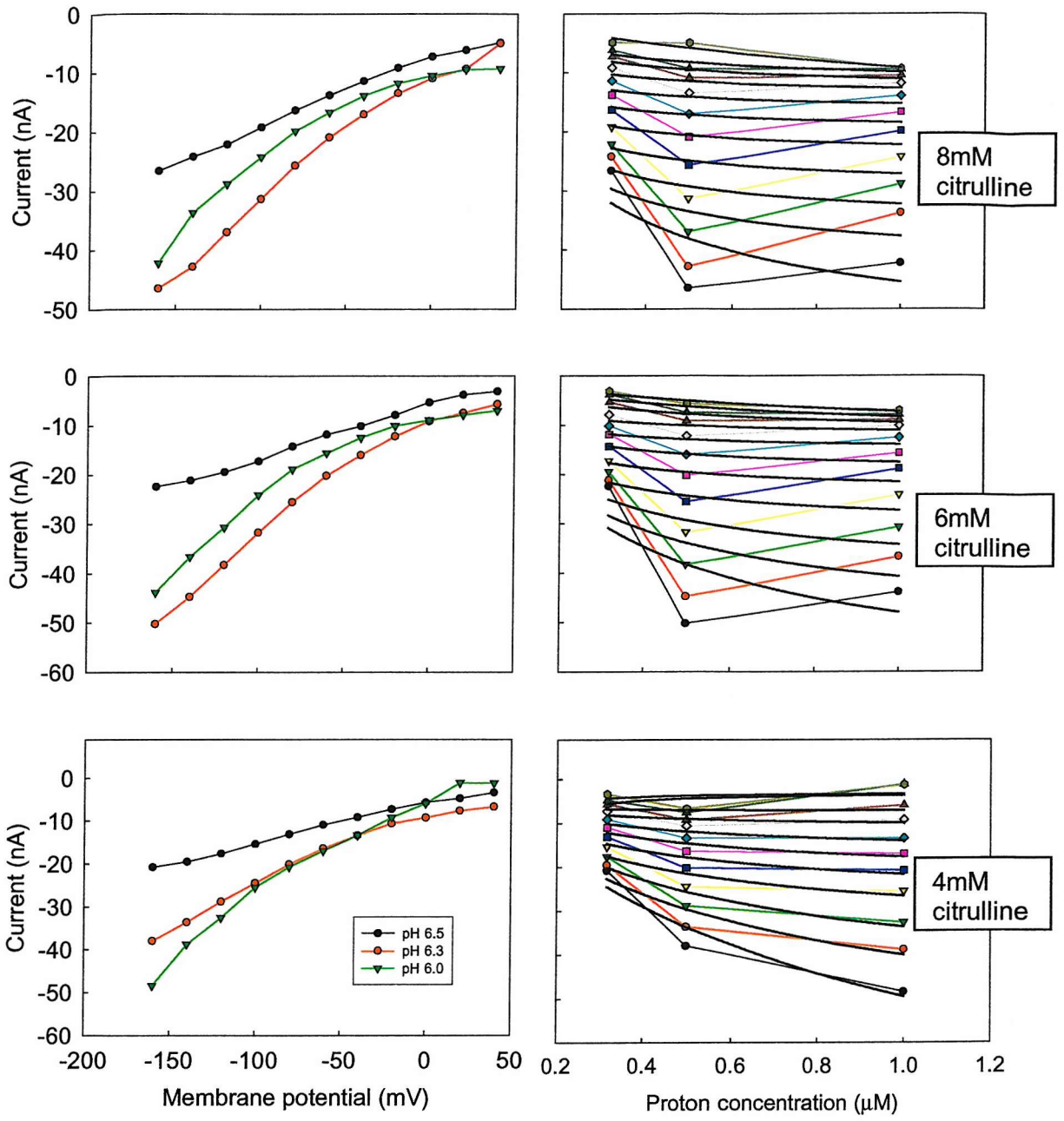

Figure A2.3-continued - Relationship between current and proton concentration for *RcAAP3*-expressing oocytes, determined from the rearrangement of the data in figure A2.1 at three citrulline concentration. Plots of current against membrane potential over a range of pH (proton concentration) (left), key on 4mM citrulline graph. Subsequent plots of current against proton concentration for voltages between -160 mV and +40 mV (right) (colour scale – key below). Calculated fits to these data are included (black lines with no symbols).

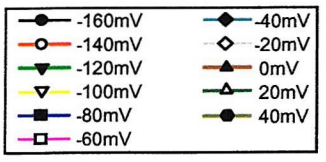

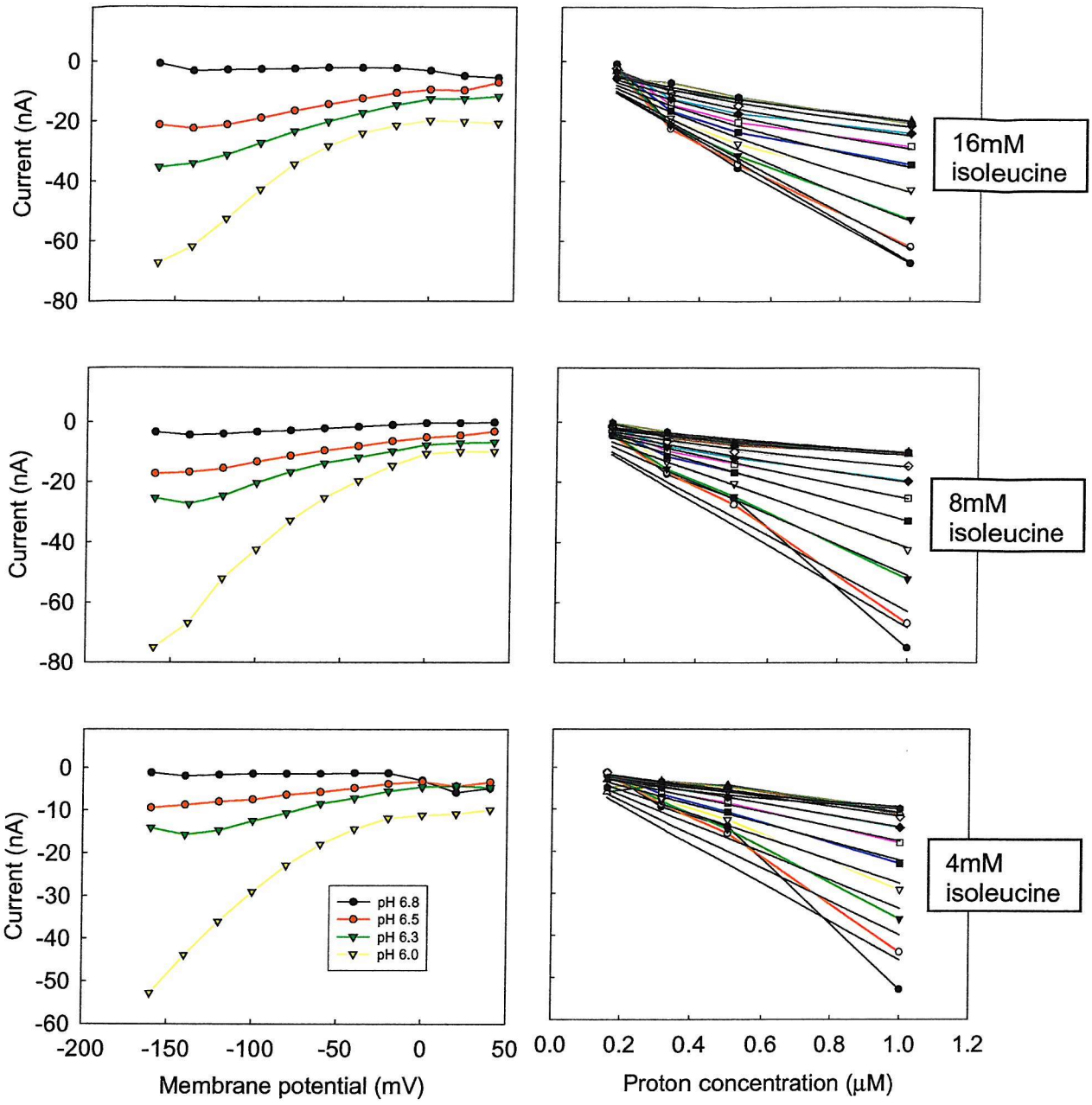

Figure A2.4 - Relationship between current and proton concentration for *RcAAP3*-expressing oocytes, determined from the rearrangement of the data in figure A2.2 at three isoleucine concentration. Plots of current against membrane potential over a range of pH (proton concentration) (left), key on 4mM isoleucine graph. Subsequent plots of current against proton concentration for voltages between -160 mV and +40 mV (right) (colour scale – key below). Calculated fits to these data are included (black lines with no symbols).

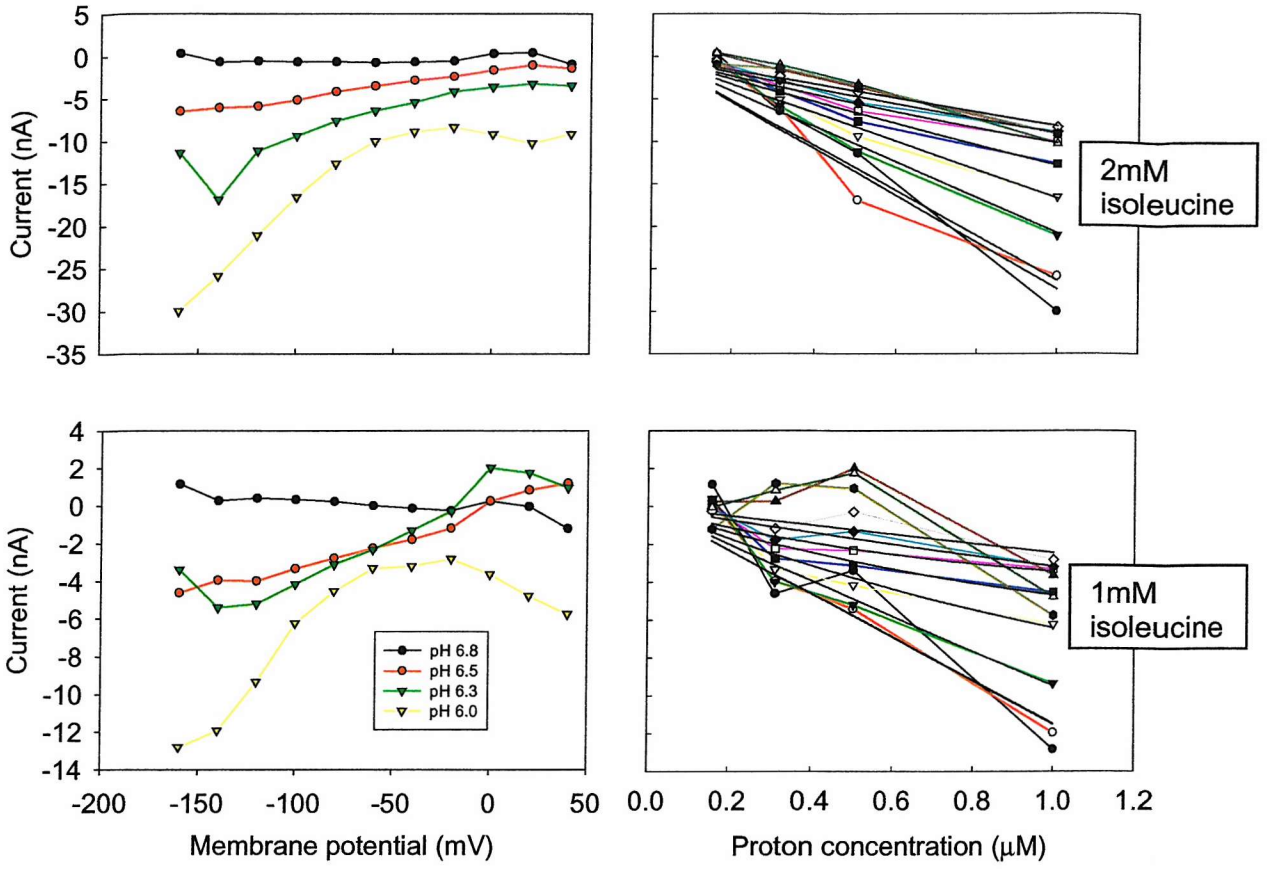

Figure A2.4 continued - Relationship between current and proton concentration for *RcAAP3*-expressing oocytes, determined from the rearrangement of the data in figure A2.2 at two isoleucine concentration. Plots of current against membrane potential over a range of pH (proton concentration) (left), key on 1mM isoleucine graph. Subsequent plots of current against proton concentration for voltages between -160 mV and +40 mV (right) (colour scale – key below). Calculated fits to these data are included (black lines with no symbols).